VPU MEDIATED ENHANCEMENT OF HUMAN IMMUNODEFICIENCY VIRUS PATHOGENESIS: THE ROLE OF CONSERVED AND UNIQUE DOMAINS IN PROTEIN FUNCTION

BY

AUTUMN JOY RUIZ

Submitted to the graduate degree program in Anatomy and Cell Biology and the Graduate Faculty of the University of Kansas in partial fulfillment of the requirements for the degree of Doctor of Philosophy

_____
Edward B. Stephens, Ph.D.
Chairperson

_____
Nancy Berman, Ph.D.

_____
Charlotte Vines, Ph.D.

_____
Michael Werle, Ph.D.

_____
Thomas Yankee, Ph.D.

Date Defended: November 22, 2010

The Dissertation Committee for Autumn Joy Ruiz
certifies that this is the approved version of the following dissertation:

VPU MEDIATED ENHANCEMENT OF HUMAN IMMUNODEFICIENCY VIRUS PATHOGENESIS: THE ROLE OF CONSERVED AND UNIQUE DOMAINS IN PROTEIN FUNCTION

_____

Edward B. Stephens, Ph.D
Chairperson

Date approved: December 13, 2010

II. Abstract

The work in this dissertation examined the biological characteristics of different HIV-1 Vpu subtypes, with an emphasis on subtypes B and C, and the potential impact of these proteins on SHIV pathogenesis. Different Vpu subtypes exhibited distinct biological properties that potentially could affect HIV-1 pathogenesis and/or transmission efficiency, including intracellular localization, efficiency in down-modulating CD4 surface expression, and the ability to enhance virion release in HeLa cells. We show for the first time that the subtype B and C Vpu proteins partitioned into detergent resistant membranes (DRMs), a property characteristic of lipid raft association. We also identified two mutants, IVV19-21AAA and W22A, that prevented this association. Additionally, we found a correlation between the ability of Vpu to stably associate with DRMs and the ability to enhance virion release in HeLa cells. Analysis of different Vpu proteins from clinical isolates identified a membrane proximal tyrosine motif (YXXΦ) that is highly conserved among all Vpu subtypes and an overlapping dileucine motif ([D/E]xxxL[L/I]) that is conserved among subtype C Vpu proteins. Substitution of the tyrosine residue in the YXXΦ motif with an alanine (Y35A) significantly inhibited SHIV replication while substitution of the primary leucine residue with a glycine (L39G) in the overlapping [D/E]xxxL[L/I] motif significantly increased the amount of virus released from C8166 cells and the mean number of viral particles per cell compared to cells inoculated with the parental $SHIV_{SCVpu}$. Recently, the enhanced virion release function of Vpu has been attributed to the antagonism of bone marrow stromal antigen 2 (BST-2) protein. This has been shown to involve the transmembrane domains (TMD) of both proteins. Our results indicate that the length of the BST-2 TMD is more important than the primary sequence both for the function and sensitivity of the protein. Additionally, we showed that the BST-2 protein expressed in pig-tailed macaques is not

antagonized by HIV-1 Vpu, but rather by SIV Nef, thus indicating a species-specific basis for this antagonism. Based on these results we continued our analyses by examining the biological characteristics of SHIV expressing either a subtype B ($SHIV_{KU\text{-}1bMC33}$) or C ($SHIV_{SCVpu}$) Vpu protein. $SHIV_{SCVpu}$ caused a more gradual rate of $CD4^+$ T cell loss and lower peak viral loads in infected pig-tailed macaques compared to macaques inoculated with $SHIV_{KU\text{-}1bMC33}$. The identification of the TMD and the putative sorting signals proximal to the membrane as key determinants in Vpu-mediated enhanced virion release prompted the hypothesis that these two regions may dictate these differences in pathogenesis. Therefore, we constructed chimeric Vpu proteins in which the N-terminus/TMD regions of the subtype B and C Vpu proteins were exchanged (VpuBC and VpuCB). Inoculation of pig-tailed macaques with $SHIV_{VpuCB}$ resulted in a more gradual loss of circulating $CD4^+$ T cells compared to $SHIV_{VpuBC}$-inoculated macaques, but more rapid than resulted in macaques inoculated with parental $SHIV_{SCVpu}$. Since both of these proteins down-modulated CD4 surface expression similar to the unmodified Vpu_{SC}EGFP1 protein, our results indicate that the differences observed in CD4 surface down-modulation *in vitro* are most likely not physiologically relevant. Finally, as pig-tailed macaques express a BST-2 protein that is not affected by the HIV-1 Vpu protein, our results suggest that the enhanced virion release function of different Vpu subtypes as observed during an intravenous inoculation may be dependent upon a different factor(s). The work presented here demonstrates a clear potential for differential signaling and functional efficiency among all HIV-1 Vpu subtypes with the ability to modify pathogenesis. Additionally, our analyses identified the TMD and membrane proximal regions as crucial components to Vpu enhancement of pathogenesis providing novel information essential for anti-retroviral therapeutic development.

III. Acknowledgments

The graduate career of a student is an exciting, challenging and humbling experience. For the past five years I have been surrounded by great minds and enormous support that have made my experience at KUMC remarkable and I would like to take this opportunity to thank those individuals who have been a part of it. First, I would like to thank my mentor, Dr. Edward B. Stephens, for all of your help and guidance. You have always encouraged me to work-hard and continually challenge myself and I hope you view this dissertation as a positive reflection of your mentorship like I do. I would also like to thank Drs. Nancy Berman, Charlotte Vines, Michael Werle, and Tom Yankee for all of their support and the time and effort they spent serving on my comprehensive exam and dissertation committees. I would also like to thank all of the members of the Microbiology, Molecular Genetics, and Immunology department as well as the Anatomy and Cell Biology department. I would like to send a special thanks to Dr. Doug Wright for his continued support and guidance throughout the years.

Thank you to the members of the Stephens' lab, Sarah Hill and Kim Schmitt. Sarah, words cannot express my gratitude. Your intellect astounds me and working alongside of you was a privilege. Thank you for always lending a helping hand when I discovered new experiments that "hate me" and for all of the random discussions that helped me to think through a problem or discover new directions. I owe a major part of my growth as a scientist to you and I thank you from the bottom of my heart.

Kim, you are an incredible friend and an amazing scientist and I would never have made it through this without you. You have been through so much these past five years and I am amazed by your perseverance and positive outlook. I thank you for all of your help and for the random questions and discussions that helped me put together this body of work. I especially

thank you for all of the times you helped me find my way when I got lost, particularly when it included shopping, movies and margaritas. You are an incredibly wonderful and gifted person and I am proud to call you my friend and my coworker.

I would also like to extend my gratitude to the former members of the Stephens' lab: Erik Pacyniak, Jean-Marie Miller, Dr. Dave Hout, Fenglan Jia, Zhengian Liu, and Istvan Adany for all of their contributions. Also, thank you to our collaborators in Dr. John Guatelli's lab at the University of California, San Diego, for all of their work and insight.

To my friends and family, I apologize that I cannot single all of you out, but please know that you mean the world to me and that I couldn't have done this without you. I love you all and I hope to make you proud.

To my mom, Echo, thank you for being the single greatest support system anyone could ever ask for. As some would say I am a "character" and I do some crazy things, but your love and support have never faltered and for that I am eternally grateful. I owe all that I am and everything I have had the opportunity to do in my life to you. You are one of the bravest, most kind-hearted, intelligent people I know and I would not have made it through this experience without you. I will never be able to thank you enough for everything you do for me, but I hope to make you as proud of me as I am to call you mom.

To my brother, Matt, you are one of the most intelligent, witty and generous persons I have ever met. You have always been an inspiration to me to continually challenge myself and keep moving forward. I admire your courage, your eagerness for learning and your limitless ability to question all that you encounter. I love you very much and I thank you for being who you are, for always being able to make me laugh and for inspiring me to be a better person.

To my dad, never does a day go by that I don't think of you. You were one of the most kind, humble and joyful people I have ever known. You supported me through everything even if it was crazy and I know you have been with me through this whole experience. You taught me to work hard, enjoy life, and help others as often as I could and I will continue to do just that. I thank you for being a wonderful father and for all of the support and love I know you still send.

To Ryan, I love you with everything that I have and all that I am. Your love and support these past few years have been immeasurable and I will forever be indebted to this experience for bringing us together. You have always believed in me even when my belief in myself wavered and that is something I hold very dear. You are incredibly kind, intelligent, outgoing and supportive and I look forward to a lifetime of nerdy scientific conversations with you. And I would definitely throw myself on a bee for you.

And finally, to my furry children, Maya and Oscar, thank you for your warm welcomes and wagging tails. You made the 100% failure rate days easier and you always made me feel successful in the end.

IV. Dedication

Dedicated to all of those who count on us for help

Table of Contents

I. Acceptance Page ..... **ii**

II. Abstract ..... **iii**

III. Acknowledgements ..... **v**

IV. Dedication ..... **viii**

V. List of Figures ..... **xii**

VI. **Chapter One: Introduction** **1**

A. Goals of the Study 1

B. Epidemiology 6

C. Classification 7

D. Geographic Distribution 11

E. Genomic Structure of Lentiviruses 14

F. Viral Replication Cycle and Current HIV-1 Therapeutic Targets 15

G. Viral Proteins 23

H. Pathogenesis 46

I. SHIV Macaque Models of HIV-1 Infection 48

J. Is Vpu an Ion Channel Protein? 54

K. Role of Vpu in CD4 Surface Down-Modulation 57

L. Role of Vpu in Enhanced Virion Release 65

M. Role of BST-2 in Release of Primate Lentiviruses Lacking a Vpu Protein 78

N. Unanswered Questions of the Vpu Protein in Viral Pathogenesis 79

VII. **Chapter Two: BST-2 Mediated Restriction of Simian-Human Immunodeficiency Virus** **83**

A. Abstract 83

B. Introduction 83

C. Results 87
D. Discussion 104
E. Experimental Methods 107

VIII. **Chapter Three: Different HIV-1 Vpu Subtypes Exhibit Distinct Biological Properties 113**

A. Abstract 113
B. Introduction 113
C. Results 115
D. Discussion 127
E. Experimental Methods 133

IX. **Chapter Four: Modulation of the Severe CD4+ T-Cell Loss Caused by a Pathogenic Simian-Human Immunodeficiency Virus by Replacement of the Subtype B Vpu with the Vpu from a Subtype C HIV-1 Clinical Isolate 141**

A. Abstract 141
B. Introduction 142
C. Results 143
D. Discussion 169
E. Experimental Methods 173

X. **Chapter Five: Membrane Raft Association of the Vpu Protein of Human Immunodeficiency Virus Type I Correlates with Enhanced Virus Release 179**

A. Abstract 179
B. Introduction 179
C. Results 182
D. Discussion 214
E. Experimental Methods 219

XI. **Chapter Six: Requirements of the Membrane Proximal Tyrosine and Dileucine-Based Sorting Signals for Efficient Transport of the Subtype C Vpu Protein to the Plasma Membrane and in Virus Release 228**

A. Abstract 228
B. Introduction 229
C. Results 231
D. Discussion 256
E. Experimental Methods 260

XII. **Chapter Seven: The Transmembrane Domain of Human Immunodeficiency Virus Type 1 Vpu is a Major Influence of the Protein on the Rate of $CD4^+$ T Cell Loss in Pig-tailed Macaques Inoculated with SHIV 268**

A. Abstract 268
B. Introduction 269
C. Results 271
D. Discussion 295
E. Experimental Methods 297

XIII. **Chapter Eight: Conclusions 304**

XIV. **References 321**

XV. **Appendix 363**

A. List of Publications 363

V. List of Figures

Chapter One: Introduction

Figure 1 Global estimates of the adults and children living with HIV/AIDS.....9

Figure 2 Phylogeny and geographic distribution of HIV isolates.....13

Figure 3 Schematic of Lentivirus genomes 17

Figure 4 Replication cycle and current HIV-1 therapeutic targets 25

Figure 5 Schematic representation of mature HIV-1 virion 27

Figure 6 Schematic representation of Vpu protein 40

Figure 7 Schematic representation of SHIV 51

Figure 8 Diagram of Vpu-mediated CD4 surface down-modulation 60

Figure 9 Potential models for Vpu antagonism of BST-2 75

Chapter Two: BST-2 mediated restriction of simian-human immunodeficiency virus

Figure 10 Sequences of pig-tailed and rhesus BST-2 clones.....89

Figure 11 Sequences of mutant BST-2 proteins used in this study 91

Figure 12 Expression of mutant BST-2 proteins 93

Figure 13 Effects of parental BST-2 proteins on SHIV release.....96

Figure 14 Effects of ptBST-2 mutant proteins on SHIV release 99

Figure 15 Effects of hBST-2 mutant proteins on SHIV release 103

Chapter Three: Different HIV-1 Vpu Subtypes Exhibit Distinct Biological Properties

Figure 16 Sequences of HIV-1 Vpu subtypes used in this study.....118

Figure 17 Intracellular localization of HIV-1 Vpu subtypes 120

Figure 18 CD4 surface down-modulation by HIV-1 Vpu subtypes 124

Figure 19 Effects of HIV-1 Vpu subtypes on SHIV particle release.....126

Figure 20 Stability of HIV-1 Vpu proteins analyzed in this study 129

Chapter Four: Modulation of the severe CD4+ T cell loss caused by a pathogenic simian-human immunodeficiency virus by replacement of the subtype B Vpu with the Vpu from a subtype C HIV-1 clinical isolate

Figure 21 Sequences of HIV Vpu proteins used in this study 146

Figure 22 CD4 surface down-modulation by subtype B and subtype C Vpu proteins.....148

Figure 23 Expression of subtype B and subtype C Vpu in SHIV inoculated cells.....150

Figure 24 Pulse Chase analysis of $SHIV_{SCVpu}$ viral proteins 154

Figure 25 Replication kinetics of $SHIV_{KU\text{-}1bMC33}$ and $SHIV_{SCVpu}$ in C8166 cells.....156

Figure 26 Electron microscopy examination of cells inoculated with $SHIV_{KU\text{-}1bMC33}$ and $SHIV_{SCVpu}$ 158

Figure 27 Envelope incorporation in $SHIV_{KU\text{-}1bMC33}$ and $SHIV_{SCVpu}$ 160

Figure 28 Circulating $CD4^+$ T cell levels and plasma viral loads in macaques inoculated with $SHIV_{KU\text{-}1bMC33}$ and $SHIV_{SCVpu}$ 163

Figure 29 Histopathology associated with $SHIV_{SCVpu}$ inoculation of macaques.....166

Figure 30 Analysis of *gag* expression in tissues isolated from macaques inoculated with $SHIV_{KU\text{-}1bMC33}$ and $SHIV_{SCVpu}$ 168

Chapter Five: Membrane raft association of the Vpu protein of human immunodeficiency virus type 1 correlates with enhanced virus release

Figure 31 Partitioning of Vpu into lipid rafts from transfected cells.....184

Figure 32 Partitioning of Vpu into lipid rafts from infected cells 187

Figure 33 Partitioning of subtype B vs subtype C Vpu into lipid rafts and effects of cholesterol depletion on Vpu partitioning into lipid rafts 191

Figure 34 Partitioning of Vpu into lipid rafts at physiological temperature.....193

Figure 35 Co-localization of Vpu with NFP-GPI following co-patching.....196

Figure 36 Detergent Resistant Membrane Fractionation of Vpu_{TM}EGFP 199

Figure 37 Sequences and protein stability of Vpu TMD mutant proteins used in this study 202

Figure 38 Partitioning of Vpu TMD mutant proteins into lipid rafts 204

Figure 39 Intracellular localization of VpuEGFPW23A 207

Figure 40 Effects of Vpu TMD mutant proteins on SHIV particle release 210

Figure 41 CD4 surface down-modulation by Vpu TMD mutant proteins.....213

Chapter Six: Requirements of the membrane proximal tyrosine and dileucine-based sorting signals for efficient transport of the subtype C Vpu protein to the plasma membrane and in virus release

Figure 42 Sequences of Vpu interface mutant proteins used in this study.....233

Figure 43 Intracellular localization of Vpu interface mutant proteins.....236

Figure 44 Co-localization of Vpu interface mutant proteins with DsRed2-Golgi marker 238

Figure 45 Quantification of surface expression of biotinylated Vpu interface mutant proteins.....240

Figure 46 Stability of Vpu interface mutant proteins 243

Figure 47 CD4 surface down-modulation by Vpu interface mutant proteins.....245

Figure 48 Replication kinetics of $SHIV_{SCVpu}$, $SHIV_{SCVpuY35A}$, $SHIV_{SCVpuL39G}$, and $SHIV_{SCVpuYL35,39AG}$ in C8166 cells 247

Figure 49 Pulse chase analysis of SHIV proteins expressed by $SHIV_{SCVpu}$, $SHIV_{SCVpuY35A}$, $SHIV_{SCVpuL39G}$, and $SHIV_{SCVpuYL35,39AG}$.....250

Figure 50 Electron microscopy examination of cells inoculated with $SHIV_{SCVpu,}$ $SHIV_{SCVpuY35A}$, $SHIV_{SCVpuL39G}$, and $SHIV_{SCVpuYL35,39AG}$.....253

Figure 51 Enumeration of the number of viral particles associated with C8166 cells infected with $SHIV_{SCVpu,}$ $SHIV_{SCVpuY35A}$, $SHIV_{SCVpuL39G}$, and $SHIV_{SCVpuYL35,39AG}$ 255

Chapter Seven: The transmembrane domain of human immunodeficiency virus type 1 Vpu is a major influence of the protein on the rate of $CD4^+$ T cell loss in pig-tailed macaques inoculated with SHIV

Figure 52 Sequences of chimeric Vpu proteins used in this study 273

Figure 53 Intracellular localization of chimeric Vpu proteins.....275

Figure 54 Stability of chimeric Vpu proteins 277

Figure 55 CD4 surface down-modulation by chimeric Vpu proteins.....279

Figure 56 Virl protein biosynthesis of SHIV expressing chimeric Vpu proteins 282

Figure 57 Replication kinetics of SHIV expressing chimeric Vpu proteins.....284

Figure 58 Electron microscopy examination of cells inoculated with $SHIV_{KU\text{-}1bMC33}$, $SHIV_{SCVpu}$, $SHIV_{VpuBC}$, and $SHIV_{VpuCB}$.....287

Figure 59 Enumeration of the number of viral particles associated with C8166 cells infected

with $SHIV_{KU\text{-}1bMC33}$, $SHIV_{SCVpu}$, $SHIV_{VpuBC}$, and $SHIV_{VpuCB}$ 289

Figure 60 Circulating $CD4^+$ T cell levels in macaques inoculated with $SHIV_{VpuBC}$ and $SHIV_{VpuCB}$ 292

Figure 61 Plasma viral loads in macaques inoculated with $SHIV_{VpuBC}$ and $SHIV_{VpuCB}$ 294

Chapter Eight: Conclusions

Figure 62 Potential models for Vpu-mediated enhanced virion release 314

VIII. Introduction

Goals of the Study

There are 9 different subtypes of HIV-1 Group M viruses responsible for the current HIV/AIDS global pandemic. Epidemiological studies have established a disproportionate global distribution of these different subtypes proposing the possibility that these different subtypes exhibit distinct virological properties that have evolved in order to promote virus spread among diverse populations. While highly active anti-retroviral therapy (HAART) has provided a reprieve in the morbidity and mortality ratios of infected patients, drug resistance and the continued spread of these viruses remain a substantial issue. More studies are needed to determine the specific genetic contributions of different HIV-1 subtypes involved in the continued propogation of these viruses. Hence, this study focused on identifying specific molecular determinants of the HIV-1 accessory protein, Vpu, involved in the enhancement of pathogenesis.

Human immunodeficiency virus type 1 (HIV-1) and several simian immunodeficiency viruses (SIV) encode for a transmembrane protein known as Viral Protein U (Vpu). While one of the smallest of the HIV-1 encoded proteins, it has two important functions within virus-infected cells. The first of these functions is the down-regulation of the CD4 receptor to prevent its interaction with the HIV-1 envelope glycoprotein. Vpu interacts with the CD4 receptor in the rough endoplasmic reticulum (RER), resulting in its re-translocation across the RER and subsequent degradation via the proteasomal pathway. The second major function of the Vpu protein is to facilitate release of virus from infected cells. Previous studies have shown that virus release is cell-type specific, suggesting that certain cells may express a restriction factor that inhibits virus release in the absence of Vpu. The exact mechanism of Vpu-mediated enhanced

virion release is still under investigation, however it has recently been attributed to the antagonism of a cellular protein known as bone marrow stromal antigen 2 (BST-2) (Neil et al., 2008; Van Damme et al., 2008).

Our laboratory has used chimeric simian-human immunodeficiency viruses (SHIV) extensively as a model for analyzing the role of the Vpu protein in viral pathogenesis. With the recent discovery of BST-2 as a restriction factor for HIV-1, we initiated our studies by examining the BST-2-mediated restriction of $SHIV_{KU-2MC4}$ and the ability of the Vpu protein to overcome this restriction. We also analyzed the role of specific amino acids within the transmembrane domain (TMD) of BST-2 in establishing Vpu susceptibility by sequentially humanizing the TMD of the pig-tailed BST-2, which is normally not sensitive to HIV-1 Vpu. Our results show that human and pig-tailed BST-2 (hBST-2 and ptBST-2) restrict SHIV release and are susceptible to the encoded Vpu (HIV-1 derived) and Nef (SIV derived) proteins, similar to results reported for HIV-1 and SIV, respectively. These results substantiate our continued use of the SHIV/macaque model as a tool for studying the effects of HIV-1 Vpu on pathogenesis. We also found that sequential "humanization" of the ptBST-2 TMD resulted in a fluctuation in sensitivity to HIV-1 Vpu, suggesting that the topology of the TMD rather than the specific amino acid identity is responsible for the interaction with Vpu. Finally, we show that the length of the TMD in human and ptBST-2 proteins is important for BST-2 restriction and susceptibility to HIV-1 Vpu. Based on our previous *in vivo* studies in which Vpu was clearly demonstrated to play a significant role in SHIV pathogenesis in the absence of a BST-2 protein that was sensitive to the Vpu protein, these studies suggest that the HIV-1 Vpu TMD may have additional functions *in vivo* unrelated to BST-2 antagonism (Hout et al., 2006b; Hout et al., 2005; McCormick-Davis et al., 2000a; Singh et al., 2001; Stephens et al., 2002).

Based on evolutionary results that have identified a variety of genotypic differences among HIV-1 subtypes including divergence in the *vpu* genes, we hypothesized that different Vpu proteins exhibit distinct molecular determinants that dictate differential function of Vpu in HIV-1 pathogenesis. Therefore, the second study presented herein examined the biological properties of several different HIV-1 Vpu protein subtypes including each protein's intracellular localization, ability to down-modulate CD4 from the cell surface, and the ability to enhance SHIV virion release in the presence of high levels of hBST-2. Our results show that Vpu protein subtypes A, A2 and C are transported to the cell surface more efficiently than Vpu proteins from subtypes B, D, F, and H, which are predominately localized within intracellular compartments. We also show that all of the proteins maintained the ability to down-modulate CD4 from the surface, even though subtypes A2 and C were significantly less efficient. We also found that the subtype F Vpu protein was the only protein unable to enhance SHIV particle release in HeLa cells, which express high levels of hBST-2. This study provided evidence in support of distinct biological determinants of Vpu function among different subtypes that may affect the ability of Vpu to enhance pathogenesis.

In light of these results we focused our analysis on the molecular differences between subtype B and subtype C Vpu proteins. Our third study further analyzed the biological properties of these two Vpu subtypes with an emphasis on their ability to modify pathogenesis using a SHIV/macaque model for disease. We consistently found that subtype C Vpu proteins were less efficient than the subtype B Vpu protein at down-modulating CD4 from the cell surface using four different subtype C Vpu proteins. We also found that a SHIV expressing a subtype C Vpu protein ($SHIV_{SCVpu}$) replicated with decreased kinetics compared to a SHIV expressing a subtype B Vpu protein ($SHIV_{KU\text{-}1bMC33}$), even though the Env and Gag proteins

were synthesized and processed similarly. We inoculated three pig-tailed macaques with $SHIV_{SCVpu}$ and monitored disease progression by analyzing the circulating $CD4^+$ T cell levels and plasma viral burdens in each macaque for up to 44 weeks. Our results show that $SHIV_{SCVpu}$ caused a more gradual rate of $CD4^+$ T cell loss and lower viral loads in pig-tailed macaques compared to those inoculated with $SHIV_{KU\text{-}1bMC33}$. This study provided evidence in support of differential modification of pathogenesis by different HIV-1 Vpu proteins and show for the first time that different Vpu proteins can influence the rate of $CD4^+$ T cell loss in the SHIV/macaque model of disease.

In order to understand the mechanisms associated with differential modification of pathogenesis by different Vpu proteins, we concentrated on identifying conserved or unique elements of each protein that govern the structural and functional features of either the subtype B or the subtype C Vpu protein. Our fourth study therefore focused on the role of the transmembrane domain in Vpu membrane association, stability and function. Since Vpu is membrane bound and known to interact with lipid raft proteins (i.e. CD4 and BST-2), we hypothesized that Vpu would also associate with lipid rafts and that specific amino acids within the TMD would dictate this association. Using biochemical and morphological techniques we demonstrated that both subtype B and subtype C Vpu proteins associate with membrane rafts in a cholesterol dependent manner. We also demonstrate a correlation between membrane raft association and the enhanced virion release function of Vpu by analyzing Vpu proteins with combinatorial substitutions within the TMD. Raft association-deficient TMD mutants were impaired in the enhanced release function in HeLa cells, but still maintained the ability to down-modulate CD4 surface expression. These results demonstrate that the two functions of Vpu

require distinct membrane localization patterns and implicate regions of the TMD as targets for inhibiting Vpu enhanced virion release function.

The fifth study presented, examined the role of two overlapping putative sorting signals in the membrane proximal region of the subtype C Vpu in intracellular transport, CD4 surface down-modulation, and virus release from the cell surface. The first is a tyrosine-based (YxxΦ) motif that is highly conserved among different Vpu subtypes and the second is a dileucine-based ([D/E]xxxL[L/I]) motif that is only highly conserved among subtype C Vpu proteins. Our results indicated that neither of these motifs is required for CD4 surface down-modulation, although elimination of both motifs together reduced the ability of the protein to down-modulate CD4 from the cell surface. In contrast, the dileucine motif significantly affected the intracellular transport of the protein. Disruption of this motif through mutagenesis resulted in a protein that was expressed at the surface at significantly reduced levels compared to the unmodified Vpu_{SC}EGFP1 protein. Examination of SHIVs expressing subtype C Vpu proteins with mutations in the tyrosine ($SHIV_{SCVpuY35A}$), dileucine ($SHIV_{SCVpuL39G}$), or both motifs ($SHIV_{SCVpuYL35,39AG}$) identified the tyrosine-based sorting motif as an essential component for efficient virus release. These analyses also indicate that the dileucine-based sorting motif not only affects intracellular trafficking, but particle release as well. Taken together, these results identify the membrane proximal region and these putative sorting signals as potential targets for anti-virals directed against Vpu.

Finally, we concluded our analysis by determining the contributions of the N-terminus/TMD and cytoplasmic domain of subtype B and subtype C Vpu proteins to the differences observed in SHIV pathogenesis in pig-tailed macaques. Chimeric Vpu proteins in which the N-terminus/TMD regions of the subtype B and subtype C Vpu proteins were

exchanged allowed us to identify the cytoplasmic domain as the determinant for localization. Since both of these proteins down-modulated CD4 surface expression similar to the unmodified Vpu_{SC}EGFP1 protein, our *in vivo* analyses allowed us to address the physiological relevance of the differential efficiencies observed among the subtype B and subtype C Vpu proteins for this function. Since we observed different rates of $CD4^+$ T cell loss in macaques inoculated with SHIV expressing either of these two chimeric proteins, the differences observed in CD4 surface down-modulation *in vitro* are most likely not physiologically relevant. SHIV expressing these two chimeric proteins, replicated in C8166 cells with intermediate kinetics compared to the parental SHIVs ($SHIV_{KU\text{-}1bMC33}$ and $SHIV_{SCVpu}$). However, the SHIV expressing the Vpu protein with the subtype B N-terminus/TMD ($SHIV_{VpuBC}$) replicated at a faster rate than the SHIV expressing the subtype C N-terminus/TMD ($SHIV_{VpuCB}$). When inoculated into pig-tailed macaques $SHIV_{VpuBC}$ resulted in a rapid loss of circulating $CD4^+$ T cells and high viral loads similar to results in macaques inoculated with $SHIV_{KU\text{-}1bMC33}$. Inoculation of three pig-tailed macaques with $SHIV_{VpuCB}$ resulted in a more gradual loss of circulating $CD4^+$ T cells than observed in $SHIV_{VpuBC}$-inoculated macaques, however more rapid than resulted in macaques inoculated with parental $SHIV_{SCVpu}$. These results demonstrate the impact of both domains of the Vpu protein on protein function and pathogenesis.

Epidemiology

Human immunodeficiency virus type 1 (HIV-1) is the causative agent of acquired immune deficiency syndrome (AIDS) (Barre-Sinoussi et al., 1983; Gallo et al., 1984). Following its discovery in 1983, HIV-1 has caused a worldwide pandemic resulting in more than 25 million deaths and the current estimate of 33 million people living with HIV-1 infections (Global

distribution of HIV-1 infections shown in Figure 1; Statistics provided by the Joint United Nations Program on HIV/AIDS (UNAIDS) and the World Health Organization (WHO)). According to the 2008 UNAIDS/WHO report on the global AIDS epidemic, there are approximately 2.7 million new infections and 2 million AIDS-related deaths per year. There is no known cure for HIV-1 infection and while the introduction of highly active anti-retroviral therapy (HAART) has led to a global stabilization of the epidemic, the levels of current and new infections are still alarmingly high. The genetic diversity of HIV-1, increasing rates of acquisition of drug resistance in treated patients and the insufficient availability of affordable treatments remain unaddressed threats posed to the regression of the epidemic and eradication of this virus. Disregard of these issues and many others will inevitably lead to the reestablishment of a growing pandemic and therefore the continued expansion of our understanding of HIV-1 molecular determinants associated with the progression of disease is critical for development of more effective treatments and vaccines.

Classification

Simian and human immunodeficiency viruses (SIV and HIV) are genetically related members of the Lentivirus genus of the Family Retroviridae. In addition to HIV-1, HIV-2 and SIV, the Genus Lentivirus also includes bovine immunodeficiency virus (BIV), feline immunodeficiency virus (FIV), visna, caprine arthritis-encephalitis virus (CAEV) and equine infectious anemia virus (EIAV) (Narayan et al., 1988). Distinct SIVs have been isolated from a multitude of primate species that include African green monkeys (SIV_{AGM}), chimpanzees (SIV_{CPZ}), mandrills (SIV_{MND}), sykes (SIV_{SYK}), and sooty mangabeys (SIV_{SMM}). While these particular isolates cause non- or mildly-pathogenic infections in their primary hosts, several SIVs

Figure 1. Global distribution of HIV-1 infections according to the UNAIDS/WHO 2008 Report on the Global AIDS Epidemic.

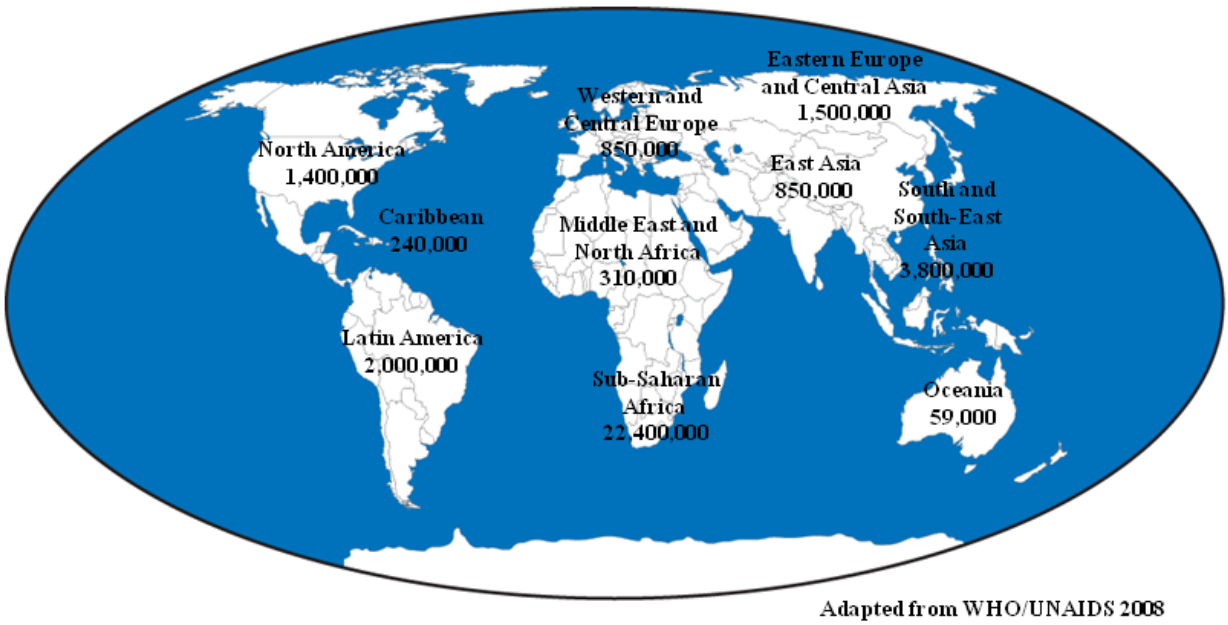

Adapted from WHO/UNAIDS 2008
Report on the Global AIDS Epidemic

have been isolated that cause AIDS-like disease from macaques that are not normally natural hosts. These include viruses isolated from Asian macaque species macaca mulatta (rhesus macaques, SIV_{MAC}) and macaca nemestrina (pig-tailed macaques, SIV_{MNE}). These isolates arose from an initial infection of a rhesus macaque that was being housed with an infected sooty mangabey. The majority of HIV isolates are classified into two groups, HIV-1 and HIV-2. HIV-1 infections are responsible for the AIDS epidemic, while HIV-2 infections are isolated to regions within Western and Central Africa. The origin of these viruses is still under investigation; however, compelling evidence exists for a zoonotic transmission between non-human and human primates. Genomic analysis of HIV-1 revealed a high percent of homology to an SIV isolated from chimpanzees (SIV_{CPZ}), while HIV-2 was more closely related to a strain isolated from sooty mangabeys (SIV_{SMM}) (Clavel et al., 1986; Gao et al., 1999; Reeves and Doms, 2002; Sharp et al., 1995). It is therefore thought that a recombinant virus formed within these two hosts that was biologically fit to transfer and replicate within a human host. Evidence supporting this theory was obtained when a specific isolate YBF30 was identified as a recombinant between HIV-1 and SIV_{CPZ} strains (Gao et al., 1999).

HIV-1 isolates are categorized into three groups, the major (M) group, the outlier (O) group, and the non-M/O (N) group. Group M isolates are responsible for more than 90% of the HIV/AIDS cases worldwide while viruses from groups O and N are primarily found in Cameroon and West Central Africa (Jaffe and Schochetman, 1998; Simon et al., 1998a; Zekeng et al., 1994). Group M contains nine different subtypes (A-D, F-H, J and K) and although this classification was originally based on *env* sequences, it applies to all regions of the genome. Some subtypes can also be further divided into sub-subtypes, including subtypes A, B and F (A1

and A2, B and B', F1 and F2). These group M viruses frequently recombine and these intersubtype recombinants are classified as either circulating recombinant forms (CRF) or unique recombinant forms (URF). Circulating recombinant forms are defined as fully sequenced viruses that have regions of genes from different subtypes within their genomes and identified in at least three epidemiologically unlinked individuals (Liner et al., 2007; Robertson et al., 2000). To date, 19 CRFs have been identified and several have played a significant role in the establishment of certain regional epidemics, including CRF01_AE and CRF02_AG (Casado et al., 2005). Unique recombinant forms have multiple combinations between different subtypes, are only found within specific individuals and are thought to be recombinations of CRFs (Liner et al., 2007; McCutchan, 2006). Finally, HIV-2 is divided into subtypes A, B and C-G (Kandathil et al., 2005). Phylogenetic representation of all HIV isolates is depicted in Figure 2.

Geographic Distribution

The original cross-species transmission of all HIV-1 groups is thought to have occurred in West Central Africa (Gao et al., 1999). Essentially all strains of HIV-1 including all group M subtypes, group N, group O and HIV-2 are found within this region. However, during progression of the epidemic, the stabilization of specific populations with certain subtypes predominating over others has occurred. The regional distributions of each major group subtype according to data collected in the WHO/UNAIDS report titled "Global and regional distribution of HIV-1 genetic subtypes and recombinants in 2004" (Hemelaar et al., 2006) is presented in Figure 2. This data suggests that subtypes A and B are major contributing factors to the growing pandemic accounting for 12% and 10% of worldwide infections, respectively. Subtype A is predominately found in West, Central and East Africa, Eastern Europe and Central Asia.

Figure 2. Phylogenetic representation and globabl/regional distribution of all HIV-1 genetic subtypes and recombinants. Data depicted according to Arien *et al.*, 2007 and Hemelaar *et al.*, 2006.

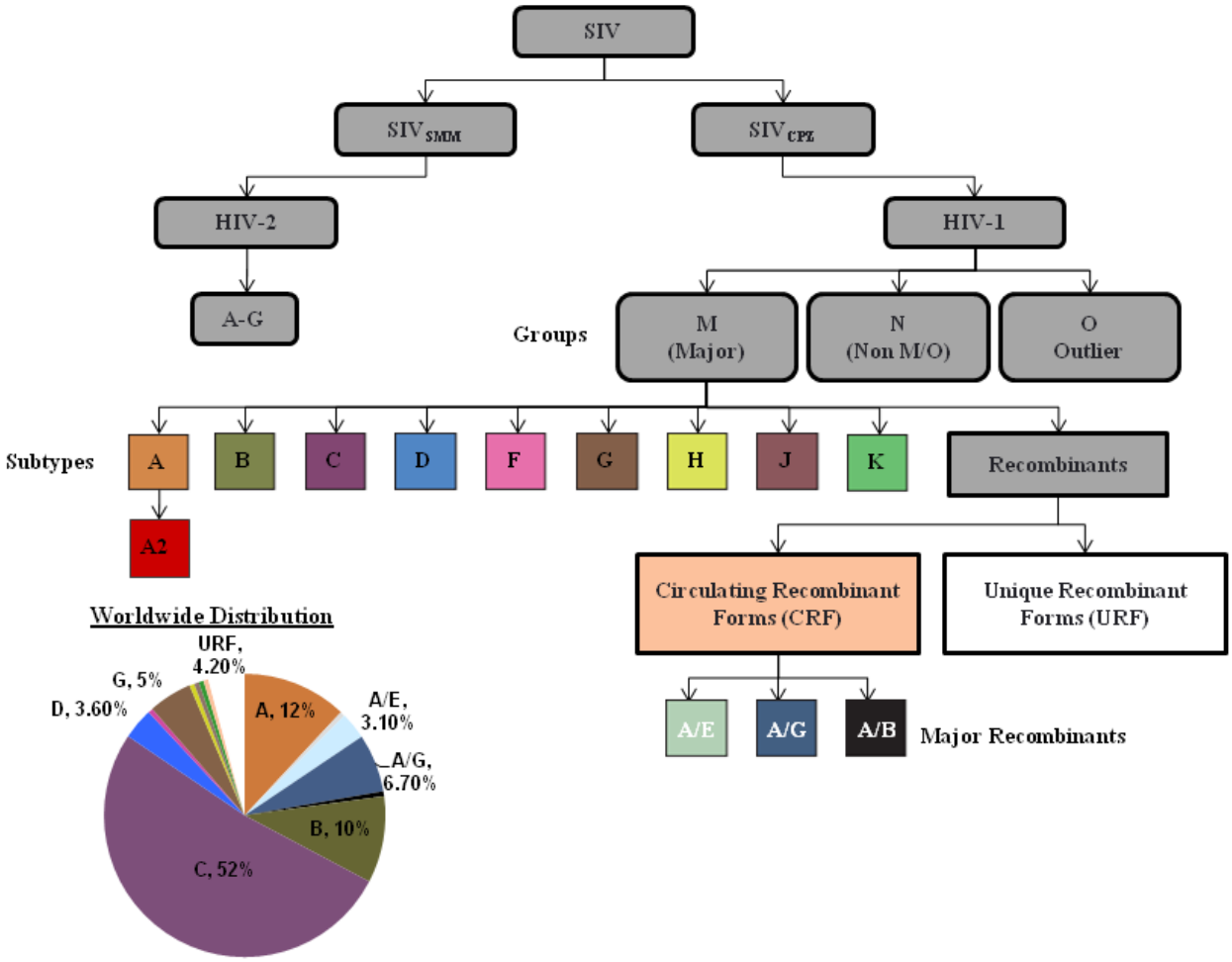

Adapted from Arien, K.K., et al. Nature Reviews Microbiology 5,141:151.Feb. 2007 and Hemelaar et al., 2006

Subtype B is responsible for 98% of HIV-1 infections in the United States and the majority of current HIV research focuses on this particular subtype. Subtype B is also prevalent in the rest of North America, Latin America, Western Europe and East Asia. Subtype C accounts for more than 50% of HIV-1 infections worldwide and is the major contributing factor to the current AIDS epidemic. The majority of subtype C infections are located in southern Africa and India. Subtype D is found mainly within North, East and Central Africa and the middle East. Subtype G infections occur mainly within West and Central Africa. Subtypes F, H, J and K only account for ~0.94% of the total number of infections worldwide. Subtype F infections are predominately found in Latin America and Central Africa while H, J and K are exclusively in Sub-Saharan Africa. The two major CRFs CRF01_AE and CRF02_AG cause infections mainly found within South/South-East Asia and West Africa, respectively. Finally, the remaining CRFs are most prevalent in East Asia, West and East Africa. CRFs account for ~18% of HIV-1 infections globally (Hemelaar et al., 2006).

Genome Structure of Lentiviruses

HIV-1, similar to all replication competent retroviruses, encodes for structural and enzymatic proteins Gag (group-specific antigen), Pol (polymerase) and Env (envelope). HIV-1 also encodes for two regulatory proteins, Tat (transcriptional activator) and Rev (regulator of virion), and 4 auxiliary proteins including the Vif (virion infectivity factor), Vpr, Vpu (viral protein U) and Nef (negative factor) (Frankel and Young, 1998). Unlike HIV-1, HIV-2 and the majority of SIVs do not express a *vpu* gene. Besides HIV-1, only SIVs isolated from chimpanzees (SIV_{CPZ}) and from select monkeys in the genus *Ceropithecus* express a Vpu homologue (Barlow et al., 2003; Cohen et al., 1988; Courgnaud et al., 2002; Dazza et al., 2005;

Huet et al., 1990; Maldarelli et al., 1993; McCormick-Davis et al., 2000b; Strebel et al., 1988). Also of note, is that some strains of SIV and HIV-2 express a *vpx* gene that has been shown to be related to the *vpr* gene. Although *vpx* was originally thought to represent an evolutionarily derived duplication of the *vpr* more recent evidence establishes divergence both in targeted substrates and functional significance (Ayinde et al., 2010; Tristem et al., 1992; Tristem et al., 1990; Tristem et al., 1998). The genomic structures of the members of the Lentivirinae subfamily are shown in Figure 3.

Viral Replication Cycle and Current HIV-1 Therapeutic Targets

HIV-1 infection is initiated by recognition and binding of the envelope glycoprotein, gp120, to the CD4 receptor and a respective co-receptor. CD4 is a 58 kDa monomeric glycoprotein expressed on the surface of ~60% of T-lymphocytes, T-cell precursors within the bone marrow and thymus, monocytes, macrophages, eosinophils, dendritic cells and microglial cells. Binding of gp120 to CD4 induces conformational changes in the V3 loop of gp120 that allow a more efficient interaction with the appropriate co-receptor. While 12 different membrane proteins have been identified as co-receptors for HIV-1, chemokine receptors CCR5 and CXCR4 have been identified as the prinicipal co-receptors for T-cell line tropic (T-tropic) and macrophage tropic (M-tropic) HIV-1 isolates, respectively (Berger et al., 1999; Deng et al., 1996; Deng et al., 1997; Doranz et al., 1996; Dragic et al., 1998; Feng et al., 1996; Liao et al., 1997). Some viruses undergo a transformation in co-receptor recognition from CCR5 to a dual-tropic phenotype (R5/X4) and finally to using the CXCR4 receptor. This adaptation is most likely due to the fact that the virus will encounter macrophages and dendritic cells (CCR5 expressing) initially during infection and T-lymphocytes (CXCR4 expressing) during the later

Figure 3. Schematic representation of several members of the Lentivirinae subfamily including HIV-1, SIV_{CPZ}, HIV-2, SIV_{SMM}, and SIV_{MAC}.

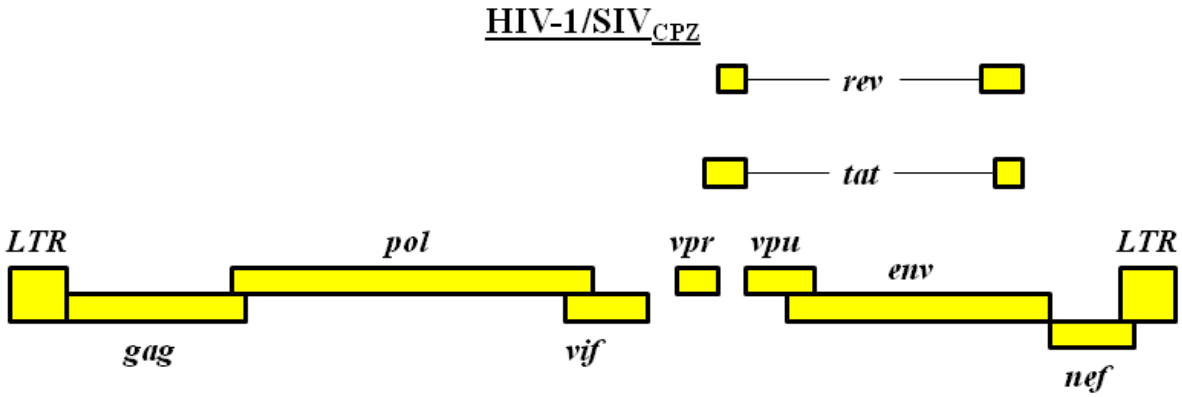
HIV-1/SIV$_{CPZ}$
rev
tat
LTR
pol
vpr
vpu
env
LTR
gag
vif
nef

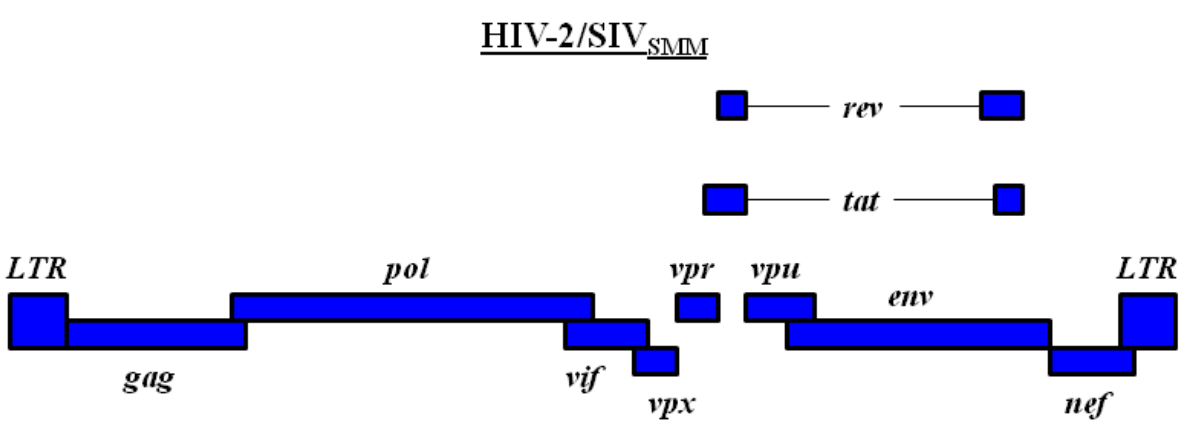
HIV-2/SIV$_{SMM}$
rev
tat
LTR
pol
vpr
vpu
env
LTR
gag
vif
vpx
nef

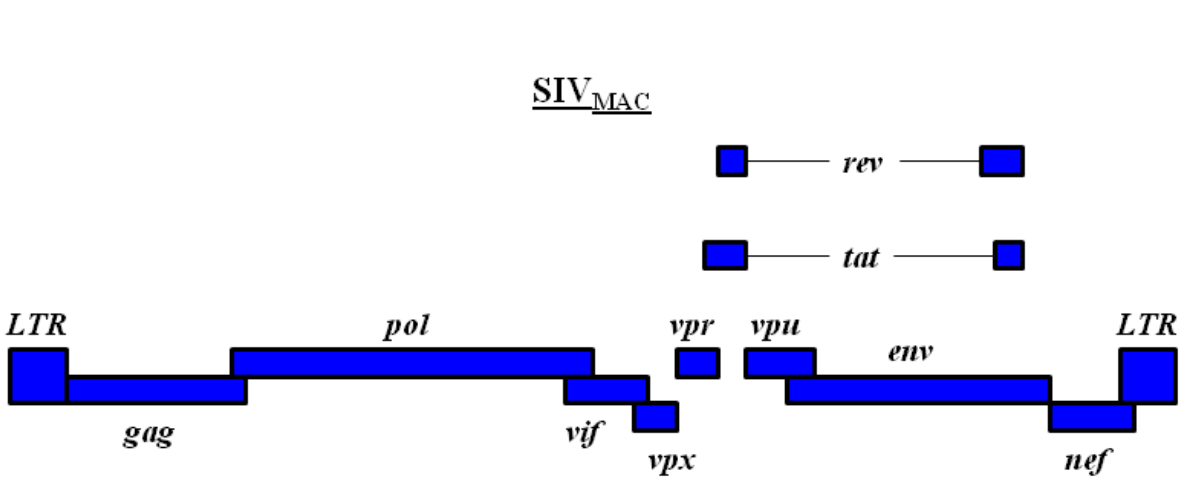
SIV$_{MAC}$
rev
tat
LTR
pol
vpr
vpu
env
LTR
gag
vif
vpx
nef

stages of infection once the virus has spread to the pheripheral lymph nodes (Coffin, 1996; Doms, 2004). Binding of gp120 to the co-receptor again induces a conformational change in gp41 exposing the fusion domain which in turn inserts into the host cell membrane. C-heptad repeat (CHR) peptides interact with N-heptad repeat (NHR) trimers to form a six-helix bundle that bring the viral envelope and target cell membrane into close proximity and eventually form a pore in the membrane (Melikyan et al., 2000; Ryser and Fluckiger, 2005). Currently there are two anti-retrovirals available for inhibiting viral entry: enfuvirtide (T20), an inhibitor of gp41 core formation, and maraviroc, an inhibitor of CCR5 (De Clercq, 2009).

The fusion of the viral and host cell membrane allows for the release of the viral nucleocapsid into the cytoplasm of the host cell. The viral core is then uncoated and the reverse transcriptase (RT) synthesizes a double stranded DNA copy of the viral genome. The uncoating and reverse transcription of the HIV-1 RNA is inhibited in lymphocytes isolated from rhesus macaques and Owl monkeys by a cellular factor known as TRIM5α, however, human TRIM5α does not inhibit HIV-1 replication as efficiently as the rhesus equivalent (Nisole et al., 2005; Towers, 2007). This cellular factor represents a potential restriction factor and studies are currently ongoing to further elucidate its biological significance. The majority of anti-retrovirals currently available target the reverse transcriptase. There are 11 reverse transcriptase inhibitors approved for clinical use in the treatment of HIV-1: seven nucleoside reverse transcriptase inhibitors (NRTIs): zidovudine, didanosine, stavudine, lamivudine, abacavir and emtricitabine; one nucleotide reverse transcriptase inhibitor (NtRTI): tenofovir; and four non-nucleoside reverse transcriptase inhibitors (NNRTIs): nevirapine, delavirdine, efavirenz and etravirine (De Clercq, 2009).

Following reverse transcription, a preintegration complex (PIC) is formed to facilitate viral DNA integration into the host chromosome. The PIC complex is around 56nm in diameter and consists of reverse transcribed viral genomic DNA, viral integrase (IN), viral protein R (Vpr), matrix protein (MA), and cellular factors that assist in translocation of the complex to the nucleus (Fouchier and Malim, 1999; Sherman et al., 2002; Sherman and Greene, 2002). The nuclear pore complex (NPC) forms an aqueous channel and when active transport occurs between the cytoplasm and nucleoplasm, macromolecules up to 25 nm in diameter are allowed to pass bidirectionally through the pore. Translocation into the nucleus is regulated by a class of proteins known as importins and exportins. Classical and non-classical nuclear import signals have been identified in the IN, MA and Vpr proteins (Bouyac-Bertoia et al., 2001; Bukrinsky et al., 1993; Jenkins et al., 1998). The exact mechanism and roles for all PIC-associated proteins in nuclear translocation and passage through the NPC are still unknown, however, at present the IN is thought to play the primary role in nuclear import with the remaining proteins providing support for the docking and transport processes (Sherman et al., 2002; Sherman and Greene, 2002). Once in the nucleoplasm, the integrase cleaves the viral and host DNA and ligates the linear viral DNA into the host genome through a reaction known as strand transfer. The IN protein binds a short sequence in the LTR and removes a dinucleotide adjacent from the highly conserved CA dinucleotide in the 3' strand of the U3 and U5 LTR domains. While there is no consensus site for host DNA integration, several lines of evidence support a non-random integration with preferential integration in transcription units for HIV-1 using symmetrical sequences (Grandgenett, 2005; Holman and Coffin, 2005; Marshall et al., 2007; Wu et al., 2005). Host cellular repair enzymes fill in the gaps between the integrated viral DNA and the host chromosomal DNA left by the integrase-mediated cleavage (Van Maele and Debyser, 2005).

Currently only one integrase inhibitor, raltegravir, is approved for clinical use and targets the strand transfer reaction rather than the 3' DNA processing event (De Clercq, 2009).

Initial transcription of the viral genome is regulated by the host cell RNA polymerase II and the basal levels of transcription are relatively low. Long terminal repeat (LTR) regions flank the viral DNA and the 3'LTR contains three distinct regions, the unique 3' end (U3), the repeated domain (R), and the unique 5' end (U5). The U3 domain allows for direct binding of the RNA polymerase II and contains several elements that promote transcription. These elements include a TATA box to which the transcription factor IID binds, three Sp1 sites, two NF-κB sites, and a "modulatory region" with binding sites for transcription factors: LEF, Ets and USF (Freed, 2001; Ross et al., 1991). The early mRNA products are doubly spliced and encode the regulatory proteins, Tat and Rev, and the accessory protein, Nef. The production of the Tat protein increases viral mRNA transcription levels by two logs and is essential for a productive infection (Dayton et al., 1986; Fisher et al., 1986). The accumulation of these early proteins promotes the transcription of the late mRNA products which encode for the structural and enzymatic components of the virion (Gag, Pol, Env) as well as the non-structural accessory proteins that facilitate viral replication and assembly, promote genomic stability and enhance virion release (Vif, Vpr, Vpu). The envelope glycoprotein precursor, gp160, is synthesized on the endoplasmic reticulum (ER) and is processed in the Golgi apparatus where it is cleaved by the host cellular protease furin, resulting in the surface glycoprotein gp120 and the transmembrane/fusion glycoprotein gp41. The structural and non-structural polyprotein precursors, the gp120/gp41 envelope complex, and two full-length copies of viral RNA are transported to the plasma membrane for assembly into virion particles (Briggs et al., 2003;

Zimmerman et al., 2002). There are currently no available anti-retrovirals targeted towards the transcriptional elements involved in HIV-1 replication.

The Gag polyprotein precursor $Pr55^{Gag}$ is essential for particle assembly as it contains the components necessary for targeting and binding the plasma membrane, promoting interactions between the virion structural components, encapsidating the viral RNA genome copies, associating with the Env glycoproteins and stimulating particle budding. $Pr55^{Gag}$ uses the cellular Endosomal Sorting Complex Required for Transport I (ESCRT-1), specifically the TSG101 and ALIX proteins, for targeting to the cellular surface and for release from the cell (Martin-Serrano et al., 2003; Stuchell et al., 2004; von Schwedler et al., 2003). The HIV-1 Gag p6 protein recruits Tsg101 and ALIX with PTAP and YPLTSL late assembly domains, respectively (Bieniasz, 2006; McDonald and Martin-Serrano, 2009; Morita and Sundquist, 2004). ALIX directly activates ESCRT-III by recruiting and activating the Snf7 subunit (McCullough et al., 2008). ESCRT-III is directly involved in the scission of the membrane neck that connects the virion to the plasma membrane. Once all of the viral particle components have been recruited to the site of assembly the immature virion buds from the plasma membrane with the host cell lipid bilayer as its outer envelope (Freed, 2002; Ono and Freed, 2001). Previously, HIV-1 assembly in T-cells was thought to occur at the plasma membrane while assembly in macrophages occurred within multi-vesicular bodies (MVB) or late endosomes (LE). However, this notion has recently come into question with increasing evidence that assembly may occur within large invaginations of the plasma membrane in macrophages that resemble MVB/LE. While more studies are necessary to fully elucidate the site of assembly in macrophages, HIV-1 assembly occurs exclusively at the plasma membrane in T-cells (Gelderblom, 1991; Ono, 2009; Orenstein et al., 1988).

The HIV-1 envelope is known to be enriched in cholesterol and both the Gag and Env proteins have been isolated in detergent resistant membrane (DRM) fractions (Aloia et al., 1993; Brugger et al., 2006; Nguyen and Hildreth, 2000). These investigators found that glycophosphatidylinositol (GPI)-anchored proteins such as Thy1, CD59, and GM-1 ganglioside were present in DRMs but that a non-raft protein, CD45, was largely absent from viral particles. It was subsequently shown that membrane rafts were critical for virus assembly and release (Ono and Freed, 2001). These investigators found that the myristylated N-terminal domain of Gag and the I domain of the NC protein were critical for raft association and that the cholesterol depleting compound, methyl-β-cyclodextrin (M-β-CD), reduced the efficiency of virus release. The palmitoylation of the gp41 envelope glycoprotein was initially shown to be important for raft targeting and infectivity but later studies showed that substitution of the cysteines at positions 764 and 837 in the cytoplasmic domain of gp41 (thus resulting in no palmitoylation) only partially affected infectivity or had no effect (Bhattacharya et al., 2004; Chan et al., 2005; Rousso et al., 2000). It was later shown that mutations in the Gag p17 protein would prevent Env incorporation into rafts and virions, suggesting that Gag regulates Env incorporation into rafts (Bhattacharya et al., 2006; Patil et al., 2010). Other investigators have shown that the HIV-1 Env has a **c**holesterol **r**ecognition/interaction **a**mino acid **c**onsensus (CRAC) domain that is responsible for raft association (Epand et al., 2006; Vishwanathan et al., 2008). There are currently no anti-retrovirals targeting virion assembly and egress approved for clinical use in HIV-1 treatment.

Once the immature virion is released from the cell the viral protease (PR) is spontaneously activated and cleaves the $Pr55^{Gag}$ and Pol polyprotein precursor ($Pr160^{Gag\text{-}Pol}$) to yield the mature Gag and Pol proteins. The virion undergoes a morphological change resulting

in a spherical particle with a visibly dense conical core containing the RNA genome copies (Ganser et al., 1999; Yeager et al., 1998). Currently, there are ten protease inhibitors (PI) approved for use in HIV-1 treatment: saquinavir, ritonavir, indinavir, nelfinavir, amprenavir, lopinavir/ritonavir, atazanavir, fosamprenavir, tipranavir and darunavir. These compounds are all designed to occupy the active site of the HIV-1 PR therefore preventing cleavage of the polyprotein precursors and in turn virion maturation (De Clercq, 2009).

An overview of the replication cycle of HIV-1 and the stages of viral infection that therapeutics are currently available is depicted in Figure 4.

Viral Proteins

While Gag is the only protein required for formation and release of virion-like particles the remaining proteins contribute to the regulation of HIV-1 replication as well as evasion of the host immune system by promoting optimal conditions intra- and extra-cellularly. A representation of a mature HIV-1 virion is depicted in Figure 5.

Gag

The *gag* gene of HIV-1 encodes for a polyprotein precursor Pr55 that is cleaved upon maturation of a virion into the proteins matrix (MA or p17), capsid (CA or p24), nucleocapsid (NC or p7) and p6. Cleavage by the protease protein (PR) also results in two spacer proteins p1 and p2. The MA protein is found at the N-terminal region of the Gag polyprotein and is 131 residues in length. It contains the M domain where a myristic acid moiety is attached to the penultimate glycine residue allowing for insertion into the host lipid bilayer and a cluster of basic residues which are thought to serve as an interface for head groups of acidic phospholipids

Figure 4. An overview of the replication cycle of HIV-1. Stages of viral infection that therapeutics are currently available for are labeled by number.

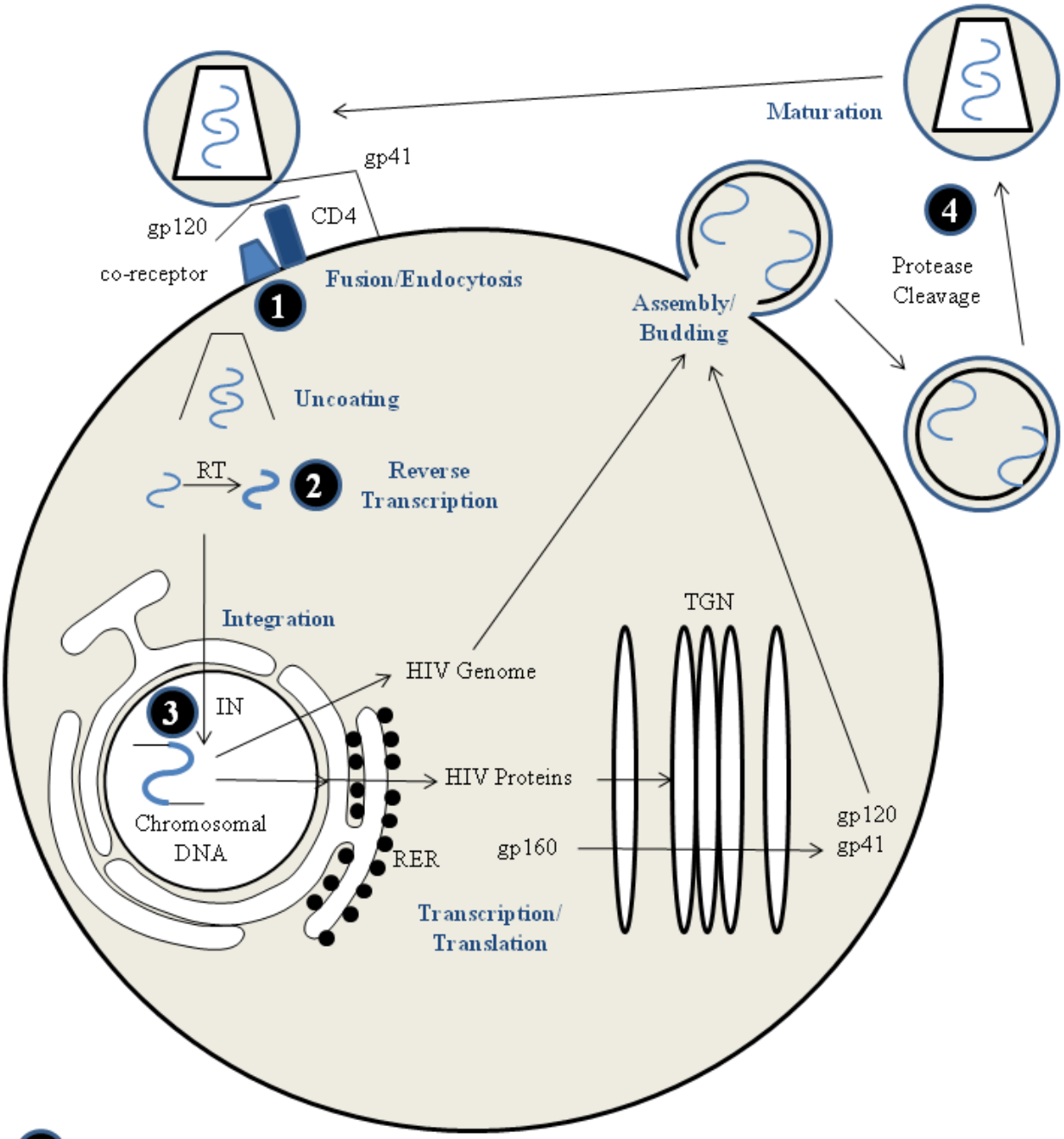

1 Fusion Inhibitors

2 RT Inhibitors

3 Integrase Inhibitors

4 Protease Inhibitors

Figure 5. Diagram of a mature HIV-1 virion.

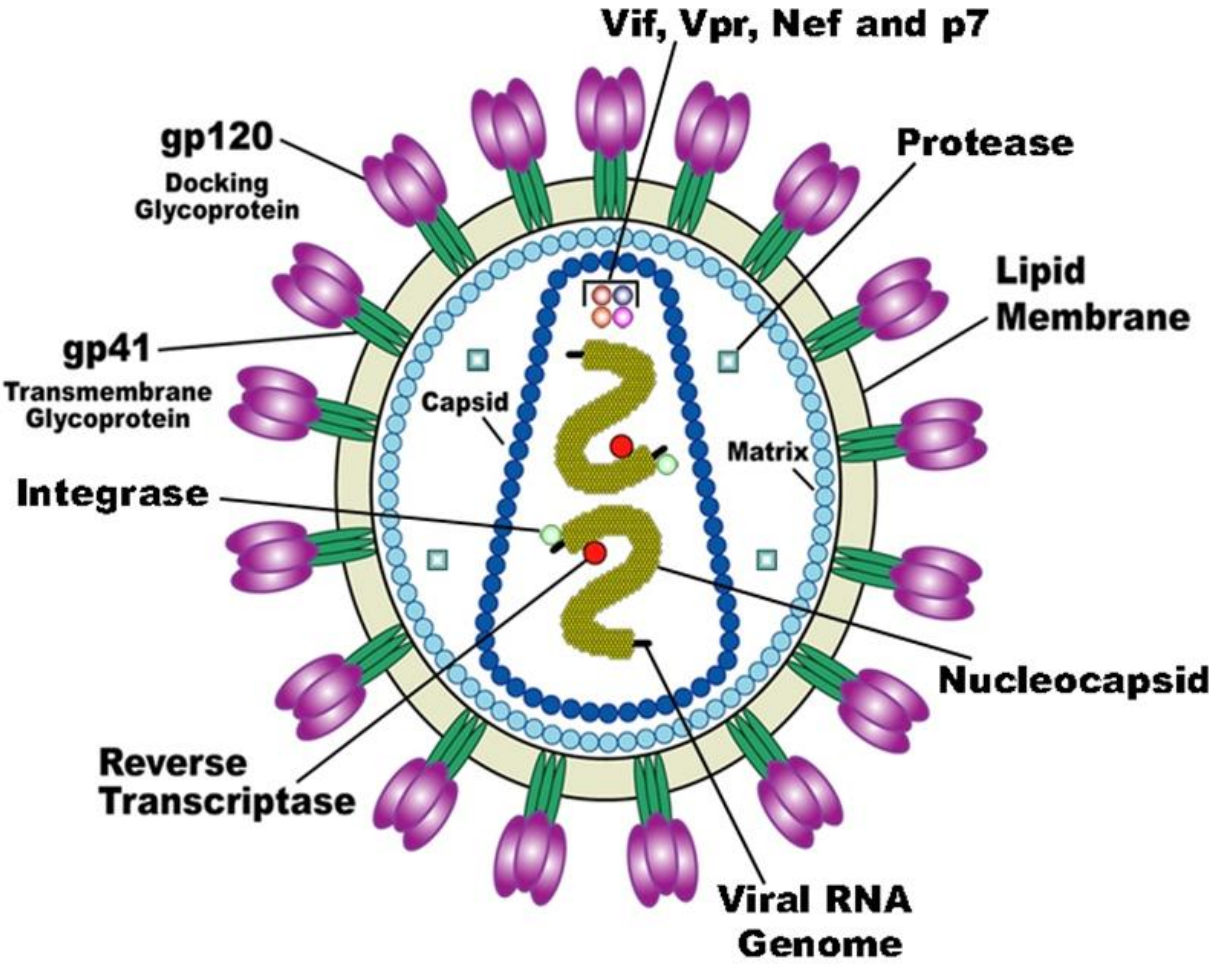

Credit: NIAID; Carl Henderson

stabilizing the interaction with the negatively charged phosphate backbone of the host membrane. One particular acidic phospholipid that is known to specifically localize to the cytoplasmic leaflet of the plasma membrane (PM), $PI(4,5)P_2$, binds specifically to the basic patch in the MA. This interaction is required for assembly and is most likely responsible for the direct targeting of Gag to membrane rafts (Chukkapalli et al., 2008; Ono et al., 2004; Saad et al., 2006). The myristoylation site is generally sequestered and the ability for Gag to insert this moiety into the host cell membrane is regulated by the CA protein. CA folds into two distinct domains: the N-terminal core and the C-terminal dimerization domain (Ono, 2009). CA multimerization causes a conformational change in the Gag protein that unmasks the myristate moiety and allows for strong binding of the precursor protein to the membrane (Saad et al., 2006). The CA protein has also been shown to incorporate cyclophilin A (CypA) for optimal infectivity of HIV-1 particles (Braaten et al., 1996; Franke et al., 1994; Luban et al., 1993; Thali et al., 1994). The incorporation of CypA into the capsid appears to stabilize the structure and may explain why the human TRIM5α protein is not as efficient at preventing "uncoating" as its rhesus counterpart (Sayah and Luban, 2004; Towers et al., 2003). The NC region of the Gag polyprotein functions to encapsidate viral genomic RNA for efficient packaging into the viral particle. The packaging signal (Ψ site) locating in the viral RNA 5' to the *gag* initiation codon is composed of four stem loop structures that allow for binding to the NC protein. NC contains two zinc finger motifs (CCHC type) each flanked by basic sequences that directly bind and stabilize the interaction with the viral RNA (Ono, 2009). Finally, the p6 region of the Gag polyprotein contains the Late (L) domain and the PTAP motif that allow for recruitment of the host ESCRT-associated complexes TSG101 and ALIX that facilitate virus particle budding from the cellular surface (Bieniasz, 2006; Gottlinger et al., 1991; Huang et al., 1995; Ono and Freed, 2004; Rudner et al., 2005).

Pol

The Pol protein is also synthesized as a precursor polyprotein in conjunction with the Gag protein, known as $Pr160^{Gag\text{-}Pol}$. The synthesis of this protein occurs following a frame-shift event during transcription and occurs at 5-10% the levels of the $Pr55^{Gag}$. This large polyprotein precursor is cleaved during maturation to yield the *pol* encoded enzymes protease (PR), reverse transcriptase (RT), and integrase (IN). A wealth of information on the reverse transcriptase is available including the three dimensional structure, mapping of resistance mutations, and its role in the virus replication cycle, however, it is beyond the scope of this dissertation and the central hypothesis, therefore it will not be discussed in great detail. The relevant aspects of these enzymes in the HIV-1 lifecycle has been discussed in the overview of viral replication.

Vif

Vif is a 192 amino acid protein and a potent regulator of HIV-1 infection (Fisher et al., 1987; Gallo et al., 1988; Strebel et al., 1987). Vif is critical for virus replication in cells termed "non-permissive" and dispensible in "permissive cells" (Gabuzda et al., 1992; von Schwedler et al., 1993). In permissive cells, the Vif protein is incorporated into virions and therefore serves as a structural protein. In non-permissive cells, Vif-deficient viruses complete entry and initiate reverse transcription but have reduced or incomplete synthesis of proviral DNA following challenge of target cells (i.e. inhibition occurs during the second round of replication) (Courcoul et al., 1995; Simon and Malim, 1996; Sova and Volsky, 1993; von Schwedler et al., 1993). The ability of Vif to impact infectivity is species-specific and the fusion of "permissive" and "non-permissive" cells yields a non-permissive phenotype (Madani and Kabat, 1998; Simon et al.,

1998b; Simon et al., 1998c). Building from these discoveries, CEM15 was identified as a dominant cellular restriction factor of Vif-deficient HIV-1(Sheehy et al., 2002).

CEM15 was found to be a member of the human apolipoprotein B mRNA editing enzyme catalytic polypeptide-like 3 family of proteins (APOBEC3) and specifically APOBEC3G. This family includes 7 members: APOBEC3A, APOBEC3B, APOBEC3C, APOBEC3D, APOBEC3E, APOBEC3F, APOBEC3G, and APOBEC3H (Chiu and Greene, 2008; Conticello et al., 2005; Jarmuz et al., 2002; Malim, 2009; OhAinle et al., 2006). These proteins are cytidine deaminases and each protein contains either one or two cytidine deaminase domains. Following the identification of APOBEC3G as an HIV-1 restriction factor, multiple investigators have examined the anti-HIV-1 properties of the other APOBEC3 proteins. The RNA editing activity of the APOBEC3 family of proteins (A3A-H) involves an active site characterized by a conserved zinc-binding motif (Cys/His-Xaa-Glu-Xaa_{23-28}-Pro-Cys-Xaa_{2-4}-Cys) (Jarmuz et al., 2002). Human A3B, A3DE, A3F and A3G all exhibit the ability to inhibit replication of Vif-deficient HIV-1 isolates, while A3A, A3C and A3H are inactive or weakly restrict HIV-1Δ*vif* (Bishop et al., 2004; Conticello et al., 2005; Dang et al., 2008; Dang et al., 2006; Doehle et al., 2005; Jarmuz et al., 2002; Liddament et al., 2004; OhAinle et al., 2006; Wiegand et al., 2004; Yang et al., 2007; Zennou and Bieniasz, 2006; Zheng et al., 2004). The actively restricting A3 proteins interact with HIV-1 viral genomic RNA and the $Pr55^{Gag}$ or $Pr160^{Gag\text{-}Pol}$ and are incorporated into budding virions. Following infection of a target cell the A3 protein interact with the RT complex as well as the viral RNA being reverse transcribed(Bogerd and Cullen, 2008; Burnett and Spearman, 2007; Khan et al., 2005; Luo et al., 2004; Luo et al., 2007; Navarro et al., 2005; Schafer et al., 2004; Svarovskaia et al., 2004; Zennou et al., 2004). During reverse transcription, the A3 protein induces deamination of

cytidines to uridines leading to an accumulation of G-to-A transitions in the newly synthesized plus strand viral DNA (Chiu and Greene, 2008; Harris et al., 2003; Malim, 2009; Mangeat et al., 2003; Mariani et al., 2003; Yu et al., 2004). More recent studies have also revealed deaminase-independent restriction functions of hA3G and considerable efforts are being made to elucidate the precise mechanisms of restriction by the APOBEC3 proteins (Chiu and Greene, 2008; Malim, 2009; Navarro et al., 2005; Newman et al., 2005).

HIV-1 has evolved to counteract the functions of these cellular restriction factors by encoding the Vif protein. Vif binds to the A3G protein as well as the Cullin5, Elongin B/C-rbx1/E3 ubiquitin ligase and induces the polyubiquitination of the A3G protein and possibly Vif itself, which subsequently leads to the proteasomal degradation of both proteins (Conticello et al., 2005; Kewalramani and Emerman, 1996; Kobayashi et al., 2005; Marin et al., 2003; Mehle et al., 2004a; Mehle et al., 2004b; Sheehy et al., 2003; Yu et al., 2003). This diminishes the cytosolic levels of A3G proteins available for virion incorporation which allows for optimal virion infectivity.

Vpx/Vpr

Vpr is a 96 amino acid virion incorporated protein expressed in both the HIV-1 and HIV-2 lineages. Vpx is a 112 amino acid virion incorporated protein whose expression is specific to the HIV-2 and SIV_{SMM} lineages. Both proteins are incorporated into budding virions through association with a dileucine motif (LXXLF) found within the p6 domain of the $Pr55^{Gag}$ precursor protein (Accola et al., 1999; Bachand et al., 1999; Cohen et al., 1990; Kewalramani and Emerman, 1996; Kondo and Gottlinger, 1996; Paxton et al., 1993; Wu et al., 1994). This

incorporation suggested that these proteins most likely play an important role in the early stages of the viral life cycle.

The Vpr protein was originally thought to be specifically dedicated to the progressive infection of macrophages, however, more recent studies have brought into question the biological significance of this protein. A variety of functions have been attributed to the HIV-1 Vpr protein including modulation of transcription (Sawaya et al., 2000), induction of apoptosis, disruption of cell cycle regulation (Chang et al., 2004), nuclear transport of the PIC (Vodicka et al., 1998), facilitation of reverse transcription (Rogel et al., 1995), suppression of immune activation (Ramanathan et al., 2002), and reduction of the mutation rate of the HIV-1 genome (Jowett et al., 1999). Vpr is able to interact with or effect a considerable number of cellular proteins including proteins involved in anti-inflammatory and immunosuppressive responses (including the glucocorticoid receptor), proteins associated with apoptotic regulation pathways (including the permeability transition pore complex), protein associated with nuclear translocation (including importin-α and several nucleoporins), and ubiquitin ligase associated proteins (Cullin 4A and DCAF-1) (Belzile et al., 2007; DeHart et al., 2007; He et al., 1995; Hrecka et al., 2007; Jacotot et al., 2001; Le Rouzic et al., 2007; Le Rouzic and Benichou, 2005; Schrofelbauer et al., 2007; Schrofelbauer et al., 2005; Tan et al., 2007; Varin et al., 2005; Vodicka et al., 1998; Wen et al., 2007; Yedavalli et al., 2005; Zeitler and Weis, 2004). While the potential of Vpr functions in HIV-1 infection is extensive, *in vitro* studies have defined the facilitation of the PIC nuclear translocation and the disruption of cell cycle regulation as the two main functions of Vpr.

Vpr contains a non-classical nuclear localization signal and interacts with proteins associated with the HIV-1 PIC as well as proteins associated with the nuclear pore complex,

including the nucleoporin human CG1, in order to facilitate docking of the PIC to the nuclear envelope (Heinzinger et al., 1994; Jenkins et al., 1998; Le Rouzic and Benichou, 2005; Vodicka et al., 1998; Zeitler and Weis, 2004). Vpr is also thought to induce herniations in the nuclear envelope that may contribute to the nuclear import of the PIC as well as the induction of G2 arrest (de Noronha et al., 2001; Le Rouzic et al., 2002).

The biological significance of the induction of G2 arrest by Vpr is controversial since Vpr was not found to be required for efficient replication in dividing cells such as cell lines and primary $CD4^+$ T cells and since macrophages do not divide and thus cell cycle regulation is irrelevant. However, while the mechanisms and significance associated with the induction of G2 arrest by Vpr remains elusive, research in recent years has provided a consensus among researchers of the proteins involved in this function. Vpr interacts with DCAF-1 using it as an adaptor to engage damaged DNA binding protein 1 (DDB1), which is a component of the Cul4A ubiquitin ligase. Vpr also recruits a yet unidentified protein that is required for entry of the cell into mitosis and uses the Cul4A ubiquitin ligase to target this unknown protein for ubiquitination and subsequent proteasomal degradation (Ayinde et al., 2010). The identification of this unknown protein is essential for understanding the biological significance of Vpr in HIV-1 function since the induction of G2 arrest may simply be a by-product of the elimination of this protein and not the direct function of Vpr. Since several HIV-1 accessory proteins have evolved to overcome host restriction factors, it is possible that Vpr evolved in a similar response. It's possible this unknown protein represents another host restriction factor that can be utilized for the development of novel anti-retrovirals.

I*n vitro* studies have ascribed several functions of Vpr to be required for HIV-1 infection, however, *in vivo* analysis of *vpr* deleted viruses questions their validity and significance. These

viruses have been shown to replicate and cause disease similar to wild-type (wt) viruses in rhesus macaques (Gibbs et al., 1995; Hoch et al., 1995; Kim et al., 2005). Further investigation is required to determine the importance of Vpr either for pathogenicity or evolutionary aspects of HIV-1 since it is clear that the *vpr* gene provides some selective advantage to the virus (Gibbs et al., 1995; Lang et al., 1993).

In contrast to *vpr* deleted viruses, vpx deficient SIV display marked attenuation for growth in macrophages. Pig-tailed macaques inoculated with *vpx* deficient viruses displayed delayed kinetics of viral replication and no disease manifestions (Hirsch et al., 1998). Rhesus macaques inoculated with similar viruses did progress to an AIDS-related death although the onset of pathogenesis was delayed and virus burdens were significantly lower than macaques inoculated with the parental virus (Gibbs et al., 1995). Also, contrary to previous hypotheses, Vpx does not simply mimic the functions of Vpr, and has been shown to be critical for infection of non-dividing macrophages, monocytes and monocyte-derived dendritic cells (Gibbs et al., 1994; Goujon et al., 2008; Goujon et al., 2007; Kawamura et al., 1994; Mahalingam et al., 2001; Ueno et al., 2003; Wolfrum et al., 2007; Yu et al., 1991). However, Vpx does interact with DCAF-1 and subsequently the DDB1-Cul4A ubiquitin ligase similar to Vpr (Bergamaschi et al., 2009; Le Rouzic et al., 2007; Sharova et al., 2008; Srivastava et al., 2008). This interaction allows Vpx to counteract a macrophage-specific restriction factor most likely by utilizing the Cul4A-DDB1^{DCAF1} complex for its degradation (Ayinde et al., 2010). The antagonism of this restriction factor promotes accumulation of HIV-2 and SIV reverse transcripts although the mechanism of restriction and how Vpx counteracts this restriction factor(s) remains to be determined.

Tat/Rev

Tat is an early transcription transactivation regulatory protein that has a variable length of 86-104 amino acids and contains two functional domains. The first domain is an activation domain that mediates interactions with host cellular machinery and the second is an arginine-rich region that is required for binding to the transactivation responsive element RNA (TAR) (Hwang et al., 2003). Post-integration of the HIV-1 genome into the host chromosome, elements including NF-κB, p50, and human deacetylase 1 (HDAC1) bind to the latent HIV-1 LTR and cause histone deacetylation and repressive changes in the chromatin structure of the LTR that causes RNA Polymerase II to initiate synthesis of short mRNAs and the virus remains latent (Pagans et al., 2005; Williams et al., 2006). During a period of stimulation (e.g. TNF-α), these complexes are removed and Tat recruits several chromatin and histone modifying complexes including the histone acetyltransferase CREB-binding protein (CBP)/p300 complex. These histone acetyltransferases (HATS) acetylate the nucleosomes on the HIV-1 promotor. Tat binds to a stem loop structure (TAR) and interacts with the P-TEFb complex, which phosphorylates/activates the RNA polymerase II. This allows the RNA polymerase II to synthesize full length HIV-1 transcripts (Garber et al., 1998; Kim et al., 2002; Williams et al., 2006).

The Tat protein also promotes transcription of the viral genome by inducing the phosphorylation of additional transcription factors including Sp1, the alpha subunit of eukaryotic initiation factor 2 (eIF2α), and NF-κB (Demarchi et al., 1999; Li et al., 2005a; Li et al., 2005b; Rossi et al., 2006; Zauli et al., 2001). The activation of these proteins induces binding to their respective sites within the LTR and subsequent facilitation of viral genome transcription.

The regulatory properties of Tat extend to the modulation of cellular gene expression as well as the induction and inhibition of apoptosis (Li et al., 2005a; Li et al., 2005b; Romani et al., 2010; Stettner et al., 2009). This ability is not limited to the infected cell as Tat is efficiently released extracellularly and can enter uninfected cells and induce transcriptional regulation (Ju et al., 2009). This property could provide an explanation for the neurodegenerative effects of HIV-1 since Tat can transverse an in-tact blood brain barrier and enter cells such as neurons and cause apoptosis (Campbell et al., 2004b; Cheng et al., 1998; de Mareuil et al., 2005; Giacca, 2005; Giunta et al., 2009; Haughey and Mattson, 2002; Vendeville et al., 2004; Wallace et al., 2006).

Transcription from the LTR leads to the generation of three major types of viral RNA transcripts: 1) full length unspliced transcripts that give rise to the $Pr55^{Gag}$ and $Pr160^{GagPol}$ precursors and the full length HIV-1 genomes packaged into virions; 2) singly spliced mRNAs which encode the Vif, Vpr, Vpu and Env proteins; and 3) doubly spliced mRNAs that give rise to the Rev, Tat and Nef proteins. Mammalian cells are restrictive to the nuclear export of unspliced or partially spliced mRNAs and HIV-1 encodes the Rev protein to overcome this barrier. Rev is a 116 amino acid protein that contains two functional domains: 1) an arginine-rich domain required for RNA binding; and 2) a leucine-rich region that acts as a nuclear export signal (Cullen, 1998). During the initial stages of infection, full length transcripts are synthesized and the multiply spliced gene products are translated in the cytoplasm (Tat, Rev, and Nef). Tat and Rev are then transported back into the nucleus via their nuclear localization signals to facilitate viral transcription. When sufficient levels of Rev are produced, nuclear export of unspliced and partially splice transcripts is initiated and translation of the Gag, Pol, Vif, Vpr, Vpu, and Env proteins takes place (Freed, 2001; Hope, 1999; Seelamgari et al., 2004).

Rev binds to a highly structured RNA element located in the *env* gene and therefore present within all unspliced or partially spliced viral transcripts, known as the Rev response element (RRE). The RRE folds into a series of five stem-loop structures and a Rev monomer initially binds to stem-loop 2 and then multimerizes with additional Rev molecules. This complex then binds to the nuclear export protein Exportin 1 as well as the Ran-GTP nuclear protein and allows for efficient export of all viral transcripts from the nucleus. Once the protein has been successfully transported across the nuclear membrane into the cytoplasm, Rev dissociates from the complex by converting Ran-GTP to Ran-GDP and is then shuttled back into the nucleus (Freed, 2001; Hope, 1999).

Vpu

The Vpu protein is a small transmembrane protein encoded by HIV-1 but not by HIV-2 (Cohen et al., 1988; Strebel et al., 1988). Structural homologues have been detected in SIV from chimpanzees (SIV_{cpz}), the mona monkey (*Cercopithecus mona*; SIV_{mon}), the greater spot-nosed monkey (*Cercopithecus nictitans*; SIV_{gsn}), mustached monkeys (*Cercopithecus cephus*; SIV_{mus}), more recently Dent's mona monkey (*Cercopithecus mona denti*; SIV_{den}) and gorillas (*Gorilla gorilla;* SIV_{gor}) (Barlow et al., 2003; Courgnaud et al., 2002; Dazza et al., 2005; Van Heuverswyn et al., 2006). Sequence analysis has shown that the *vpu* from SIV_{cpz} is most closely related to the *vpu* from HIV-1 both in amino acid sequence and CD4 down-modulation function (Gomez et al., 2005; McCormick-Davis et al., 2000b). While one of the smallest of the HIV-1 proteins, it has two important functions within virus-infected cells, which will be discussed in detail in a later section. The first of these functions is the down-regulation of the CD4 receptor to prevent its interaction with the HIV-1 envelope glycoprotein. Vpu interacts with the CD4

receptor in the rough endoplasmic reticulum (RER), resulting in its re-translocation across the RER and subsequent degradation via the proteasomal pathway (Schubert et al., 1998; Schubert et al., 1996a; Vincent et al., 1993; Willey et al., 1992a). The second major function of the Vpu protein is to facilitate release of virus from infected cells. Previous studies have shown that virus release is cell type specific, suggesting that certain cells may express a restriction factor that inhibits virus release in the absence of Vpu. Recently, bone marrow stromal antigen 2 (BST-2/HM1.24/CD317/tetherin) has been identified as this factor (Neil et al., 2008; Van Damme et al., 2008).

The Vpu protein is 77-86 amino acids in length and is comprised of a short N-terminal region, a transmembrane domain (TMD), and a longer cytoplasmic domain (CD) (Figure 6). Vpu is translated on the rough endoplasmic reticulum (RER) with the TMD also serving as an uncleaved leader sequence. The signal sequence is bound by the signal recognition particle (SRP) which subsequently binds to the SRP receptor on the RER. The nascent Vpu protein is inserted into the RER membrane and synthesis of the remainder of the protein is completed. The CD of Vpu has two predicted α-helical domains separated by a hinge region characterized by two canonical casein kinase II sites (S/T-X-X-E/D) (Maldarelli et al., 1993; Schubert et al., 1992). The most variable regions of the protein are the N-terminal region (including parts of the transmembrane domain) and the far C-terminal region of the protein (McCormick-Davis et al., 2000b). However, there are several highly conserved amino acids and domains among most *vpu* species. The most highly conserved region is the hinge region, which reflects its importance in Vpu function and will be discussed later. There are several invariant amino acids found in the

Figure 6. Schematic diagram of the membrane orientation of the consensus subtype B Vpu protein (strain HXB2 with a correct methionine at the N-terminus). The amino acids within the hexagons represent amino acids that were found to be invariant among all *vpu* subtypes (Chen *et al.*, 1993).

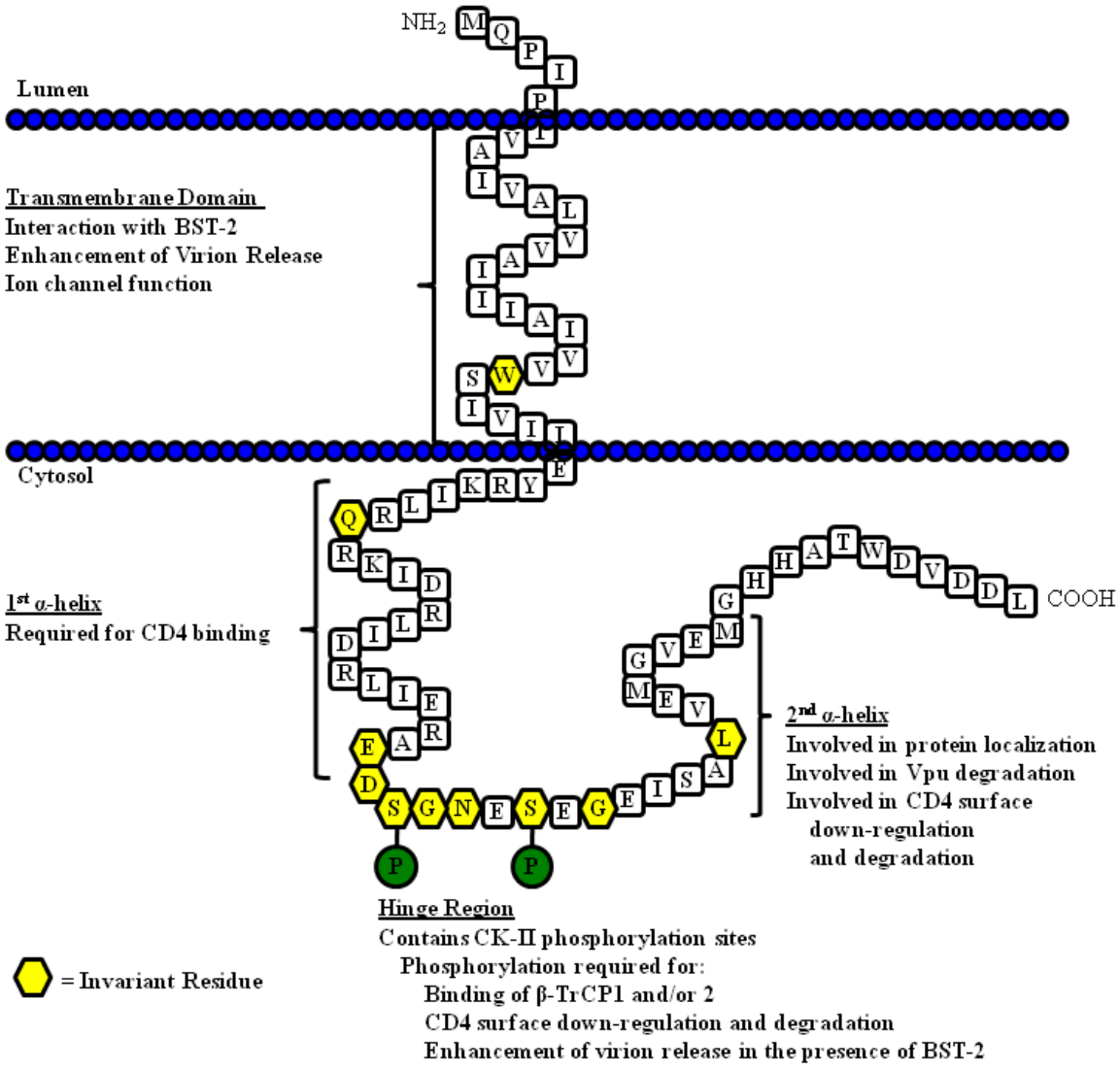
NH2
Lumen
Transmembrane Domain
Interaction with BST-2
Enhancement of Virion Release
Ion channel function
Cytosol
1st α-helix
Required for CD4 binding
2nd α-helix
Involved in protein localization
Involved in Vpu degradation
Involved in CD4 surface
down-regulation
and degradation
COOH
Hinge Region
Contains CK-II phosphorylation sites
Phosphorylation required for:
Binding of β-TrCP1 and/or 2
CD4 surface down-regulation and degradation
Enhancement of virion release in the presence of BST-2
= Invariant Residue

transmembrane region and the cytoplasmic domain. The first is the invariant tryptophan at position 23 of the corrected HXB2 Vpu protein (position 22 in the uncorrected protein). This amino acid with its ring structure is probably involved in stabilizing the TMD within the lipid bilayer (Park and Opella, 2005). There is also an invariant glutamine at position 35 within the first α-helical domain and an invariant leucine at position 63 within the second α-helical domain. The function of G35 is unknown and the L63 will be discussed in a later section. The second highly conserved domain is the tyrosine-based motif YXXΦ (where Φ is a hydrophobic amino acid) located at the TMD/CD interface. Unlike the other transmembrane glycoprotein of HIV-1, gp120/gp41, Vpu has no predicted N-linked glycosylation sites.

While the three-dimensional structure of the entire Vpu protein has yet to be solved, the structure of the TMD has been determined by nuclear magnetic resonance (NMR) spectroscopy in micelle and bilayer samples (Park et al., 2003). These investigators used the peptide $Vpu_{2–30+}$, which was a 36-residue polypeptide that consists of residues 2–30 from the N terminus of Vpu and a six-residue "solubility tag" at its C terminus. They found that the $Vpu_{2–30+}$ has a TM α-helix spanning residues 8–25 with an average tilt of 13^{o}. They found that the helix was kinked slightly at the isoleucine at position 17, which results in tilts of 12^{o} for residues 8–16 and 15^{o} for residues 17–25. These investigators subsequently showed that the tilt angle of the helix was inversely proportional to hydrophobic thickness of the lipid bilayer (Park and Opella, 2005).

Env

Similar to Gag and Pol, the Env protein is synthesized as a polyprotein (gp160). The envelope protein is synthesized on the RER similar to the Vpu protein except that the signal sequence of Env is cleaved by signal peptidase. The function of the Env protein is to recognize

and bind to the CD4 molecule for viral entry, it is not surprising that this event also occurs in the RER between nascent CD4 and gp160 molecules leading to the formation of gp160-CD4 complexes. This interaction sequesters both proteins in the RER preventing processing and transport to the cell surface leading to their eventual transport to lysosomes for destruction (Piguet et al., 1999b). This does down-regulate CD4 from the cell surface which has been shown to be beneficial for viral replication. This interaction has been shown to be relieved by the Vpu protein as described above by permitting transport, cleavage into gp120/gp41 subunits, and addition and processing of N-glycans.

The gp160 precursor protein is transported to the Golgi where it oligomerizes and undergoes heavy glycosylation modification mainly involving N-linked high-mannose-type oligosaccharides. These N-linked glycans are processed as the protein is transported to different compartments of the Golgi. These glycans allow for proper folding and conformational stability of the glycoproteins and ultimately provide a host-derived "mask" of carbohydrates that aide in the evasion of immune recognition and neutralization of viral infectivity by host antibody and cellular immune responses (Pantophlet and Burton, 2006; Poignard et al., 2001; Wyatt et al., 1998). The resulting glycoprotein is cleaved by host encoded proteases resulting in two mature heterodimers consisting of the surface glycoprotein, gp120, and the transmembrane or fusion glycoprotein, gp41 (Deng et al., 1996; Wyatt et al., 1998). The two glycoproteins remain associated through weak noncovalent interactions and are transported to the surface for incorporation into budding virions (Wyatt et al., 1998). The expression of the gp120/gp41 complexes on the surface of infected cells can cause fusion of two or more cells leading to the formation of multinucleated giant cells known as syncitia (Yao et al., 1993).

The gp120 protein consists of five variable regions (V1-V5) and five constant regions (C1-C5). The functional domains of this protein are responsible for recognition and binding of the HIV-1 receptor, CD4 (achieved by residues within a hydrophobic pocket surrounding a phenylalanine at position 43 (Phe43) formed mainly by segments within the C2, C3 and C4 domains), and the co-receptor, generally either CCR5 or CXCR4 (associated with V3 loop) (Deng et al., 1996; Krambovitis and Spandidos, 2006; Pantophlet and Burton, 2006; Wyatt and Sodroski, 1998). The interaction of the gp120 with CD4 causes a conformational change in the variable loop regions V1, V2 and V3. This allows the V3 loop to bind to the coreceptor which is mediated by charge-charge interactions. The CXCR4 and CCR5 coreceptors have regions of either strong negative or strong positive charge, respectively, that interacts with differential regions of the V3 loop that possess an opposing charge (Doms and Peiper, 1997; Kwong et al., 2000; Moulard et al., 2000; Sullivan et al., 1998). The interaction of the V3 loop with a co-receptor causes further conformational changes that allow for dissociation of the gp41 from gp120. The gp41 protein consists of three separate domains, the ectodomain, the transmembrane domain and the cytoplasmic domain. This protein anchors the envelope complex (gp120/gp41) in the viral membrane and catalyzes the fusion (via insertion of a hydrophobic fusion peptide into the host cell membrane) of the viral and host cell lipid bilayers during virus entry (Chen et al., 1995; Lu et al., 1995; Weissenhorn et al., 1997).

Nef

Nef is a small myristoylated early protein in HIV-1 infection that is polymorphic in length (200-215 amino acids). A myristic acid moiety is attached to the N-terminal region of Nef during protein processing and is required for membrane association. Nef is mainly localized

in the perinuclear region and less abundantly at the plasma membrane. While Nef is dispensable for viral replication, it has been established as a major determinant of pathogenicity. Several *in vivo* studies have demonstrated that *nef*-deficient viruses caused lower virus burdens and severity of disease both in humans and rhesus macaques (Foster and Garcia, 2008). Nef appears to serve as an adaptor protein that redirects specific host cellular proteins to atypical pathways in order to promote viral replication. Four major functions of Nef have been demonstrated *in vitro* including the: 1) down-regulation of CD4 from surface of infected cells; 2) down-regulation of major histocompatibility complex class 1 (MHC-1); 3) regulation of cellular signaling and activation; and 4) enhancement of virion infectivity (Aiken, 1997; Aiken et al., 1996; Anderson et al., 1994; Arora et al., 2000; Atkins et al., 2008; Campbell et al., 2004a; Chowers et al., 1994; Garcia and Miller, 1991; Greenberg et al., 1998b; Lundquist et al., 2002; Luo et al., 1997; Mangasarian et al., 1997; Miller et al., 1994; Noviello et al., 2008; Pizzato et al., 2007; Renkema et al., 1999; Schwartz et al., 1996; Simmons et al., 2001; Wei et al., 2005; Wonderlich et al., 2008).

The down-modulation of CD4 from the surface of infected cells is the most extensively studied functions of the Nef protein and appears to be the major factor in Nef modification of viral pathogenesis. Nef interacts with and accumulates CD4 molecules into clathrin coated pits at the cellular surface by the membrane proximal region of the cytoplasmic tail of CD4 (Anderson et al., 1994; Garcia and Miller, 1991; Grzesiek et al., 1996; Hua and Cullen, 1997). Nef contains a canonical dileucine motif (^{160}EXXXLL^{165}) and a diacidic motif (^{174}[E/D]D^{175}) that are required for binding adaptor protein 2 (AP-2) and down-regulation of the CD4 molecule (Chaudhuri et al., 2007; Coleman et al., 2005; Craig et al., 1998; Greenberg et al., 1998a; Lindwasser et al., 2008). The vacuolar membrane ATPase (V-ATPase) appears to bind both the

C-terminal region of Nef and the μ2 subunit of AP-2 connecting the the CD4/Nef/AP-2 complex to the endocytic pathway (Geyer et al., 2002). This combination of events increases the internalization rate of CD4 and diverts the molecule from being recycled to being degraded via the lysosome.

Nef also down-regulates MHC-I from the cellular surface by interacting with an adaptor protein (AP-1) (Roeth et al., 2004). The main function of AP-1 is to direct proteins at the trans-Golgi network (TGN) to the endolysosomal pathways (Robinson and Bonifacino, 2001). The exact mechanism by which Nef down-regulates MHC-I is still under investigation, however, it has been suggested that Nef serves as an adaptor between AP-1 and newly synthesized MHC-I molecules. This data is supported by the discovery of a ternary complex between Nef, the cytoplasmic tail of MHC-I and AP-1 (Noviello et al., 2008; Wonderlich et al., 2008). Normally, newly synthesized MHC-I molecules would become phosphorylated and transported to the plasma membrane for antigen presentation, however in the presence of Nef, these hypophosphorylated molecules are prevented from becoming phosphorylated and through the interaction with AP-1 are redirected to the lysosomes for degradation (Kasper et al., 2005; Roeth et al., 2004). Nef has also been shown to increase the rate of endocytosis of MHC-I molecules on the surface through the recruitment of phosphofurin acidic cluster sorting protein 1 and/or 2 (PACS1/2). This allows for activation of the endocytic pathway and through a yet unknown mechanism Nef is able to prevent the recycling of the MHC-I containing vesicles to the plasma membrane and rather deliver the MHC-I molecules to the lysosome for degradation (Blagoveshchenskaya et al., 2002; Foster and Garcia, 2008; Swann et al., 2001).

Finally, Nef has been demonstrated to impact infectivity of viral particles released from an infected cell and is thought to occur through several different mechanisms (Chowers et al.,

1994; Miller et al., 1994). Campbell *et al.* demonstrated that disruption of the actin cytoskeleton was able to overcome the defect observed in *nef*-deficient viruses suggesting that Nef is able to somehow counteract the barrier presented by the actin cytoskeleton (Campbell et al., 2004a). Pizzato *et al.* provided another possible mechanism suggesting that a yet unknown protein distinct from CD4 inhibits the function of HIV-1 Env and that Nef down-regulates this protein through a Dynamin 2/clathrin-mediated mechanism thereby counteracting its effects on the Env protein (Pizzato et al., 2007). Finally, additional studies have suggested that Nef may protect the viral core from post-fusion degradation (Qi and Aiken, 2007, 2008).

LTR

The HIV-1 genome is flanked by two long terminal repeat (LTR) regions. These regions allow for integration into the host cellular DNA and do not encode for any viral proteins. The 5'LTR contains the transactivation-response elements (TAR) where the Tat protein binds and the promoter enhancer binding sites and allows for the recruitment of host cellular transcriptional machinery to promote viral replication as described above in the overview of viral replication.

Pathogenesis

HIV-1 is characterized by the progressive depletion of the $CD4^+$ subset of the T cell population resulting in severe immunosuppression and ultimately the development of AIDS and increased susceptibility to opportunistic infections. The exact mechanism for the depletion of the $CD4^+$ T cell population remains unknown, however it is generally thought to be associated both with the cytopathic effects of the virus as well as the over activation of the immune system.

HIV-1 can be transmitted through sexual intercourse, intravenously (most likely through contaminated needles (healthcare workers or drug users) or transfusion of blood products), or vertically from mother to child. During the primary or acute phase of infection viral loads are high in the peripheral blood and the virus disseminates throughout the host especially localizing to the primary and secondary lymphoid organs. This phase is generally accompanied by a short flu-like illness (Hirsch and Curran, 1996). There are three general patterns of disease progression that occur following infection: 1) typical progressor; 2) rapid progressor; and 3) long-term non-progressor. After several weeks, a typical progressor will enter into a clinically asymptomatic or latent stage of infection, which has a mean time of 10 years in untreated patients. This stage is accompanied by steady levels of viral replication and slow continual depletion of $CD4^+$ T cells. The continuous damage of the immune system eventually results in an increase in viral loads and progression to a symptomatic stage of infection followed by advancement into the AIDS stage which is characterized by severe clinical symptoms and/or opportunistic infections (Hirsch and Curran, 1996). Clinical AIDS is established when an infected individuals circulating $CD4^+$ T cell levels drop below 200 cells/µl or if they exhibit one of the AIDS defining clinical conditions as defined by the Center for Disease Control and Prevention (CDC). Around 5-10% of individuals infected with HIV-1 are rapid progressors and generally develop AIDS within 3-4 years. These individuals do not mount a stage of clinical latency, but rather continually exhibit high viral loads and a rapid decrease in circulating $CD4^+$ T cell levels (Arens et al., 1993; Bollinger et al., 1996; Demarest et al., 2001). Finally, around 5% of HIV-1 patients are termed long-term non-progressors (LTNP). These individuals initially exhibit high viral loads during the acute phase of infection and then continually present with low virus burdens for an extended period of infection. The circulating $CD4^+$ T cell levels of LTNPs

remain stable at or above 600 cells/µl and are devoid of clinical symptoms (Rinaldo et al., 1995). Several studies have suggested a correlation between deletions or premature truncations of accessory proteins especially the *nef* gene and long-term nonprogressive infections (Deacon et al., 1995; Kirchhoff et al., 1995; Kondo et al., 2005; Salvi et al., 1998; Yamada and Iwamoto, 2000).

In addition to severe lymphoid depletion, HIV-1 is also known to cause HIV-1 associated nephropathy (HIVAN) and HIV-1 associated dementia (HAD) during the late stages of infection. Relatively 10% of HIV-1 infected individuals develop HIVAN and 90% of these patients are African American (Winston and Klotman, 1996). HIVAN is characterized by focal segmental glomerulosclerosis (FSGS), elevated serum nitrogen levels, and microproteinuria (Rao, 1991; Szczech, 2001). Patients progressively lose renal function and ultimately develop end stage renal disease which has a mortality rate of ~50% within one year post-initiation of dialysis (Szczech, 2001). Approximately 15-25% of HIV-1 infected patients develop HAD without anti-retroviral treatment. HIV-1 invades the central nervous system (CNS) early after infection and while the exact mechanisms by which HIV-1 traverses the blood brain barrier are still unknown, it is most likely attributed to infiltration by infected macrophages (microglia) and/or lymphocytes and neuronal injury caused by release of neurotoxic factors (Cunningham et al., 1997; Gartner, 2000; Kaul et al., 2001; Li et al., 1992; Smit et al., 2001; Williams et al., 2001).

SHIV Macaque Models of HIV-1 Infection

As Vpu is only expressed in HIV-1 and some SIV_{CPZ} strains, examination of the role of Vpu in viral pathogenesis is limited by the lack of a relevant animal model. Chimeric viruses composed of HIV-1 *tat, rev, vpu,* and *env* genes in a genetic background of $SIV_{MAC}239$, known

as SHIVs, have permitted extensive research on the role of HIV-1-specific genes products in a pathogenic macaque model (Figure 7). These viruses provide an alternative non-human primate model of HIV-1 disease that allows for examination of unique biological motifs within the HIV-1 gp160 as well as the biological role of the HIV-1 *vpu*. The initial SHIV constructed (SHIV-4) was able to infect rhesus and pig-tailed macaques and cause a persistent infection, however no loss of $CD4^+$ T cells nor development of an AIDS-like disease was observed (Li et al., 1992). This virus was subsequently passaged through a series of rhesus and pig-tailed macaques to yield pathogenic variants that replicate to extremely high titers, cause rapid $CD4^+$ T cell loss and the development of AIDS within six months to one year post-inoculation. Several of these SHIVs could cause end-stage renal and neurological disease similar to disease observed within HIV-1 infected human hosts and also use CXCR4 as a coreceptor for virus entry into cells, which is not observed in SIV infections (Chen et al., 1997; Choe, 1998; Edinger et al., 1997; Joag et al., 1996; Joag et al., 1998a; Karlsson et al., 1997; Kimata et al., 1999; Liu et al., 1999; Narayan et al., 1999; Raghavan et al., 1997; Reeves et al., 1999; Shibata et al., 1997; Stephens et al., 1997; Stephens et al., 2000). The two main pathogenic variants used within our laboratory are $SHIV_{KU\text{-}1bMC33}$ and $SHIV_{KU\text{-}2MC4.}$ Both variants contain the US.HXB2 laboratory adapted subtype B *vpu* gene and have both been shown to cause rapid $CD4^+$ T cell loss and development of AIDS (Liu et al., 1999; McCormick-Davis et al., 2000a).

During the derivation and selection of these viruses our laboratory provided evidence indicating that the Vpu protein plays an important role in the modification of SHIV pathogenesis. The initial indication was observed during the sequential characterization of the pathogenic $SHIV_{KU\text{-}1}$ virus (an uncloned virus isolated from the cerebrospinal fluid of a pig-tailed macaque). This study demonstrated an association between the reversion of the *vpu* to an open reading

Figure 7. Schematic representation of chimeric simian-human immunodeficiency viruses (SHIVs). SIV encoded genes are shown in blue. HIV-1 encoded genes are shown in yellow.

SHIV

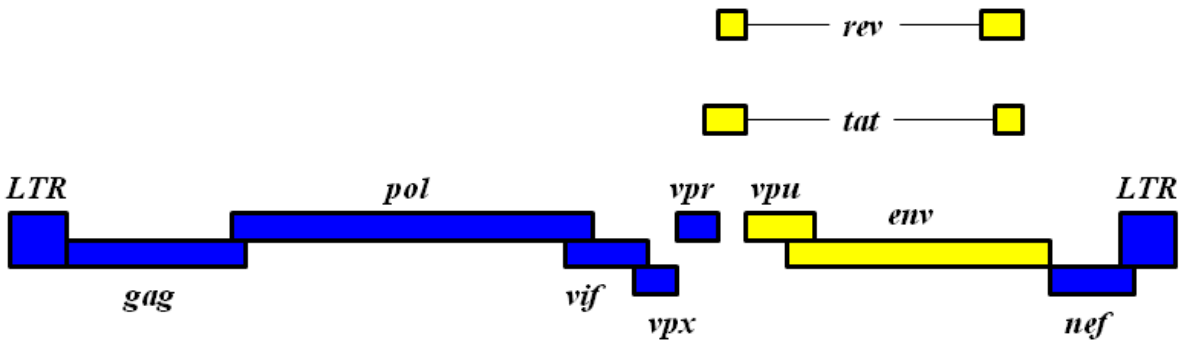

frame (start codon changed from ACG (SHIV-4) to ATG ($SHIV_{KU-1}$)) and the selection of virus variants that caused a second phase of $CD4^+$ T cell loss and the development of AIDS (McCormick-Davis et al., 1998). This study also identified consensus mutations within the *env* and *nef* genes that correlated with the reversion of the *vpu* to an open reading frame (Joag et al., 1997; McCormick-Davis et al., 1998). The construction of the pathogenic molecular clone $SHIV_{KU-1bMC33}$ that contained these consensus mutations in *tat, rev, vpu, env*, and *nef* was completed in order to create a reproducibly pathogenic virus clone (Stephens et al., 2002). Similarily, a reproducibly pathogenic clone of the $SHIV_{KU-2}$ cell-free virus stock (an uncloned virus isolated from the CSF of a rhesus macaque), $SHIV_{KU-2MC4}$, was constructed. Of note is the ability of $SHIV_{KU-2MC4}$ to cause severe glumerulosclerosis of the kidney and lentiviral encephalitis (Liu et al., 1999).

The role of Vpu in pathogenesis was indicated further with the construction of two separate deletion mutants. In the first study, a mutant in which 42 of the total 82 amino acids of Vpu were deleted (Singh et al., 2001). The Vpu protein expressed by this virus was truncated and non-membrane and the virus was designated $\Delta vpuSHIV_{KU-1bMC33}$. The inoculation of this virus into four separate macaques caused a moderate to no decline in $CD4^+$ T cells in three macaques and a rapid decrease in $CD4^+$ T cells and neurological disease in the final macaque (50O). The severe $CD4^+$ T cell loss and neurological disorder of macaque 50O was attributed to significant amino acid substitutions and deletions within the Nef and Env proteins. Also, inoculation of a virus isolated from the lymph node of macaque 50O into four additional macaques demonstrated reproducible development of severe $CD4^+$ T cell loss and development of AIDS (Singh et al., 2001). These results taken to together support the conclusion that Vpu

does increase pathogenicity of SHIV however, individual macaques can select for compensating mutations within other genes, especially *env* and *nef*.

Finally, an additional study was completed to confirm the role of Vpu in pathogenesis with a virus where the entire coding region of *vpu* upstream of *env* gene was deleted (no*vpu*$SHIV_{KU\text{-}1bMC33}$). Three macaques were inoculated with this virus and none developed a significant drop in $CD4^+$ T cells or any disease manifestations (Stephens et al., 2002). Taken together, these studies demonstrate that the HIV-1 Vpu protein plays a significant role in the pathogenesis of SHIV in macaques.

These SHIV viruses have allowed our laboratory to conduct extensive *in vivo* studies examining the role of specific amino acids and motifs within the Vpu protein in SHIV pathogenesis. Of note are our studies involving the transmembrane domain (TMD) and hinge region of Vpu that contains the two casein kinase II phosphorylation sites. Inoculation of macaques with a SHIV expressing a Vpu with a scrambled TMD ($SHIV_{TM}$) that presumably disrupted ion channel function resulted in no $CD4^+$ T cell loss and no development of any other disease manifestations (Hout et al., 2005). Additional analysis of the role of the potential role of the ion channel function of Vpu was conducted using a SHIV expressing a Vpu in which the TMD was exchanged with that of the M2 protein of the Influenze A virus, a known viroporin ($SHIV_{M2}$). Macaques inoculated with $SHIV_{M2}$ exhibited high viral loads, rapid $CD4^+$ T cell loss and histological lesions consistent with lymphoid depletion similar to macaques inoculated with the parental $SHIV_{KU\text{-}1bMC33}$ (Hout et al., 2006b). Taken together, these results indicate that the TMD of Vpu is important for Vpu-mediated modification of SHIV pathogenesis and may potentially be associated with the ion channel properties of Vpu.

As mentioned, our laboratory also confirmed the role of the hinge region casein kinase II phosphorylated serine residues in Vpu modification of viral pathogenesis using a SHIV expressing a Vpu protein in which the two serine residues at positions 52 and 56 were substituted with glycines ($SHIV_{S52,56G}$). Of the four pig-tailed macaques inoculated with this SHIV, one exhibited rapid $CD4^+$ T cell loss and histological lesions consistent with inoculation with a parental SHIV, while the others developed no or gradual $CD4^+$ T cell loss. It was later confirmed that the virus isolated from the macaque that developed rapid $CD4^+$ T cell loss had reverted the glycine residues back to serines (Singh et al., 2003). At the time this study was conducted, it was assumed that these phosphorylation sites were only required for Vpu-mediated down-modulation of CD4 from the cell surface, leading to the conclusion that this was an essential function of Vpu in enhancing pathogenesis *in vivo*. However, more recent studies, which will be discussed later, have suggested a role for these residues in the enhancement of virion release function of Vpu as well as CD4 down-modulation and therefore indicates that the specific contributions of each of the functions of Vpu in modifying pathogenesis still remain unknown.

Is Vpu an Ion Channel Protein?

Several studies suggest that Vpu may have ion channel activity. In the early descriptions of the Vpu protein, its structure was compared to the M2 protein of influenza as it had: a) a similar topology in the membrane having a short N-terminal region; b) an uncleaved leader/transmembrane domain and longer cytoplasmic domain; and c) a similar length and two casein kinase II phosphorylation sites. The H^+ ion channel of M2 has been extensively characterized and is considered the prototypical "viroporin." It is the best characterized of this

class of viral proteins, which also includes the 6K protein of Sindbis virus (SV), and the 2B protein of poliovirus, to name a few (Gonzalez and Carrasco, 2003). The initial evidence that Vpu could form an ion channel arose from studies showing that expression of Vpu in frog oocytes results in a conductance that is weakly selective for cations (Ewart et al., 1996; Schubert et al., 1996b). Modeling studies have suggested that a pentameric structure for the Vpu TMD would be optimal for the formation of such a channel (Cordes et al., 2001; Grice et al., 1997; Lopez et al., 2002; Sansom et al., 1998; Wray et al., 1999). These same investigators later showed that two derivatives of the Na^+/K^+ antiporter amiloride, dimethyl amiloride (DMA) and hexamethylene amiloride (HMA), inhibited Vpu-mediated virion release and replication in monocyte-derived macrophage cultures (Ewart et al., 2002; Ewart et al., 2004). However, we have found that these compounds affected the cell cycle regulation when T-cells were treated with concentrations required to inhibit viral replication (unpublished data).

Previous studies of the M2 protein have shown that the H-X-X-X-W motif within the TMD was essential for ion channel activity with the histidine being the proton sensor and the tryptophan being the actual pore (Okada et al., 2001; Takeuchi et al., 2003; Tang et al., 2002). The drugs amantadine and rimantadine are known as M2 ion channel blockers (Okada et al., 2001; Takeuchi et al., 2003; Tang et al., 2002). Substitution of the M2 TMD histidine residue with an alanine resulted in a constitutively open channel, indicating its importance to channel activation (Holsinger and Lamb, 1991; Holsinger et al., 1994; Pinto et al., 1992; Tang et al., 2002). As previously mentioned our laboratory constructed a SHIV in which the TMD of Vpu was exchanged with the TMD of M2 (Hout et al., 2006b). This virus, $SHIV_{M2}$, was capable of causing a severe loss of $CD4^+$ T cells and AIDS when inoculated into macaques. In addition, we found that unlike the parental $SHIV_{KU\text{-}1bMC33}$, replication of the $SHIV_{M2}$ virus was sensitive to an

M2 ion channel blocker, rimantadine. This study showed that drugs targeting the TMD of Vpu (in this case a chimeric Vpu with the TMD of the M2 protein) could reduce virus release from infected cells. If one compares the sequence of the Vpu and M2 TMDs, the subtype B Vpu contains the sequence A-X-X-X-W in approximately the same position as M2 with the tryptophan being invariant in Vpu (McCormick-Davis et al., 2000b). We subsequently showed that substitution of the alanine in this motif with a histidine residue resulted in a SHIV ($SHIV_{VpuA19H}$) that became more sensitive to rimantadine than the $SHIV_{M2}$ virus (Hout et al., 2006a). These results indicate that a single amino acid substitution within the TMD of the Vpu protein converts a rimantadine-resistant SHIV to a rimantadine-sensitive SHIV. In a subsequent study, Park and Opella used NMR spectroscopy to analyze the structure of the TMD with the alanine to histidine substitution They showed that in C14 phospholipid bicelles, the unmodified TMD has a tilt angle of 30^o but that the A18H had a tilt angle of 41^o, indicating that the introduced histidine altered the structure of the helix in the bicelle. These investigators also showed that the isoleucine at position 15 and the tryptophan at position 22 of A18H but not the unmodified TMD were perturbed by the presence of rimantadine. Finally, they showed that the rotation angle of H18 and W22 in A18H were almost identical to H37 and W41 of the M2 protein (A18H, 41^o, M2, 38^o). Taken together, these studies indicate that the TMD of Vpu can be designed to bind the influenza antiviral rimantadine. Whether the ion channel activity of Vpu is functionally required for the virus release function is still controversial. However, these studies do provide "proof of concept" that Vpu could be a target for novel antiviral drugs.

The Role of Vpu in CD4 Surface Down-Modulation

During virus entry, the HIV-1 Env glycoprotein binds to the CD4 receptor and subsequently with a chemokine co-receptor, normally CCR5 on macrophages and CXCR4 on T helper cells. Thus, expression of CD4 molecules on the surface of cells is essential to HIV-1 infection, however, once infection has occurred, expression of CD4 poses several problems in the virus replication cycle. Newly synthesized CD4 molecules are capable of forming complexes with the Env precursor gp160 in the endoplasmic reticulum (ER) preventing transport and processing of the two cleavage products, gp120 and gp41, to the site of assembly (Crise et al., 1990; Jabbar and Nayak, 1990; Levesque et al., 2003; Stevenson et al., 1988; Willey et al., 1992b). High CD4 surface expression can lead to the retention of nascent virions at the plasma membrane and/or superinfection of cells by cell-free or cell-associated virus (Klimkait et al., 1990; Schubert et al., 1996a; Vincent et al., 1993; Wildum et al., 2006; Yao et al., 1993). Finally, CD4 surface expression has been shown to decrease viral infectivity by incorporating CD4 molecules and inactive CD4-gp120 complexes into the virion (Cortes et al., 2002; Levesque et al., 2003; Tanaka et al., 2003). While the physiological significance of each of these potential complications is still under investigation, there is a clear indication that CD4 degradation is important for HIV-1 replication. HIV-1 has developed several mechanisms to down-modulate both intracellular and surface expression of CD4 molecules promoting productive virion assembly and release. These mechanisms are mediated by two accessory proteins encoded for by HIV-1: Nef and Vpu. These two proteins regulate CD4 expression at different cellular compartments and by distinct mechanisms. HIV-1 Nef functions by acting on mature CD4 molecules present at the plasma membrane or in late endosomes. Nef accelerates clathrin-mediated endocytosis of CD4 molecules from the cell plasma membrane and targets them to the

lysosomes for destruction (Garcia and Miller, 1991; Piguet et al., 1998; Piguet et al., 1999a). HIV-1 Vpu is expressed from the same mRNA as Env and is responsible for counteracting the effects of CD4 molecules early within the biosynthetic pathway. The general mechanism by which HIV-1 Vpu counteracts the problems presented by CD4 molecules has been well studied. Research conducted over the past several years has focused on the characterization of specific molecular components involved in this process and the consequences that this CD4 down-modulation has on pathogenesis and cellular homeostasis *in vitro* and *in vivo* (Figure 8).

Following synthesis of Vpu in the ER, it binds to a specific motif, LSEKKT, within the cytoplasmic domain of CD4 between residues 414 and 419 (Bour et al., 1995; Chen et al., 1993; Lenburg and Landau, 1993; Vincent et al., 1993). Binding of the CD4 molecule by Vpu is required for its subsequent degradation; however, it is not sufficient (Bour et al., 1995; Buonocore et al., 1994; Schubert et al., 1994; Tiganos et al., 1997). Previous studies have shown that both α-helical domains within the CD of HIV-1 Vpu are structurally important for CD4 down-modulation from the cell surface with only the first α-helix being required for binding (Tiganos et al., 1997). These investigators showed that disruption of the predicted secondary structure of the two cytoplasmic α-helical domains eliminates Vpu-mediated CD4 surface down-modulation (Tiganos et al., 1997). These investigators showed that expression of a Vpu protein with amino acid substitutions in the first α-helical domain but not in the second α-helical domain affected binding to CD4. Also, deletion of the C terminal 23 residues within HIV-1 Vpu strain HXB2 or substitution of residues V65 thru M71 with the amino acid sequence ALGMAL, eliminates Vpu-mediated CD4 surface down-regulation, but not CD4 binding (Pacyniak et al., 2005; Tiganos et al., 1997). Taken together, these studies indicate that primary and secondary structures are important for Vpu-mediated CD4 surface down-regulation and that the first α-

Figure 8. Down-modulation of cell surface CD4 expression by Vpu. In the rough endoplasmic reticulum, Vpu binds CD4 through an interaction between the first α-helix within the cytoplasmic domain of Vpu and a specific motif within the cytoplasmic domain of CD4 (LSEKKT). Vpu is phosphorylated by several different isoforms of casein kinase II. This phosphorylation recruits and binds the cellular F-box protein β-TrCP. CD4 is then ubiquitinated via the $SCF^{\beta\text{-}TrCP}$ E3 Ub ligase complex after which it is shunted to the proteasome for degradation through an unknown mechanism.

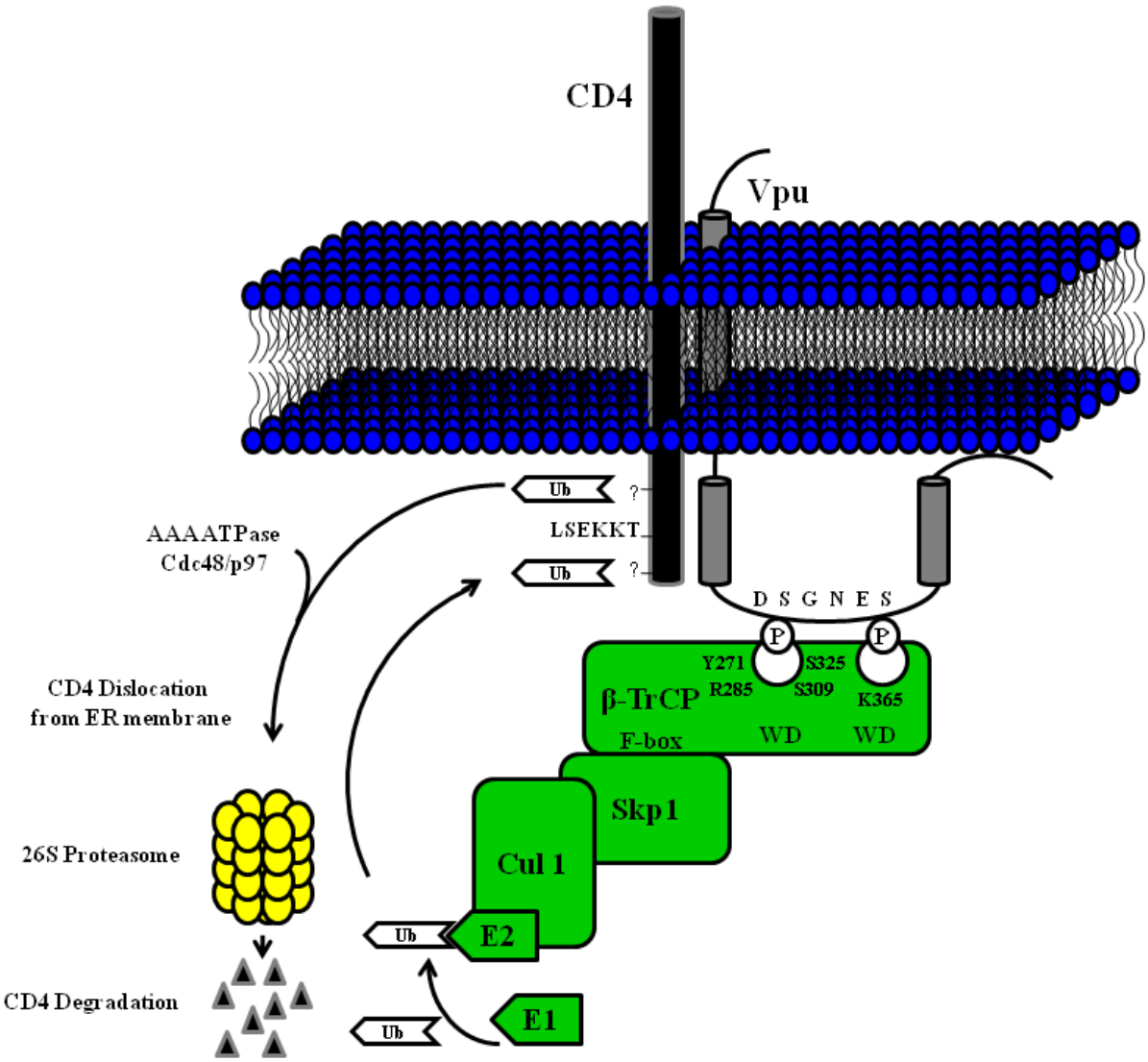
CD4
Vpu
Ub
?
LSEKKT
Ub
?
AAAATPase
Cdc48/p97
D S G N E S
P
P
Y271
R285
S325
S309
K365
β-TrCP
F-box
WD
WD
CD4 Dislocation
from ER membrane
Skp1
Cul 1
26S Proteasome
Ub
E2
CD4 Degradation
Ub
E1

helical region of the cytoplasmic domain of Vpu appears to be involved in the interaction with CD4. We recently completed a study that systematically analyzed the importance of each amino acid in the predicted second α-helical domain (Hill et al., 2010). In this study, each amino acid was substituted with an alanine residue. We identified an additional amino acid, L63 within the second α-helix of HIV-1 Vpu strain HXB2 that is required for CD4 surface down-modulation (Hill et al., 2010). In this study, we also identified a second amino acid, V68, which is necessary but is not sufficient for complete CD4 surface down-regulation. The L63 residue is conserved among all HIV-1 Vpu subtypes. While Tiganos and colleagues showed that substitution of this residue with a proline did disrupt Vpu-mediated CD4 degradation, a proline substitution eliminated the ability to distinguish between a primary role of the hydrophobic amino acid residue at this position and its structural role in the predicted second α-helical domain (Tiganos et al., 1997). Substitution of this residue with alanine or valine, which maintains the predicted secondary structure, did not disrupt binding to CD4 or β-TrCP, but did eliminate CD4 surface down-modulation. Interestingly, substitution of this residue with either an isoleucine or a glycine resulted in partial function in CD4 down-modulation, suggesting that the length of the side chain is important. Similar results were obtained for mutant Vpu with similar substitutions of the valine at position 68 although to a lesser extent. These mutants will be useful in determining the specific role of the second α-helix in the process of CD4 degradation.

The Vpu protein is phosphorylated at residues S52 and S56 (positions from HIV_{NL4-3} clone) present within two highly conserved casein kinase II phosphorylation sites (S/T-XX-D/E) (Schubert et al., 1994). This phosphorylation is required for CD4 degradation, but not CD4 binding (Bour et al., 1995; Paul and Jabbar, 1997). The phosphorylated Vpu protein recruits and binds the cellular F-box protein β-TrCP generating a CD4-Vpu-β-TrCP ternary complex (Binette

et al., 2007; Margottin et al., 1998). The signal for recognition of ligands, including HIV-1 Vpu, by β-TrCP is the phosphorylation of one or two serine residues present within a conserved motif, $DS^{P}GxxS^{P}$. Both phosphoserines have distinct orientations within the protein complex that allow them to make specific contacts with the WD-repeat β-propeller domain of β-TrCP (Coadou et al., 2003; Evrard-Todeschi et al., 2006; Megy et al., 2005; Wu et al., 2003). Biochemical analyses of the HIV-1 Vpu protein showed that the first phosphoserine interacts with the binding pocket of the β-TrCP WD-repeat domain (residues Y271, R285, S309 and S325). The second phosphoserine interacts with a basic patch in the β-TrCP WD-repeat domain centered around residue K365. The hydrophobic amino acids surrounding the $DS^{P}GxxS^{P}$ motif also strengthen the interaction of Vpu with the β-TrCP by forming electrostatic, hydrogen and van der Waals bonds with specific residues within the binding pocket (Coadou et al., 2003; Evrard-Todeschi et al., 2006; Megy et al., 2005; Wu et al., 2003).

The F-box protein β-TrCP recruits the other components of the E3 ubiquitin ligase complex (Skp1 and Cullin1) and mediates the ubiquitination of the CD4 molecule in *trans*. A homologue of β-TrCP known as β-TrCP2 or HOS was shown to be sufficient for Vpu-mediated CD4 down-modulation (Besnard-Guerin et al., 2004; Butticaz et al., 2007). Silencing of both homologues with siRNA was required for the inhibition of Vpu-mediated CD4 surface down-regulation (Butticaz et al., 2007). The process by which Vpu mediates CD4 down-regulation resembles the ER-associated protein degradation process (ERAD); however, the exact mechanism by which CD4 is poly-ubiquitinated and transported to the cytosol for degradation is not completely understood. Meusser and Sommer reconstituted HIV-1 Vpu-mediated CD4 degradation in *Saccharomyces cerevisiae* to determine the role of ERAD proteins in this process (Meusser and Sommer, 2004). In this system, CD4 was translocated across the ER membrane

but, unlike human cells where CD4 is stable the CD4 was rapidly degraded in the absence of Vpu and depended on the presence of the yeast ERAD proteins and a functional proteasome. The rapid degradation of CD4 was eliminated in yeast defective in ERAD-dependent ubiquitination ligases, but could be restored by the expression of Vpu and human β-TrCP. Also, in the ERAD-defective yeast CD4 was shown to be ubiquitinated in the presence of phosphorylated Vpu and β-TrCP providing evidence supporting the *trans*-polyubiquitination of the CD4 by the $SCF^{\beta\text{-}TrCP}$ E3 Ub ligase complex. The degradation of CD4 was shown to be dependent on the presence of four lysine residues within the cytosolic tail of CD4 (Meusser and Sommer, 2004). Similar results were obtained for the polyubiquitination of the CD4 cytoplasmic domain mediated by the $SCF^{\beta\text{-}TrCP}$ E3 Ub ligase complex in human cells (Binette et al., 2007). However, CD4 down-regulation was not completely dependent on ubiquitination of the four cytoplasmic lysine residues suggesting a role for other serine or threonine residues present within the CD4 cytoplasmic tail. This study also provided evidence for the involvement of an ERAD protein, the AAA ATPase (ATPases Associated with diverse cellular Activities) Cdc4/p97 by showing disruption of Vpu-mediated CD4 down-regulation through the expression of a transdominant negative mutant of this ATPase. This protein is involved in dislocation of ERAD substrates and this group also provides evidence for dislocation of the CD4 molecule that is dependent on its poly-ubiquitination. These data provide a better understanding of the specific mechanism by which Vpu mediates CD4 degradation and continued studies are needed to determine all proteins involved in the process and possible targets for therapeutics.

The HIV-1 Vpu protein has been found to escape degradation during the process of CD4 down-regulation and degradation (Margottin et al., 1998; Schubert et al., 1994). In a recent study Vpu degradation was shown to occur in cells arrested in early mitosis by a proteasome-mediated process (Estrabaud et al., 2007). The Vpu protein was shown to become phosphorylated at a downstream phosphoserine residue (S61 in HIV_{HXB2}) inducing recruitment of an unknown E3 ubiquitin ligase complex for ultimate degradation (Estrabaud et al., 2007). Mutation of this residue resulted in the accumulation of HIV-1 Vpu within cells and increased release of HIV-1 particles from HeLa cells in comparison to HeLa cells infected with wild-type virus. Vpu-mediated CD4 degradation was not affected by mutation of this serine residue. These investigators indicated that phosphorylation of this residue was involved in regulating Vpu degradation. We previously analyzed the Vpu sequences from over 100 strains of HIV-1 group M with representation of all different subtypes (McCormick-Davis et al., 2000b). Our results indicate that a serine residue at this position is a relatively rare occurrence (BRU, HXB2 strains) and extrapolation to Vpu proteins from "clinical isolates" may not be possible. Whether the serine present at position 64 in the majority of HIV-1 Vpu proteins is phosphorylated and can substitute for the serine at position 61 remains to be elucidated. While our results are in agreement regarding serine 61 and degradation of Vpu, substitution of residues L63 and V68 with alanines also resulted in slower turnover of HXB2 Vpu in transfected cells (Hill et al., 2010). Taken together, these results indicate that other amino acids within the second α-helical domain also contribute to the regulation of Vpu degradation.

The Role of Vpu in Enhanced Virion Release

The ability of Vpu to enhance the release of virions from infected cells exemplifies viral antagonism of an intrinsic host defense mechanism. The interferon-induced transmembrane protein BST-2 (CD317, HM1.24 or tetherin) restricts the release of nascent virions from the cell surface, while the Vpu protein relieves this restriction. Although the mechanisms involved in this process are not fully elucidated, current data suggest that BST-2 blocks release by directly retaining mature, nascent HIV-1 virions on the cell surface, while Vpu counteracts BST-2 by removing it from sites of virion assembly and budding at the plasma membrane. These relationships allow Vpu to be considered an antagonist of the innate, interferon-induced, immune response to enveloped viruses.

BST-2 is an interferon-induced, lipid raft-associated, type II integral membrane protein with an unusual topology. It contains a short cytoplasmic N-terminus followed by a transmembrane domain, a central extracellular domain predicted to form a coiled-coil that contains two N-linked glycosylation sites, and a C-terminal cleavage site predicted to form a glycosyl-phosphatidylinositol (GPI) anchor (Ishikawa et al., 1995; Kupzig et al., 2003). This unusual membrane topology in which BST-2 interacts with the lipid bilayer twice, has suggested a membrane-spanning model of tethering in which one end of BST-2 is embedded in the membrane of the host cell and the other in the membrane of the budded virion. As a GPI-anchored protein, BST-2 is found within the cholesterol-enriched lipid domains from which HIV-1 (and other enveloped viruses) bud (Kupzig et al., 2003; Nguyen and Hildreth, 2000; Ono et al., 2004; Ono and Freed, 2001). The protein is found on the plasma membrane and within the endosomal system, including the *trans*-Golgi network (Dube et al., 2009; Kupzig et al., 2003; Neil et al., 2008; Van Damme et al., 2008). BST-2 co-localizes with HIV-1 Gag in a punctate

distribution along the plasma membrane of cells expressing HIV-1, consistent with a direct tethering mechanism (Jouvenet et al., 2009; Mitchell et al., 2009; Neil et al., 2008; Van Damme et al., 2008). This mechanism appears to involve the incorporation of BST-2 into nascent virions (Perez-Caballero et al., 2009). So far, the molecular requirements for virion-tethering within BST-2 include the cytoplasmic domain, the predicted coiled-coil ectodomain, and the GPI anchor (Goffinet et al., 2009; Neil et al., 2008). BST-2 forms disulfide linked dimers and is heterogeneously glycosylated (Andrew et al., 2009; Barlow et al., 2003; Kaletsky et al., 2009; Perez-Caballero et al., 2009). However, the importance of dimerization and glycosylation in BST-2 function is not completely understood. Kaletsky and colleagues treated 293T cells expressing the HIV Gag-Pol and human BST-2 with DTT (dithiothreitol) and showed that it had no ability to elute restricted HIV from the cell surface, suggesting that cysteine-mediated dimerization alone does not mediate the restriction of virion release (Kaletsky et al., 2009). However, the exact role of glycosylation and dimerization in conjunction with other protein-protein interactions in the tethering process remain unknown. The ability of BST-2 to restrict the release of virus like particles (VLPs) derived from viral proteins from members of diverse viral families including all retroviruses tested, filoviruses, and an arenavirus (Lassa), suggests that it does not interact with any specific viral component, but rather the viral lipid envelope, an unknown receptor, or itself (Jouvenet et al., 2009). In the latter scenario, cell-associated BST-2 would interact with virion-associated BST-2, potentially via the protein's coiled-coil extracellular domain. A recent study by Andrew and colleagues provided further insight into the mechanism by which BST-2 restricts HIV-1 release (Andrew et al., 2009). Disruption of individual intermolecular disulfide bonds by point and 2 or 3 mutations of three cysteine residues within the extracellular domain (C53A, C63A, or C91A) revealed that no individual cysteine was

sufficient to abolish dimerization or antiviral activity of the BST-2 protein. However, mutation of all three cysteine residues abrogated both dimer formation and antiviral activity of the protein against Vpu deficient HIV-1. Further analysis of the triple cysteine mutant provided evidence that the lack of antiviral activity was not due to a mislocalization of the protein. This group also used point mutational analysis to investigate the role of glycosylation in BST-2 function. The two asparagines residues potentially involved in glycosylation (N65 and 92) were mutated in combination to glutamine and the ability of the mutant to inhibit HIV-1 release was analyzed. The results indicated that the mutant inhibited Vpu deficient HIV-1 release to a similar extent as a wild-type BST-2 protein suggesting that glycosylation is not required for the antiviral activity of BST-2. Also of note, is that neither the triple-cysteine mutant nor the glycosylation deficient mutant affected Vpu sensitivity (Andrew et al., 2009).

Another study by Perez-Caballero and colleagues also analyzed the role of cysteine-mediated dimerization and glycosylation in BST-2 antiviral activity (Perez-Caballero et al., 2009). This study used a series of point mutations, deletions and domain exchanges within the BST-2 protein in order to elucidate the importance of these residues and domains for antiviral activities. Similar to the Andrew's study, this group also determined that any of the three cysteine residues could mediate dimerization, and that mutation of all three residues completely abolished dimer formation. In slight contrast to the previous study this group found that while mutation of all three cysteines significantly decreased the antiviral activity of the protein, a weak phenotype was still observed. The effects of glycosylation on the antiviral activities of BST-2 were also evaluated through mutagenesis of the two asparagine residues within the extracellular domain (N65A and N92A). They found that N92A but not N65A markedly impaired the antiviral properties of BST-2. In stark contrast to the Andrew's study, amino acid substitutions

at both positions essentially inactivated the protein. This group evaluated the biological properties of these mutant proteins along with a secreted protein that lacked both the N-terminal transmembrane domain as well as the putative GPI anchor. These results revealed that glycosylation was essential for secretion and localization to the plasma membrane, suggesting a role in proper folding and transport and potentially not for direct tethering of virions. Deletion of the majority of the coiled-coil domain inhibited BST-2 function, but allowed for localization to the plasma membrane and formation of disulfide linked homodimers. Deletion of either the N-terminal transmembrane domain or the GPI anchor signal completely abolished the block of particle release, however both of these mutants were incorporated into budding virions as dimers. This group further analyzed the potential orientation of the BST-2 protein within the cellular and viral membranes by using these two mutants. Interestingly, the delTM mutant was able to be completely digested with subtilisin treatment of purified virions suggesting that this protein was anchored in the viral membrane by only the GPI anchor. This group also analyzed BST-2 incorporation into virions using gold immunolabeling and backscatter electron detection providing further evidence for virion incorporation. These experiments revealed that the delGPI mutant BST-2 preferentially localized to sites of particle budding while the WT and delTM BST-2 proteins were associated with budding particles but were not enriched at sites of assembly. This group suggests that the N-terminal transmembrane domain is essential for localization to these sites. The importance of the specific amino acids within the BST-2 protein for interaction with viral proteins is still under analysis, however this group developed an artificial BST-2 protein (art-tetherin) to test the role of the domains in antiviral activity. This protein consisted of the N-terminal region of the transferrin receptor (TfR), the 75 residue coiled-coil from the cytoplasmic dimeric protein, dystrophia myotonica protein kinase (DMPK), an HA-tag following

the coiled-coil domain, and the C-terminal region of the urokinase plasminogen activator receptor (uPAR). This artificial protein inhibited the release of both HIV-1 and Ebola virion like-particles, however did not display a susceptibility to the HIV-1 Vpu protein that has been previously reported (Perez-Caballero et al., 2009). The construction and analysis of this artificial protein provides a significant advance in the development of potential therapeutics. While this study provides evidence for a direct mechanism of tethering for the BST-2 protein it does not completely eliminate the possibility for other indirect mechanisms of action.

Vpu relieves the restriction of virion release imposed by BST-2. This relationship accounts for the long observed *vpu* phenotype of enhanced efficiency of viral release, and it explains why certain cell types such as HEK293 do not support this phenotype as they do not express BST-2 constitutively. To counteract BST-2, Vpu appears to remove the protein from sites of virion assembly along the plasma membrane (Jouvenet et al., 2009; Mitchell et al., 2009; Van Damme et al., 2008). In cells expressing Vpu, the overall level of BST-2 at the cell surface is reduced (Bartee et al., 2006; Gupta et al., 2009a; Mitchell et al., 2009). This reduction occurs rapidly, within sixteen hours of viral gene expression, consistent with the time frame in which progeny virions begin to bud from infected cells. The molecular mechanisms by which Vpu modulates BST-2 likely involves an interaction between the two proteins and the recruitment of a specific SCF E3 ubiquitin ligase complex containing the substrate adaptor β-TrCP to BST-2 by Vpu (Gupta et al., 2009a; Mitchell et al., 2009). In support of an interaction between Vpu and BST-2, the proteins co-localize microscopically in endosomal vesicles and can be co-immunoprecipitated from cellular lysates (Douglas et al., 2009; Neil et al., 2008; Van Damme et al., 2008). Though not yet formally shown, the transmembrane domains (TMDs) of Vpu and BST-2 likely mediate this interaction within the lipid bilayer. Conversely, BST-2 orthologues of

non-human primates are neither virologically counteracted nor removed from the cell surface by Vpu (Gupta et al., 2009a; McNatt et al., 2009; Rong et al., 2009). This resistance to Vpu maps to the BST-2 TMD (Gupta et al., 2009a; McNatt et al., 2009; Rong et al., 2009). McNatt and colleagues constructed plasmids expressing human *bst-2* genes with point mutations within the TMD that correlated with residues found in the TMD of the rhesus BST-2 protein (McNatt et al., 2009). This group concluded that no single change in the human BST-2 TMD abolished Vpu sensitivity. However, several combinatorial mutations elicited an increase in resistance including delGI,T45I (where residues G25 and I26 were deleted and residue T45 was substituted with an isoleucine) and delGI,I33V,I36L (where residues G25 and I26 were deleted, residue I33 was substituted with a valine and residue I36 was mutated to a leucine). McNatt also noted that residues V30 and P40 impart a distinct contribution to Vpu sensitivity. Exchange of the TMDs from human and rhesus BST-2 conferred complete resistance of human BST-2 and sensitivity of the rhesus BST-2 protein to HIV-1 Vpu (McNatt et al., 2009). Gupta also emphasized the importance of residue T45 in the human BST-2 protein, concluding that mutation of this residue to an isoleucine substantially reduces the sensitivity of human BST-2 to HIV-1 Vpu, without affecting antiviral activity. These investigators also noted that substitution of this residue abrogates the Vpu mediated depletion of cellular steady state levels of BST-2, providing additional evidence in favor of the importance of BST-2 degradation for the virus to overcome its antiviral effects (Gupta et al., 2009a). Both groups, as well as that of Rong and colleagues, agree that the TMD of human BST-2 is not only necessary but is also sufficient for the species specificity of Vpu-responsiveness (Gupta et al., 2009a; McNatt et al., 2009; Rong et al., 2009). These data support a model in which the TMDs of the two proteins interact, potentially directly, although the structural basis of this interaction remains to be elucidated. The study by Perez-

Caballero and colleagues provided further evidence for the interaction of HIV-1 Vpu with the transmembrane domain of BST-2 and the incorporation of BST-2 into virions (Perez-Caballero et al., 2009). This group hypothesized that if the incorporation of BST-2 into virions was important for the restriction of particle release, then the HIV-1 Vpu protein should prevent incorporation of the delGPI mutant BST-2 but have no affect on the delTM mutant incorporation. Analysis of virions from 293T cells stably expressing these mutant proteins in the presence and absence of HIV-1 Vpu provided evidence in favor of this hypothesis (Perez-Caballero et al., 2009).

The importance of Vpu-mediated surface down-regulation and the intracellular depletion of BST-2 with respect to the virologic effect of Vpu in spreading infections is not without controversy. Several groups have shown that HIV-1 Vpu causes intracellular depletion and surface down-regulation of human BST-2 in cell lines including HeLa, HEK 293T (exogenously expressed), and A3.01 CD4-positive T lymphoid cells, and these effects correlate with the enhancement of virion release (Bartee et al., 2006; Douglas et al., 2009; Goffinet et al., 2009; Gupta et al., 2009a; Mitchell et al., 2009; Van Damme et al., 2008). However, Miyagi and colleagues further investigated the roles of HIV-1 Vpu and the surface down-regulation and intracellular depletion of BST-2 on the kinetics of viral replication during spreading infections (Miyagi et al., 2009). This group observed minimal changes in the surface expression of BST-2 during the course of infection of CEMx174 and H9 cells, while *vpu* clearly contributed to the net production of cell-free virions. The authors concluded that Vpu enhances virus release in the absence of either surface down-regulation or intracellular depletion of BST-2. This conclusion relies on the assumptions that the accumulation of cell-free virions during spreading infections is a simple correlate of the efficiency of virion release from infected cells and that no other

functions of Vpu are relevant to the rate of viral spread. These assumptions may not be correct: the absence of *vpu* enhances the rate of cell-to-cell viral spread (Gummuluru et al., 2000) and the down-regulation of CD4 by Vpu may affect viral propagation, as reviewed above. In contrast to the conclusions of Miyagi *et al*., Rong and colleagues showed that BST-2 specifically decreased the replication rate of *vpu*-negative HIV-1 in a dose-dependent manner (Rong et al., 2009). These investigators used an inducible system to express BST-2 in the CD4-positive T cell line SupT1, which lacks endogenous BST-2. The ability of Vpu to counteract BST-2 in this system directly correlated with the depletion of BST-2 levels.

Several questions regarding the mechanism of down-regulation of BST-2 by Vpu remain to be answered. In addition to interacting with BST-2, Vpu recruits to BST-2 a β-TrCP-containing E3 ubiquitin ligase complex to modulate the protein either directly or indirectly via ubiquitination (Douglas et al., 2009; Mangeat et al., 2009; Mitchell et al., 2009). As discussed above, the cytoplasmic domain of Vpu contains the sequence $DS^{p}GxxS^{P}$ which recognizes the cellular proteins β-TrCP-1 and -2, which are F-box proteins and substrate adaptors for SCF E3 ubiquitin-ligase complexes. The interaction of Vpu with β-TrCP was first described as the basis for the down-regulation of CD4 by Vpu, however, evidence that a related process occurs in the case of BST-2 include the observations that: 1) the $DS^{P}GxxS^{P}$ sequence in Vpu is required both for optimal virion release and the down-regulation of BST-2, and 2) expression of a dominant-negative β-TrCP or knockdown of endogenous β-TrCP inhibits both the Vpu-mediated enhancement of virion release and the down-regulation of BST-2. Although a consensus is now emerging regarding a key role of β-TrCP as a Vpu co-factor in counteracting BST-2, a number of questions remain. First, is BST-2 ubiquitinated in response to Vpu? Second, what is the consequence of such Vpu-mediated ubiquitination? Evidence has been presented in support of

various outcomes: proteasomal degradation of BST-2, lysosomal degradation of BST-2, and/or post-endocytic endosomal trapping with partial lysosomal degradation (Douglas et al., 2009; Goffinet et al., 2009; Gupta et al., 2009a; Gupta et al., 2009b; Iwabu et al., 2009; Mitchell et al., 2009). In support of the latter, the plasma membrane clathrin adaptor AP-2 and endosomal acidification are required for optimal down-regulation of BST-2 from the cell surface by Vpu (Mitchell et al., 2009). The K5 protein of the Kaposi Sarcoma Virus has also been identified as an antagonist of human BST-2, and the data supporting this inhibition parallel to some extent the results reported for the Vpu protein (Mansouri et al., 2009). The observation that lysines in the short amino-terminal domain of BST-2 are ubiquitinated by the K5 protein resulting in the rapid degradation of BST-2 provides increased incentive for determining if and how BST-2 is ubiquitinated in response to Vpu. Such information would provide a better understanding of the fate of BST-2 following its interaction with Vpu, and it might embrace multiple mechanisms for the down-regulation and degradation of BST-2, some of which could be cell-type specific. Notably, cell type differences and/or experimental formats (transient expression of exogenous BST-2 versus constitutive expression of endogenous protein) could contribute to the different mechanisms proposed thus far for the counteraction of BST-2 by Vpu. Nevertheless, a model is now apparent in which the transmembrane and cytoplasmic domains of Vpu each contribute to the counteraction of BST-2: the transmembrane domain via an interaction with BST-2 and the cytoplasmic domain via recruitment of an E3 ubiquitin ligase complex to cellular membranes containing BST-2. The effect of these interactions is the altered localization of BST-2 within the cell and the counteraction of restricted virion release (See Figure 9 for potential model).

As is a caveat of all *in vitro* studies, the importance and validity of these conclusions will not be fully substantiated until observed within a physiologically relevant *in vivo* host system.

Figure 9. Possible mechanisms by which Vpu enhances virion release from cells. Vpu allows efficient transport of Env proteins to the site of virion assembly. Vpu is synthesized on the rough endoplasmic reticulum and binds CD4 releasing gp160 for processing and cleavage into gp120/gp41 which may be transported to the site of assembly. Vpu may function as a viroporin. Vpu resides within the rough endoplasmic reticulum, *trans*-Golgi network and at the cell surface. It is unknown whether the ability of Vpu to serve as an ion channel functions to enhance virion release at any of these intracellular locations. Vpu removes BST-2 from the site of virion assembly. In the absence of Vpu, BST-2 is expressed at the cell surface. The orientation used by BST-2 to "tether" virions to the surface remains unknown, however, the GPI anchor resides within lipid rafts where HIV-1 virions assemble and bud. This potentiates a model where the N-terminal transmembrane remains anchored within the cell membrane while the C-terminal GPI anchor is embedded in the virion membrane. BST-2 is internalized from lipid rafts on the cell surface by clathrin-mediated endocytosis. Two tyrosine residues within the N-terminal cytoplasmic tail are required for an interaction with a Δα-adaptin of the AP-2 complex (Masuyama et al., 2009). It is possible that in the presence of Vpu the targeting of endocytosed BST-2 containing vesicles is altered for endo-lysosomal degradation. Vpu may also potentially interact with BST-2 in *trans*-Golgi network and target it for lysosomal or proteasomal degradation.

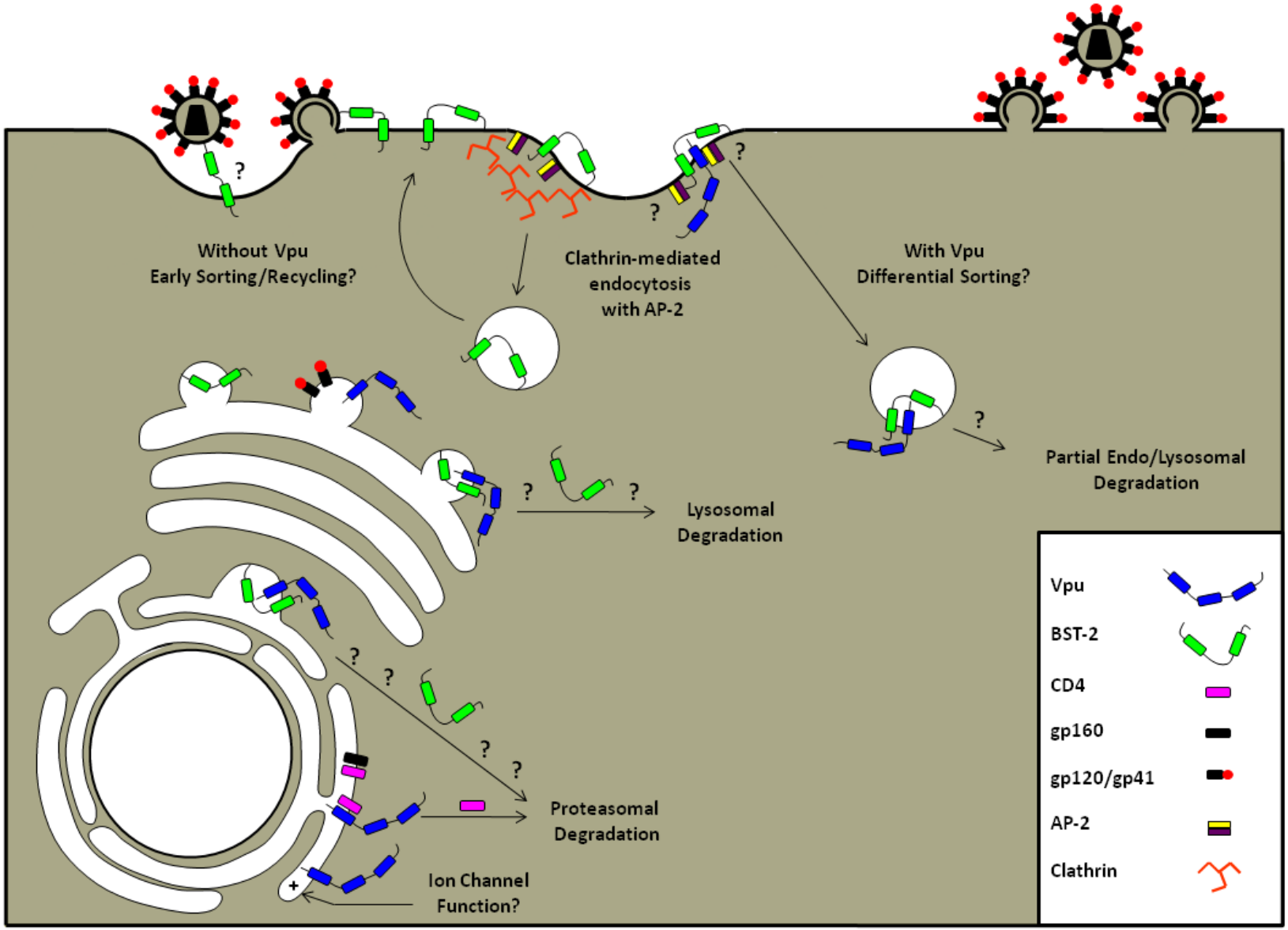
Without Vpu
Early Sorting/Recycling?
Clathrin-mediated
endocytosis
with AP-2
With Vpu
Differential Sorting?
Partial Endo/Lysosomal
Degradation
Lysosomal
Degradation
Proteasomal
Degradation
Ion Channel
Function?
Vpu
BST-2
CD4
gp160
gp120/gp41
AP-2
Clathrin

Pig-tailed (pt) and rhesus (rh) macaque BST-2 proteins have been shown to have antiviral effects on HIV-1 replication that are not Vpu sensitive (McNatt et al., 2009). However, recent studies have determined that SIV Nef is an inhibitor of these orthologues (Jia et al., 2009; Zhang et al., 2009). More research is needed to increase our understanding of the mechanisms by which BST-2 restricts virion release and how Vpu and Nef antagonize this restriction. This will allow us to establish the most effective way to study the role of these interactions *in vivo* and to determine the potential of BST-2 as an antiviral therapeutic. Further research is also needed to determine if specific interactions (indirect or direct) exist between the Vpu and/or the Nef proteins and pt/rhBST-2 proteins that could be used to study the effects of BST-2 *in vivo.* The SHIV/macaque model of disease is an excellent tool for studying the *in vitro* and *in vivo* effects of human and non-human primate BST-2 proteins, because it expresses both the HIV-1 Vpu protein and the $SIV_{mac}239$ Nef gene. SHIVs could potentially be engineered to express Vpu or Nef proteins with mutations that abrogate specific interactions without affecting other functions of both proteins. The intrinsic antiviral defenses encoded by human and non-human primate hosts now includes the TRIM family, APOBEC3 and BST-2 proteins, providing multiple avenues to the development of approaches to the design of novel therapies. The analysis of these endogenous antiviral agents also provides evidence of evolutionary pressure for multiple families of viruses to acquire new or positively selected genes that contribute to species tropism and the barriers to cross-species transmission.

A recent study by a collaborative group analyzed the role of BST-2 in the adaption of Vpu and Nef proteins as well as the potential effects of BST-2 on the evolution of pandemic and non-pandemic HIV-1 strains (Sauter et al., 2009). This group analyzed a panel of *vpu* constructs representing nearly all primate lentiviruses that encode this gene including, HIV-1 groups M, N

and O; SIV_{cpz}; SIV_{gor}; SIV_{gsn}; SIV_{mon}; and SIV_{mus}. The salient results of this study were a selection of the Vpu proteins as a BST-2 antagonist following the transmission of SIV_{cpz} to humans and the differences in the HIV-1 groups both in CD4 down-regulation and BST-2 antagonism. The strains representing the HIV-1 group M both degraded CD4 and used Vpu to antagonize BST-2 rather than Nef of SIV_{cpz}. In contrast, the strains that represent HIV-1 group N antagonize BST-2 but do not degrade CD4, while HIV-1 group O strains down-modulate CD4 but do not antagonize BST-2. This combination of functions may have contributed significantly to the ability of HIV-1 group M strains but not groups N and O to cause the current HIV-1 pandemic. This group observed similar conserved features in all the primate lentivirus Vpus as previously reported by our group (Gomez et al., 2005; Sauter et al., 2009) including a hydrophobic N-terminal transmembrane domain; a putative central α-helical region containing one or two serine residues known to be phosphorylated and required for CD4 down-regulation (Paul and Jabbar, 1997; Schubert and Strebel, 1994); and an acidic C-terminal region. All Vpu proteins except those representative of the HIV-1 group N strains induced CD4 degradation to varying degrees. These results provide evidence for the importance of CD4 degradation in causing disease since the HIV-1 group O strains are able to cause disease in humans, even though this group of viruses has not caused a pandemic. The Vpu proteins isolated from SIV_{cpz}, SIV_{gor} and HIV-1 group O were not efficient at antagonizing BST-2 derived from their respective hosts or those from other species. Only HIV-1 Vpus (group M and N) were capable of counteracting BST-2 proteins derived from humans, chimpanzees and gorillas. The Vpu homologs from SIV_{gsn}, SIV_{mon} and SIV_{mus} were able to antagonize BST-2 proteins both from their respective hosts as well as from other monkey species. Due to the inability of SIV_{cpz}, SIV_{gor} and HIV-1 group O Vpus to counteract BST-2 proteins, this group analyzed the

antagonistic abilities of their respective Nef proteins. The Nef proteins from SIV_{cpz} and SIV_{gor} were shown to effectively counteract the BST-2 proteins derived from their respective hosts but not human BST-2. The sensitivity of these BST-2 proteins was mapped to the same five amino acid region identified by others in the N terminal cytoplasmic domain (Jia et al., 2009; Sauter et al., 2009; Zhang et al., 2009). This group identified trends among all species of viruses and BST-2 proteins with a few exceptions. These few exceptions underline the importance of understanding the role of specific amino acids within both the restriction factor proteins as well as those of the viral proteins for the development of potential therapeutics. This study provides multiple lines of evidence for the facilitation of cross-species transmission by evolutionary pressure imposed by endogenous restriction factors. These adaptations may be key in understanding the ability of specific strains to cause a pandemic and the possible development of therapeutics targeting these regions.

The Role of BST-2 in Release of Primate Lentiviruses Lacking a Vpu Protein

Recent studies have addressed the question of how retroviruses that lack a *vpu* gene, including multiple primate lentiviruses, are efficiently released from cells that express BST-2. Two reports have investigated the ability of $SIV_{mac}239$ Env and Nef proteins to counteract multiple primate BST-2 proteins (Jia et al., 2009; Zhang et al., 2009). While $SIV_{mac}239$ Env was found to possess no antagonistic abilities towards either rhesus or pig-tailed BST-2 (rhBST-2; ptBST-2) proteins, the $SIV_{mac}239$ Nef protein did. The ability of several different Nef proteins from different primate lentiviruses to counteract various primate BST-2 proteins revealed a species-specific bias towards antagonism (Zhang et al., 2009). Both groups showed that the release of SIVΔNef could be inhibited by several primate BST-2 proteins. Both groups

investigated the potential for specific regions or amino acids within the BST-2 proteins that conferred susceptibility to the SIV Nef protein, and both identified an amino acid motif that included residues D/GDIW$_{14-17}$, which is present within the cytoplasmic domain of pig-tailed and rhesus BST-2 but absent in human BST-2. Their results also revealed that this region could be inserted into the human BST-2 protein and impart susceptibility to the SIV Nef protein (Jia et al., 2009; Zhang et al., 2009). Mutation of either the myristoylation site within the N-terminal region of SIV Nef or residues that affect the down-regulation of CD4 completely abolished the ability to counteract BST-2 whereas mutation of a site specifically involved in the down-regulation of MHC-I had no effect (Zhang et al., 2009). SIV$_{mac}$239 Nef down-regulated surface BST-2 in 293T cells stably expressing HA-tagged rhesus BST-2, similar to the results obtained for cell surface down-regulation of human BST-2 by Vpu (Jia et al., 2009). Thus, it appears that SIV$_{mac}$239 Nef functions similarly to HIV-1 Vpu in the counteraction of BST-2 proteins in a species-specific manner.

Unanswered Questions of the Vpu Protein in Viral Pathogenesis

The new exciting data from the last several years has brought some clarity to the role of Vpu in the virus replication cycle and its role in virus pathogenesis. One question that needs to be addressed is whether CD4 down-modulation is more important *in vivo* than the release of infectious virus from cells. Unfortunately, the macaque models do not express a BST-2 protein that is susceptible to HIV-1 Vpu. Thus, macaque models may be able to assess the role of CD4 down-modulation in virus pathogenesis but not virus release. Several studies have shown that a mutant Vpu with either asparagine or glycine substitutions at positions 52 and 56 (Vpu2/6) abolishes Vpu binding to β-TrCP and subsequently CD4 surface down-modulation (Margottin et

al., 1998; Schubert et al., 1994; Singh et al., 2003). Previous studies suggested that the TMD and CD of Vpu were specifically responsible for virus release and CD4 down-modulation, respectively(Schubert et al., 1996a). However, several studies have since provided evidence for contributions of both domains in all of the biological activities of Vpu (Douglas et al., 2009; Hout et al., 2005; Mitchell et al., 2009; Tiganos et al., 1998). Our laboratory has used a simian-human immunodeficiency virus (SHIV) macaque model to study the specific contributions of the HIV-1 Vpu protein to pathogenesis. Using this model our laboratory showed that macaques inoculated with SHIV expressing a Vpu protein with the two serines of the CK-II sites changed to glycines did not lose circulating $CD4^+$ T cells and maintained significantly lower viral loads than macaques inoculated with parental SHIV (Singh et al., 2003). This study suggested that the ability of Vpu to down-modulate CD4 expression directly correlates to the progression of disease in macaques. More recent studies have presented data for the requirement of Vpu binding to β-TrCP for BST-2 surface down-regulation and subsequent release of virions from the cell surface, suggesting that CD4 down-modulation and virus release may involve a common cellular cofactor (Douglas et al., 2009; Mitchell et al., 2009). Thus, elimination of the CK-II sites may have pleiotropic effects on different Vpu functions. These results extend the still unanswered question of "What is the specific contribution of Vpu mediated CD4 degradation to disease progression *in vivo*?" Therefore, the isolation of mutants that affect one function but not the other are needed to definitely address each function in its role in disease progression. It will be interesting to use the macaque model to study the pathogenesis of SHIVs expressing a Vpu protein that binds CD4 and β-TrCP, but is deficient in CD4 surface down-modulation (such as the Vpu_{L63A} and Vpu_{V68A}).

As discussed above, two recent studies have shown that SIV Nef proteins can counteract the BST-2 proteins of non-human primates; pointing to a new role for Nef in lentiviral pathogenesis (Jia et al., 2009; Zhang et al., 2009). However, these studies raise an interesting question about how hBST-2 affects the replication of $SIV_{mac}239$ in CEMx174 cells. This human B-T hybrid cell line expresses copious amounts of hBST-2, and hBST-2 inhibits the release of $SIV_{mac}239$ derived virions (Jia et al., 2009; Miyagi et al., 2009; Zhang et al., 2009). This is somewhat surprising, as many researchers have grown $SIV_{mac}239$ and $SIV_{mac}239\Delta$Nef stock viruses in this cell line (Hammes et al., 1989; Joag et al., 1994; Kestler et al., 1991; Stephens et al., 1998; Yoon et al., 1998). This apparent paradox again raises the question of the extent to which BST-2 restricts the rate of viral replication during multi-cycle, spreading infection.

Perhaps the key question is how the enhancement of virion release by Vpu relates to pathogenesis in the host. During HIV-1 infection of humans or SIV infection of macaques the depletion of CD4+ T cells in the secondary lymphoid organs ultimately results in AIDS, not the depletion of circulating CD4+ T cells. Since CD4+ T cells in these organs are generally in close proximity to one another (e.g., in the paracortical region of the lymph nodes, the periarterial lymphatic sheath of the spleen, and the lymphoid aggregates and Peyer's patches of the gut associated lymphoid tissue), and tethered particles may be infectious, the efficient spread of virus by cell-to-cell transmission may occur even in the absence of Vpu. On the other hand, the observation that three lentiviral proteins, HIV-1 Vpu, SIV-Nef and HIV-2 Env, each counteract BST-2 to enhance virion release, weighs in favor of a key role for this phenotype in the replication of these viruses. Finally, few Vpu proteins from strains other than laboratory-adapted subtype B viruses have been studied. Subtype B HIV-1 isolates account for only 5-10% of the total HIV-1 infections worldwide. Future studies will determine if the counteraction of BST-2

and the enhancement of virion release are common to most or all HIV-1 subtypes and non-human primate lentiviruses that encode the Vpu protein, or if it is instead a phenotype of only a subset of *vpu* genes.

VII. Chapter 2: BST-2 mediated restriction of simian-human immunodeficiency virus

Abstract

Pathogenic simian–human immunodeficiency viruses (SHIV) contain HIV-1 Vpu and SIV Nef, both shown to counteract BST-2 (HM1.24; CD317; tetherin) inhibition of virus release in a species-specific manner. We show that human and pig-tailed BST-2 (hBST-2 and ptBST-2) restrict SHIV particle release and are susceptible to the encoded Vpu and Nef proteins, identifying $SHIV_{KU\text{-}2MC4}$ as a beneficial tool for studying mechanisms of BST-2 mediated viral restriction. We also found that sequential "humanization" of the transmembrane domain (TMD) of the ptBST-2 protein resulted in a fluctuation in sensitivity to HIV-1 Vpu. Finally, we show that the length of the transmembrane domain in human and ptBST-2 proteins is important for BST-2 restriction and susceptibility to Vpu. Taken together, our results emphasize the importance of tertiary structure in BST-2 antagonism and suggest that the HIV-1 Vpu transmembrane domain may have additional functions *in vivo* unrelated to BST-2 antagonism.

Introduction

Human bone marrow stromal cell antigen 2 (BST-2; HM1.24; CD317 or tetherin) was recently identified as a potent inhibitor of the release of multiple enveloped viruses including HIV-1 and SIV (Jouvenet et al., 2009; Kaletsky et al., 2009; Neil et al., 2008; Van Damme et al., 2008). While the exact cellular function of human BST-2 (hBST-2) in the human host is unclear, it has been shown to play a role in regulating the growth and development of B cells, to be involved in the organization of the subapical actin cytoskeleton in polarized epithelial cells (Rollason et al., 2009), and most recently to function as a ligand for ILT7, a receptor that inhibits IFN production from plasmacytoid dendritic cells (Cao et al., 2009). BST-2 is an interferon-

induced, lipid raft-associated, type II integral membrane protein with an unusual topology that is similar in membrane orientation to a neuro-pathogenic form of the prion protein (PrP) (Kupzig et al., 2003). It contains a short cytoplasmic N-terminus followed by a transmembrane domain (TMD), a central extracellular domain predicted to form a coiled-coil structure, and a C-terminal cleavage site predicted to form a glycosyl-phosphatidylinositol (GPI) anchor (Ishikawa et al., 1995; Kupzig et al., 2003). This topology supports membrane-spanning models of restriction of virion release, in which the protein would form dimers providing a physical, protease-sensitive link between the cellular and viral membranes (Perez-Caballero et al., 2009). This model is supported by evidence that hBST-2 is incorporated into nascent virions and that the formation of cysteine-linked dimers is required for hBST-2 restriction of HIV-1 virion release (Ali et al., 2010; Andrew et al., 2009; Fitzpatrick et al., 2010; Habermann et al., 2010; Perez-Caballero et al., 2009). Several studies have provided evidence that viruses including HIV-1 and SIV have evolved to acquire activity against the anti-viral properties of BST-2. The HIV-1 group M Vpu proteins counteract specifically the restriction of human, chimpanzee and gorilla BST-2 proteins, with the exception of Vpu from strains JR-CSF and YU-2, which also antagonized BST-2 proteins derived from Greater-spot nosed and African green monkeys (Jouvenet et al., 2009; Neil et al., 2008; Sauter et al., 2009; Van Damme et al., 2008). The Nef proteins isolated from SIV_{MAC}, SIV_{CPZ}, SIV_{GOR}, and SIV_{AGM} also antagonize the effects of certain non-human primate BST-2 proteins, including those isolated from rhesus (rhBST-2) and pig-tailed (ptBST-2) macaques (Jia et al., 2009; Sauter et al., 2009; Zhang et al., 2009). Similar to other known intrinsic viral restriction factors such as the APOBEC3 and TRIM families of proteins, the ability of specific viral proteins to counteract BST-2 restriction is species-specific (Gupta et al., 2009a; Jia et al., 2009; McNatt et al., 2009; Zhang et al., 2009). Specific domains and amino acids

within these proteins mediate this specificity, allowing small evolutionary changes to confer susceptibility to cross-species infection (Gupta et al., 2009a; Jia et al., 2009; McNatt et al., 2009; Yap et al., 2005; Zhang et al., 2009). The interaction of Vpu with hBST-2 involves the TMDs of both proteins (Douglas et al., 2009; McNatt et al., 2009; Rong et al., 2009). Several studies have identified amino acids within the human, rhesus and tantalus monkey BST-2 proteins required for Vpu sensitivity/resistance. These studies found several combinations of substitutions within the transmembrane domain of hBST-2 that reduced susceptibility to Vpu, including delGI,T45I (where glycine and isoleucine residues at positions 25 and 26 were deleted in combination with the substitution of a threonine at position 45 with an isoleucine) and delGI, I33V, I36L (where the glycine and isoleucine residues at positions 25 and 26 were deleted in combination with the substitution of the isoleucine at position 33 with a valine and mutation of the isoleucine at position 36 to a leucine). These studies also noted the importance of the proline residue at position 40 in sensitivity to Vpu (McNatt et al., 2009). More recent studies focused on the specific role of amino acids within the BST-2 proteins from non-human primates in the susceptibility and resistance to SIV_{MAC} Nef proteins. Several groups obtained similar results that identified an amino acid motif that is present within the cytoplasmic domain (D/GIWK14–17) of pig-tailed and rhBST-2 as important for SIV Nef susceptibility. These investigators showed that this motif could be inserted into the hBST-2 protein and impart susceptibility to the SIV Nef protein (Jia et al., 2009; Zhang et al., 2009).

Simian–human immunodeficiency viruses (SHIVs) have been used extensively for in vivo studies to understand the role of HIV-1 Vpu and Env proteins as well as other SIV proteins in viral pathogenesis. These chimeric viruses express both the HIV-1 Vpu and SIV_{MAC} Nef proteins shown to counteract BST-2 orthologues from human and non-human primates and

possibly represent a useful virus to study these interactions. However, during the selection of pathogenic clones of these viruses, consensus mutations were introduced into several of the encoded genes, especially in the *env* and *nef* genes (Liu et al., 1999; McCormick-Davis et al., 1998). While studies have established that Vpu does not interact with or require other HIV-1 proteins in order to counteract the hBST-2 protein, it is unknown whether the antagonistic abilities of Vpu would be altered in the context of a SHIV. It is also unknown whether the mutations introduced into the other viral proteins encoded within the pathogenic molecular clones of SHIV, specifically Env and Nef, would result in an altered ability to counteract BST-2 proteins expressed by different species (specifically pig-tailed and rhesus macaque BST-2 proteins). In this study, we examined the ability of the pathogenic molecular clone $SHIV_{KU-2MC4}$ to counteract both hBST-2 and ptBST-2, with specific emphasis on the Vpu and Nef proteins. We also assess the characteristics and anti-viral activities of hBST-2 and ptBST-2 proteins with specific amino acid exchanges in the context of SHIVs lacking the HIV-1 *vpu* gene, the SIV *nef* gene, or both. Our results indicate that $SHIV_{KU-2MC4}$ can serve as a model for studying the anti-viral properties of BST-2 proteins and the antagonistic mechanism(s) associated with the Vpu and Nef proteins. We also demonstrate that the transmembrane domain of the BST-2 protein is a determinant of HIV-1 Vpu susceptibility, however, the length of the domain may play more of a role in this rather than specific amino acids and or combinations of residues.

Results

Comparison of the sequence of pig-tailed and rhesus *bst-2* genes

We amplified and sequenced the *bst-2* genes from five rhesus macaques (CX54, AH64, AS05, AS34 and AS89) and seven pig-tailed macaques (CC8X, W004, W005, W006, W007, W013, and W018). The genes isolated from the rhesus macaques exhibited considerable variability compared to genes isolated from pig-tailed macaques, most notably in the N-terminal regions (Figure 10). We observed a 50:50 distribution of arginine and cysteine at position 9, a 60:40 ratio of aspartic acid to glycine at position 14, a 70:30 distribution of valine to isoleucine at position 29 and finally an 80:20 ratio of leucine to proline at position 43. In contrast the pig-tailed sequences did not show significant variability with the exception of one sequence that had a leucine instead of a methionine at position 13. Based on the sequence analysis, we cloned the ptbst-2 gene for expression studies.

Analysis of human and ptBST-2 mutants

We constructed a series of mutations in the human and pig-tailed *bst-2* genes. These are presented in Figure 11. We first examined the expression of each mutant BST-2 protein by transfection of 293 cells with vectors expressing each mutant protein and subsequent Western blot analysis of the cell lysates (Figure 12). Substitution of the leucine and glycine residues at positions 24 and 25 in hBST-2 with alanines or isoleucines (hBST-2-LG/AA or hBST-2-LG/II) consistently resulted in higher levels of expression, suggesting that these mutations may increase the half-life of these proteins. The only other protein with altered expression was the ptBST-2-(ΔDDWIK/+LG). This amino acid substitution resulted in decreased protein expression, which could be due to altered stability of the protein and was not further studied.

Figure 10. Sequence analysis of *bst-2* genes amplified from rhesus (A) and pig-tailed (B) macaques. RNA was isolated from either spleen tissue or PBMC from five rhesus macaques and seven pig-tailed macaques. The *bst-2* gene was amplified from each of these samples and bulk sequenced. The sequences obtained from the rhesus macaques are presented along with the sequences of rhBST-2 from the genomic database. The BST-2 proteins used in this study for both rhesus and pig-tailed macaques were used as references and the dashes represent similar identity.

A

```
CX54 PBMC       1 MAPILYDYRKMPMDDIWKEDGDKRCKLVVGILGLLVIVLLGVLLIFFIIKANSEACQDGLRAVMECRNVT
AH64 SPLEEN      1 ------------------------------------------------------------------------
AS05 SPLEEN     1 --------C----G----------------------------P---------------------------
AS34 SPLEEN     1 --------C-------------------------------------------------------------
AS89 SPLEEN     1 --------C----G----------------------------P---------------------------
CB554098        1 ------------------------------------------------------------------------
FJ943431        1 --------C-------------------I-----------------------------------------
FJ943432        1 --------C----G--------------I-----------------------------------------
GQ304749        1 ------------------------------------------------------------------------
NM_001161666    1 -------------G--------------I-----------------------------------------

CX54 PBMC      71 YLLQQELAEAQRGFRDAEAQAVTCNQTVMALMASLDAEKAQGRKKVEELEGEITTLNHKLQDASAEVERL
AH64 SPLEEN    71 ------------------------------------------------------------------------
AS05 SPLEEN    71 ----------------------------------------H-------------------------------
AS34 SPLEEN    71 ------------------------------------------------------------------------
AS89 SPLEEN    71 ----------------------------------------H-------------------------------
CB554098       71 ------------------------------------------------------------------------
FJ943431       71 ------------------------------------------------------------------------
FJ943432       71 ------------------------------------------------------------------------
GQ304749       71 ------------------------------------------------------------------------
NM_001161666   71 ------------------------------------------------------------------------

CX54 PBMC     141 RRENHVLNARIADTDSASPQDSSCAAEPPLLILLLGLSALLL*
AH64 SPLEEN   141 ---------------------------------------------*
AS05 SPLEEN   141 ---------------------------------------------*
AS34 SPLEEN   141 ---------------------------------------------*
AS89 SPLEEN   141 ---------------------------------------------*
CB554098      141 ---------------------------------------------*
FJ943431      141 ----------------G-S----------V------------*
FJ943432      141 ---------------------------------------------*
GQ304749      141 ---------------------------------------------*
NM_001161666  141 ------------------S-----------------------*
```

B

```
CC8X PBMC       1 MAPILYDYCKMPMDDIWKEDGDKRCKLVVGILGLLVIVLLGVLLIFFIIKANSEACQDGLRAVMECRNVT
WO04 PBMC       1 ------------------------------------------------------------------------
WO05 PBMC       1 ------------L-----------------------------------------------------------
WO06 PBMC       1 ------------------------------------------------------------------------
WO07 PBMC       1 ------------------------------------------------------------------------
WO13 PBMC       1 ------------------------------------------------------------------------
WO18 PBMC       1 ------------------------------------------------------------------------

CC8X PBMC      71 YLLQQELAEAQRGFRDAEAQAVTCNQTVMALMASLDAEKAQGRKKVEELEGEITTLNHKLQDASAEVERL
WO04 PBMC      71 ------------------------------------------------------------------------
WO05 PBMC      71 ------------------------------------------------------------------------
WO06 PBMC      71 ------------------------------------------------------------------------
WO07 PBMC      71 ------------------------------------------------------------------------
WO13 PBMC      71 ------------------------------------------------------------------------
WO18 PBMC      71 ------------------------------------------------------------------------

CC8X PBMC     141 RRENHVLNARIADTDSASSQDSSCAAEPPLLILLLGLSALLL*
WO04 PBMC     141 ---------------------------------------------*
WO05 PBMC     141 ---------------------------------------------*
WO06 PBMC     141 --------------Y--------------------------*
WO07 PBMC     141 ---------------------------------------------*
WO13 PBMC     141 ---------------------------------------------*
WO18 PBMC     141 ---------------------------------------------*
```

Figure 11. The amino acid sequence of the N-terminal region of human and pig-tailed BST-2 proteins, and the BST-2 mutants analyzed in this study.

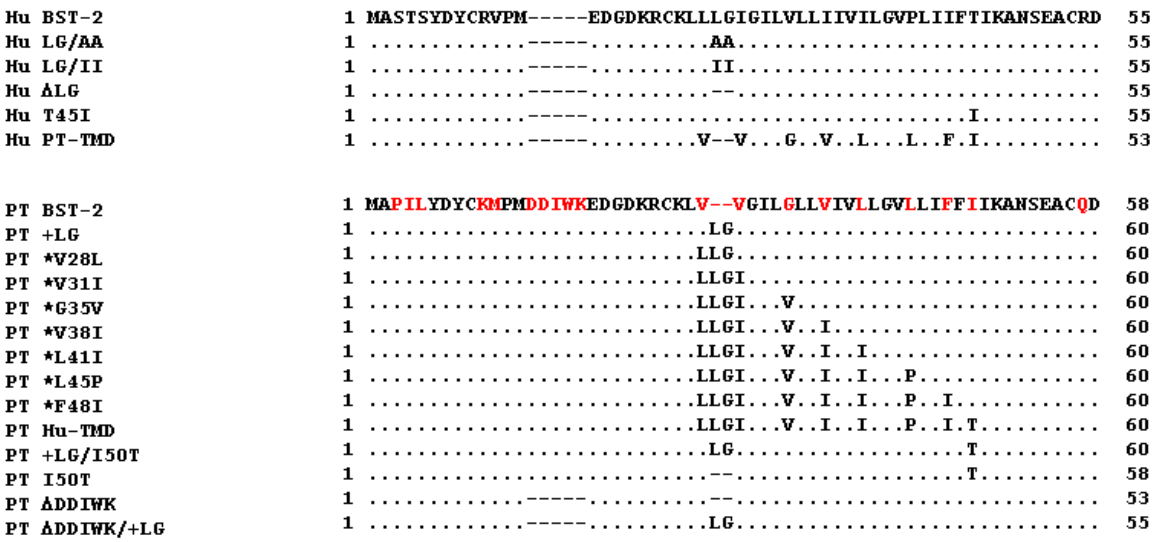
Hu BST-2 1 MASTSYDYCRVPM-----EDGDKRCKLLLGIGILVLLIIVILGVPLIIFTIKANSEACRD 55
Hu LG/AA 1 .....-----.....AA..... 55
Hu LG/II 1 .....-----.....II..... 55
Hu ΔLG 1 .....-----.....--..... 55
Hu T45I 1 .....-----.....I..... 55
Hu PT-TMD 1 .....-----.....V--V...G..V..L...L..F.I..... 53
PT BST-2 1 MAPILYDYCKMPMDDIWKEDGDKRCKLV--VGILGLLVIVLLGVLLIFFIIKANSEACQD 58
PT +LG 1 .....LG..... 60
PT *V28L 1 .....LLG..... 60
PT *V31I 1 .....LLGI..... 60
PT *G35V 1 .....LLGI...V..... 60
PT *V38I 1 .....LLGI...V..I..... 60
PT *L41I 1 .....LLGI...V..I..I..... 60
PT *L45P 1 .....LLGI...V..I..I...P..... 60
PT *F48I 1 .....LLGI...V..I..I...P..I..... 60
PT Hu-TMD 1 .....LLGI...V..I..I...P..I.T..... 60
PT +LG/I50T 1 .....LG.....T..... 60
PT I50T 1 .....--.....T..... 58
PT ΔDDIWK 1 .....-----.....--..... 53
PT ΔDDIWK/+LG 1 .....-----.....LG..... 55

Figure 12. Expression of parental and mutant BST-2 proteins analyzed in this study. 293 cells were transfected with vectors expressing each of the BST-2 proteins. At 48 hours, cell lysates were collected and the nuclei were removed through centrifugation. The lysates were boiled in sample reducing buffer and protein expression was examined through Western blot analysis using a rabbit polyclonal anti-BST-2 antibody (NIH). Panel A. 293 cells transfected with vectors expressing human parental and mutant BST-2 proteins. Panel B. 293 cells transfected with vectors expressing pig-tailed parental and mutant BST-2 proteins.

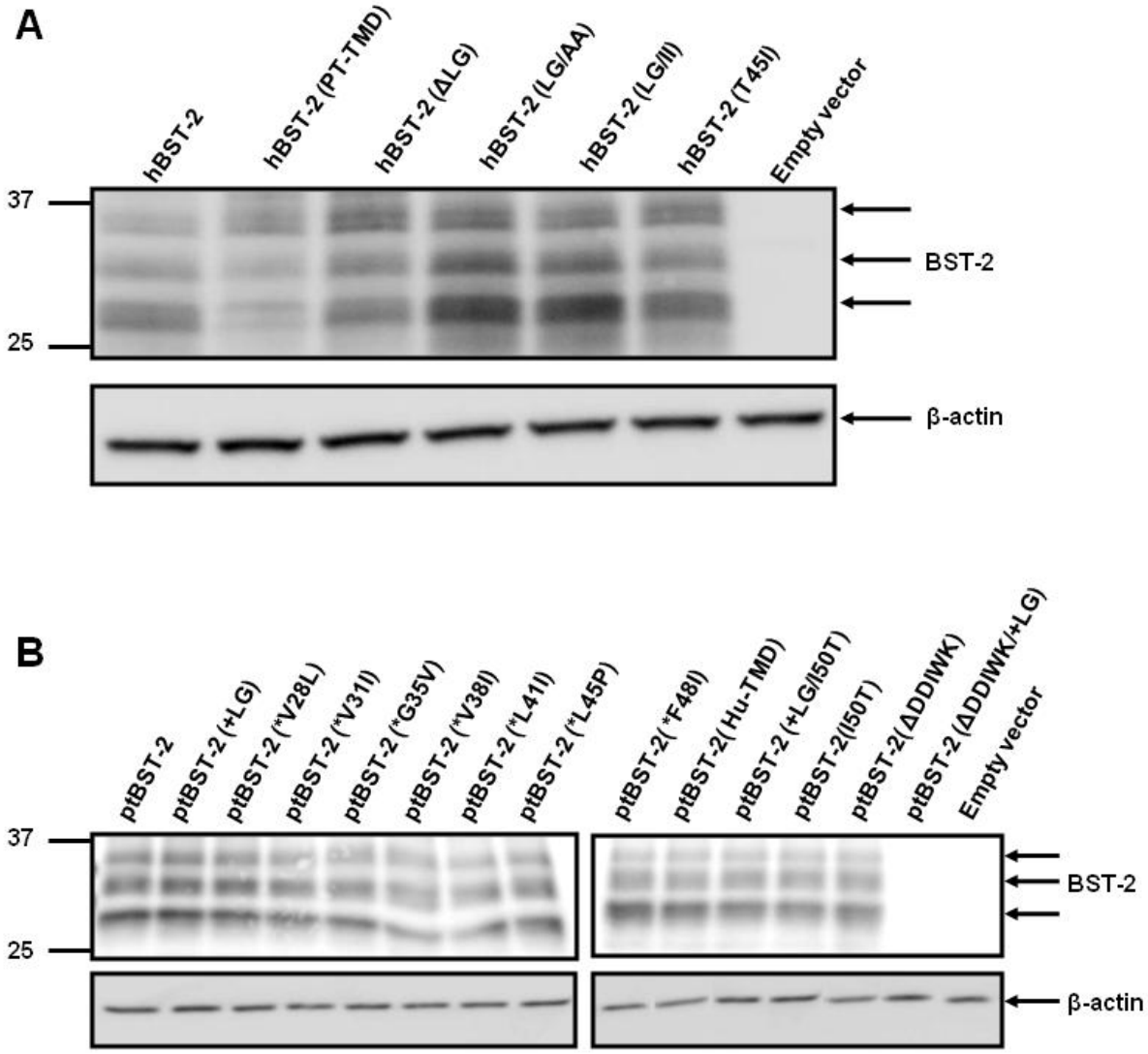
A
hBST-2
hBST-2 (PT-TMD)
hBST-2 (ΔLG)
hBST-2 (LG/AA)
hBST-2 (LG/II)
hBST-2 (T45I)
Empty vector
37
25
BST-2
β-actin
B
ptBST-2
ptBST-2 (+LG)
ptBST-2 (*V28L)
ptBST-2 (*V31I)
ptBST-2 (*G35V)
ptBST-2 (*V38I)
ptBST-2 (*L41I)
ptBST-2 (*L45P)
ptBST-2 (*F48I)
ptBST-2 (Hu-TMD)
ptBST-2 (+LG/I50T)
ptBST-2 (I50T)
ptBST-2 (ΔDDIWK)
ptBST-2 (ΔDDIWK/+LG)
Empty vector
37
25
BST-2
β-actin

SHIV can serve as models for studying BST-2 mediated restriction

In order to examine the ability of the wild-type hBST-2 and ptBST-2 proteins to restrict virus release, we used parental $SHIV_{KU-2MC4}$ to construct three SHIVs that did not express either HIV-1 Vpu ($SHIV_{\Delta Vpu}$), SIV Nef ($SHIV_{\Delta Nef}$) or both proteins ($SHIV_{\Delta Vpu/\Delta Nef}$). HEK 293 cells were co-transfected with plasmids expressing one of the four SHIVs and each of the BST-2 constructs. At 48 hours post-transfection, the supernatants were collected and cleared by centrifugation, the cells were lysed and the nuclei and cellular debris cleared by centrifugation. The supernatants and cell lysates were used to quantify the percent p27 antigen release from cells and the supernatants were also evaluated for 50% tissue culture infectious doses ($TCID_{50}$) (Figure 13). The percent release of p27 in the context of each SHIV in the presence and absence of each BST-2 protein is shown in Figure 13A. All samples were normalized to their respective SHIV empty vector controls. Significance in the restriction of p27 release for the $SHIV_{KU-2MC4}$ samples was determined with respect to the parental $SHIV_{KU-2MC4}$ empty vector control using a Student's t-test (▲). Significance in the restriction of p27 release for the $SHIV_{\Delta Vpu}$, $SHIV_{\Delta Nef}$, and $SHIV_{\Delta Vpu/\Delta Nef}$ samples was calculated with respect to the $SHIV_{KU-2MC4}$ in the presence of each respective BST-2 using a Student's t-test (*). The level of infectious virus released was determined using TZM-bl indicator cells (Figure 13B). The results are represented as the average $\log_{10}$ infectious units. Significance in the restriction of infectious units released was determined with respect to the appropriate empty vector control (•) since Nef has significant effects on virion infectivity that are not associated with BST-2 incorporation (Aiken and Trono, 1995; Chowers et al., 1994). All four SHIVs exhibited similar p27 release in the absence of any BST-2 protein. In the presence of hBST-2, $SHIV_{\Delta Vpu}$ and $SHIV_{\Delta Vpu/\Delta Nef}$ viruses exhibited a significant decrease in p27 release from cells while $SHIV_{\Delta Nef}$ had no decrease in p27 release.

Figure 13. BST-2 dependent down-regulation of SHIV virion release from cells transfected with hBST-2 and ptBST-2. Panel A. p27 release assay. 293 cells were co-transfected with vectors expressing proviral DNA from one of four SHIVs ($SHIV_{KU-2MC4}$, $SHIV_{\Delta Vpu}$, $SHIV_{\Delta Nef}$ or $SHIV_{\Delta Vpu/\Delta Nef}$) and a vector expressing either the hBST-2 or ptBST-2 protein. At 48 hours post-transfection, the supernatants and cell lysates were collected and cleared of cellular debris and nuclei by centrifugation. The p27 content of both the supernatant and cell lysate from each sample was quantified using a p27 antigen capture assay (Zeptometrix) and the percent p27 release calculated. All conditions were run at least three separate times, normalized to their respective SHIV empty vector controls, and the average percent p27 release and standard error calculated. Significance in the restriction of p27 release for the $SHIV_{KU-2MC4}$ samples was determined with respect to the parental $SHIV_{KU-2MC4}$ empty vector control using a Student's *t*-test (▲). Significance in the restriction of p27 release for the $SHIV_{\Delta Vpu}$, $SHIV_{\Delta Nef}$, and $SHIV_{\Delta Vpu/\Delta Nef}$ samples was calculated with respect to the $SHIV_{KU-2MC4}$ in the presence of each respective BST-2 using a Student's *t*-test (*). Panel B. Infectious units assay using TZM-bl indicator cells. Supernatants from transfections described above were added to the TZM-bl cells and serially diluted. At 48 hours post-infection, cells were washed, fixed, and stained for 2 hours. The $TCID_{50}$ for each supernatant was calculated based on wells containing cells expressing β-galactosidase. All conditions were run at least three times and the $TCID_{50}$ calculated. The average $TCID_{50}$ and standard error were calculated. Significance in the restriction of infectivity was determined with respect to the parental SHIV empty vector control using a Student's *t*-test with $p \leq 0.05$ considered significant (•).

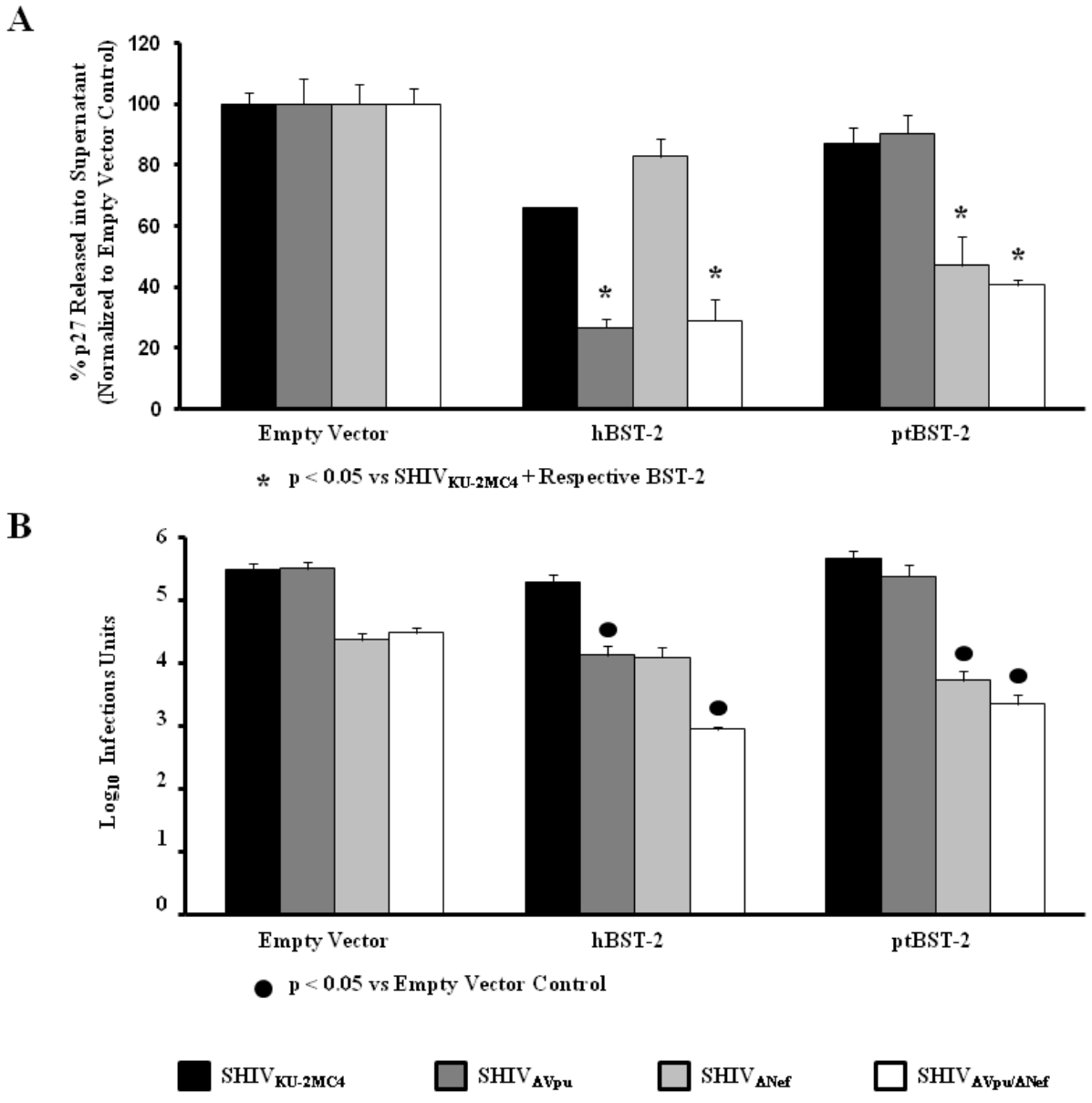
A
% p27 Released into Supernatant (Normalized to Empty Vector Control)
120
100
80
60
40
20
0
Empty Vector
hBST-2
ptBST-2
* p < 0.05 vs SHIV KU-2MC4 + Respective BST-2
B
Log10 Infectious Units
6
5
4
3
2
1
0
Empty Vector
hBST-2
ptBST-2
● p < 0.05 vs Empty Vector Control
SHIV KU-2MC4
SHIV ΔVpu
SHIV ΔNef
SHIV ΔVpu/ΔNef

Similar results were observed in the infectious units assay. In the presence of ptBST-2 protein, only $SHIV_{\Delta Nef}$ and $SHIV_{\Delta Vpu/\Delta Nef}$ showed a decrease in p27 release as well as infectious units released. These results are in congruence with those published by other investigators that found that hBST-2 is susceptible to HIV-1 Vpu and ptBST-2 is sensitive to the SIV Nef (Neil et al., 2008; Van Damme et al., 2008; Zhang et al., 2009), indicating that these SHIVs can serve as models for studying the individual and additive effects of different BST-2 proteins.

Mutant ptBST-2 antagonism of SHIV release

Previous studies showed that the transmembrane domain of the hBST-2 protein dictates its interaction with and susceptibility to HIV-1 Vpu (Gupta et al., 2009a; McNatt et al., 2009; Rong et al., 2009). We determined if cumulative consecutive amino acid substitutions in the transmembrane domain of the ptBST-2 would result in a gradual increase in sensitivity to Vpu. We generated a library of ptBST-2 constructs with successive "humanizing" amino acid substitutions starting from the amino terminal end of the TMD with an insertion of two amino acids, a leucine and a glycine, at positions 29 and 30. We transfected each construct into 293 cells in conjunction with one of four different simian–human immunodeficiency virus expressing plasmids. The supernatants and cell lysates were used to quantify the percent p27 antigen release from cells and the supernatants were also evaluated for the number of infectious doses ($TCID_{50}$) (Figure 14). The percent release of p27 in the context of each SHIV in the presence and absence of each BST-2 protein is shown in Figure 14A. Results and significance are expressed and calculated similar to Figure 13A. The level of infectious virus released was determined using TZM-bl indicator cells (Figure 14B). Again, the results and significance are expressed and calculated as described for Figure 13B. Surprisingly, a gradual increase in sensitivity to Vpu

Figure 14. BST-2 dependent down-regulation of SHIV virion release from cells transfected with vectors expressing ptBST-2 mutants. Panel A. p27 release assay. 293 cells were cotransfected with vectors expressing proviral DNA from one of four SHIVs ($SHIV_{KU-2MC4}$, $SHIV_{\Delta Vpu}$, $SHIV_{\Delta Nef}$ or $SHIV_{\Delta Vpu/\Delta Nef}$) and a vector expressing either the hBST-2 or ptBST-2 protein. At 48 hours post-transfection, the supernatants and cell lysates were collected and cleared of cellular debris and nuclei by centrifugation. The p27 content of both the supernatant and cell lysate from each sample was quantified using a p27 antigen capture assay (Zeptometrix) and the percent p27 release calculated. All conditions were run at least three separate times, normalized to their respective SHIV empty vector controls, and the average percent p27 release and standard error calculated. Significance in the restriction of p27 release for the $SHIV_{KU-2MC4}$ samples was determined with respect to the parental $SHIV_{KU-2MC4}$ empty vector control using a Student's *t*-test (▲). Significance in the restriction of p27 release for the $SHIV_{\Delta Vpu}$, $SHIV_{\Delta Nef}$, and $SHIV_{\Delta Vpu/\Delta Nef}$ samples was calculated with respect to the $SHIV_{KU-2MC4}$ in the presence of each respective BST-2 using a Student's *t*-test (*). Panel B. Infectious units assay using TZM-bl indicator cells. Supernatants from transfections described above were added to the TZM-bl cells and serially diluted. At 48 hours post-infection, cells were washed, fixed, and stained for 2 hours. The $TCID_{50}$ for each supernatant was calculated based on wells containing cells expressing β-galactosidase. All conditions were run at least three times and the average $TCID_{50}$ and standard error were calculated. Significance in the restriction of infectivity was determined with respect to the parental SHIV empty vector control using a Student's *t*-test with $p \leq 0.05$ considered significant (•).

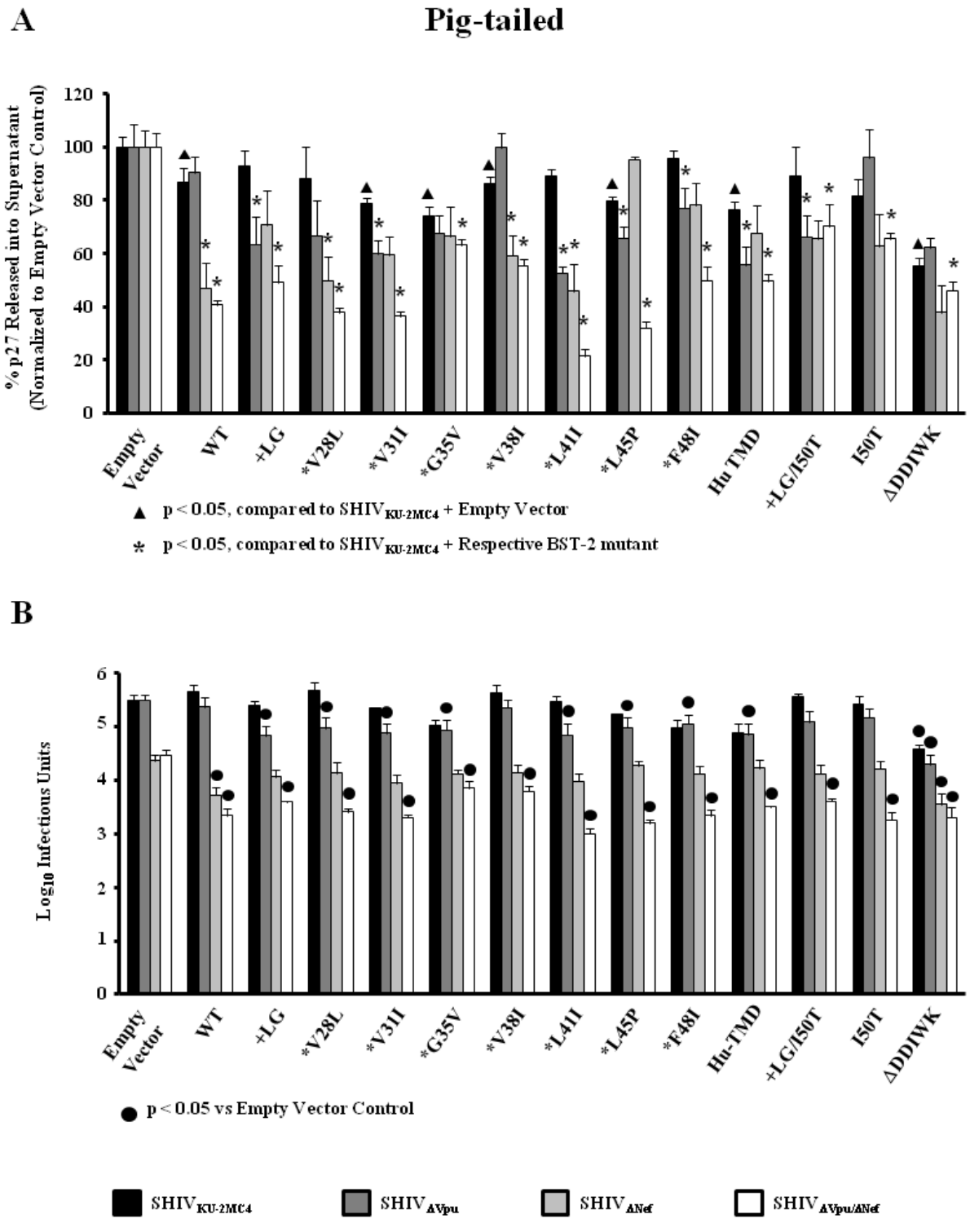
A
Pig-tailed
% p27 Released into Supernatant (Normalized to Empty Vector Control)
120
100
80
60
40
20
0
Empty Vector
WT
+LG
*V28L
*V31I
*G35V
*V38I
*L41I
*L45P
*F48I
Hu TMD
+LG/I50T
I50T
ΔDDIWK
▲ p < 0.05, compared to SHIV KU-2MC4 + Empty Vector
* p < 0.05, compared to SHIV KU-2MC4 + Respective BST-2 mutant
B
Log10 Infectious Units
6
5
4
3
2
1
0
Empty Vector
WT
+LG
*V28L
*V31I
*G35V
*V38I
*L41I
*L45P
*F48I
Hu-TMD
+LG/I50T
I50T
ΔDDIWK
● p < 0.05 vs Empty Vector Control
SHIV KU-2MC4
SHIV ΔVpu
SHIV ΔNef
SHIV ΔVpu/ΔNef

was not observed. We observed that most mutations resulted in BST-2 sensitivity to HIV-1 Vpu but the level was random in distribution. Mutations that significantly increased sensitivity to Vpu, including substitution of the leucine at position 41 with an isoleucine, did not retain this phenotype with additional "humanizing" amino acid substitutions. This indicates that the substitutions were not sufficient for the interaction with and antagonism by HIV-1 Vpu and suggests that their effect on the spatial orientation of the TMD within the membrane is also important.

The length of the transmembrane domain is important for hBST-2 susceptibility to Vpu

Our results shown in Figure 14 indicated that insertion of the two residues in the transmembrane domain of ptBST-2 alone significantly increased the susceptibility to HIV-1 Vpu. These results were confirmed by quantifying the level of infectious virus released using TZM-bl indicator cells (Figure 14B). These results suggested that the length of the transmembrane domain may be important for Vpu antagonism. To test this hypothesis, we generated additional hBST-2 constructs with different amino acid substitutions in the transmembrane domain. These constructs included hBST-2 proteins in which the TMD was replaced with the TMD from ptBST-2 (hBST-2-PT-TMD), the leucine and glycine residues at positions 24 and 25 were substituted with alanines (hBST-2-LG/AA), the residues at positions 24 and 25 were substituted with hydrophobic, isoleucine residues (hBST-2-LG/II), or the two residues were deleted (hBST-2-ΔLG). These plasmids were used in the same virion release assay described above to determine the percent virion release (Figure 15A). The hBST-2-PT-TMD protein was no longer susceptible to any viral protein, similar to results that have been published previously (Douglas et al., 2009; McNatt et al., 2009). The hBST-2-ΔLG protein

exhibited similar results to hBST-2-PT-TMD, while the hBST-2-LG/AA and hBST-2-LG/II proteins produced results similar to the wild-type protein. These data suggest that alteration of the length of the transmembrane domain and not necessarily the hydrophobic nature of the amino acid residues at these positions contributed to the resistance to HIV-1 Vpu. These results were confirmed by quantifying the levels of infectious virus released using TZM-bl indicator cells (Figure 15B). The results and significance for both assays are expressed and calculated as described for Figure 13.

Deletion of residues 13–17 in the ptBST-2 decreases sensitivity to SHIV Nef

In order to study the susceptibility of the ptBST-2 mutants to the SIV_{MAC} Nef protein encoded in our SHIVs, we generated a construct that expressed a protein with a deletion in the region previously shown to be sufficient for antagonism by Nef. Deletion of residues 13–17 within this region (ptBST-2-ΔDDIWK) decreased susceptibility of the protein to SIV_{MAC} Nef and resulted in a decrease in p27 released from cells transfected with all four SHIV constructs (Figure 14A). These results are in accordancewith those published previously that residues 14–17within the rhesus BST-2 protein determine susceptibility to SIV_{MAC} Nef. Again, these results were confirmed using TZM-bl cell assays that indicated a similar level of infectious virus (Figure 14B).

Figure 15. BST-2 dependent down-regulation of SHIV virion release from cells transfected with vectors expressing hBST-2 mutants. Panel A. p27 release assay. 293 cells were co-transfected with vectors expressing proviral DNA from one of four SHIVs ($SHIV_{KU-2MC4}$, $SHIV_{\Delta Vpu}$, $SHIV_{\Delta Nef}$ or $SHIV_{\Delta Vpu/\Delta Nef}$) and a vector expressing either the hBST-2 or ptBST-2 protein. At 48 hours post-transfection, the supernatants and cell lysates were collected and cleared of cellular debris and nuclei by centrifugation. The p27 content of both the supernatant and cell lysate from each sample was quantified using a p27 antigen capture assay (Zeptometrix) and the percent p27 release calculated. All conditions were run at least three separate times, normalized to their respective SHIV empty vector controls, and the average percent p27 release and standard error calculated. Significance in the restriction of p27 release for the $SHIV_{KU-2MC4}$ samples was determined with respect to the parental $SHIV_{KU-2MC4}$ empty vector control using a Student's *t*-test (▲). Significance in the restriction of p27 release for the $SHIV_{\Delta Vpu}$, $SHIV_{\Delta Nef}$, and $SHIV_{\Delta Vpu/\Delta Nef}$ samples was calculated with respect to the $SHIV_{KU-2MC4}$ in the presence of each respective BST-2 using a Student's *t*-test (*). Panel B. Infectious units assay using TZM-bl indicator cells. Supernatants from transfections described above were added to the TZM-bl cells and serially diluted. At 48 hours post-infection, cells were washed, fixed, and stained for 2 hours. The $TCID_{50}$ for each supernatant was calculated based on wells containing cells expressing β-galactosidase. All conditions were run at least three times and the average $TCID_{50}$ and standard error were calculated. Significance in the restriction of infectivity was determined with respect to the parental SHIV empty vector control using a Student's *t*-test with $p \leq 0.05$ considered significant (•).

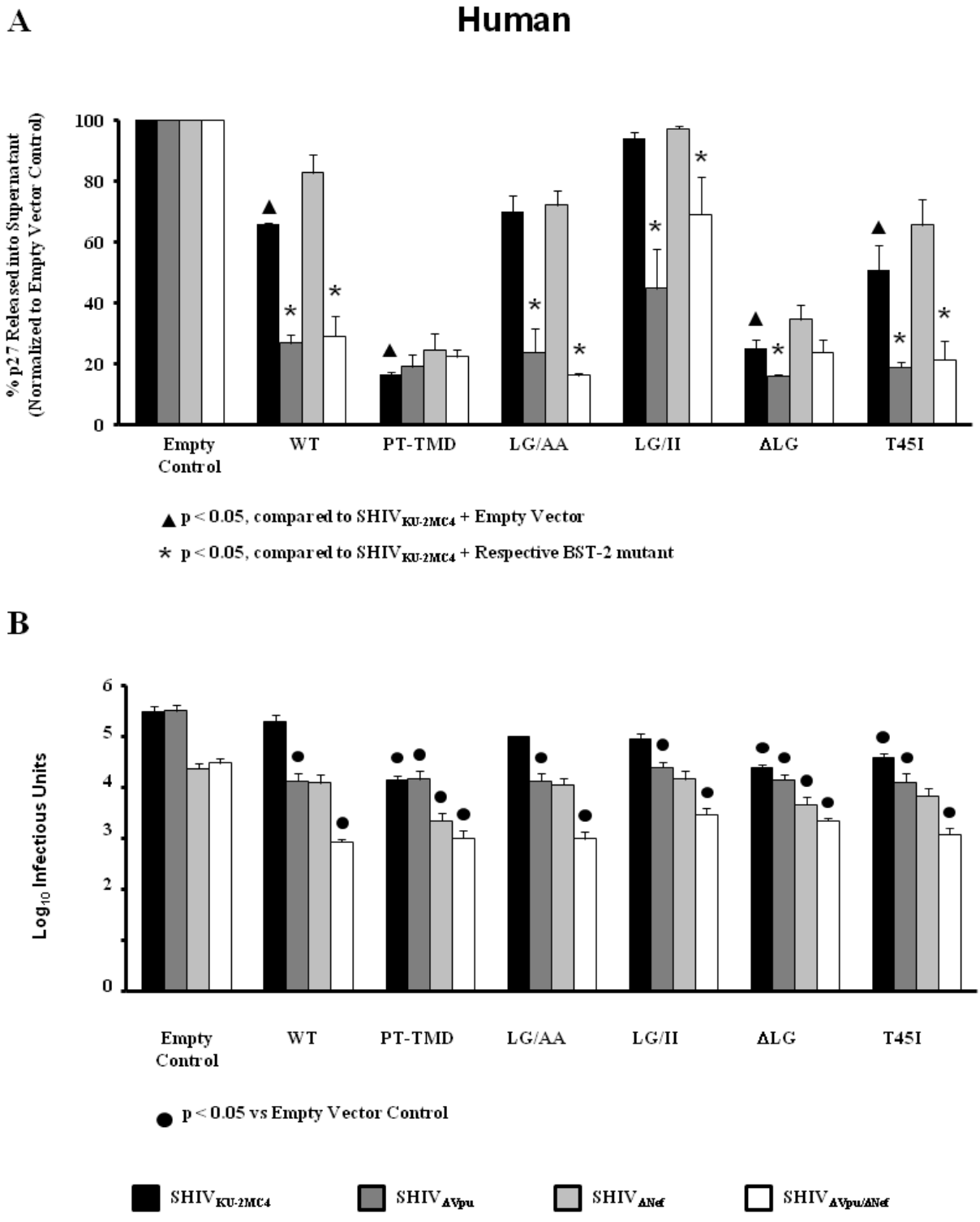
A
Human
% p27 Released into Supernatant (Normalized to Empty Vector Control)
100
80
60
40
20
0
Empty Control
WT
PT-TMD
LG/AA
LG/II
ΔLG
T45I
▲ p < 0.05, compared to SHIV KU-2MC4 + Empty Vector
* p < 0.05, compared to SHIV KU-2MC4 + Respective BST-2 mutant
B
Log10 Infectious Units
6
5
4
3
2
0
Empty Control
WT
PT-TMD
LG/AA
LG/II
ΔLG
T45I
● p < 0.05 vs Empty Vector Control
SHIV KU-2MC4
SHIV ΔVpu
SHIV ΔNef
SHIV ΔVpu/ΔNef

Discussion

Previous studies have shown that BST-2 restricts HIV-1 and SIV_{MAC} in a species-specific manner with these effects being counteracted by HIV-1 Vpu and SIV Nef (Jia et al., 2009; McNatt et al., 2009; Neil et al., 2008; Van Damme et al., 2008; Zhang et al., 2009). SHIVs that express both of these proteins have been used extensively to study the effects of these and other viral proteins in vivo. Thus, one goal of these studies was to determine if SHIVs would counter human and pig-tailed BST-2 proteins and if specific mutations in these primate BST-2 proteins would increase or decrease sensitivity to Vpu and Nef. We approached this by characterizing BST-2-mediated restriction of the unmodified $SHIV_{KU-2MC4}$ and three additional SHIVs that did not express Vpu, Nef or both proteins. Our results demonstrate that SHIVs display similar properties as HIV-1 and SIV with respect to human and pig-tailed BST-2. That is, $SHIV_{\Delta Vpu}$ was restricted by hBST-2 while $SHIV_{\Delta Nef}$ was inhibited by ptBST-2. This suggests that the amino acid substitutions in the Nef protein during adaptation of $SHIV_{KU-2MC4}$ to cause disease in rhesus and pig-tailed macaques did not result in a loss of Nef antagonism against ptBST-2.

The resistance of the ptBST-2 to SHIV Vpu and its sensitivity to SHIV Nef allowed us to characterize the role of individual residues within the transmembrane domain of the ptBST-2 associated with these properties. While previous studies presented data on the role of the individual residues of the hBST-2 TMD, we used a series of cumulative sequential amino acid substitutions to "humanize" the ptBST-2 TMD (Gupta et al., 2009a; McNatt et al., 2009; Rong et al., 2009). Our results are in accordance with these groups in that the two amino acid deletions in the ptBST-2 TMD (L29 and G30) are key residues involved in the susceptibility to HIV-1 Vpu. However, our analysis of a series of proteins with a progressive "humanizing" of the TMD revealed a fluctuation in sensitivity to HIV-1 Vpu. All of the ptBST-2 transmembrane domain

mutants displayed susceptibility to HIV-1 Vpu, SIV Nef or both. However, the four mutations that displayed the most interesting effects were ptBST-2(+LG), ptBST-2(*G35V), ptBST-2(*V38I) and ptBST-2(*L41I). Insertion of the leucine and glycine at positions 29 and 30 clearly increased the sensitivity of the protein to HIV-1 Vpu without significantly altering the susceptibility to SIV Nef. Substitution of the glycine at position 35 with a valine eliminated the sensitivity to SHIV Vpu gained with the preceding mutations. This substitution also seemed to eliminate sensitivity to SHIV Nef. Mutation of the valine at position 38 to an isoleucine resulted in a complete loss of the sensitivity to HIV-1 Vpu gained with mutation of the preceding residues, but again without alteration of SHIV Nef susceptibility. Finally, substitution of the leucine at position 41 with an isoleucine resulted in an increased sensitivity to HIV-1 Vpu and an increase in the additive effects of Vpu and Nef. Any alterations in Nef susceptibility observed with the transmembrane domain mutations are most likely due to an alteration in the positioning of the cytoplasmic tail along the membrane. These results suggest that the overall structure, the spatial orientation of amino acids in the membrane, or possibly the tilt angle of the TMD in the membrane may be important factors. Insertion of the leucine and glycine at positions 29 and 30 into the ptBST-2 resulted in the most observable effect on the antagonism by Vpu leading us to hypothesize that the length of the transmembrane domain was important for this interaction. We tested this hypothesis by constructing three mutants of hBST-2 with either deletion of the LG (ΔLG), or substitution with amino acids with either a small hydrophobic side group (LG/AA) or a larger hydrophobic side group (LG/II). The hBST-2ΔLG deletion restricted particle release of all four SHIVs tested, while the LG/AA and LG/II mutants remained highly sensitive to Vpu and resistant to Nef. These results indicate that the length and not the degree of hydrophobicity of these amino acids is critical in defining susceptibility to HIV-1 Vpu.

The level of surface expression of hBST-2 compared to ptBST-2 is unknown and it is possible that differences in these levels may help explain the possible differences in viral restriction efficiency as well as mechanisms of antagonism by viral proteins. Differences in surface expression could be due to differences in protein expression, internalization rates and/or turnover rates of each species of protein. Studies examining these properties are necessary in order to further elucidate the mechanisms by which different species of BST-2 proteins restrict virion release and how they are antagonized by different viral proteins. Studies within our laboratory suggest that there are differences in expression levels of the hBST-2 compared to the ptBST-2 and present a possible explanation for the differences in restriction efficiency observed in this study (unpublished data). However, the studies presented herein reflect intraspecies analysis and do not indicate cross-species examination. This study introduces SHIV as an in vitro model for studying BST-2 mediated restriction laying a basis for future studies that could lead to an in vivo model. These results also emphasize the necessity for studies focused on the structural components of BST-2 and their contributions to the anti-viral properties of the protein. These studies support the findings by (Perez-Caballero et al., 2009) that the amino acid identity of the protein is less significant than the structural properties in virion restriction. Taken together, these results provide a basis for the development of new small molecule inhibitors designed to mimic the effects of BST-2 on multiple enveloped viruses.

The physiological relevance of the anti-HIV activity of BST-2 has not yet been demonstrated in vivo. Previously published studies from our laboratory demonstrate that a functional Vpu protein is important for pathogenicity of SHIV in the pig-tailed macaque model, which expresses a Vpu resistant BST-2, suggesting a role for other functions of Vpu in viral pathogenesis (Hout et al., 2005; McCormick-Davis et al., 2000a; Singh et al., 2003; Singh et al.,

2001; Stephens et al., 2002). Of note are our studies using a SHIV expressing the Vpu_{M2} protein ($SHIV_{M2}$). This protein has been shown to down-regulate CD4 from the surface of $CD4^+$ cells, however it is unable to rescue virion release from cells expressing high levels of BST-2 (data not shown). $SHIV_{M2}$ caused a loss of $CD4^+$ T cells within one month, high viral loads and histological lesions in infected macaques (Hout et al., 2006b). These studies provide evidence for additional functions of the Vpu transmembrane domain *in vivo* unrelated to BST-2 antagonism, which are potentially related to the ion channel properties exhibited by Vpu. Regardless of the physiological relevance of its anti-viral properties, BST-2 does represent a significant *in vitro* tool for examining the effects of different Vpu proteins, be they distinct subtypes or mutants, on protein function. Just as the BST-2 transmembrane domain has amino acids/structures that are critical for interactions with Vpu, there are most likely amino acids within the Vpu transmembrane domain that are also critical for these interactions. It will be of interest to identify these residues and determine if they are conserved in different subtypes of HIV-1.

Materials and Methods

Plasmid Construction

The human bst-2 (hBST-2) gene was amplified from a plasmid expressing a full length cDNA of hBST-2 (Origene) using oligonucleotides containing 5′ BamHI and 3′ XhoI sites. The fragment was ligated into a pcDNA3.1(+) expression vector (Promega) digested with BamHI and XhoI restriction enzymes. The plasmid was sequenced to ensure no mutations were introduced during the cloning process. The pig-tailed bst-2 (ptBST-2) and rhesus bst-2 (rhBST-2) genes were amplified from cDNA generated from PBMC isolated from uninfected juvenile pig-tailed

and rhesus macaques using a reverse-transcriptase polymerase chain reaction (RT-PCR). Oligonucleotides used contained 5′ BamHI and 3′ NotI restriction sites. The resulting fragment was ligated into a pcDNA3.1(+) expression vector (Promega) digested with BamHI and NotI restriction enzymes. Mutations introduced into all plasmids were accomplished using a QuikChange site-directed mutagenesis kit (Stratagene) according to the manufacturer's protocol. All plasmids were sequenced to ensure the validity of the mutations and that no other mutations were introduced during the cloning process.

Sequence Analysis of ptBST-2 and rhBST-2 Variants

The *bst-2* gene was amplified from five and seven different rhesus and pig-tailed macaque spleen tissues or PBMC, respectively, using a one-tube Titan reverse-transcriptase kit (Roche). The resulting fragments were purified using a Qiaquick Gel Extraction kit (Qiagen) and subjected to sequence analysis.

Proviral DNA Plasmid Construction

The construction of molecular clone $SHIV_{KU-2MC4}$ has been described previously (Liu et al., 1999). In order to construct $SHIV_{\Delta Vpu}$, $SHIV_{\Delta Nef}$, and $_{SHIV\Delta Vpu/\Delta Nef}$ another molecular clone Δ*vpu*Δ*nef*SHIVPPc was used and the construction of this clone has been described previously (Joag et al., 1998b). A 1444 base pair (bp) fragment was removed from$SHIV_{KU-2MC4}$ using restriction enzymes SphI and NheI. This fragment was replaced with the corresponding 1382 bp fragment of Δ*vpu*Δ*nef*SHIVPPc. The resulting construct expressed a Vpu protein with a 62 bp

deletion and an inactive start codon ($SHIV_{\Delta Vpu}$). A 525 bp fragment was removed from $SHIV_{KU\text{-}2MC4}$ using restriction enzymes BamHI and NcoI. This fragment which encodes for part of the *gp41* and *nef* genes was replaced with the corresponding 321 bp fragment of Δ*vpu*Δ*nef*SHIVPPc. The resulting construct expressed a *nef* gene with a 204 bp deletion that included the start codon ($SHIV_{\Delta Nef}$). A 525 bp fragment was removed from $SHIV_{\Delta Vpu}$ using restriction enzymes BamHI and NcoI. This fragment which encoded for part of the *gp41* and *nef* genes was replaced with the corresponding 321 bp fragment of Δ*vpu*Δ*nef*SHIVPPc. The resulting construct expressed a *vpu* gene with a 62 bp deletion and an inactive start codon and a *nef* gene with a 204 bp deletion that included the start codon ($SHIV_{\Delta Vpu/\Delta Nef}$).

Cell Lines and Transfections

The TZM-bl cell line was was obtained through the NIH AIDS Research and Reference Reagent Program, Division of AIDS, NIAID, NIH: TZM-bl from Dr. John C. Kappes, Dr. Xiaoyun Wu and Tranzyme Inc. The HEK 293 and TZM-bl cell lines were maintained in DMEM supplemented with 10% fetal bovine serum (FBS), gentamicin (5 μg per ml) and penicillin/streptomycin (100 U/100 μg per ml, respectively). Both cell lines were transfected using a cationic polymer (polyethylenimine) transfection reagent (ExGen™ 500, MBI Fermentas) using the manufacturer's protocol.

Western Blot Assays

Human 293 cells (10^5) were seeded into each well of a 24-well tissue culture plate 24 hours prior to transfection. Cells were transfected as described above with 1 μg of plasmid expressing full length SHIV proviral DNA (either $SHIV_{KU\text{-}2MC4}$, $SHIV_{\Delta Vpu}$, $SHIV_{\Delta Nef}$, and/or $SHIV_{\Delta Vpu/\Delta Nef}$) and empty vector or 10 ng of plasmid expressing various untagged *bst-2* genes. Cells were incubated at 37C in 5% CO2 atmosphere for 48 hours. Cells were lysed in 200 μl of 1X RIPA buffer (50 mM Tris–HCl, pH 7.5; 50 mM NaCl; 0.5% deoxycholate; 0.2% SDS; 10 mM EDTA) and the nuclei removed through high speed centrifugation. Cell lysates were made 1X with sample reducing buffer (100 mM Tris–HCl pH 6.8, 30% glycerol, 2% SDS, 10% 2-mercaptoethanol, 0.05% bromophenol blue) and boiled for 5 minutes. Samples were separated on SDS-PAGE gels and transferred to PVDF membrane. BST-2 proteins were detected using a rabbit polyclonal anti-BST-2 primary antibody obtained through the AIDS Research and Reference Reagent Program, Division of AIDS, NIAID, NIH: Anti-Bst-2 (cat# 11722) from Drs. Klaus Strebel and Amy Andrew (1:1000 dilution). The secondary antibody used was an alkaline phosphatase-conjugated goat anti-rabbit IgG (whole molecule) (Sigma). Alkaline phosphatase substrate used was CDP-Star (Sigma) for chemiluminescent detection and an LAS-4000 Imager (Fujifilm) was used for the visualization and analysis of proteins.

Virion Release Assays

Human 293 cells (10^5) were seeded into each well of a 24-well tissue culture plate 24 hours prior to transfection. Cells were transfected as described above with 1 μg of plasmid expressing full length SHIV proviral DNA (either $SHIV_{KU\text{-}2MC4}$, $SHIV_{\Delta Vpu}$, $SHIV_{\Delta Nef}$, or

$SHIV_{\Delta Vpu/\Delta Nef}$) and 10 ng of plasmid expressing various untagged *bst-2* genes. Cells were incubated at 37C in 5% CO_2 atmosphere for 48 hours. Supernatants were collected and cellular debris removed through low speed centrifugation. Cells were lysed in 200 µl of 1X RIPA buffer (50 mM Tris–HCl, pH 7.5; 50 mM NaCl; 0.5% deoxycholate; 0.2% SDS; 10 mM EDTA) and the nuclei removed through high speed centrifugation. The amount of p27 present within the virion containing supernatant and the cell lysates was determined using a commercially available p27 ELISA kit (Zeptometrix Incorporated) and percent p27 release calculated. All conditions were run at least three separate times, normalized to the empty vector control, and the average percent p27 release and standard error calculated. Significance in the restriction of p27 release for the $SHIV_{KU-2MC4}$ samples was determined with respect to the parental $SHIV_{KU-2MC4}$ empty vector control using a Student's *t*-test with $p<0.05$ considered significant. Significance in the restriction of p27 release for the $SHIV_{\Delta Vpu}$, $SHIV_{\Delta Nef}$, and $SHIV_{\Delta Vpu/\Delta Nef}$ samples was calculated with respect to the $SHIV_{KU-2MC4}$ in the presence of each respective BST-2 using a Student's *t*-test with $p<0.05$ considered significant.

Infectious Units Release Assays

TZM-bl cells (10^4) cells were seeded into each well of a 96-well tissue culture plate 24 hours prior to infection. Supernatants collected from either the 293 cells co-transfected with SHIV and BST-2 expressing plasmids as described above were added to the TZM-bl cells and serially diluted. At 48 hours post-infection, cells were washed twice in 1X PBS and fixed in a solution of 0.25% glutaraldehyde and 0.8% formaldehyde in PBS for 5 minutes at room temperature. The cells were washed three times in 1X PBS and covered in staining solution (400

μg per ml X-gal, 4 mM $MgCl_2$, 4 mM $K_3Fe(CN)_6$, 4 mM $K_4Fe(CN)_6$–$3H_2O$ in phosphate-buffered saline) and incubated for 2 hours at 37C. Cells were washed once in 1X PBS and then covered in 1X PBS during counting. The $TCID_{50}$ for each supernatant was calculated based on wells containing cells expressing β-galactosidase. All conditions were run at least three times and the $TCID_{50}$ calculated. The average $TCID_{50}$ and standard error were calculated. Significance in the restriction of infectivity was determined with respect to the parental SHIV empty vector control using a Student's *t*-test with $p<0.05$ considered significant.

VIII. Chapter 3: Different HIV-1 Vpu Subtypes Exhibit Distinct Biological Properties

Abstract

Vpu proteins from HIV-1 group M isolates degrade the virus CD4 receptor and inhibit human BST-2 (hBST-2) in order to enhance viral pathogenesis. In this study, we examined the biological properties of several different HIV-1 Vpu subtype isolates including each protein's intracellular localization, ability to down-modulate CD4 from the cell surface, and the ability to enhance SHIV virion release in the presence of high levels of human BST-2 (hBST-2). Our findings indicate that Vpu protein subtypes A, A2 and C are transported to the cellular plasma membrane more efficiently than Vpu proteins from subtypes B, D, F, and H, which are predominately localized within intracellular compartments. We also show that while all isolates maintained the ability to down-modulate CD4 from the cell surface, subtypes A2 and C were significantly less efficient. Finally, all isolates save subtype F were able to overcome hBST-2 restriction of virion release in HeLa cells. Taken together, these results indicate that different HIV-1 Vpu subtypes exhibit distinct biological properties that potentially regulate the ability of Vpu to enhance pathogenesis and could provide a partial explanation for the disproportionate global distribution of HIV-1 subtypes and the ability of HIV-1 to cause a pandemic.

Introduction

HIV-1 employs several intrinsic mechanisms to ensure viral evolution and survival, including integration into the host genome, a high mutation rate and the ability to evade the immune system. The rapid evolution and continued transmission of HIV-1 into diverse geographic populations has led to unprecedented genetic diversity observed in the current pandemic. Since its introduction into the human population, the pandemic causing HIV-1 Group

M viruses have diverged into nine classifiable subtypes (A, B, C, D, F, G, H, J, and K), sub-subtypes (A1, A2, F1, and F2), circulating recombinant forms and unique recombinant forms. Epidemiological studies have revealed a disproportionate distribution of each subtype both geographically and based on modes of transmission (Arien et al., 2007; Hemelaar et al., 2006; Hu et al., 1999; Neilson et al., 1999; Renjifo et al., 1998). While the trends associated with transmission routes are still controversial, the prevalence of particular subtypes, specifically the worldwide predominance of subtype C viruses, is certain.

The predominance of the subtype C viruses could be due to genetic differences between subtypes, modes of transmissions or differences in socio-cultural behaviors. Evolutionary studies have revealed an array of genotypic differences among HIV-1 subtypes, however these phylogenetically based analyses do not examine the mechanisms by which these genetic differences impact the pathogenicity of the virus. Additional studies have addressed the viral fitness of different HIV-1 subtype isolates, both in PBMC and *ex vivo* tissues. These studies found that subtype C viruses were less fit in peripheral blood mononuclear cell (PBMC) competition assays when compared to all other HIV-1 Group M subtypes (Arien et al., 2005; Ball et al., 2003). However, the subtype C viruses were found to have similar replicative fitness to subtype B viruses in Langerhan cells suggesting that subtype C viruses may be more efficiently transmitted (Ball et al., 2003). Finally, a study comparing the fitness and transmission efficiency of 33 different CCR5 (R5) and CXCR4-tropic (X4) HIV-1 isolates in PBMC and *ex vivo* tissues demonstrated a general order of replicative fitness in PBMC where subtype B and D isolates were slightly more fit than subtype A viruses and significantly more fit than 12 different subtype C viruses (Abraha et al., 2009). However, when analyzed in primary human explants of penial, cervical and rectal tissues, the R5-tropic subtype C viruses were able to compete with all

other R5 isolates. These results suggest that subtype C HIV-1 isolates may exhibit similar transmission efficiencies, but are less fit compared to other Group M HIV-1 isolates to cause disease. Taken together, these studies suggest that different HIV-1 subtypes may have adapted specific molecular determinants to promote prosperity within specific host populations. However, more studies are needed to identify these specific molecular determinants and discern their potential as therapeutic targets.

In this study, we examined the biological properties of seven different HIV-1 Vpu isolates (VpuA, VpuA2, VpuB, VpuC, VpuD, VpuF1, and VpuH). Using a VpuEGFP reporter system developed in our laboratory previously, we determined the intracellular localization of each Vpu isolate and their ability to down-modulate CD4 from the cell surface (Singh et al., 2003). In addition to the down-modulation of CD4 from the cell surface, Vpu also enhances virion release to promote virus spread. Therefore, we also analyzed the ability of each Vpu isolate to enhance virion release using $SHIV_{\Delta Vpu}$, which has been previously described (Ruiz et al., 2010b). Taken together, our results suggest that specific molecular determinants within different Vpu subtypes mediate protein trafficking and function and in turn, affect the role of the Vpu in HIV-1 pathogenesis.

Results

Sequence analysis of different HIV-1 Vpu subtypes

The sequences of the different HIV-1 Vpu subtypes analyzed in this study are depicted in Figure 16. All of the isolates contain a potential tyrosine motif (YxxΦ) proximal to the transmembrane domain. Vpu subtypes A2 (92UG037) and C (96BW16B01) contain a putative dileucine motif ([D/E]xxxL[L/I] overlapping the conserved tyrosine motif. The importance of

these motifs will be discussed later (Chapter 5). The residues that are invariant among all HIV-1 Vpu subtypes are displayed in purple. Each Vpu protein contains an N-terminal region followed by an uncleaved leader sequence/transmembrane domain and a cytoplasmic domain. Two casein kinase II phosphorylation sites that are required for CD4 surface down-regulation are found within the cytoplasmic domain in the "hinge" region.

Different HIV-1 Vpu subtypes are more readily transported to the cellular surface

Previous studies in our laboratory demonstrated that while both a subtype B Vpu isolate (US.HXB2) and a subtype C Vpu isolate (96BW16B01) were localized predominately within the ER and Golgi compartments, the subtype C Vpu isolate was efficiently expressed at the cellular surface (Pacyniak et al., 2005). Based on these results we first analyzed the ability of each of our Vpu subtype isolates to be transported to the cell surface using confocal microscopy. We constructed a series of plasmids expressing each of the *vpu* genes fused in frame to the gene for enhanced green fluorescence protein (eGFP) similar to pc*vpuegfp* and pcvpu_{SC}*egfp* plasmids whose construction has been described previously (Pacyniak et al., 2005; Singh et al., 2003). We transfected human 293 cells with vectors expressing Vpu_{SA}EGFP, Vpu_{SA2}EGFP, VpuEGFP, Vpu_{SC}EGFP1, Vpu_{SD}EGFP, Vpu_{SF}EGFP, or Vpu_{SH}EGFP. At 48 hours post-transfection, these cells were analyzed by laser scanning confocal microscopy. As shown in Figure 17, the Vpu_{SA}EGFP and Vpu_{SA2}EGFP were observed at the cell plasma membrane similar to Vpu_{SC}EGFP1. In contrast, the Vpu_{SD}EGFP, Vpu_{SF}EGFP, or Vpu_{SH}EGFP proteins resided predominately within intracellular compartments similar to VpuEGFP.

Figure 16. Sequence alignment of Vpu proteins used in this study. Residues highlighted in purple are invariant among all Vpu subtypes. The two casein kinase II phosphorylation sites are denoted with (*) symbols. The putative transmembrane domain (black), tyrosine motif (blue), and dileucine motifs (green) within each isolate are identified by color and top-line.

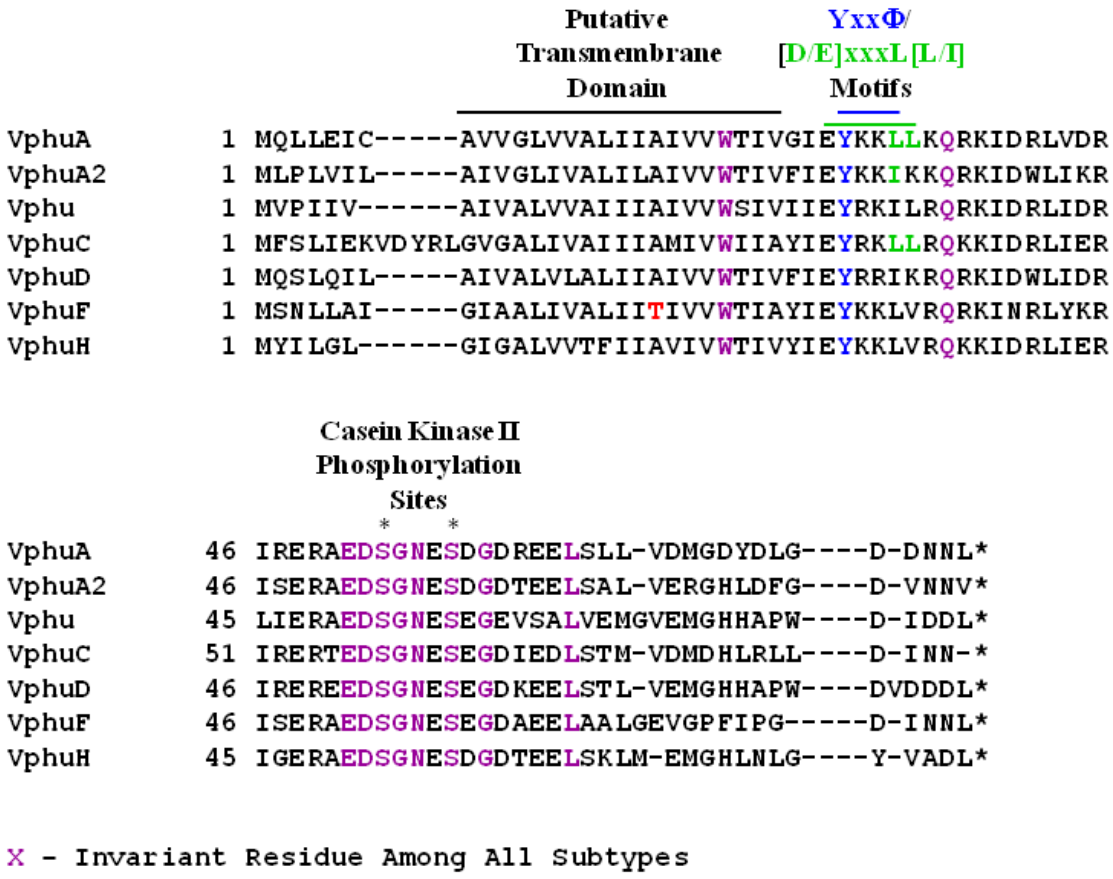

X - Invariant Residue Among All Subtypes

Figure 17. Intracellular localization of Vpu isolates used in this study. 293 cells were transfected with vectors expressing EGFP, Vpu_{SA}EGFP, Vpu_{SA2}EGFP, VpuEGFP, Vpu_{SC}EGFP1, Vpu_{SD}EGFP, Vpu_{SF}EGFP, or Vpu_{SH}EGFP. At 48 hours, cells expressing EGFP were identified and images collected using laser scanning confocal microscopy as described in the Materials and methods section. Panel A. 293 cell transfected with a vector expressing EGFP. Panel B. 293 cell transfected with a vector expressing Vpu_{SA}EGFP. Panel C. 293 cell transfected with a vector expressing Vpu_{SA2}EGFP. Panel D. 293 cell transfected with a vector expressing VpuEGFP. Panel E. 293 cell transfected with a vector expressing Vpu_{SC}EGFP1. Panel F. 293 cell transfected with a vector expressing Vpu_{SD}EGFP. Panel G. 293 cell transfected with a vector expressing Vpu_{SF}EGFP. Panel H. 293 cell transfected with a vector expressing Vpu_{SH}EGFP.

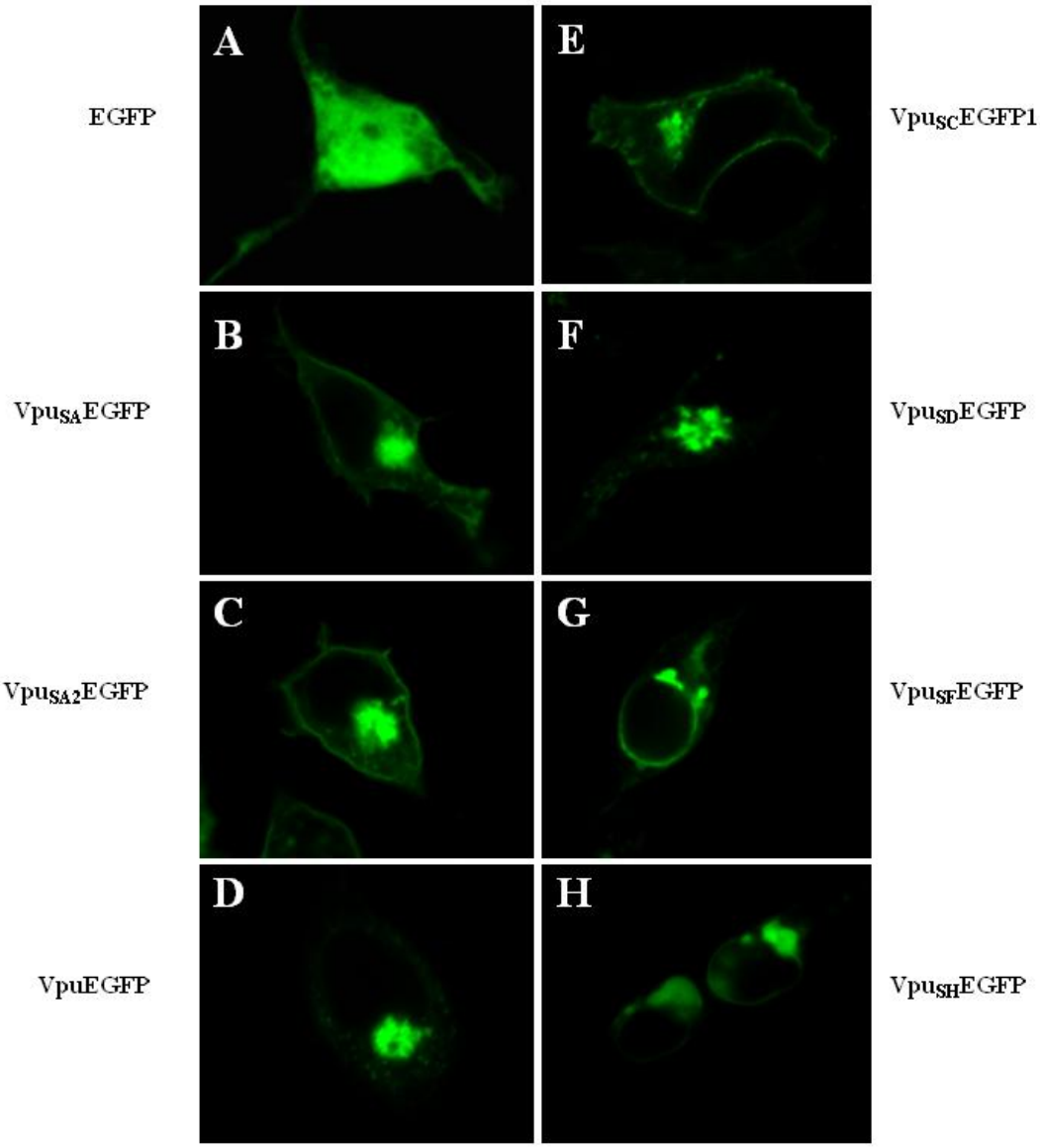
A
E
EGFP
VpuSCEGFP1
B
F
VpuSAEGFP
VpuSDEGFP
C
G
VpuSA2EGFP
VpuSFEGFP
D
H
VpuEGFP
VpuSHEGFP

The ability to down-regulate CD4 from the cell surface is maintained among different HIV-1 Vpu subtypes

We analyzed cell surface CD4 expression in the presence of each Vpu isolate with the subtype B (VpuEGFP) as a positive control. HeLa $CD4^+$ cells were transfected with vectors expressing Vpu_{SA}EGFP, Vpu_{SA2}EGFP, VpuEGFP, Vpu_{SC}EGFP1, Vpu_{SD}EGFP, Vpu_{SF}EGFP, or Vpu_{SH}EGFP. At 48 hours post-transfection, these cells were immunostained for CD4 and analyzed by flow cytometry to measure the intensity of cell surface CD4 expression. As shown in Figure 18, CD4 surface expression was significantly decreased in the presence of all Vpu isolates. Of the seven isolates, the CD4 surface expression in the presence of Vpu_{SA2}EGFP and Vpu_{SC}EGFP1 was statistically distinct from the other subtypes when evaluated using a Student's *t*-test, with a $p<0.05$ considered significant.

HIV-1 Vpu subtype F isolate 93BR020 does not enhance virion release in the presence of hBST-2

In order to examine the ability of each Vpu isolate to counteract BST-2 we co-transfected HeLa cells, that constitutively express hBST-2, with a vector expressing $SHIV_{\Delta Vpu}$ (as described in Chapter 1) and each of the Vpu subtypes. In order to eliminate the EGFP fusion tag as a variable we constructed vectors expressing codon-optimized *vpu* genes (pcVphuA, pcVphuA2, pcVphu, pcVphuC, pcVphuD, pcVphuF, and pcVphuH) and used these plasmids for exogenous expression of each Vpu isolate. At 48 hours post-transfection, the supernatants were collected and cleared by centrifugation, and the cells were lysed and the nuclei removed by centrifugation. The cleared supernatants and cell lysates were used to quantify the percent p27 antigen release from cells and the supernatants were also evaluated for the 50% tissue culture infectious dose ($TCID_{50}$) (Figure 19). The percent release of p27 in the presence of each Vpu isolate is shown in

Figure 19A. All samples were normalized to the $SHIV_{KU-2MC4}$ co-transfected with empty vector control and the average p27 release and standard error calculated. Significance in the enhancement of p27 release in the presence of each Vpu isolate was determined with respect to the $SHIV_{KU-2MC4}$ empty vector control using a Student's *t*-test (*). The level of infectious virus released was determined using the TZM-bl indicator cell line (Figure 19B). The results are represented as the average log_{10} infectious units and the significance in infectious units released was again determined with respect to the $SHIV_{KU-2MC4}$ empty vector control. All Vphu isolates except VphuF significantly enhanced p27 release compared to the $SHIV_{\Delta Vpu}$ empty vector control. A caveat of this assay was our inability to confirm Vphu protein expression and stability, specifically VphuF, within each sample as there is no antibody available that recognizes each of these different isolates. We addressed this issue using two distinct approaches: 1) reverse-transcriptase-PCR (RT-PCR) analysis on RNA isolated from the samples described above to confirm mRNA expression; and 2) conducting similar assays with vectors expressing Vpu fusion proteins and Western blot analysis using a mouse monoclonal anti-EGFP antibody (Clontech). All samples examined to generate the data represented in Figure 19 were positive for Vphu mRNA expression as determined by RT-PCR (Figure 19C). Assays conducted with the VpuEGFP fusion proteins yielded similar results and protein expression was confirmed by Western blot analysis (data not shown). It was clear however, that the EGFP fusion tag significantly interfered with Vpu-mediated enhancement of virion release in the context of hBST-2 antagonism. Therefore, data presented in Figure 19 is based on the results obtained with the native proteins.

Figure 18. All Vpu proteins maintain CD4 surface down-modulation function. HeLa CD4+ cells were transfected with plasmids expressing EGFP, Vpu_{SA}EGFP, Vpu_{SA2}EGFP, VpuEGFP, Vpu_{SC}EGFP1, Vpu_{SD}EGFP, Vpu_{SF}EGFP, or Vpu_{SH}EGFP. At 48 hours, live cells were immunostained for CD4. Cells expressing EGFP or EGFP fusion proteins were assessed for CD4 surface expression using flow cytometry. CD4 expression in cells expressing the various Vpu proteins was normalized to CD4 expression in EGFP expressing cells. (*) symbol above bar represents Vpu isolates that were significantly less efficient at down-modulating CD4 from the cell surface compared to VpuEGFP, with a $p < 0.05$ considered significant.

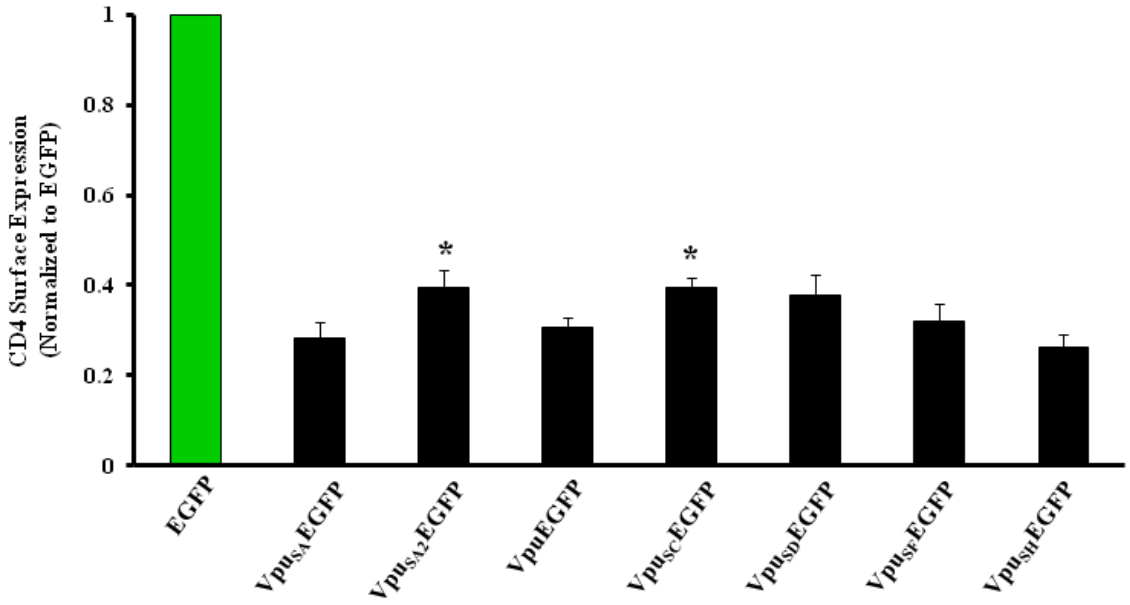

* Significant Compared to VpuEGFP; $p \leq 0.05$

Figure 19. HIV-1 Vpu subtype F protein does not enhance virion release in the presence of hBST-2. HeLa cells were co-transfected with $SHIV_{\Delta Vpu}$ and vectors expressing codon-optimized Vpu proteins (VphuA, VphuA2, Vphu, VphuC, VphuD, VphuF, or VphuH). At 48 hours, the culture medium was collected and assayed for p27 and infectious virus released from the cells. Panel A. The level of p27 released from transfected cells. Significance in the enhancement of p27 release was calculated with respect to the $SHIV_{KU\text{-}2MC4}$ empty vector using a Student's *t*-test, with $p \leq 0.01$ considered significant (*). Panel B. The level of infectious virus released as determined by infection of TZM-bl cells and staining for the presence of β-galactosidase activity at 48 hours post-inoculation as described in the Materials and methods section. Significance in the enhancement of infectious units released was determined with respect to the Vphu sample using a Student's *t*-test, with $p \leq 0.01$ considered significant (*). Panel C. Confirmation of transfection and mRNA expression of each Vphu protein as determined by RT-PCR analysis of RNA isolated from transfected cells (representative of all samples analyzed).

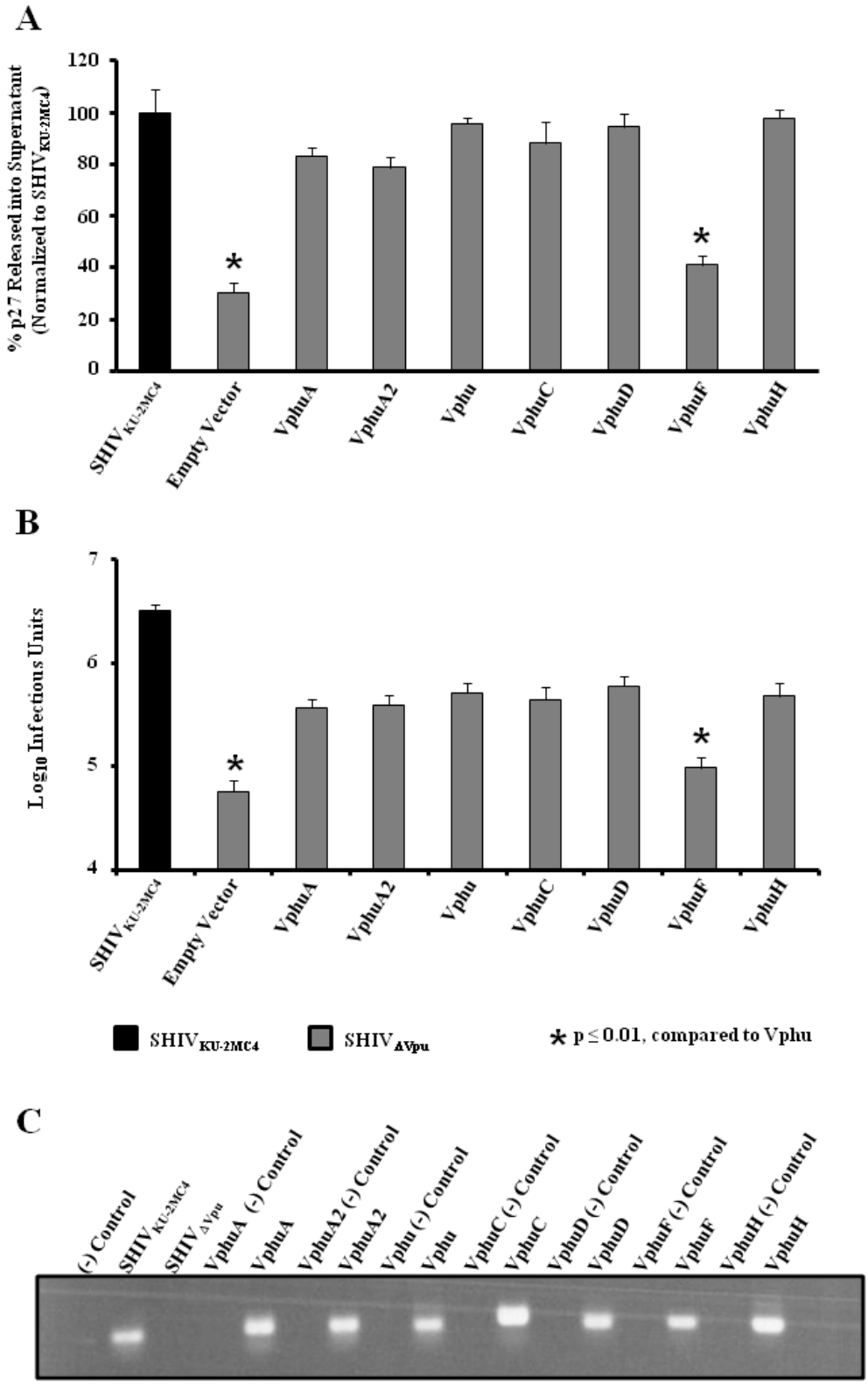
A
% p27 Released into Supernatant (Normalized to SHIV KU-2MC4)
120
100
80
60
40
20
0
*
*
SHIV KU-2MC4
Empty Vector
VphuA
VphuA2
Vphu
VphuC
VphuD
VphuF
VphuH
B
Log10 Infectious Units
7
6
5
4
*
*
SHIV KU-2MC4
Empty Vector
VphuA
VphuA2
Vphu
VphuC
VphuD
VphuF
VphuH
SHIV KU-2MC4
SHIV ΔVpu
* p ≤ 0.01, compared to Vphu
C
(-) Control
SHIV KU-2MC4
SHIV ΔVpu
VphuA (-) Control
VphuA
VphuA2 (-) Control
VphuA2
Vphu (-) Control
Vphu
VphuC (-) Control
VphuC
VphuD (-) Control
VphuD
VphuF (-) Control
VphuF
VphuH (-) Control
VphuH

The inability of Vpu subtype F isolate 93BR020 to enhance virion release may in part be due to enhanced turnover of the protein

One possible explanation for the inability of VphuF to enhance SHIV release in the presence of high quantities of hBST-2 could be due to the stability of the protein. We performed pulse-chase analysis of each of the Vpu/EGFP isolates to examine the rate of protein turnover. As shown in Figure 20, all of the Vpu isolates, except the subtype F protein, had between 40-60% of the protein remaining following a 6 hour chase period. The subtype F Vpu protein had approximately 25% protein remaining at the 6 hour chase period, which was significantly reduced compared to the VpuEGFP. These results suggest that the protein stability could contribute to the results observed in Figure 19.

Discussion

HIV-1 Group M isolates are responsible for more than 90% of HIV/AIDS cases worldwide (Jaffe and Schochetman, 1998; Simon et al., 1998a; Zekeng et al., 1994). The disproportionate dissemination of subtypes could be due to random introduction into distinct populations, susceptibilities of different hosts based on genetics or transmission routes, and/or specific adaptations of the viruses. While research over the years has provided great insight into specific mechanisms and molecular determinants of all of the HIV-1 encoded proteins, the majority of these studies have been conducted on several subtype B laboratory-adapted strains. Therefore, the potential for viral genetic determinants of the divergence of specific subtypes has remained elusive. Several studies have been conducted comparing the relative fitness of different HIV-1 subtypes, providing evidence in support of specific properties exhibited by subtype C viruses that exacerbated their persistence in certain geographic populations

Figure 20. Pulse-chase analyses of the Vpu fusion proteins. 293 cells were transfected with vectors expressing Vpu_{SA}EGFP, Vpu_{SA2}EGFP, VpuEGFP, Vpu_{SC}EGFP1, Vpu_{SD}EGFP, Vpu_{SF}EGFP, or Vpu_{SH}EGFP. At 48 hours post-transfection, cells were starved for methionine/cysteine and radiolabled for 1 hour as described in the Materials and methods section. The radiolabel was removed, cells washed and incubated in excess cold methionine/cysteine for 0-6 hours. The cells were lysed and processed for immunoprecipitation assays using a rabbit anti-EGFP serum. The immunoprecipitates were collected on protein A-Sepharose beads, boiled and visualized by SDS PAGE (10% gel) and standard autoradiographic techniques. Untransfected 293 cells served as a negative control (Lane C). The numbers above each lane represent the length of time chased in cold medium (Panel A). The percent of the protein remaining at the 6 hour chase period was determined by densitometry (Panel B). Significance was determined using a Student's *t*-test, with a $p<0.05$ considered significant (*).

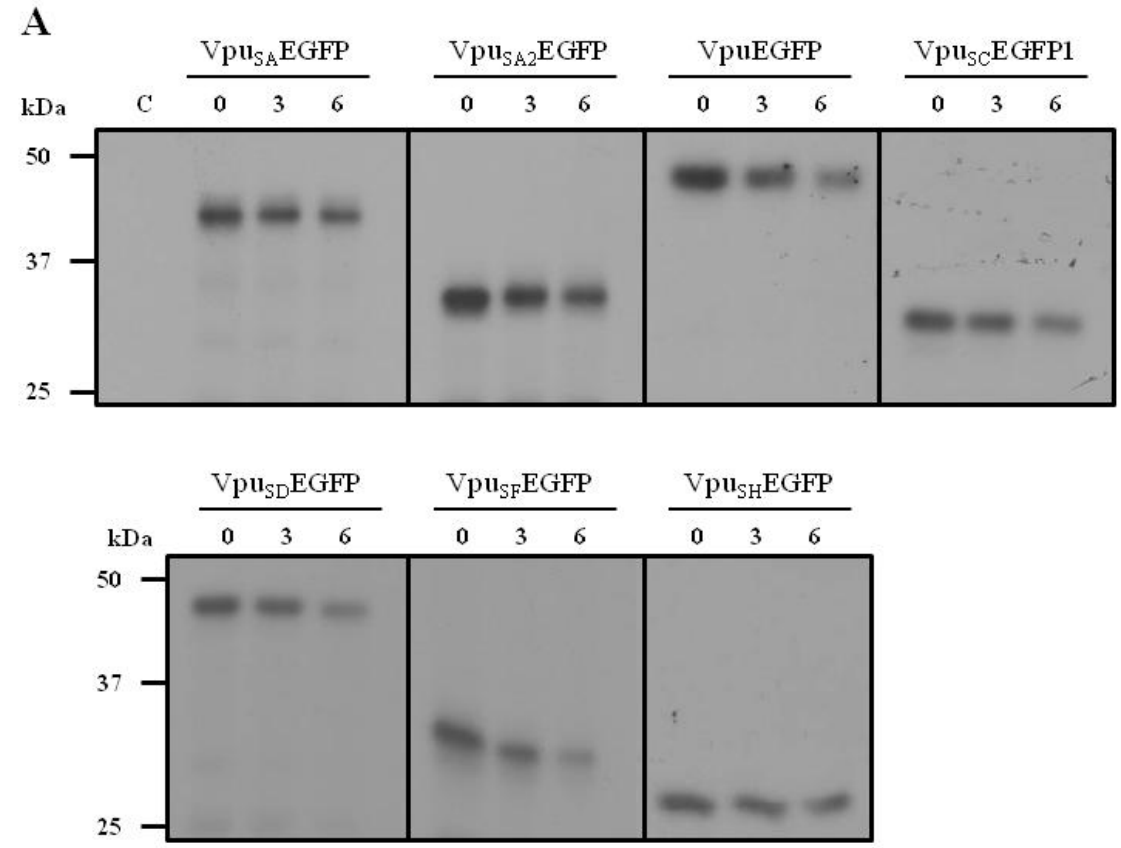
A
VpuSAEGFP
VpuSA2EGFP
VpuEGFP
VpuSCEGFP1
kDa
C
0 3 6
50
37
25
VpuSDEGFP
VpuSFEGFP
VpuSHEGFP

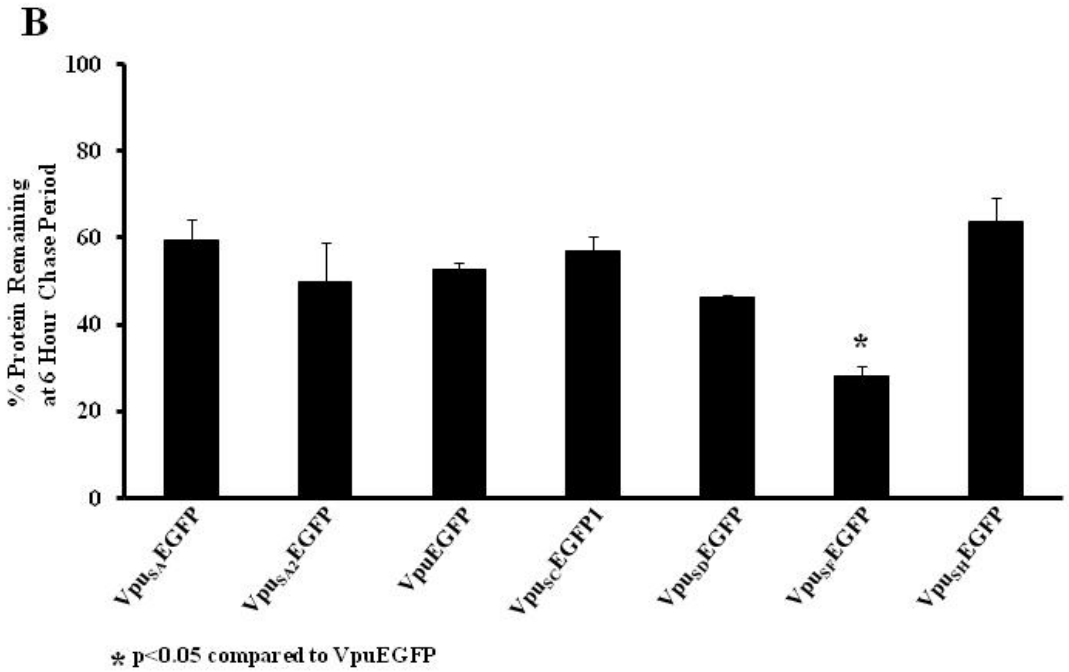
B
% Protein Remaining at 6 Hour Chase Period
100
80
60
40
20
0
*
VpuSAEGFP
VpuSA2EGFP
VpuEGFP
VpuSCEGFP1
VpuSDEGFP
VpuSFEGFP
VpuSHEGFP
* p<0.05 compared to VpuEGFP

(Abraha et al., 2009; Arien et al., 2005; Ball et al., 2003). Few studies have been conducted on specific genomic contributions of different subtypes to overall viral pathogenesis. Hence, this study focused on an accessory protein involved in the enhancement of HIV-1 pathogenesis, Vpu, and the distinct biological properties that contribute to this phenotype.

In previous studies our laboratory showed that a subtype B Vpu isolate (US.HXB2) and a subtype C Vpu isolate (C.96BW16B01) are transported to the cell surface with distinct efficiencies (Pacyniak et al., 2005; Singh et al., 2003). In this study we expanded our analyses of distinct biological properties exhibited by different HIV-1 Vpu subtypes. All of the isolates examined maintained the ability to down-modulate CD4 from the cell surface. Although the subtype A2 and C isolates were statistically less efficient at down-regulating CD4 molecules, the biological significance of these differences remains unknown. All Vpu proteins, except the subtype F Vpu isolate enhanced SHIV virion release in HeLa cells, which express high amounts of hBST-2. We observed that subtype A, A2 and C Vpu proteins more efficiently trafficked to the cell surface compared to the other Vpu proteins. While it does not appear that the plasma membrane localization pattern affects the ability to down-modulate CD4 from the surface, it may have residual effects on the enhanced release function of Vpu. It will be interesting to examine the replication kinetics of SHIV expressing these individual Vpu isolates in $CD4^+$ T cells as well as in macrophages in order to further elucidate the impact that these distinct properties have on pathogenesis and potentially transmission. Further studies are needed to identify the specific determinants, specifically signals that mediate intracellular protein trafficking and protein-protein interactions involved in both functions of Vpu, within each of these proteins.

During the conduction of these studies a collaborative group published a similar study evaluating the conservation of Vpu function among different human and non-human primate

lentiviruses (Sauter et al., 2009). Sauter *et al.* demonstrated that both functions of Vpu were maintained among different *vpu*-containing lentiviruses, however, there were several important differences. This group noted that the Vpu proteins from all 26 Group M HIV-1 isolates maintained the ability to down-regulate CD4 from the surface, albeit at different efficiencies, as did all 10 of the Group O Vpu proteins evaluated. However, this function was not conserved among the rare Group N HIV-1 Vpu proteins. These investigators also observed the maintenance of this function among 17 different SIV Vpu proteins, similar to results previously published by our laboratory (Gomez et al., 2005). In contrast, the ability to antagonize BST-2 was highly divergent among the different isolates and host-specific adaptations were found to be extremely important. Vpu proteins from SIV_{GSN}, SIV_{MUS} and SIV_{MON} were only active against monkey-derived BST-2 while Vpu from HIV-1 Group M isolates only counteracted hBST-2. HIV-1 Group N Vpu proteins also maintained the ability to counteract hBST-2, however the Group O Vpu proteins tested did not. Also of note was the finding that SIV_{CPZ} uses its Nef protein to antagonize BST-2 rather than the Vpu protein. This result was interesting since $SIV_{GSN,}$ SIV_{MUS}, SIV_{MON}, and SIV_{CPZ} all share a common ancestor and HIV-1 is thought to be derived from a cross-species transmission of SIV_{CPZ} (Gao et al., 1999; Schindler et al., 2006). Based on these results, this group suggested that the evolution of the HIV-1 Group M Vpu proteins to antagonize hBST-2 while maintaining its ability to down-modulate CD4 contributed the global spread of these viruses over those of HIV-1 Group N, Group O, and HIV-2. While the results of this group are extremely beneficial to the understanding of the evolution of different Vpu isolates and support the idea that there are specific differences among species and potentially subtypes of Vpu proteins, they do not address the question of the physiological relevance of Vpu-mediated BST-2 antagonism. All of the experiments within this study were

conducted in a 293T cell line and do not address the potential for differences in functionality of each Vpu isolate in different cells including macrophages, dendritic cells and $CD4^+$ T-lymphocytes. It would be interesting to see if similar results would be obtained in these different cell types and if not whether cell-type or subtype-specific molecular determinants could be identified.

Since the subtype F Vpu isolate used in our study maintained the ability to down-modulate CD4 from the cellular surface, but was completely devoid of any hBST-2 antagonistic function, it represents a potentially beneficial tool in beginning to determine: 1) whether BST-2 antagonism is physiologically relevant; 2) whether Vpu uses mechanisms not related to BST-2 antagonism to enhance virion release; and 3) the separation of importance for the two independent functions of Vpu in HIV-1 pathogenesis. Additional studies examining the enhanced virion release function of this isolate in macrophages, dendritic cells and $CD4^+$ T-lymphocytes/PBMC are needed to determine if this isolate is in fact completely devoid of the ability to enhance virion release. Studies determining the ability of this isolate to serve as an ion channel are also needed. These results would provide the necessary data for speculation on the possibility for additional mechanisms of Vpu-mediated enhancement of virion release and the physiological relevance of BST-2 antagonism. Also, if the subtype F Vpu isolate does lack the ability to enhance virion release, it would provide a wild-type Group M Vpu protein that could be used to test the sufficiency of CD4 surface down-modulation to modify pathogenesis using the SHIV macaque model of disease.

The subtype F Vpu isolate is also a useful tool to determine specific residues that may contribute to the enhanced virion release function of Vpu. Sequence analysis comparing our subtype F Vpu isolate to the HXB2 subtype B Vpu isolate used in our study as well as the two

subtype F Vpu isolates examined in Sauter *et al.,* 2009, revealed a threonine residue at position 19 that may be responsible for the failure to antagonize BST-2. Sequence analysis of another subtype C Vpu isolate (C.96BW.H51), which preliminary results within our laboratory suggests is also deficient in counteracting hBST-2, also revealed a threonine at this position, suggesting this residue could represent a potential anti-retroviral target. It will be interesting to determine whether this residue is responsible for the observed affects and whether substitution of a threonine at this position in fully functional Vpu proteins would result in a loss of function.

To date, the major drawback of all studies conducted with the intention of determining whether subtype contributes to the progression and global distribution of different HIV-1 isolates is the limited number of isolates examined. However, the number of studies being conducted is increasing resulting in an accumulation of the number of different isolates being analyzed. Also, through the analyses of different isolates, we and other investigators have been able to identify specific targets within specific isolates allowing for examination of the prevalence of these targeted regions/residues within other isolates.

Materials and Methods

Plasmids, Viruses and Cell Culture

The construction of plasmids expressing the subtype B Vpu (US.HXB2) and subtype C Vpu (96BW16B01) proteins fused to the gene for enhanced green fluorescent protein (EGFP) has been described previously (Pacyniak et al., 2005; Singh et al., 2003). Vpu genes from other HIV-1 subtypes were amplified from near-full-length clones (VpuA, cat# 1743 (92UG037) obtained through the AIDS Research and Reference Reagent Program, Division of AIDS, NIAID, NIH: HIV-1 92UG037 from The UNAIDS Network for HIV Isolation and

Characterization**;** VpuA2**,** cat# 6175 (94CY017.41) obtained through the AIDS Research and Reference Reagent Program, NIAID, NIH: p94CY017.41 from Drs. Stanley A. Trask, Feng Gao, Beatrice H. Hahn, and the Aaron Diamond AIDS Research Center; VpuD, cat# 4003 (84ZR085) obtained through the AIDS Research and Reference Reagent Program, Division of AIDS, NIAID, NIH: p84ZR085.1 (Near-Full-Length) from Drs. Beatrice Hahn and Feng Gao, and the UNAIDS Network for HIV Isolation and Characterization; VpuF, cat# 2329 (93BR020) obtained through the AIDS Research and Reference Reagent Program, Division of AIDS, NIAID, NIH: HIV-1 93BR020 from The UNAIDS Network for HIV Isolation and Characterization; VpuH, cat# 4005 (90CF056) obtained through the AIDS Research and Reference Reagent Program, Division of AIDS, NIAID, NIH: p90CF056.1 (Near-Full-Length) from Drs. Beatrice Hahn and Feng Gao, and the UNAIDS Network for HIV Isolation and Characterization) with 5' and 3' NcoI restriction sites. These fragments were purified using a Qiaquik Gel Extraction kit (Qiagen) and directly cloned into pGEMT-Easy by T/A overhang. All plasmids were digested with the NcoI restriction endonuclease and the resulting fragments were subcloned into NcoI digested CIAP treated pEGFP vector (Clontech Laboratories) that has a NcoI site at the 5' end of the gene for fusion to the gene expressing enhanced green fluorescent protein (EGFP). The resulting plasmids were sequenced to ensure that: (1) the *vpu* genes were valid and inserted in the correct orientation and (2) the Vpu/EGFP fusions were in frame. All *vpu*/*egfp* fusion genes were then purified following digestion of the plasmids with KpnI and StuI which are found on opposing sides of the gene fusions. These fragments were then directly ligated into a pcDNA3.1(+) expression vector digested with KpnI and EcoRV. The resulting plasmids contained each *vpu* gene fused in frame to the gene for EGFP under the control of the CMV immediate early promoter. A similar plasmid was constructed that expressed only EGFP. The

plasmids were identified as follows: pc*vpu*$_{SA}$*egfp*; pc*vpu*$_{SA2}$*egfp*; pc*vpu*$_{SD}$*egfp*; pc*vpu*$_{SF}$*egfp*; pc*vpu*$_{SH}$*egfp*.

Codon optimized sequences of HIV-1 Vpu genes from the different clinical isolates described above (VphuA (92UG037); VphuA2 (94CY017.41); VphuC (96BW16B01); VphuD (84ZR085); VphuF (93BR020); VphuH (90CR056)) were synthesized with 5' KpnI and 3' XbaI restriction sites and subcloned into a pUC57 vector (GenScript USA Inc.). Each construct was digested using restriction enzymes KpnI and XbaI and subcloned into a pcDNA3.1(+) expression vector (Promega). All plasmids were sequenced to ensure the validity of the gene and that no mutations were introduced during the cloning process. The codon optimized subtype B Vphu was obtained through the NIH AIDS Research and Reference Reagent Program, Division of AIDS, NIAID, NIH: pcDNA-Vphu from Dr. Stephan Bour and Dr. Klaus Strebel. (cat# 10076).

The construction of molecular clone SHIV$_{KU-2MC4}$ has been described previously (Liu et al., 1999). In order to construct SHIV$_{\Delta Vpu}$, another molecular clone Δ*vpu*Δ*nef*SHIVPPc was used and the construction of this clone has been described previously (Joag et al., 1998b). A 1444 base pair (bp) fragment was removed from SHIV$_{KU-2MC4}$ using restriction enzymes SphI and NheI. This fragment was replaced with the corresponding 1382 bp fragment of Δ*vpu*Δ*nef*SHIVPPc. The resulting construct expressed a Vpu protein with a 62 bp deletion and an inactive start codon (SHIV$_{\Delta Vpu}$).

The HeLa cell line was obtained through the AIDS Research and Reference Reagent Program, Division of AIDS, NIAID, NIH: (specify cell line) from Dr. Richard Axel. The 293 and HeLa cell lines were maintained in Dulbecco's minimal essential medium (DMEM) supplemented with 10% fetal bovine serum, gentamicin (5 ug per mL) and penicillin/streptomycin (100 U per mL and 100 μg per mL, respectively). The TZM-bl cell line

was obtained through the NIH AIDS Research and Reference Reagent Program, Division of AIDS, NIAID, NIH: TZM-bl from Dr. John C. Kappes, Dr. Xiaoyun Wu and Tranzyme Inc. The HeLa $CD4^+$ cell line was obtained through the AIDS Research and Reference Reagent Program, Division of AIDS, NIAID, NIH: HeLa CD4 Clone 1022 from Dr. Bruce Chesebro. TZM-bl cells were maintained in Dulbecco's minimal essential medium supplemented with 10% fetal bovine serum, gentamicin (5 µg per mL), and penicillin/streptomycin (100 U per mL and 100 µg per mL, respectively). HeLa $CD4^+$ cells were maintained in Dulbecco's minimal essential medium supplemented with 10% fetal bovine serum, gentamicin (5 µg per mL), penicillin/streptomycin (100 U per mL and 100 µg per mL, respectively) and G-418 (1 mg per mL).

Laser Scanning Confocal Fluorescence Microscopy Analysis

Plasmids expressing VpuEGFP fusion proteins were transfected into 293 cells to assess subcellular localization using a cationic polymer (polyethylenimine) transfection reagent (ExGen^{TM} 500, MBI Fermentas) according to the manufacturer's instructions. Briefly, 10^5 cells were seeded onto cover slips in each well of a 6-well tissue culture plate 24 hours prior to transfection. Plasmid DNA (4.75 µg) was diluted in 300 µl of 150 mM sodium chloride solution and vortexed gently. Polyethylenimine was then added to the solution, vortexed and allowed to stand at room temperature for 10 minutes. The 293 cells were washed and 3.0 mL of media was added. The polyethylenimine/DNA mixture was added to the cells dropwise and the cultures were incubated at 37C in 5% CO_2 atmosphere. At 48 hours post-transfection, cells were washed in phosphate buffered saline (PBS, pH 7.2) and fixed in ice cold 2% paraformaldehyde for 5 minutes. The cells were washed again in PBS and the cover slips mounted onto microscope

slides using mounting media (Slowfade Antifade, Molecular Probes). The cells were imaged with a Zeiss LSM 510 confocal microscope in the upright configuration. The objective used was a 63X 1.4n.a. Plan Apochromat. Images were captured at 12 bit resolution with a pixel array of 2048 x 2048 and a zoom of 2.0X. The EGFP was excited with light at 488 nm with a constant laser intensity, and the emitted light was collected after passing through a 505 nm long pass filter. The amplifier offset and gain were identical for all images. The pinhole was set to 96 µm which at this wavelength represents one airey unit. The optical section had a width of 0.7 µm.

Pulse-Chase Analysis to Assess Protein Stability

Plasmids expressing VpuEGFP fusion proteins were transfected into 293 cells to assess the rate of protein degradation using the ExGen^{TM} 500 transfection reagent. Briefly, $2.5x10^5$ cells were seeded into 35 mm dishes 24 hours prior to transfection. Plasmid DNA (3 µg) was diluted in 300 µl of 150 mM sodium chloride solution and vortexed gently. Polyethylenimine was then added to the solution, vortexed and allowed to stand at room temperature for 10 minutes. The 293 cells were washed and 3.0 mL of media was added. The polyethylenimine/DNA mixture was added to the cells dropwise and the cultures were incubated at 37C in 5% CO_2 atmosphere. At 48 hours post-transfection, the medium was removed and cells were incubated in methionine/cysteine-free medium at 37C for 2 hours. The cells were then radiolabeled with 200 µCi of ^{35}S-Translabel (methionine and cysteine, MP Biomedical) for 1 hour. The radiolabel was chased in DMEM containing 100X unlabeled methionine/cysteine medium for 0, 3 and 6 hours. VpuEGFP proteins were immunoprecipitated using a rabbit anti-EGFP antiserum and collected on Protein A-Sepharose beads on a rotator for 18 hours. Non-transfected 293 cells, starved, radiolabeled and chased for 0 hours served as a negative control.

Beads were washed three times with 1X radioimmunoprecipitation buffer (RIPA: 50 mM Tris-HCl, pH 7.5; 50 mM NaCl; 0.5% deoxycholate; 0.2% SDS; 10 mM EDTA) and the samples resuspened in 1X sample reducing buffer. Samples were boiled and the VpuEGFP proteins separated by SDS-PAGE (10% gel). Proteins were then visualized using standard autoradiographic techniques. All conditions were run in duplicate, the pixel densities of each band determined using ImageJ software, normalized to the hour 0 sample, and the average percent protein remaining calculated. Significance in percent protein remaining was determined using a Student's *t*-test with $p<0.05$ considered significant.

CD4 Surface Expression Analysis

For analysis of cell surface CD4 expression in the presence of each Vpu subtype, 2.5 x 10^5 HeLa $CD4^+$ cells were seeded into each well of a 6-well tissue culture plate 24 hours prior to transfection. Cells were transfected with vectors expressing each VpuEGFP protein as described above. Cells transfected with a vector expressing EGFP only were used as the control. At 48 hours post-transfection, cells were removed from the plate using Ca^{2+}/Mg^{2+}-free PBS containing 10 mM EDTA and stained with Phycoerythrin-Cyanine 5 (PE-Cy5) conjugated anti-CD4 antibody (BD Bioscience). Cells were analyzed using an LSRII flow cytometer determining the mean fluorescence intensity (MFI) of PE-Cy5 for transfected (EGFP positive) and untransfected (EGFP negative) cells within the same well. An MFI ratio was calculated for each sample with the EGFP only control normalized to 1.0. Normalized ratios from at least three separate experiments were averaged and the standard error calculated. Significance was determined by comparing all groups to the EGFP only control as well as the VpuEGFP sample using a Student's *t*-test with a $p<0.05$ considered significant.

Virion Release Assays

Hela cells (10^5) were seeded into each well of a 24-well tissue culture plate 24 hours prior to transfection. Cells were transfected as described above with 1 µg of plasmid expressing full length SHIV proviral DNA (either $SHIV_{KU\text{-}2MC4}$ or $SHIV_{\Delta Vpu}$) and 500 ng of plasmid expressing each Vphu subtype. Cells were incubated at 37C in 5% CO_2 atmosphere for 48 hours. Supernatants were collected and cellular debris removed through low speed centrifugation. Cells were lysed in 250 µl of 1X RIPA buffer and the nuclei removed through high speed centrifugation. The amount of p27 present within the supernatant and the cell lysates was determined using a commercially available p27 ELISA kit (Zeptometrix Incorporated) and the percent of p27 release calculated. All conditions were run at least three separate times and the average percent p27 release and standard error calculated. Significance with respect to the $SHIV_{\Delta Vpu}$ control was calculated using a Student's *t*-test with a $p<0.05$ considered significant.

Infectious Units Release Assays

TZM-bl cells (10^4) expressing luciferase and β-galactosidase genes under the control of an HIV-1 promoter were seeded into each well of a 96-well tissue culture plate 24 hours prior to infection. Supernatants collected from HeLa cells co-transfected with $SHIV_{\Delta Vpu}$ and Vphu subtype expressing plasmids as described above were added to the TZM-bl cells and serially diluted (10-fold). At 48 hours post-infection, cells were washed twice in 1X PBS and fixed in a solution of 0.25% glutaraldehyde and 0.8% formaldehyde in PBS for 5 minutes at room temperature. The cells were washed three times in 1X PBS and covered in staining solution (400 µg per mL X-gal, 4 mM $MgCl_2$, 4 mM $K_3Fe(CN)_6$, 4 mM $K_4Fe(CN)_6$-$3H_2O$ in phosphate

buffered saline) and incubated for 2 hours at 37C. Cells were washed once in 1X PBS and then covered in 1X PBS during counting. The $TCID_{50}$ for each supernatant was calculated based on wells containing cells expressing β-galactosidase. All conditions were run at least three times and the $TCID_{50}$ calculated. The average $TCID_{50}$ and standard error were calculated. Significance in the restriction of infectivity was determined with respect to the $SHIV_{KU\text{-}2MC4}$ sample using a Student's *t*-test with $p<0.05$ considered significant.

IX. Chapter 4: Modulation of the Severe $CD4^+$ T Cell Loss Caused by a Pathogenic Simian-Human Immunodeficiency Virus by Replacement of the Subtype B Vpu with the Vpu from a Subtype C HIV-1 Clinical Isolate

Abstract

Previously, we showed that the Vpu protein from human immunodeficiency virus type 1 (HIV-1) subtype C was efficiently targeted to the cell surface suggesting that this protein has biological properties that differ from the well-studied subtype B Vpu protein. In this study, we have further analyzed the biological properties of the subtype C Vpu protein. Flow cytometric analysis revealed that the subtype B Vpu (strain HXB2) was more efficient at down-regulating CD4 surface expression than the Vpu proteins from four subtype C clinical isolates. We constructed a simian-human immunodeficiency virus, designated as $SHIV_{SCVpu}$, in which the subtype B *vpu* gene from the pathogenic $SHIV_{KU\text{-}1bMC33}$ was substituted with the *vpu* from a clinical isolate of subtype C HIV-1 (strain C.96BW16B01). Cell culture studies revealed that $SHIV_{SCVpu}$ replicated with slightly reduced kinetics when compared with the parental $SHIV_{KU\text{-}1bMC33}$ and that the viral Env and Gag precursor proteins were synthesized and processed similarly compared to the parental $SHIV_{KU\text{-}1bMC33}$. To determine if substitution of the subtype C Vpu protein affected the pathogenesis of the virus, three pig-tailed macaques were inoculated with $SHIV_{SCVpu}$ and circulating $CD4^+$ T cell levels and viral loads were monitored for up to 44 weeks. Our results show that $SHIV_{SCVpu}$ caused a more gradual decline in the rate of $CD4^+$ T cells in pig-tailed macaques compared to those inoculated with parental subtype B $SHIV_{KU\text{-}1bMC33}$. These results show for the first time that different Vpu proteins of HIV-1 can influence the rate at which $CD4^+$ T cell loss that occurs in the SHIV/pig-tailed macaque model.

Introduction

All the naturally occurring primate lentiviruses encode for Tat, Rev, Nef, Vif and Vpr accessory proteins. In addition to these accessory proteins, human immunodeficiency virus type 1 virus (HIV-1) and a select number of simian immunodeficiency virus (SIV) isolates (SIV_{CPZ}, SIV_{DEN}, SIV_{GSN}, SIV_{MON}, SIV_{MUS}) also encode for a Vpu protein (Barlow et al., 2003; Courgnaud et al., 2002; Dazza et al., 2005; Huet et al., 1990). Previously, we and others demonstrated that different HIV-1 Vpu subtypes exhibit distinct biological properties that could alter their ability to modify transmission and/or pathogenicity (See Chapter 3). This included the intracellular localization of the different proteins, their ability to down-modulate CD4 from the cell surface, and their ability to enhance SHIV virion release in the presence of hBST-2. These studies, however, did not explore the physiological relevance of these differences. Hence, this study focused on determining whether subtypes that exhibit distinct biological properties also differentially modify pathogenesis. Because SIV_{MAC} strains commonly used in pathogenicity studies do not encode for the Vpu protein, we have used the pathogenic simian human immunodeficiency virus (SHIV), which has the *tat, rev, vpu* and *env* genes of HIV-1 in a genetic background of the SIV_{MAC}239, to analyze the role of Vpu in pathogenicity. Infection with these pathogenic SHIVs results in high viral loads, a rapid loss of $CD4^+$ T cells within one month of infection, and severe depletion within lymphoid organs such as the thymus, lymph nodes and spleen. To date, all studies assessing the role of Vpu in macaques have been performed using the well-studied subtype B Vpu protein from a laboratory-adapted HIV-1 isolate (NL4-3). Based on our previous examination of seven different HIV-1 Vpu proteins, we chose to further analyze the biological properties of subtype C Vpu.

Previously, we reported that a clinical isolate of subtype C Vpu (C.96BW16B01) was: 1) more efficiently transported to the cell surface compared to other Vpu proteins; 2) maintained the ability to degrade CD4, although slightly less efficiently than other Vpu proteins; and 3) maintained the ability to enhance virion release in the presence of hBST-2. Other investigators have also shown that while subtype C HIV-1 isolates are less replicatively fit in peripheral blood mononuclear cell (PBMC) competition assays, they display equal fitness in Langerhan cells as well as in penial, cervical and rectal tissue explants (Abraha et al., 2009; Arien et al., 2005; Ball et al., 2003). These studies suggest that subtype C viruses may have evolved to be more efficiently transmitted sexually and less virulent in order to ensure long-term persistence within the host, which may contribute to the predominance of subtype C HIV-1 viruses worldwide. In this study, we report that the trend of slightly diminished CD4 down-modulation compared to the subtype B Vpu protein was maintained among four separate subtype C Vpu isolates. Also, using the pathogenic molecular clone, $SHIV_{KU\text{-}1bMC33}$, we report on the construction of a SHIV in which the subtype B *vpu* was exchanged with the *vpu* from a clinical isolate of subtype C HIV-1 ($SHIV_{SCVpu}$). Our results show that following inoculation into macaques, $SHIV_{SCVpu}$ had a decreased rate of $CD4^+$ T cell loss compared with the parental $SHIV_{KU\text{-}1bMC33}$. These results show for the first time that different Vpu proteins can influence the rate of $CD4^+$ T cell loss in the SHIV/macaque model.

Results

CD4 down-regulation by subtype B and C Vpu proteins

The sequence of the subtype B and C Vpu proteins analyzed in this study are shown in Figure 21. Previously, we showed that fusion of the Vpu protein to enhanced green fluorescent

protein (EGFP) still resulted in the ability to down-modulate cell surface CD4 (Hout et al., 2005; Singh et al., 2003). We analyzed the efficiency of cell surface CD4 down-regulation by the subtype B and C Vpu fusion proteins. HeLa CD4+ cells were transfected with vectors expressing either the subtype B or C Vpu fusion proteins. At 48 hours post-transfection, live cells were immunostained for CD4 and analyzed by flow cytometry to measure the intensity of cell surface CD4 expression. As shown in Figure 22, the cells transfected with the vector expressing the subtype B fusion (VpuEGFP) consistently down-regulated CD4 more efficiently ($p<0.008$) than cells transfected with the vector expressing the subtype C Vpu fusion protein (Vpu_{SC}EGFP1). We also analyzed the ability of three additional subtype C Vpu fusions to EGFP (IN21068, BW04.07, and BW06.H51) fusion proteins to down-regulate CD4 surface expression. As shown in Figure 22, all three Vpu proteins were significantly less efficient ($p<0.05$) at preventing CD4 surface expression compared to the HXB2 Vpu protein.

The $SHIV_{SCVpu}$ virus expresses the Vpu protein within infected cells

We analyzed the expression of the Vpu protein in C8166 cultures inoculated with parental $SHIV_{KU\text{-}1bMC33}$ or $SHIV_{SCVpu}$. Cultures were inoculated with equivalent amounts of virus and at 5 days post-inoculation, cells were radiolabeled and Vpu proteins immunoprecipitated from cell lysates. As shown in Figure 23, a protein with a relative molecular mass (Mr) of 16,000 was immunoprecipitated from $SHIV_{KU\text{-}1bMC33}$-inoculated cultures. A Vpu protein was also immunoprecipitated from $SHIV_{SCVpu}$-inoculated C8166 cultures with a slightly slower mobility in SDS–PAGE, which may be due to the larger size (85 vs. 82 amino acids) of the subtype C Vpu protein (Figure 23).

Figure 21. Comparison of the Vpu sequences analyzed in this study.

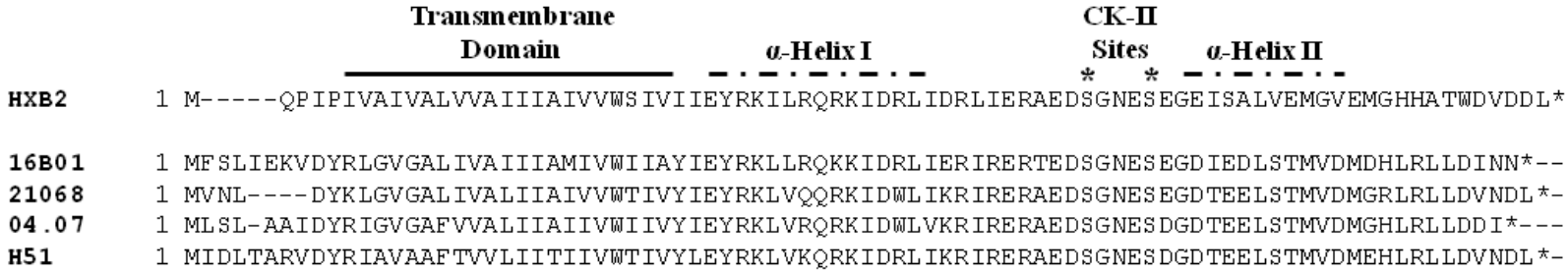
Transmembrane Domain
α-Helix I
CK-II Sites
α-Helix II
HXB2 1 M-----QPIPIVAIVALVVAIIIAIVVWSIVIIEYRKILRQRKIDRLIDRLIERAEDSGNESEGEISALVEMGVEMGHHATWDVDDL*
16B01 1 MFSLIEKVDYRLGVGALIVAIIIAMIVWIIAYIEYRKLLRQKKIDRLIERIRERTEDSGNESEGDIEDLSTMVDMDHLRLLDINN*--
21068 1 MVNL----DYKLGVGALIVALIIAIVVWTIVYIEYRKLVQQRKIDWLIKRIRERAEDSGNESEGDTEELSTMVDMGRLRLLDVNDL*-
04.07 1 MLSL-AAIDYRIGVGAFVVALIIAIIVWIIVYIEYRKLVRQRKIDWLVKRIRERAEDSGNESDGDTEELSTMVDMGHLRLLDDI*---
H51 1 MIDLTARVDYRIAVAAFTVVLIITIIVWTIVYLEYRKLVKQRKIDRLIKRIRERAEDSGNESDGDTEELSTMVDMEHLRLLDVNDL*-

Figure 22. The subtype C Vpu is less efficient at down-modulating surface CD4 than the subtype B Vpu protein. HeLa $CD4^+$ cells were transfected with plasmids expressing EGFP, VpuEGFP, Vpu_{SC}EGFP1, Vpu_{SC}(95IN21068)EGFP, Vpu_{SC}(96BW06.H51), or Vpu_{SC}(96BW04.07). At 48 hours, live cells were immunostained for CD4. Cells expressing EGFP or EGFP fusion proteins were assessed for CD4 surface expression using flow cytometry. CD4 expression in cells expressing the various Vpu proteins was normalized to CD4 expression in EGFP expressing cells. (*) symbol above bar represents Vpu isolates that were less efficient at down-modulating CD4 from the cell surface compared to VpuEGFP, with a $p < 0.05$ considered significant.

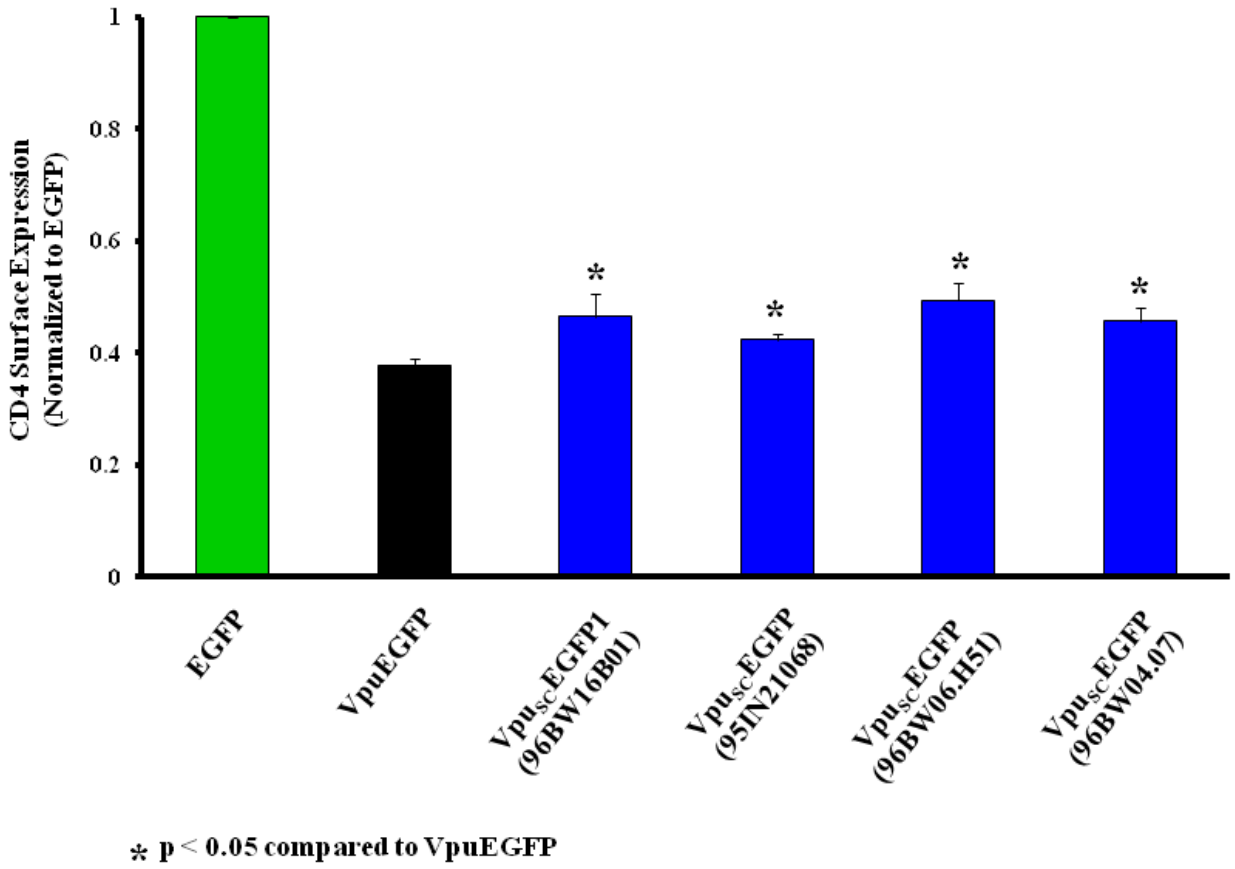

* $p < 0.05$ compared to VpuEGFP

Figure 23. The Vpu protein is expressed in C8166 cells infected with $SHIV_{SCVpu}$. C8166 cells were infected with $SHIV_{KU\text{-}1bMC33}$ or $SHIV_{SCVpu}$ for 5 days. The cells were incubated in DMEM lacking methionine and cysteine for 2 hours. Cells were radiolabeled with 500 µCi of ^{35}S Translabel (ICN Biomedical) for 12 hours. Supernatants were removed, cells lysed in 1X RIPA buffer and the nuclei removed through centrifugation. Cell lysates were immunoprecipitated using an antisera generated against the cytoplasmic domain of the subtype B Vpu protein and protein A-Sepharose beads. Immune precipitates were washed and separated on a 10% SDS-PAGE gel and visualized using standard autoradiography techniques. (Lane 1) Vpu proteins immunoprecipitated from $SHIV_{KU\text{-}1bMC33}$-inoculated cultures. (Lane 2) Vpu proteins immunoprecipitated from $SHIV_{SCVpu}$-inoculated cultures. (Lane 3) Vpu proteins immunoprecipitated from uninfected cultures.

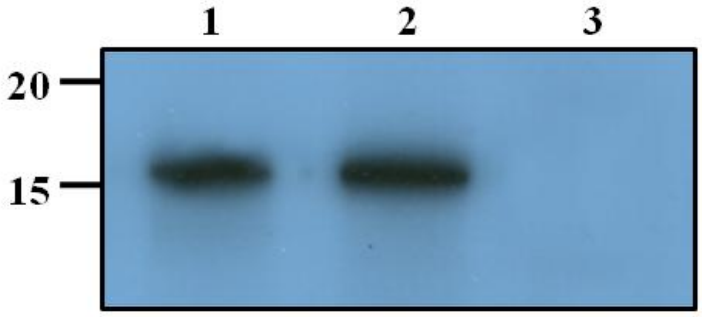
1
2
3
20
15

Pulse-chase analysis reveals that $SHIV_{SCVpu}$ precursor proteins are synthesized and processed with similar kinetics compared to parental $SHIV_{KU\text{-}1bMC33}$

Previous studies have shown that Vpu expression results in more efficient release of virus particles from infected cells. We used pulse-chase analysis to determine if substitution of the subtype B *vpu* for the subtype C *vpu* would result in similar release of viral structural proteins from infected cells. These results indicate that the substitution of the subtype B *vpu* with the subtype C *vpu* did not significantly alter the processing of Gag and Env precursor proteins (Figure 24).

$SHIV_{SCVpu}$ replicates with delayed kinetics and is less cytopathic compared to parental $SHIV_{KU\text{-}1bMC33}$

We analyzed the growth kinetics of the parental $SHIV_{KU\text{-}1bMC33}$ and the $SHIV_{SCVpu}$ following inoculation of C8166 cell cultures. As shown in Figure 25, $SHIV_{SCVpu}$ replicated with reduced kinetics as compared to the parental $SHIV_{KU\text{-}1bMC33}$. While the amount of p27 released appeared to be delayed by 2 days, the rate of p27 release from 7 to 10 days was reproducibly similar. At the end of the experiment, the amount of p27 released from $SHIV_{SCVpu}$-inoculated cultures was 86% of the p27 found in the parental $SHIV_{KU\text{-}1bMC33}$-inoculated cultures. However, the kinetics of p27 release was different from C8166 cells inoculated with $SHIV_{TM}$, which has a scrambled transmembrane domain (Hout et al., 2005), or from cultures inoculated with no*vpu*$SHIV_{KU\text{-}1bMC33}$, which lacks the *vpu* sequences prior to the *env* (Stephens et al., 2002). We also compared the pattern of virus maturation in cultures inoculated with parental $SHIV_{KU\text{-}1bMC33}$ and $SHIV_{SCVpu}$ using electron microscopy. The results shown in Figure 26 indicate that $SHIV_{SCVpu}$ matures from the cell surface similar to parental $SHIV_{KU\text{-}1bMC33}$. The reduced kinetics

of p27 release was also reflected in the time before the appearance of syncytial cytopathology. With the parental $SHIV_{KU\text{-}1bMC33}$, cytopathology generally appears 3 to 4 days post-inoculation, whereas $SHIV_{SCVpu}$-inoculated cultures displayed cytopathology starting 5 to 6 days post-inoculation. Additionally, the syncytia formation did not appear to be as extensive as $SHIV_{KU\text{-}1bMC33}$, suggesting that this subtype C Vpu protein could influence the ability to form syncytia in culture (data not shown).

The subtype C Vpu does not influence the incorporation of envelope glycoprotein into viral particles

We determined if substitution of the subtype B *vpu* with the subtype C *vpu* would influence the incorporation of Env into viral particles. $SHIV_{KU\text{-}1bMC33}$ and $SHIV_{SCVpu}$ were used to infect C8166 cells and radiolabeled at 6 days post-inoculation. The virus containing culture medium was harvested and virus pelleted through a 20% sucrose cushion. The pellet was lysed and the SHIV proteins immunoprecipitated using an anti-SHIV serum. The immunoprecipitated proteins were analyzed by SDS–PAGE and densitometry to determine the ratio of Gag p27 protein to Env gp120. As shown in Figure 27, the ratio of immunoprecipitated p27 to gp120 was approximately equal for the two viruses, $SHIV_{KU\text{-}1bMC33}$ (ratio 4.31) and $SHIV_{SCVpu}$ (ratio 4.89), suggesting that exchanging the subtype B *vpu* for the subtype C *vpu* did not influence the level of Env (gp120) associated with particles.

Figure 24. Pulse-chase analysis of the $SHIV_{SCVpu}$ proteins. C8166 cells were inoculated with 10^3 $TCID_{50}$ of either $SHIV_{KU\text{-}1bMC33}$ or $SHIV_{SCVpu}$. At 7 days post-infection, the medium was removed and the cells were incubated in DMEM lacking methionine and cysteine for 2 hours. The cells were radiolabeled for 30 minutes with 1mCi per ml of ^{35}S-Translabel (ICN Biomedical) and the radiolabel chased for various periods of time (0-6 h) in DMEM containing 100X unlabeled methionine/cysteine. SHIV proteins were immunoprecipitated from cell lysates using plasma pooled from several pig-tailed macaques infected previously with non-pathogenic SHIV-4 and protein A-Sepharose beads as described in the Materials in methods section. Immune precipitates were washed and separated on a 10% SDS-PAGE gel and visualized using standard autoradiography techniques. Uninfected C8166 cells, radiolabeled and chased for 6 hours, served as a negative control (C). Panel A. Results of pulse-chase analysis of viral proteins immunoprecipitated from $SHIV_{KU\text{-}1bMC33}$ infected cell lysates. Panel B. Results of pulse-chase analysis of viral proteins immunoprecipitated from $SHIV_{SCVpu}$ infected cell lysates.

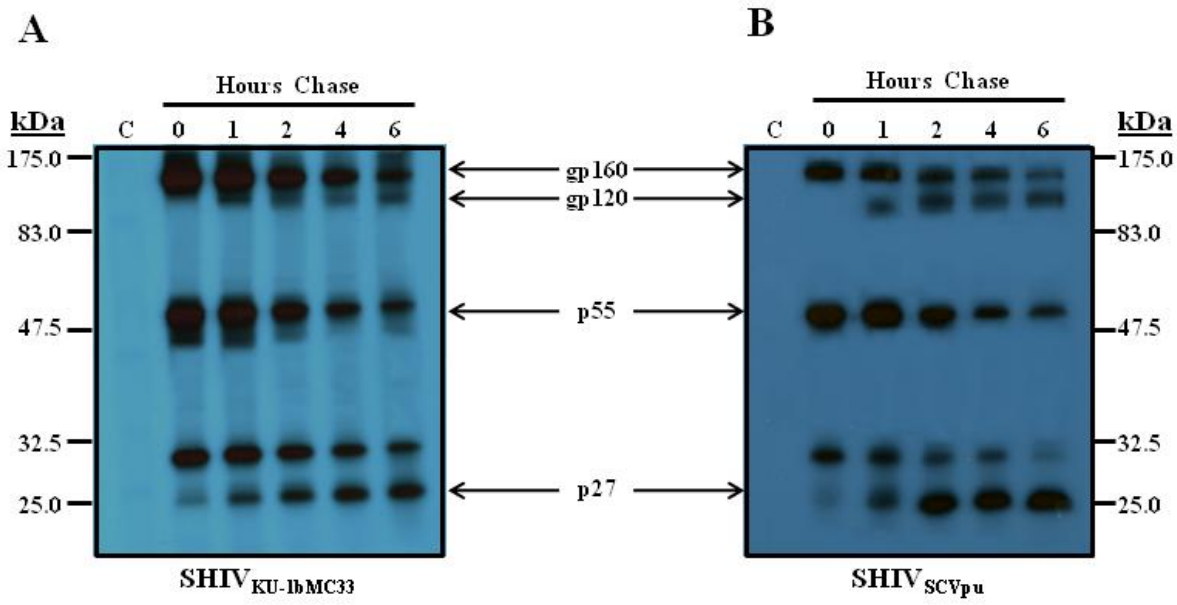
A
B
Hours Chase
kDa
C
0
1
2
4
6
175.0
83.0
47.5
32.5
25.0
gp160
gp120
p55
p27
SHIV KU-1bMC33
SHIV SCVpu

Figure 25. The kinetics of replication of $SHIV_{KU\text{-}1bMC33}$ and $SHIV_{SCVpu}$ in C8166 cell cultures. Cultures of C8166 cells were inoculated with either $SHIV_{KU\text{-}1bMC33}$ or $SHIV_{SCVpu}$. Aliquots of the culture medium were assayed for the presence of p27 antigen. The growth curves were performed in triplicate and the mean of the three experiments plotted.

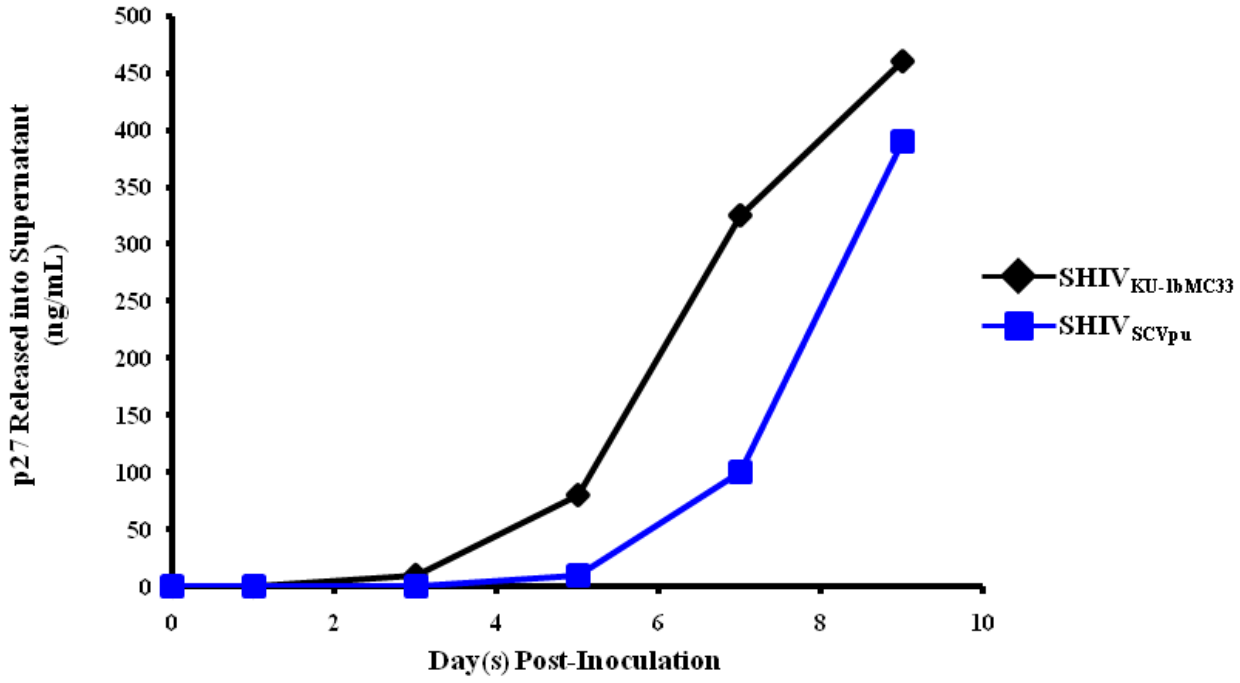
p27 Released into Supernatant (ng/mL)
500
450
400
350
300
250
200
150
100
50
0
0
2
4
6
8
10
Day(s) Post-Inoculation
SHIV KU-1bMC33
SHIV SCVpu

Figure 26. Electron microscopy examination of C8166 cells inoculated with $SHIV_{KU-1bMC33}$ or $SHIV_{SCVpu}$. C8166 cells were inoculated with either $SHIV_{KU-1bMC33}$ or $SHIV_{SCVpu}$ for 7 days. Cells were washed three times with PBS and processed for electron microscopy as described in the Materials and methods section. Panel A. C8166 cells inoculated with $SHIV_{SCVpu}$. Panel B. C8166 cells inoculated with parental $SHIV_{SCVpu}$ showing a virus particle maturing at the cell surface. Panel C. C8166 cells inoculated with parental $SHIV_{KU-1bMC33}$. Panel D. C8166 cells inoculated with parental $SHIV_{KU-1bMC33}$ showing a particle maturing at the cell surface.

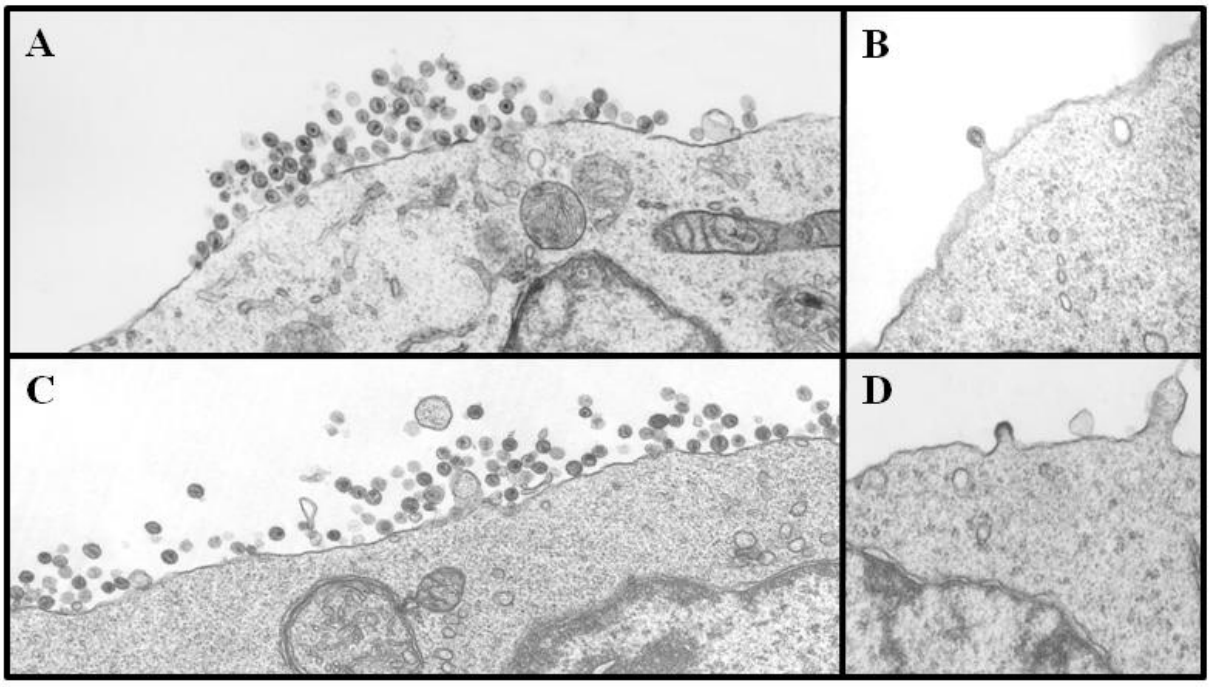
A
B
C
D

Figure 27. Envelope incorporation into $SHIV_{KU\text{-}1bMC33}$ and $SHIV_{SCVpu}$ virions. C8166 cells were inoculated with either $SHIV_{KU\text{-}1bMC33}$ or $SHIV_{SCVpu}$ for 6 days. At 6 days post-inoculation, cultures were radiolabeled as described in the Materials and methods section. The virus culture supernatants were centrifuged through a 20% sucrose cushion and lysed for immunoprecipitation. SHIV proteins were immunoprecipitated from cell lysates using plasma pooled from several pig-tailed macaques inoculated previously with SHIV-4 and protein A-Sepharose beads as described in the Materials and methods section. Uninfected C8166 cells served as a negative control. All immunoprecipitates were washed and separated on a 10% SDS-PAGE gel and visualized using standard autoradiography techniques. (Lane 1) Proteins immunoprecipitated from $SHIV_{SCVpu}$ infected cell lysates. (Lane 2) Proteins immunoprecipitated from uninfected cell lysates. (Lane 3) Proteins immunoprecipitated from $SHIV_{KU\text{-}1bMC33}$ infected cells. Molecular weight markers (kDa) are to the right of the gel.

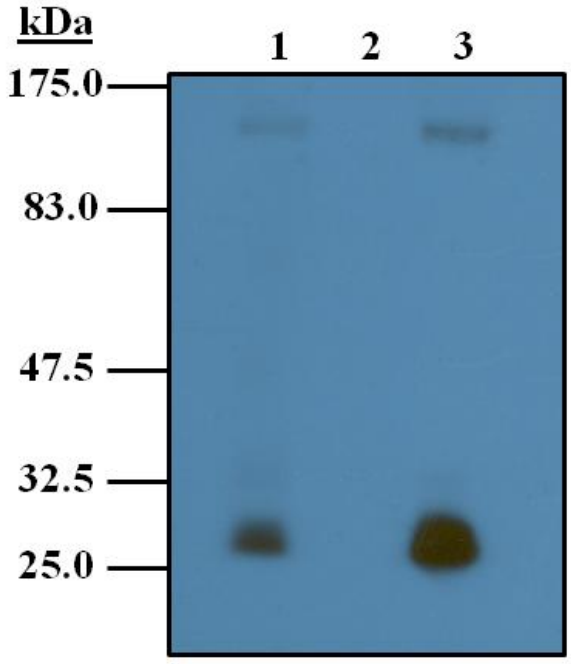
kDa
1
2
3
175.0
83.0
47.5
32.5
25.0

The rate of $CD4^+$ T cell loss was decreased and viral loads lower in $SHIV_{SCVpu}$ inoculated macaques

To determine whether the $SHIV_{SCVpu}$ was capable of causing disease in pig-tailed macaques, three macaques (CX56, CX57, and PLG2) were inoculated with $SHIV_{SCVpu}$ and $CD4^+$ T cells, and viral loads followed for up to 44 weeks. Macaque CX56 and CX57 were euthanized in a moribund condition at 36 and 44 weeks post-inoculation. Macaque PLG2 was euthanized at 40 weeks post-inoculation following development of severe enteritis. The circulating $CD4^+$ T cell levels are shown in Figure 28A and indicate that all three macaques developed a gradual decline in the levels of circulating $CD4^+$ T cells during the course of their infection. The rate of circulating $CD4^+$ T cell loss in macaques inoculated with $SHIV_{SCVpu}$ was clearly decreased compared to parental $SHIV_{KU\text{-}1bMC33}$ (Figure 28B). The rate of $CD4^+$ T cell loss was found to be statistically significant ($p \leq 0.01$). We also found that the early peak viral loads (between 1 and 3 weeks) in macaques inoculated with $SHIV_{SCVpu}$ were approximately 10-fold less than in macaques inoculated with the parental $SHIV_{KU\text{-}1bMC33}$ (Figures 28C and D).

Sequence analysis of the vpu gene isolated from $SHIV_{SCVpu}$ inoculated macaques

We analyzed the sequence of the *vpu* genes amplified from PBMC at different times post-inoculation and three lymphoid tissues (spleen, thymus and mesenteric lymph node) at necropsy. In all three macaques, we found scattered amino acid substitutions at different times post-inoculation but no consensus amino acid substitutions (data not shown).

Figure 28. Circulating $CD4^+$ T cell levels and plasma viral loads following inoculation of macaques with $SHIV_{KU1b\text{-}MC33}$ and $SHIV_{SCVpu}$. Panel A. The levels of circulating $CD4^+$ T cells in macaques (2000, ♦; CM4G, ■; CM4K, ▲) following inoculation with $SHIV_{KU\text{-}1bMC33}$. Panel B. The levels of circulating $CD4^+$ T cells in macaques (CX56, ♦; CX57, ■; PLg2, ▲) following inoculating with $SHIV_{SCVpu}$. Panel C. Plasma viral RNA levels in macaques (2000, ♦; CM4G, ■; CM4K, ▲) following inoculation with $SHIV_{KU\text{-}1bMC33}$. Panel D. Plasma viral RNA levels in macaques (CX56, ♦; CX57, ■; PLg2, ▲) following inoculating with $SHIV_{SCVpu}$. RNA samples were subjected to real-time RT-PCR and Taqman probe homologous to the SIV *gag* gene. Standard curves were generated using five dilutions of viral RNA of known concentrations.

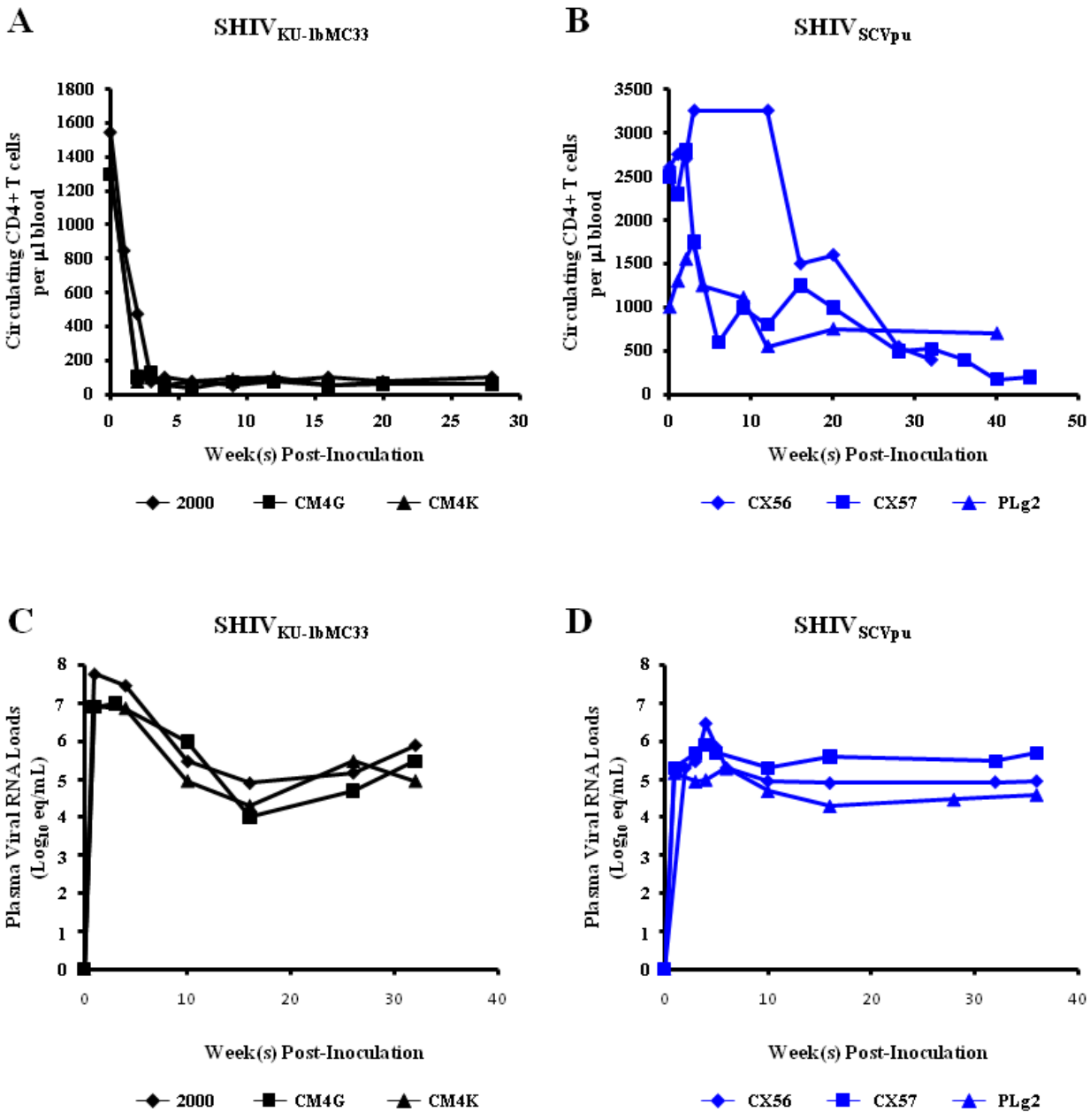
A
SHIV KU-1bMC33
Circulating CD4+ T cells per µl blood
1800
1600
1400
1200
1000
800
600
400
200
0
0
5
10
15
20
25
30
Week(s) Post-Inoculation
2000
CM4G
CM4K
B
SHIV SCVpu
Circulating CD4+ T cells per µl blood
3500
3000
2500
2000
1500
1000
500
0
0
10
20
30
40
50
Week(s) Post-Inoculation
CX56
CX57
PLg2
C
SHIV KU-1bMC33
Plasma Viral RNA Loads (Log10 eq/mL)
8
7
6
5
4
3
2
1
0
0
10
20
30
40
Week(s) Post-Inoculation
2000
CM4G
CM4K
D
SHIV SCVpu
Plasma Viral RNA Loads (Log10 eq/mL)
8
7
6
5
4
3
2
1
0
0
10
20
30
40
Week(s) Post-Inoculation
CX56
CX57
PLg2

The pathology in lymphoid organs at necropsy was similar to the parental $SHIV_{KU\text{-}1bMC33}$

We examined the histological sections from tissues of macaques inoculated with $SHIV_{SCVpu}$ at necropsy and compared the lesions to those observed following inoculation with parental $SHIV_{KU\text{-}1bMC33}$. No significant histological lesions were observed in the 15 regions of the brain and spinal cord (central nervous system; CNS), the heart, liver, lungs, kidney, or pancreas. The lack of histological lesions in the CNS is not surprising as the parental $SHIV_{KU\text{-}1bMC33}$ is not a neuropathogenic virus. As shown in Figure 29, the $SHIV_{SCVpu}$ inoculated macaque CX56 developed severe atrophy of the thymus, marked lymphoid depletion with little follicular activity in the lymph nodes, and moderate lymphoid depletion in the spleen. These lesions were similar to that seen in macaques inoculated with parental $SHIV_{KU\text{-}1bMC33}$. Macaque CX57 developed similar lymphoid depletion in the thymus and lymph nodes but no significant lesions were found in the spleen. Macaque PLG2 developed severe enteritis and protracted diarrhea. This macaque developed thymus atrophy and moderate depletion in the lymph nodes. The distribution of virus in the various visceral organs was determined by PCR for viral *gag* and *2-LTR* sequences. All three macaques were positive for *gag* sequences in all 13 visceral organs despite exsanguination with 1 liter of saline (data not shown). We also examined tissue RNA for the presence of viral RNA. As shown in Figure 30, viral RNA sequences were detected in RNA sequences isolated from 7 of 13, 7 of 13, and 6 of 13 visceral organs from CX56, CX57, and PLG2, respectively. The majority of the tissue RNAs that were positive for the presence of viral RNA sequences were from lymphoid organs. We also analyzed the RNA samples of tissues from 15 regions of the CNS for viral RNA sequences. Macaques CX56, CX57, and PLG2 had no regions of the brain and spinal cord that were positive for viral RNA sequences (data not shown).

Figure 29. Histopathology associated with $SHIV_{SCVpu}$ infection of macaques. Hematoxylin and eosin stains of sections from the thymus (Panels A and B), mesenteric lymph node (Panels C and D), and spleen (Panels E and F) from a non-infected age-matched macaque (Panels A, C, and E) and macaque CX56 (Panels B, D, and F).

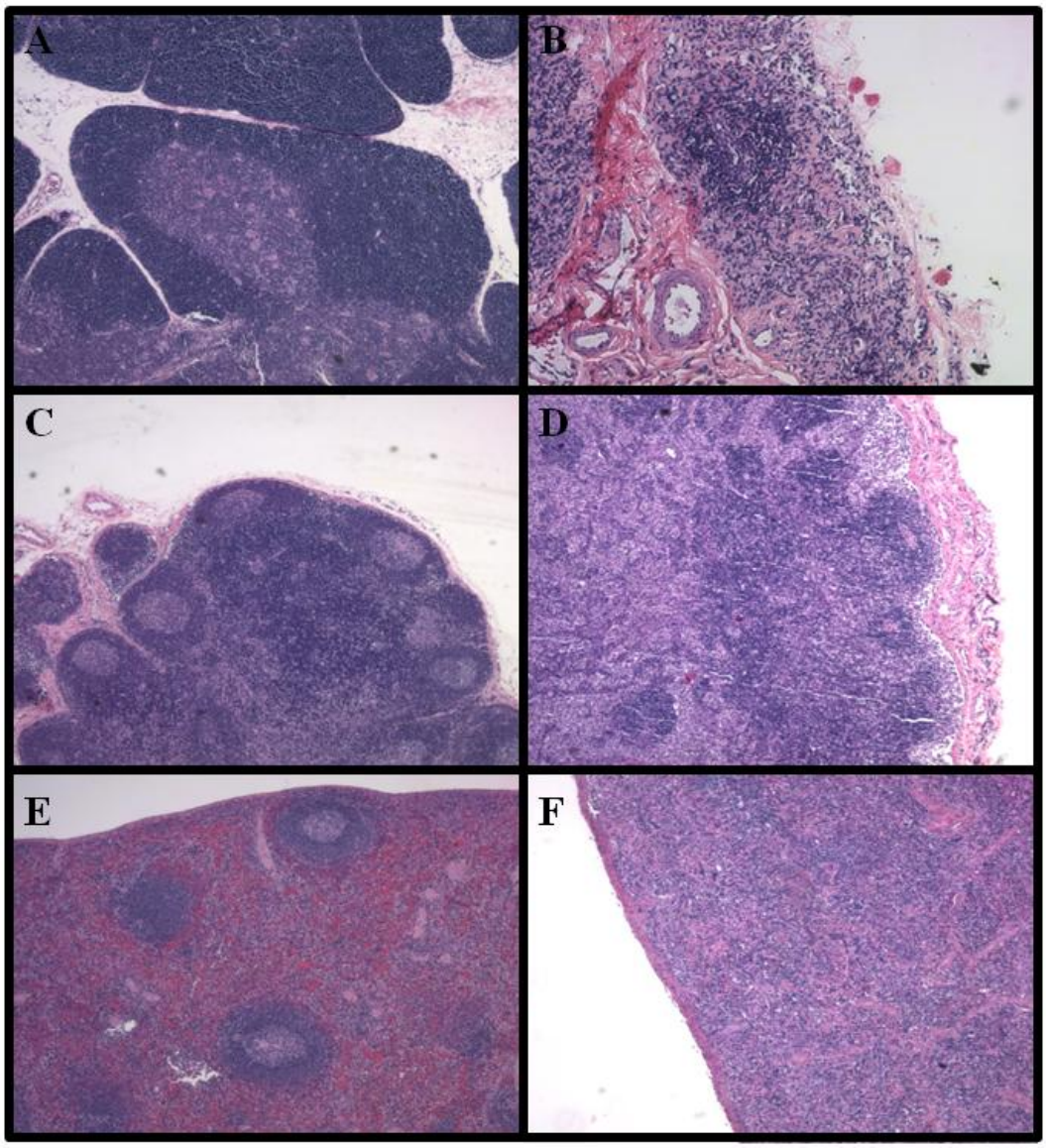
A
B
C
D
E
F

Figure 30. Distribution of virus in macaques CX56, CX57, and PLg2. Viral sequences were amplified using RT-PCR from RNA samples isolated from visceral and lymphoid organs from macaques CX56 (Panel A), CX57 (Panel B), and PLg2 (Panel C). The order of the gels are: (Lane 1) Positive control (RNA from SHIV infected C8166 cells), (Lane 2) Negative control (RNA isolated from lymph node of an uninfected macaque), (Lane 3) Heart, (Lane 4) Liver, (Lane 5) Lung, (Lane 6) Kidney, (Lane 7) Pancreas, (Lane 8) Salivary gland, (Lane 9) Mesenteric lymph node, (Lane 10) Axillary lymph node, (Lane 11) Inguinal lymph node, (Lane 12) Small intestine, (Lane 13) Spleen, (Lane 14) Thymus, and (Lane 15) Tonsil.

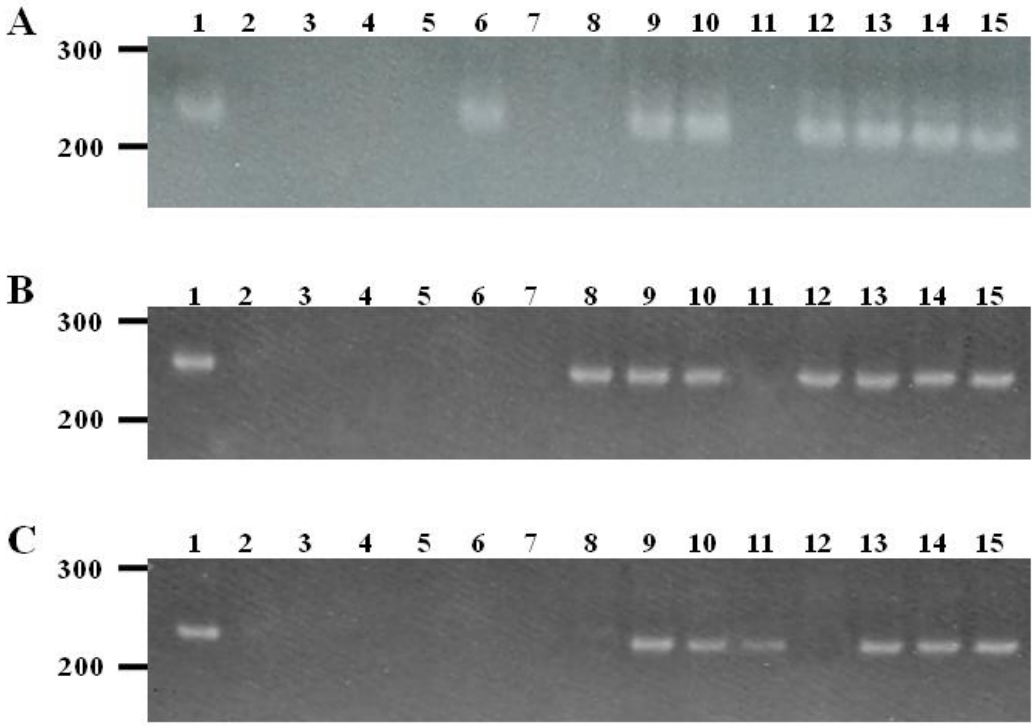
A
1 2 3 4 5 6 7 8 9 10 11 12 13 14 15
300
200
B
1 2 3 4 5 6 7 8 9 10 11 12 13 14 15
300
200
C
1 2 3 4 5 6 7 8 9 10 11 12 13 14 15
300
200

Discussion

The vast majority of HIV-1 infections are in Sub-Saharan Africa, where an estimated 60–70% of infected people reside (UNAIDS, 2008). Within the HIV-1 Group M pandemic, subtype C has increased in prevalence over the past 10 years, accounting for approximately 50% of the infections worldwide (Essex, 1999; Hemelaar et al., 2006; Takeb et al., 2004), and is most prominent in east Africa, south Africa, India and parts of China. In one study, both NSI/R5 and SI/X4 subtype C HIV-1 isolates were found to be significantly less fit in PBMC competition assays compared to all other group M isolates of the same phenotype (Ball et al., 2003). More recently, in a study that evaluated the replicative fitness of representative strains from subtypes A, B, C, D and CRF01_AE, the subtype C viruses had less replicative fitness in PBMC compared to the other subtypes. However, the subtype C isolates still replicated 100-fold higher than HIV-2 or group O isolates (Arien et al., 2005; Arien et al., 2007). Although less fit for replication in PBMC, the subtype C viruses were found to be similar to subtype B viruses for replicative fitness in skin-derived Langerhans cells, suggesting that these viruses might be more efficiently transmitted (Ball et al., 2003). In another study, subtype C HIV-1 was associated with the increased vaginal shedding of virus (John-Stewart et al., 2005). These data suggest that the relatively poor replication efficiency of subtype C in PBMCs (and possibly lymphoid organs) may be related to slower disease progression, hence, longer survival of the human host, which in turn could lead to increased time for transmission (Ball et al., 2003; Quinones-Mateu et al., 2000).

The subtype C Vpu protein has structural motifs that differ from the well-studied subtype B Vpu protein, and these may be associated with different biological properties of these two proteins (Hout et al., 2004). The subtype C Vpu proteins have an additional potential CK-II site

(TMVD) downstream from the two consensus sites. Other, potentially interesting sequence motifs unique to the subtype C Vpu proteins are two canonical dileucine motifs (E/D-X-X-X-L-L/I), one proximal to the transmembrane domain and one towards the carboxyl terminus of the Vpu protein. An acidic residue located at position 4, 5, or 6 upstream of the dileucine motif has been shown by investigators to be required for the efficient internalization of several proteins (Bonifacino and Traub, 2003). Dileucine motifs are known to interact with adaptor protein complexes AP-1, AP-2, and AP-3, resulting in the recruitment of cargo into clathrin coated pits and clathrin-coated vesicles (Bonifacino and Traub, 2003). Previous studies have implicated dileucine-based motifs in the sorting of membrane proteins to cellular sites such as the trans-Golgi network (TGN), endosomes, lysosomes, and plasma membrane (Bonifacino and Traub, 2003). The HIV-1 Nef protein associates with the inner side of the cell plasma membrane via its myristylated amino terminus. Importantly, the HIV-1 Nef, which also interacts with and down-regulates CD4 from the surface of infected cells, has a dileucine motif at the carboxyl terminus. This dileucine motif is required for CD4 down-regulation (Aiken et al., 1994; Bresnahan et al., 1998; Craig et al., 1998; Goldsmith et al., 1995). Our analysis indicates that the subtype C Vpu proteins from Indian and African subtype C isolates have "DM-GRLRLL" or "DMDGLRLL" motifs close to the carboxyl terminus, which closely fit the consensus motif described above. Thus, if these sequences are found to be responsible for altered biological properties, it has potential significance to HIV-1 pathogenesis, since subtype C isolates represent approximately 50% of the HIV-1 infections worldwide (Takeb et al., 2004).

In addition to differences regarding structural motifs, the subtype B and C have different biological properties. Using a reporter system that fused the Vpu protein to enhanced green fluorescent protein (EGFP), we previously showed that the subtype B Vpu protein is

predominantly localized in the Golgi complex of the cell while the subtype C Vpu protein was transported to the cell plasma membrane (Pacyniak et al., 2005). In our data presented here, we used flow cytometric analysis to compare the efficiency of subtype C Vpu proteins at down-regulating CD4 from the cell surface. These studies revealed that the efficiency of subtype B Vpu CD4 down-regulation was statistically different than four subtype C Vpu proteins. Although the physiological significance of this difference is currently unknown, these results demonstrate a potentially additional distinction in the biological properties of the subtype C and B Vpu proteins.

In previous studies using a pathogenic molecular clone of simian–human immunodeficiency virus known as $SHIV_{KU\text{-}1bMC33}$, we showed that the subtype B Vpu protein contributes to the profound $CD4^+$ T cell loss following inoculation into pig-tailed macaques (Hout et al., 2005; Singh et al., 2003; Singh et al., 2001; Stephens et al., 2002). These studies showed that the two casein kinase II sites and the transmembrane domain contribute to the rapid $CD4^+$ T cell loss following inoculation into macaques. Furthermore, we showed that the Vpu transmembrane domain could be replaced with the TM domain of the M2 protein of influenza A virus and retain pathogenicity in pig-tailed macaques (Hout et al., 2006b). Thus, this model has been useful in the molecular analysis of those domains of Vpu that are necessary for disease progression. Attempts have been made to construct pathogenic SHIVs expressing the *env* gene from subtype C HIV-1 (Chen et al., 2000; Ndung'u et al., 2001). In one of these studies, investigators constructed a SHIV expressing an R5 envelope glycoprotein (including the C-terminal end of the Vpu protein which contains the most amino acid divergence between the subtype B and C Vpu proteins) from a subtype C HIV-1 isolate (strain CHN19). These investigators found that this virus was capable of replicating in pig-tailed macaque PBMC but

not rhesus macaque PBMC. They observed that with serial passage in pig-tailed macaques, the virus replicated more efficiently. However, these macaques never developed significant $CD4^+$ T cell loss and functionality of this chimeric Vpu was not determined (Chen et al., 2000). In another study, a SHIV was constructed with the majority of the subtype C *env* gene (the gp120 region starting just past the vpu ORF and part of gp41) into a SHIV89.6P based virus (Ndung'u et al., 2001). This virus was found to replicate in both rhesus and pig-tailed macaques. This virus was capable of replicating to high peak viral loads in rhesus macaques but did not result in significant $CD4^+$ T cell loss. In our studies presented here, we have concentrated on the contribution of the subtype C Vpu in the pathogenic SHIV/macaque model system. We hypothesized that if a SHIV expressing a Vpu protein from another subtype of HIV-1 (in this case, subtype C) still resulted in severe $CD4^+$ T-cell loss, it would suggest that the divergent sequence of this Vpu (particularly the carboxyl terminus) was not a factor in disease progression. Our results presented here indicate that a SHIV constructed with the Vpu from a subtype C Vpu ($SHIV_{SCVpu}$) significantly differed in the rate of $CD4^+$ T cell loss compared to parental pathogenic $SHIV_{KU\text{-}1bMC33}$. As $SHIV_{SCVpu}$ and parental $SHIV_{KU\text{-}1bMC33}$ are identical with the exception of the *vpu* gene and the overlapping *env* sequences (which do not appear to significantly affect envelope glycoprotein synthesis and processing), these results suggest that the efficiency of the CD4 down-regulation by the Vpu protein may correlate with the rate of $CD4^+$ T cell loss *in vivo*. As previously suggested, Vpu may use alternative mechanisms unassociated with BST-2 antagonism that are also important in the SHIV macaque model of disease, which also may correlate with the rate of $CD4^+$ T cell loss. A potential caveat of this study is that the expressed Vpu may not be reflective of all subtype C Vpu proteins. Although a valid concern, the subtype C Vpu protein we used to construct $SHIV_{SCVpu}$ is similar to other

subtype C Vpu sequences from Botswana (data not shown). Further, our experiments examining the down-regulation of CD4 from the cell surface revealed similarities among the four subtype C Vpu proteins (both from Botswana and India) when compared to the HXB2. Whether the decreased rate of $CD4^+$ T cell loss in $SHIV_{SCVpu}$-inoculated macaques was due to the rate of turnover of the Vpu protein in cells *in vivo*, the magnitude of CD4 down-regulation or the ability to influence virus release within infected cells remains to be determined.

Materials and Methods

Plasmids and Cell Culture

The construction of plasmids expressing a subtype B *vpu* (US.HXB2) and subtype C *vpu* (96.BW16B01) gene have been described previously (Pacyniak et al., 2005; Singh et al., 2003). These fragments were purified using a Qiaquik Gel Extraction kit (Qiagen) and directly cloned into pGEMT-Easy by T/A overhang. All plasmids were digested with the NcoI restriction endonuclease and the resulting fragments were subcloned into NcoI digested CIAP treated pEGFP vector (Clontech Laboratories) that has a NcoI site at the 5' end of the gene for enhanced green fluorescent protein (EGFP). The resulting plasmids were sequenced to ensure that (1) the *vpu* genes were valid and inserted in the correct orientation and (2) the Vpu/EGFP junction was in frame. All *vpu*/*egfp* fusion genes were then purified following digestion of the plasmids with KpnI and StuI which are found on opposing sides of the gene fusions. These fragments were then directly ligated into a pcDNA3.1(+) expression vector digested with KpnI and EcoRV. The resulting plasmids contained each *vpu* gene fused in frame to the gene for EGFP under the control of the CMV immediate early promoter. A similar plasmid was constructed that expressed only EGFP.

C8166 cells were maintained in RPMI-1640 supplemented with 10% fetal bovine serum, 10 mM Hepes buffer, pH 7.3, 2mM glutamine, penicillin/streptromycin (100 U per mL and 100 µg per mL, respectively) and gentamicin (5 µg per mL).

Construction of SHIV

The derivation of $SHIV_{KU\text{-}1bMC33}$ has been described previously (McCormick-Davis et al., 2000a; Singh et al., 2003; Stephens et al., 2002). In order to construct $SHIV_{SCVpu}$ a plasmid containing the 96BW16B01 *vpu* and *env* genes was used to amplify a 258 bp fragment with a NsiI site at the 5' end of the *vpu* gene and a KpnI site within the *env* gene. The amplicon was gel purified according to a Millipore isolation protocol and ligated into a pGEMT-Easy vector (Promega). Insertion of the 258 bp amplicon into SHIV was accomplished in a three step process. First, the pUC19ΔSN#12 plasmid, which has the SphI/KpnI fragment of $SHIV_{KU\text{-}1bMC33}$ in a pUC19 background and a NsiI site introduced at the beginning of the subtype B *vpu* gene was digested with NsiI and KpnI restriction endonucleases and gel purified to remove the vpu containing fragment. The 258 bp amplicon containing the *scvpu* gene was directly ligated into this purified digested plasmid yielding pUC*scvpu*. For introduction of *scvpu* into the plasmid containing the 3' end of SHIV, both the pUC*scvpu* and p3'-$SHIV_{KU\text{-}1bMC33}$ were digested with SphI and KpnI, gel purified, and ligated. The resulting plasmid p3'-$SHIV_{SCVpu}$ was sequenced to ensure that the *tat, rev, vpu* and *env* genes did not have any mutations during the cloning process. For the production of $SHIV_{SCVpu}$, p3'$SHIV_{SCVpu}$ and p5'SHIV-4 were digested with SphI overnight, purified, ligated and used to transfect C8166 cells as previously described (Hout et al., 2006b; Hout et al., 2005; McCormick-Davis et al., 2000a; McCormick-Davis et al., 2000b; Singh

et al., 2003; Stephens et al., 2002). Stocks were prepared, titrated in C8166 cells and stored at -80C until used.

Viral Replication Kinetics Assessment

Standard p27 assays (Beckman Coulter, SIV core antigen kit) were used to assess release of viral particles from cells infected with $SHIV_{KU\text{-}1bMC33}$ and $SHIV_{SCVpu}$. Cultures of 10^6 C8166 cells were inoculated with equivalent amounts of infectious cell free virus (10^3) for 4 hours. At the end of 4 hours, the cells were washed three times in fresh medium. The cells were resuspended in C8166 growth medium and this was considered the 0 time point of the assay. Cultures were incubated at 37C in a 5% CO_2 atmosphere and aliquots of the culture were removed at 0, 1, 3, 5, 7, and 9 days post-inoculation with fresh medium added to the cultures at days 3 and 6. The culture medium was separated from the cells by centrifugation and assayed for p27 according to the manufacturer's instructions.

Macaques and Virus Inoculation

Pig-tailed macaques were obtained from the Caribbean Primate Center in Puerto Rico. All macaques were housed in the AAALAC-approved animal facility at the University of Kansas Medical Center. Three pig-tailed macaques (CX56, CX57, and PLG2) were inoculated intravenously with 10^4 $TCID_{50}$ of $SHIV_{SCVpu}$. These macaques were euthanized at 36 to 44 weeks post-inoculation. We previously reported on the circulating $CD4^+$ T cell levels and virus loads in macaques inoculated with pathogenic $SHIV_{KU\text{-}1bMC33}$ (Singh et al., 2003; Stephens et al., 2002). EDTA-treated blood was collected weekly for 6 weeks, then at 3-week intervals for the next 6 weeks, and thereafter at monthly intervals.

Processing of Blood Samples

The PBMCs were prepared by centrifugation on Ficoll-Hypaque gradients as described previously (Joag et al., 1996; Joag et al., 1994). Ten-fold dilutions of PBMCs (10^6 cells/ml) were inoculated into replicate cultures and were examined for development of cytopathic effects as previously described (McCormick-Davis et al., 2000a; McCormick-Davis et al., 2000b; Stephens et al., 2002). Alterations in the circulating $CD4^+$ lymphocytes levels after experimental inoculations were monitored sequentially by flow cytometric analysis (Becton Dickinson). T-lymphocyte subsets were labeled with OKT4 (CD4; Ortho Diagnostics Systems, Inc), SP34 (CD3; Pharmingen) or FN18 (CD3; Biosource International) monoclonal antibodies.

Processing of Tissue Samples at Necropsy

At the time of euthanasia, animals were anesthetized by administration of 10 mg/kg ketamine (IM) followed by an intravenous administration of sodium pentobarbital at 20–30 mg/kg. A laparotomy was performed on the animal and exsanguinated by aortic cannulation. The chest was opened, the left ventricle cannulated, the right atrium nicked, and the animal perfused with 1 liter of cold pyrogen-free Ringer's saline. All aspects of the animal studies were performed according to the institutional guidelines for animal care and use at University of Kansas Medical Center. At necropsy, tissues from the heart, kidney, liver, lungs, axillary lymph nodes (LN), mesenteric LN, inguinal LN, pancreas, salivary gland, small intestine, spleen, thymus, and tonsil were fixed in 10% neutral buffered formalin and embedded in paraffin. Sections (5 μm) were stained with hematoxylin and eosin for routine histological examination by Dr. David Pinson, a board certified veterinary pathologist. In addition, the right half of the brain

and spinal cord were dissected into frontal, motor, parietal, temporal and occipital cortices, corpus callosum, thalamus, basal ganglia, midbrain, pons, medulla, cerebellum, cervical, thoracic and lumbar spinal cord and were also processed as above. In addition to each of the visceral organs, regions of the CNS were also frozen in liquid nitrogen for DNA isolation. PCR amplification and sequence analysis of *gag* DNA was extracted from the visceral organs and different regions of the CNS as previously described (McCormick-Davis et al., 2000a) and used to amplify viral *gag* sequences. We also analyzed tissues for the presence of viral RNA, indicative of actively replicating virus. RNA was extracted from approximately 30 mg of each tissue from each visceral organ using an RNeasy kit (Qiagen) according to the manufacturer's instructions. RNA samples were digested with DNase I for 30 min. Samples were run on agarose formaldehyde gels before and after DNase treatment to check for the presence of contaminating DNA. RNA samples were amplified by using primers for the SHIV *gag* gene and the Easy-A One-Tube RT-PCR System (Stratagene). The amplified *gag* fragment is 240 base pairs.

Plasma Virus Loads

Plasma viral RNA loads were determined on RNA extracted from EDTA-treated plasma. Virus was pelleted and RNA extracted using the Qiagen viral RNA kit (Qiagen). RNA samples were analyzed by real-time RT-PCR using *gag* specific primers and a 5'FAM and 3'TAMRA labeled Taqman probe that was homologous to the SIV *gag* gene. Standard curves were prepared using a series of six 10-fold dilutions of viral RNA of known concentration. The

sensitivity of the assay was 100 RNA equivalents per milliliter. Samples were analyzed in triplicate and the number of RNA equivalents was calculated per ml of plasma.

Sequence Analysis of the *vpu* Gene

The *vpu* was amplified from DNA samples isolated from several tissues taken at necropsy to examine the sequence of *vpu*. For sequence analysis, the PCR products from three separate PCRs were separated by electrophoresis in a 1% agarose gel, isolated, and each PCR reaction directly sequenced. Cycle sequencing reactions were done using the BigDye Terminator Cycle Sequencing Ready Reaction Kit with AmpliTaq DNA polymerase, FS (PE Applied Biosystems) and sequence detection was conducted with an Applied Biosystems 377 Prism XL automated DNA sequencer and visualized using the ABI Edit view program. Sequences were compared to the intact sequences from $SHIV_{SCVpu}$. Sequences showing differences were confirmed by molecularly cloning the PCR fragments into the pGEMT-Easy vector (Promega) followed by sequencing as described above.

X. Chapter 5: Membrane Raft Association of the Vpu Protein of Human Immunodeficiency Virus Type 1 Correlates with Enhanced Virus Release

Abstract

The Vpu protein of human immunodeficiency virus type 1 (HIV-1) is known to enhance virion release from certain cell types. To accomplish this function, Vpu interacts with the restriction factor known as bone marrow stromal cell antigen 2 (BST-2)/tetherin. In this study, we analyzed whether the Vpu protein is associated with microdomains known as lipid or membrane rafts. Our results indicate that Vpu partially partitions into detergent resistant membrane (DRM) fractions when expressed alone or in the context of simian-human immunodeficiency virus (SHIV) infection. The ability to be partitioned into rafts was observed with both subtype B and C Vpu proteins. The use of cholesterol lowering Lovastatin/M-β-cyclodextrin and co-patching experiments confirmed that Vpu can be detected in cholesterol rich regions of membranes. Finally, we present data showing that raft association-defective transmembrane mutants of Vpu have impaired enhanced virus release function, but still maintain the ability to down-regulate CD4.

Introduction

Viral protein U (Vpu) encoded by human immunodeficiency virus type I (HIV-1) augments viral pathogenesis by down-modulating CD4 molecules from the surface of infected cells and enhancing virion release (Fujita et al., 1997; Klimkait et al., 1990; Ruiz et al., 2010a; Schubert et al., 1998). Membrane association is critical for both activities although an earlier study indicated that the primary structure of the transmembrane domain was irrelevant for CD4

down-modulation (Schubert et al., 1996a). The ability of Vpu to enhance virion release from some cell types has been attributed to antagonism of the cellular protein bone marrow stromal antigen 2 (BST-2; also known as CD317, HM1.24 and tetherin) (Neil et al., 2008; Van Damme et al., 2008). BST-2 localizes to the sites of HIV-1 budding and provides a physical, protease-sensitive link between the cellular and viral membranes (Perez-Caballero et al., 2009). BST-2 is a type II integral membrane protein that is anchored into the cell membrane by an amino terminal transmembrane domain and by a glycophosphatidylinositol (GPI) anchor at the carboxyl terminal region. GPI anchored proteins are often found in membrane microdomains known as membrane rafts and fully processed BST-2 has been shown to partition to these domains (Kupzig et al., 2003). A more recent study documented a punctate distribution of BST-2 on the surface of HIV-1 infected cells and that removal of the GPI anchor resulted in BST-2 being exclusively associated with sites of assembly suggesting that BST-2 may partition to multiple types of microdomains with distinct membrane compositions (Perez-Caballero et al., 2009). As it is documented that the subtype B Vpu is neither incorporated into virions nor is it present at the sites of HIV-1 assembly and maturation, the location of Vpu mediated antagonism of BST-2 has remained in question (Strebel et al., 1989). However, since BST-2 may partition to multiple, compositionally distinct rafts during intracellular processing, it may interact with Vpu in rafts distinct from those essential to HIV-1 maturation and egress. The mechanism(s) by which Vpu counteracts BST-2 are under investigation but the down-regulation of BST-2 from the cellular surface, increased degradation of BST-2 and sequestration at alternate intracellular sites are all potentially dependent co-partitioning to similar membrane rafts.

Membrane rafts are essential to HIV-1 replication as the assembly and budding of virions is a dynamic process that is dependent upon the association of viral proteins with these microdomains (Ono and Freed, 2001). HIV-1 proteins Gag, Env and Nef have been identified as membrane raft associated proteins and the partitioning to these microdomains is essential for assembly, budding and enhancement of viral infectivity (Alexander et al., 2004; Nguyen and Hildreth, 2000). Membrane rafts are enriched in cholesterol and sphingolipids forming tightly packed, highly ordered regions within the membrane. The presence of cholesterol and sphingolipids in rafts confers resistance to solubilization by some non-ionic detergents such as Triton X-100 at low temperatures. Due to their insolubility, membrane rafts are often referred to as detergent resistant membranes (DRMs). Because the isolation of DRMs is accomplished at 4C and isolated DRMs are 0.1 to 1μm vesicles, some investigators have questioned their existence in live cells. However, more recent studies have shown that DRMs can also be isolated by extraction at physiological temperature (Chen et al., 2009). Additionally, morphological approaches (confocal microscopy; atomic force microscopy, and fluorescence resonance energy transfer) have been used to study *in situ* localization of membrane rafts (Kusumi and Suzuki, 2005; Pralle et al., 2000; Prior et al., 2003; Sharma et al., 2004).

In this study, we employed both biochemical and morphological approaches to determine whether Vpu associates with membrane rafts and further characterized the potential for this association to affect both functions of Vpu. We report here that Vpu partially partitions to detergent resistant membrane microdomains in a cholesterol dependent manner. We also demonstrate the involvement of the transmembrane domain in this partitioning and identify targeted mutations within this domain that abolish membrane raft association. Furthermore, membrane raft association of the Vpu protein correlates with the enhancement of virion release

function, but not CD4 surface down-regulation. Taken together, these results establish that separate Vpu functions require distinct membrane localization patterns, implicate specific regions of the transmembrane domain as targets for disrupting Vpu function and provide further evidence for the importance of membrane rafts in HIV-1 pathogenesis.

Results

The subtype B Vpu protein partially partitions to the detergent resistant membrane fractions

We transfected 293 cells with a vector expressing a codon-optimized version of the subtype B Vpu (Vphu) and at 48 hours the DRMs were isolated on sucrose gradients using ultracentrifugation. Fractions were collected from the top of the gradients, the proteins concentrated and analyzed by Western blotting. Vphu was detected predominantly in the soluble fractions at the bottom of the gradient (Figure 31; upper panel) where a non-raft protein (transferrin receptor) was located (Figure 31; lower panel). However, the Vphu protein was also detected in fractions at the top of the gradient that corresponded to the DRMs. The DRM fractions were identified by the presence of Flotillin 1 (a raft protein) (Figure 31; middle panel). All experiments were performed at least twice, and the blots shown are representative of all experiments. These results provide evidence that Vpu is partially partitioned into membrane raft proteins.

Vpu is detected in the DRM fractions isolated from virus infected cells

We next determined if Vpu could be detected in DRM fractions from virus-infected cells. C8166 cells were inoculated with 10^4 $TCID_{50}$ of simian-human immunodeficiency virus

Figure 31. Vpu partitions into detergent resistant membrane (DRM) fractions. 293 cells were transfected with a plasmid expressing the Vphu protein. At 48 hours, cells were lysed in ice cold DRM buffer containing 1% Triton X-100, and raft proteins separated from non-raft proteins on discontinuous sucrose gradients by ultracentrifugation as described in the Materials and methods section. Fractions were collected from the top of the gradient, and Vpu proteins detected by Western blot analysis using a rabbit Vpu anti-serum (upper panel) or stripped and reprobed with either an antibody directed against raft protein Flotillin 1 (middle panel) or the non-raft protein transferrin receptor (lower panel). Fraction 1 is the top of the gradient and fraction 12 the bottom of the gradient.

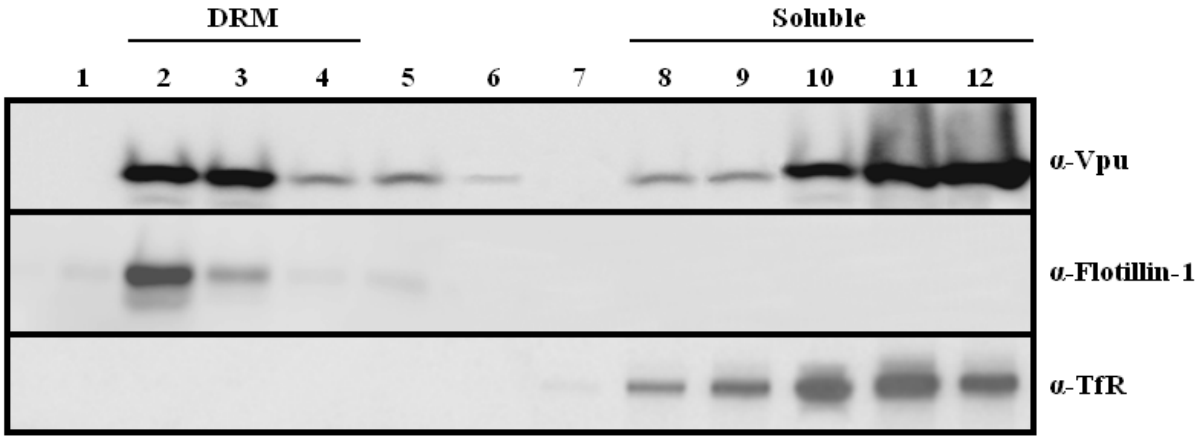
DRM
Soluble
1
2
3
4
5
6
7
8
9
10
11
12
α-Vpu
α-Flotillin-1
α-TfR

expressing an intact subtype B Vpu protein ($SHIV_{KU\text{-}1bMC33}$) or no Vpu protein (no*vpu*$SHIV_{KU\text{-}1bMC33}$) and incubated for 5 days. At 5 days, cells were starved and radiolabeled with ^{35}S-methionine/cysteine for 2 hours followed by DRM extraction and isolation by ultracentrifugation. Fractions containing the DRMs (fractions 1-3; I (insoluble)), the middle of the gradient (fraction 6-7; M (middle)), and the soluble non-raft proteins (fractions 10-12; S (soluble)) were each pooled, the Vpu proteins immunoprecipitated using a rabbit Vpu anti-serum, and then the proteins separated by SDS-PAGE. Aliquots were analyzed by Western blot for Flotillin 1 or transferrin receptor (TfR). Vpu could be detected in both the DRM and soluble fractions, but very little was detected in fractions collected from the middle of the gradient (Figure 32). All experiments were performed at least twice, and the blots shown are representative of all experiments. These results indicate that Vpu could also be detected in DRMs isolated from virus-infected T cells.

Vpu fusion proteins also partition to DRMs

To facilitate the detection of Vpu in different compartments of the cell, we previously developed a vector that expressed Vpu fused to the protein enhanced green fluorescent protein (VpuEGFP) (Pacyniak et al., 2005; Singh et al., 2003). In order to determine if the VpuEGFP protein would also partition to the DRM fractions, 293 cells were transfected with vectors expressing either the subtype B fusion protein (VpuEGFP) or the subtype C Vpu protein (Vpu_{SC}EGFP1) and fractionated as described above. Both the VpuEGFP and Vpu_{SC}EGFP1 were detected in the DRM fractions, indicating that these tagged proteins could be used to study raft association (Figure 33A-B). All experiments were performed at least twice, and the blots shown are representative of all experiments.

Figure 32. Vpu expressed in virus-infected cells also partitions into DRM fractions. C8166 cells were inoculated with 100 ng of $SHIV_{KU\text{-}1bMC33}$ or no*vpu*$SHIV_{KU\text{-}1bMC33}$ and incubated for 5 days. At this time cells were starved for methionine/cysteine for 2 hours and radiolabeled for 2 hours with 1 mCi of ^{35}S-methionine/cysteine. The cells were harvested by low speed centrifugation, washed, and lysed in ice cold DRM buffer containing 1% Triton X-100. Raft proteins were separated from non-raft proteins using discontinuous sucrose gradients by ultracentrifugation as described in the Materials and methods section. Fractions 1-3, 6-7 and 10-12 were pooled and the Vpu proteins immunoprecipitated using a rabbit Vpu anti-serum and immunoprecipitates collected on protein A-Sepharose beads. The remaining supernatants were analyzed by Western blot for Flotillin 1 and transferrin receptor. The proteins were separated using SDS-PAGE and proteins visualized using standard autoradiographic techniques.

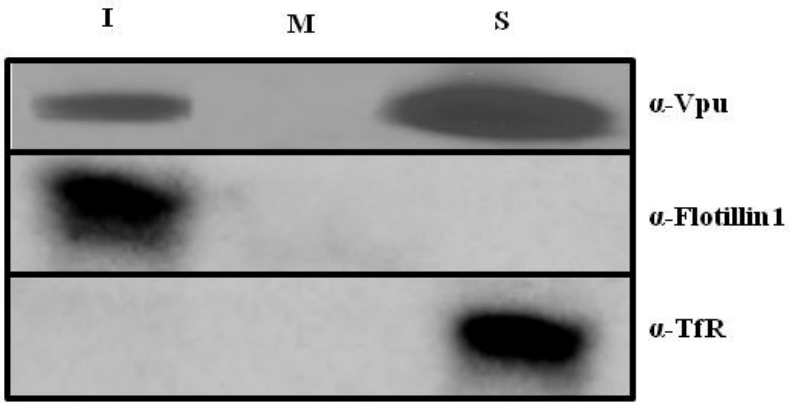
I
M
S
α-Vpu
α-Flotillin1
α-TfR

Cholesterol depletion abolishes the ability of VpuEGFP and Vpu_{SC}EGFP1 to be partitioned to the DRM fractions

As membrane rafts are rich in cholesterol, compounds that reduce cholesterol levels in cells such as M-β-cyclodextrin (M-β-CD) or statins disrupt membrane raft formation (Keller and Simons, 1998; Scheiffele et al., 1999). We examined if Lovastatin/M-β-CD treatment would reduce the level of Vpu in DRM fractions. 293 cells were transfected with vectors expressing VpuEGFP or Vpu_{SC}EGFP1, treated with 4 μM Lovastatin for 48 hours and with M-β-CD for the last 30 minutes prior to cell lysis. The cells were lysed as described above, DRM and soluble fractions separated by ultracentrifugation and fractions collected as described above. All experiments were performed at least twice, and the blots shown are representative of all experiments. The results clearly indicate that there were reduced levels of Vpu B and C fusion proteins in the DRM fractions following treatment with Lovastatin and M-β-CD, indicating that Vpu resistance to Triton-X-100 is cholesterol dependent and likely correlates with raft association (Figure 33A-B). The observation of Flotillin 1 in rafts of Lovastatin/M-β-CD treated cells may relate to the ability of Flotillin 1 to occupy detergent-resistant, buoyant complexes that do not rely on cholesterol for their integrity and has been previously reported (Browman et al., 2006; Gkantiragas et al., 2001). Companion monolayers of 293 cells treated with Lovastatin and M-β-CD showed no toxicity/cell death compared to untreated cells using microscopy (Figure 33C-D) and trypan blue staining (data not shown).

Vpu partially partitions into membrane rafts isolated at physiological temperature

Classical methods of the isolation of DRMs involve solubilization at 4C, which has been challenged by some investigators. Therefore, we also examined Vpu partitioning into membrane

raft fractions when the extraction was performed at 37C. 293 cells were transfected with a vector expressing VpuEGFP and at 48 hours post-transfection the cells were lysed in DRM37 buffer plus 1% Triton-X-100 and rafts isolated as described in the Materials and methods section (Chen et al., 2009). Rafts were separated from non-rafts by ultracentrifugation and fractions collected. The fractions were analyzed by Western blotting for the presence of Vpu, Flotillin 1, and transferrin receptor. The raft (Flotillin 1) and non-raft (TfR) markers were predominantly localized at the top and bottom of the gradients, respectively (Figure 34). Vpu was detected in both raft and non-raft fractions, similar to what we observed with solubilization of cells in the presence of 1% Triton-X-100 at 4C. All experiments were performed at least twice, and the blots shown are representative of all experiments. These results show that the Vpu protein could be detected in DRMs at physiological temperature as well as at 4C.

The subtype C Vpu protein co-localizes with a patched membrane raft protein

To further verify that Vpu is found in membrane rafts, we employed co-patching techniques for aggregating membrane rafts to a size visible by confocal microscopy and then examined if Vpu_{SC}EGFP1 co-localized with a known membrane raft protein. We used plasmids expressing either a fluorescent or non-fluorescent form of YFP with an ER translocation signal and a GPI anchor sequence. This protein is recognized by a mouse anti-GFP antibody (Clontech) in live cells, as the YFP portion of the protein is found extracellularly. While all known Vpu proteins are found in small amounts at the cell surface, most are prominently retained in the Golgi apparatus, making visualization of raft association difficult in live cells. Most live cell methods of raft detection involve surface staining or aggregation of rafts by cholera toxin or antibody co-patching. To increase the likelihood of visualizing Vpu in

Figure 33. Vpu fusion proteins also partition into DRM fractions and cholesterol depletion reduces the amount of VpuEGFP and Vpu_{SC}EGFP1 in DRM fractions. Left side of panels A and B. 293 cells were transfected with vectors expressing either VpuEGFP (Panel A) or Vpu_{SC}EGFP1 (Panel B) proteins. At 48 hours, cells were lysed in ice cold DRM buffer containing 1% Triton X-100, and raft proteins separated from non-raft proteins on discontinuous sucrose gradients by ultracentrifugation as described in the Materials and methods section. Fractions 1-3 (I), fractions 6-7 (M) and 10-12 (S) were pooled, concentrated and the Vpu proteins detected by Western blot analysis using a mouse anti-EGFP antibody. Right side of panels A and B. 293 cells were transfected with vectors expressing either VpuEGFP (Panel A) or Vpu_{SC}EGFP1 (Panel B) proteins. Following transfection, cells were incubated in the presence of 4 μM Lovastatin for 48 hours. Thirty minutes prior to lysis, M-β-CD was added to a final concentration of 10 mg/ml. Cells were processed as described for the untreated samples. Panels C-D. Micrographs of untreated cultures (Panel C) or those treated with Lovastatin/M-β-CD (Panel D).

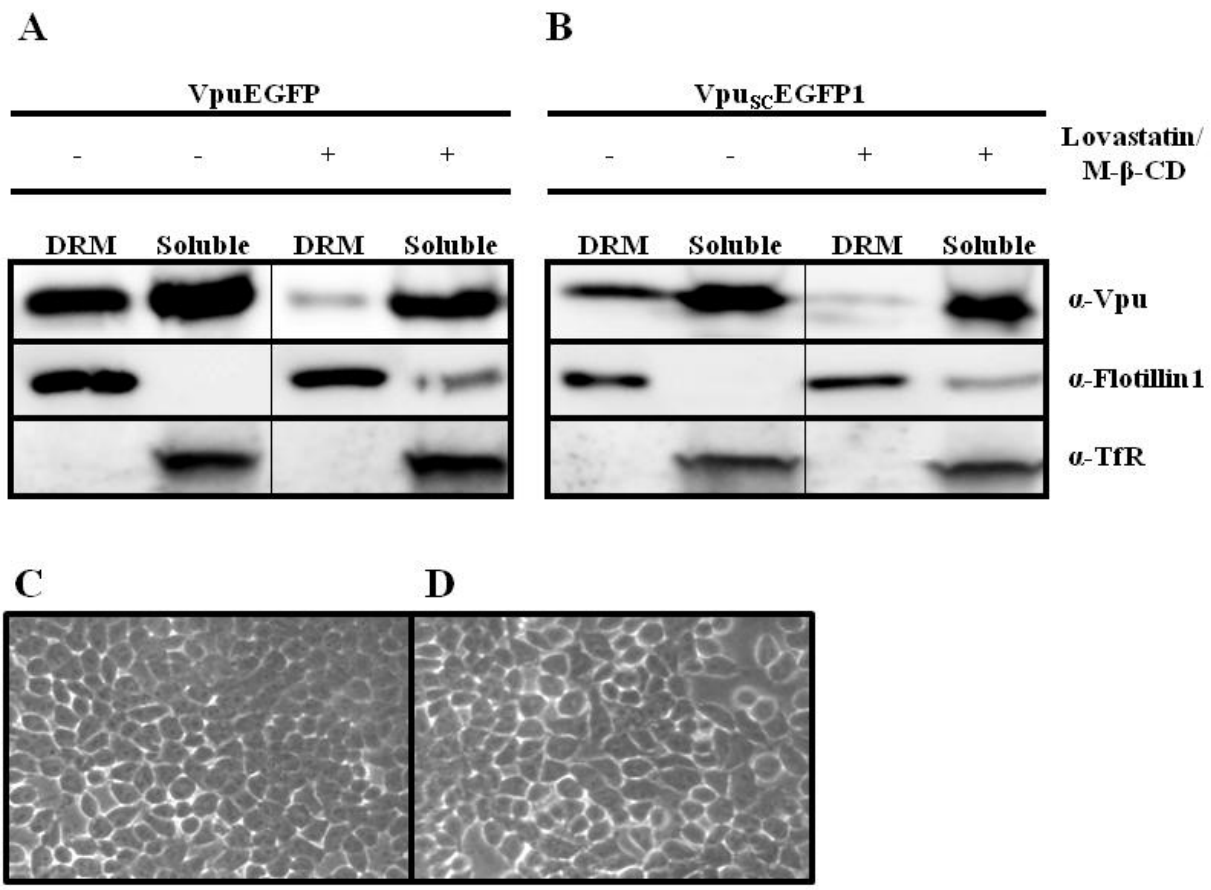
A
B
VpuEGFP
Vpu$_{SC}$EGFP1
- - + +
Lovastatin/
M-β-CD
DRM Soluble DRM Soluble
DRM Soluble DRM Soluble
α-Vpu
α-Flotillin1
α-TfR
C
D

Figure 34. Vpu partitions into membrane rafts isolated at physiological temperature. 293 cells were transfected with a vector expressing VpuEGFP and incubated at 37C. At 48 hours post-transfection, cells solubilized in DRM37 buffer containing 1% Triton-X-100 and raft proteins separated from non-raft proteins using discontinuous flotation sucrose gradients and ultracentrifugation as described in the Materials and methods section. Fractions were collected and VpuEGFP, Flotillin 1 or transferrin receptor detected by Western blot analysis using antibodies described in the Materials and methods section. Panel A. Detection of VpuEGFP. Panel B. Detection of Flotillin 1. Panel C. Detection of transferrin receptor. Fraction 1 is the top of the gradient and fraction 9 the bottom of the gradient.

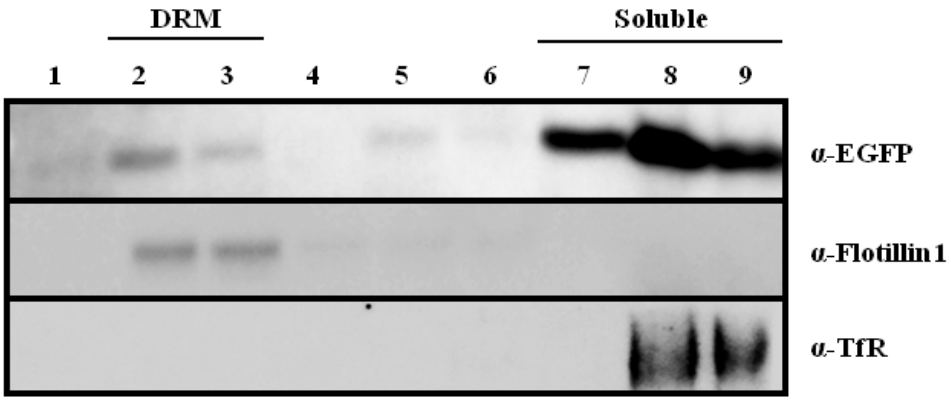
DRM
Soluble
1
2
3
4
5
6
7
8
9
α-EGFP
α-Flotillin1
α-TfR

membrane rafts by antibody co-patching, we utilized a Vpu protein which is predominantly found at the cell surface, Vpu_{SC} (Pacyniak et al., 2005). We used several controls to validate this approach. First, cells were transfected with a plasmid expressing Vpu_{SC}EGFP1 and live stained with anti-GFP as described in the Materials and methods (Figure 35A-C). As expected, these cells show no staining, since the EGFP tag of Vpu_{SC}EGFP1 is cytoplasmic. We next transfected cells with the plasmid expressing the fluorescent YFP-GPI, fixed and then stained with mouse anti-GFP (Figure 35D-F). The antibody staining in Figure 35F shows nearly complete co-localization at the cell surface, indicative of antibody specificity to the extracellular YFP tag. Finally, we transfected cells with the plasmid expressing the fluorescent YFP-GPI, stained and then fixed the live cells at 37C as described in Materials and methods (Figure 35G-I). This induces aggregation of the membrane rafts, making them visible by standard microscopy. Note the punctate staining of the co-patched YFP-GPI compared to the pre-fixed (i.e. fixed and then stained) sample. To determine if Vpu_{SC}EGFP1 would co-localize with this membrane raft protein, we used a plasmid expressing a non-fluorescent version of the same YFP-GPI construct (NFP-GPI), which produces no background (data not shown). This allowed us to use the Vpu_{SC}EGFP1 protein without having overlapping fluorescent signals. Cells were co-transfected with plasmids expressing NFP-GPI and Vpu_{SC}EGFP1, then stained at 37C and fixed post-stain (Figure 35J-O). Vpu_{SC}EGFP1 partially co-localized with the patches of NFP-GPI, indicating that Vpu is found in at least some GPI-anchored protein containing membrane rafts. This provides additional evidence that Vpu is a membrane raft protein and has the potential to partition into rafts similar to the BST-2 protein (a known GPI, lipid raft associated protein).

Figure 35. Co-patching experiments reveal that Vpu_{SC}EGFP1 partially co-localizes with NFP-GPI. Panels A, D, G, J, and M are fluorescent micrographs using a filter for YFP/EGFP . Panels B, E, H, K, and N are fluorescent micrographs for Cy5. Panels C, F, I, L, and O are a merge of the two fluorescent micrographs to the left. Panels A-C. 293 cells were transfected with vector expressing Vpu_{SC}EGFP1. Panels D-F. 293 cells were transfected with a vector expressing YFP-GPI and fixed prior to staining (i.e. pre-fixed). Panels G-I. 293 cells were transfected with a vector expressing YFP-GPI and co-patched. Panels J-O. 293 cells were transfected with both Vpu_{SC}EGFP1 and NFP-GPI and co-patched.

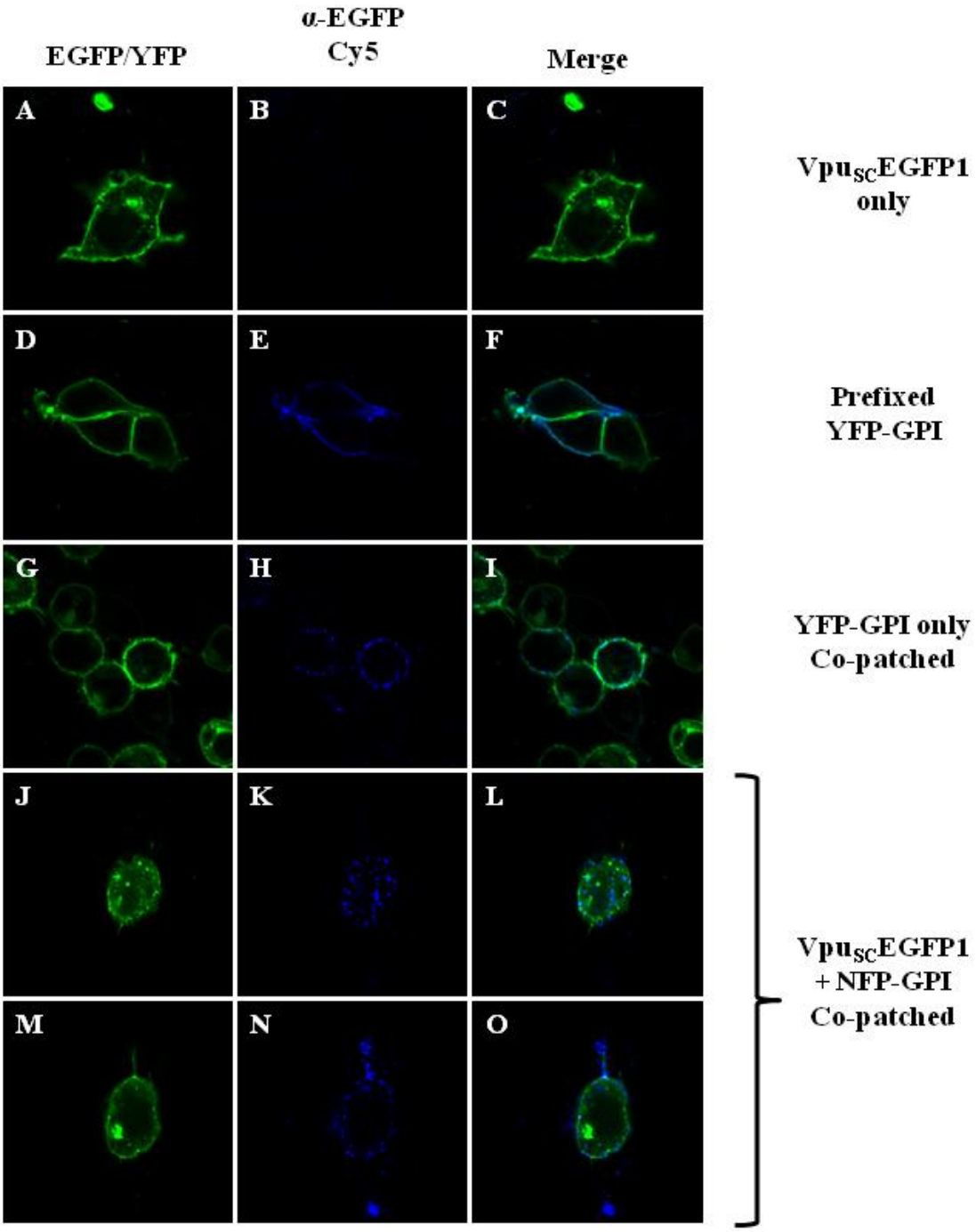
EGFP/YFP
α-EGFP
Cy5
Merge
A
B
C
D
E
F
G
H
I
J
K
L
M
N
O
Vpu$_{SC}$EGFP1
only
Prefixed
YFP-GPI
YFP-GPI only
Co-patched
Vpu$_{SC}$EGFP1
+ NFP-GPI
Co-patched

The transmembrane domain of Vpu is involved in raft association

We next determined if amino acids within the transmembrane domain were involved in the transport of VpuEGFP to membrane rafts. Previous studies have shown that scrambling the hydrophobic amino acids of the transmembrane domain (VpuRD or Vpu_{TM}EGFP) results in a protein that is membrane bound, transported to similar compartments within the cell, but unable to enhance virus release. The VpuRD protein maintained the capability of binding CD4 and inducing CD4 degradation, while the Vpu_{TM}EGFP protein was unable to down-modulate surface expression of CD4 (Hout et al., 2005; Schubert et al., 1996a). We determined if the Vpu_{TM} fused to EGFP (Vpu_{TM}EGFP) would partition to raft fractions. The results shown in Figure 36 indicate that Vpu_{TM}EGFP partitioned exclusively to the detergent soluble fractions of the gradient. All experiments were performed at least twice, and the blots shown are representative of all experiments. Appropriate controls for raft isolation and purity were performed and are shown. These results provide genetic evidence for the specificity of Vpu partitioning to the DRM fractions.

Characterization of Vpu transmembrane mutants

Based on the above results suggesting the involvement of the transmembrane domain in raft association, we constructed a series of vectors expressing Vphu proteins with 1-3 amino acid changes in the transmembrane domain (Figure 37A). We first analyzed the stability of these mutants using pulse-chase analysis. 293 cells were transfected with each mutant or the unmodified Vphu. At 48 hours, the cells were starved and radiolabeled with ^{35}S-methionine/cysteine and then the radiolabel chased in cold excess methionine/cysteine for 0 and 6 hours. All conditions were run at least in duplicate and the average percent protein remaining

Figure 36. Scrambling the transmembrane domain prevents VpuEGFP raft association. 293 cells were transfected with vectors expressing either VpuEGFP or Vpu_{TM}EGFP proteins. At 48 hours, cells were lysed in ice cold DRM buffer containing 1% Triton X-100, and raft proteins separated from non-raft proteins on discontinuous sucrose gradients by ultracentrifugation as described in the Materials and methods section. Fractions were collected from the top of the gradient, and fractions from the top (1-3; I) middle (6-7; M) and bottom (10-12;S) were analyzed for the presence of Vpu, Flotillin 1 and transferrin receptor proteins by Western blot analysis using antibodies described in the Materials and methods section.

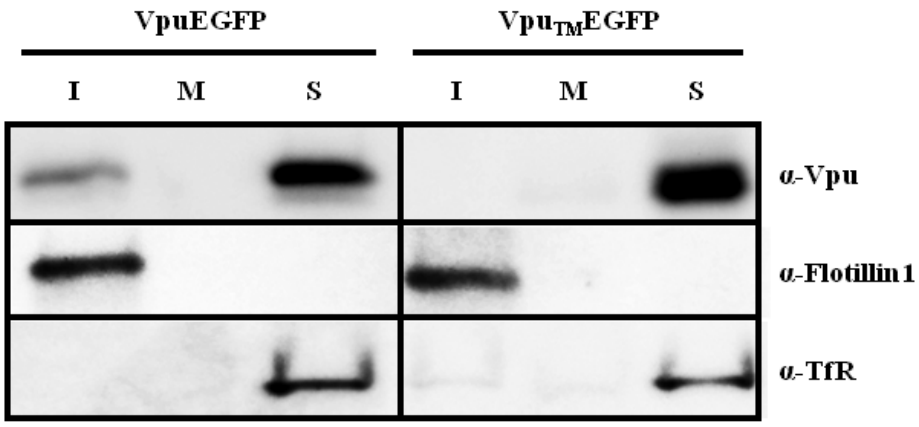
VpuEGFP
Vpu$_{TM}$EGFP
I
M
S
I
M
S
α-Vpu
α-Flotillin1
α-TfR

and standard deviation calculated. The results indicate that the majority of the Vphu mutants had a similar stability or were more stable than the unmodified Vphu, which had 47% remaining at the 6 hour chase period (Figure 37B-C). The average protein remaining at the 6-hour chase period for Vphu mutants W22A and SI23,24AA was lower than for the unmodified Vphu protein (28% and 38%, respectively).

Identification of critical amino acids in the transmembrane domain of Vpu that are required for membrane raft association

We determined if one or more amino acid residues within the transmembrane domain were critical for membrane raft association. Vectors expressing these mutant Vphu proteins were transfected into 293 cells and at 36 hours the DRMs were isolated as described above. All experiments were performed at least twice, and the blots shown are representative of all experiments. Appropriate controls for raft isolation and purity were performed and are shown. We found that two mutants, W22A and IVV19-21AAA had no detectable Vpu in the DRM fractions (Figure 38A). Additionally, substitution of the W22 with the more hydrophobic leucine did not affect raft association (Figure 38B). Taken together, these results suggest that membrane raft association can be manipulated by substituting specific amino acids in the TM domain.

The W22A mutant is localized to the same compartments as the unmodified VpuEGFP

As the W22A mutant appeared to have the greatest effect on raft association, we determined if this mutant displayed localization within the cells distinct from the observed with the unmodified Vpu protein. 293 cells were transfected with vectors expressing either VpuEGFP

Figure 37. Characterization of Vphu transmembrane mutants. Panel A. Sequences of the series of transmembrane mutants constructed and used in this study. Panel B. Pulse chase analysis of the Vphu transmembrane mutants. 293 cells were transfected with either the unmodified Vphu or the Vphu TM mutants. At 48 hours, cells were starved for methionine/cysteine and radiolabled for 1 hour as described in the Materials and methods section. The radiolabel was removed, cells washed and incubated in excess cold methionine/cysteine for 0 or 6 hours. The cells were lysed and processed for immunoprecipitation assays using a rabbit Vpu anti-serum. The immunoprecipitates were collected on protein A-Sepharose beads, boiled and visualized by SDS PAGE (12% gel) and standard autoradiographic techniques. The numbers above each lane represent the length of time chased in cold medium. Panel C. Graphical representation of the percent protein remaining for each Vphu TM mutant at the 6-hour post-chase timepoint.

A

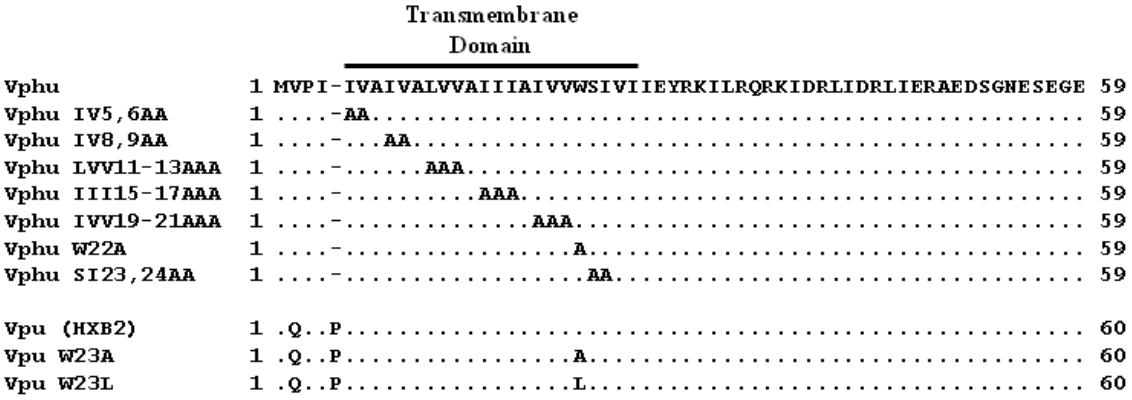
Transmembrane Domain
Vphu 1 MVPI-IVAIVALVVAIIIAIVVWSIVIIEYRKILRQRKIDRLIDRLIERAEDSGNESEGE 59
Vphu IV5,6AA 1 ....-AA..... 59
Vphu IV8,9AA 1 ....-...AA..... 59
Vphu LVV11-13AAA 1 ....-......AAA..... 59
Vphu III15-17AAA 1 ....-.........AAA..... 59
Vphu IVV19-21AAA 1 ....-.............AAA..... 59
Vphu W22A 1 ....-.................A..... 59
Vphu SI23,24AA 1 ....-.................AA..... 59
Vpu (HXB2) 1 .Q..P..... 60
Vpu W23A 1 .Q..P.................A..... 60
Vpu W23L 1 .Q..P.................L..... 60

B

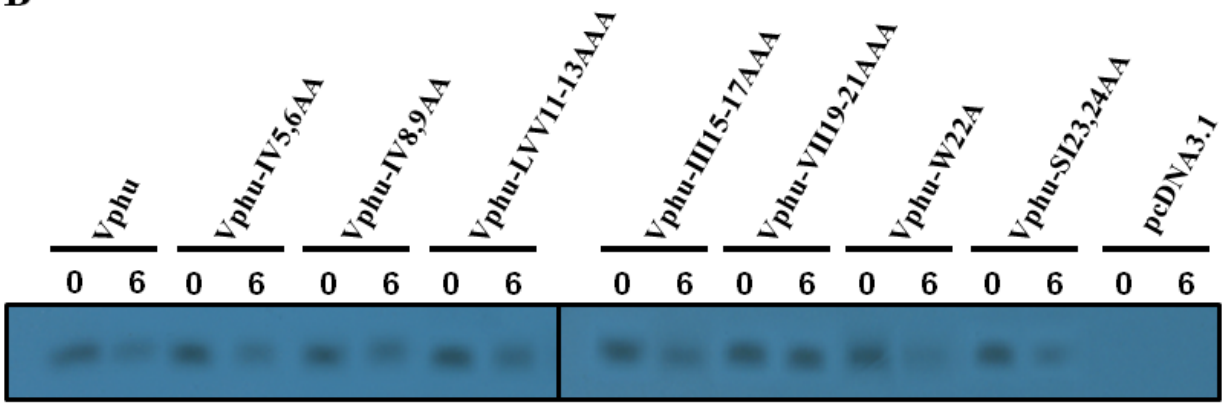
Vphu
Vphu-IV5,6AA
Vphu-IV8,9AA
Vphu-LVV11-13AAA
Vphu-III15-17AAA
Vphu-VIII19-21AAA
Vphu-W22A
Vphu-SI23,24AA
pcDNA3.1
0 6 0 6 0 6 0 6 0 6 0 6 0 6 0 6 0 6

C

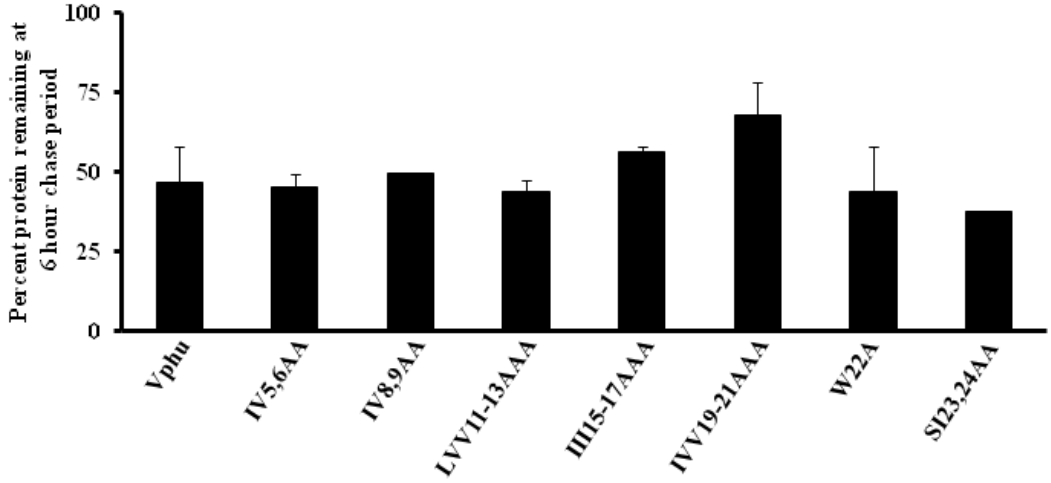
Percent protein remaining at 6 hour chase period
100
75
50
25
0
Vphu
IV5,6AA
IV8,9AA
LVV11-13AAA
III15-17AAA
IVV19-21AAA
W22A
SI23,24AA

Figure 38. Identification of Vphu transmembrane mutants that are not associated with membrane rafts. 293 cells were transfected with vectors expressing each of the Vphu TM mutants described in Figure 7A. At 48 hours, DRMs were extracted and isolated as described in the Materials and methods section. Fractions 1-3 (rafts; I), 5-6 (middle of the gradient; M) and 10-12 (non-raft; S) were pooled and analyzed for the presence of Vpu, Flotillin 1, and transferrin receptor. Panel A. Fractions from 293 cells transfected with vectors expressing each of the Vphu mutants described in Figure 7A. Panel B. Fractions from 293 cells transfected with vectors expressing either VpuEGFPW23A or VpuEGFPW23L described in Figure 7A.

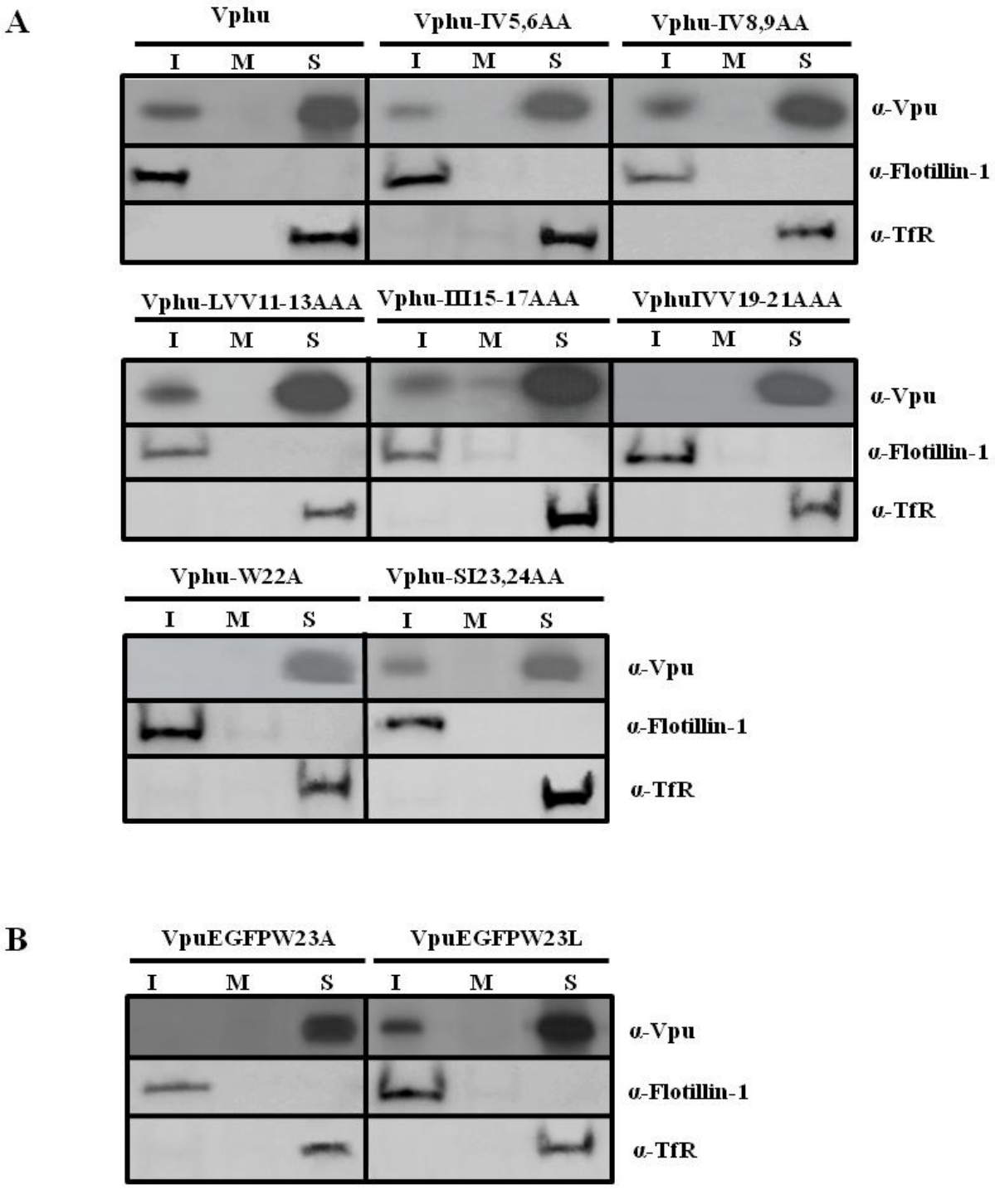
A
Vphu
Vphu-IV5,6AA
Vphu-IV8,9AA
I M S I M S I M S
α-Vpu
α-Flotillin-1
α-TfR
Vphu-LVV11-13AAA
Vphu-III15-17AAA
VphuIVV19-21AAA
I M S I M S I M S
α-Vpu
α-Flotillin-1
α-TfR
Vphu-W22A
Vphu-SI23,24AA
I M S I M S
α-Vpu
α-Flotillin-1
α-TfR
B
VpuEGFPW23A
VpuEGFPW23L
I M S I M S
α-Vpu
α-Flotillin-1
α-TfR

or VpuEGFPW23A (W residue is at position 23 in the corrected Vpu sequence fused to EGFP) and ER, Golgi or membrane markers. The results indicate that the VpuEGFP (Figure 39A-I) and the VpuEGFPW23A (Figure 39J-R) were localized to similar compartments, suggesting that transport to the intracellular compartments was not the reason for the lack of raft association by the W22A/W23A mutants.

Membrane raft association correlates with enhanced virus release

We examined these same mutants for the ability to enhance virus release from infected cells. For these experiments, we used HeLa cells, which express bone marrow stromal antigen 2 (BST-2). Vpu has been shown to directly interact with BST-2 to permit enhanced virus release from infected cells (Douglas et al., 2009). HeLa cells were co-transfected with plasmids expressing the Vphu mutants described above and $SHIV_{\Delta Vpu}$ and assessed for p27 release as described in the Materials and methods section. All conditions were run at least four separate times and the average percent p27 release and standard error calculated. The results indicate that Vpu mutants W22A and IVV19-21AAA and to a lesser extent LVV11-13AAA showed a significant decrease in p27 release, which correlated well with the lack of association with membrane rafts (Figure 40A). Analysis of infectious virus released also showed the same general pattern when compared to the p27 assays (Figure 40B). Significance of the p27 and infectious virus release for each virus mutant was assessed by comparison to the Vphu control with a $p \leq 0.01$ considered significant.

Figure 39. VpuEGFPW23A and VpuEGFP are localized to similar compartments. 293 cells were transfected with a vectors expressing either VpuEGFP or VpuEGFPW23A and ER-DsRed2, Golgi-DsRed2 or Membrane-DsRed2 as described in the Materials and methods section. At 48 h, cells were processed for confocal microscopy. Figure 9A-I. 293 cells transfected with VpuEGFP. Panels A, D, and G are fluorescent micrographs showing expression of VpuEGFP. Panels B, E, and H are fluorescent micrographs showing expression of DsRed2 proteins. Panels C, F, and I are a merge of the two panels to the left. Panels A-C. 293 cells transfected with VpuEGFP and ER-DsRed2. Panels D-F. 293 cells transfected with VpuEGFP and Golgi-DsRed2. Panels G-I. 293 cells transfected with VpuEGFP and Mem-DsRed2. Figures 9J-R. 293 cells transfected with VpuEGFPW23A. Panels J, M, and P are fluorescent micrographs showing expression of VpuEGFPW23A. Panels K, N, and Q are fluorescent micrographs showing expression of DsRed2 proteins. Panels L, O, and R are a merge of the two panels to the left. Panels J-L. 293 cells transfected with VpuEGFPW23A and ER-DsRed2. Panels M-O. 293 cells transfected with VpuEGFPW23A and Golgi-DsRed2. Panels P-R. 293 cells transfected with VpuEGFPW23A and Mem-DsRed2.

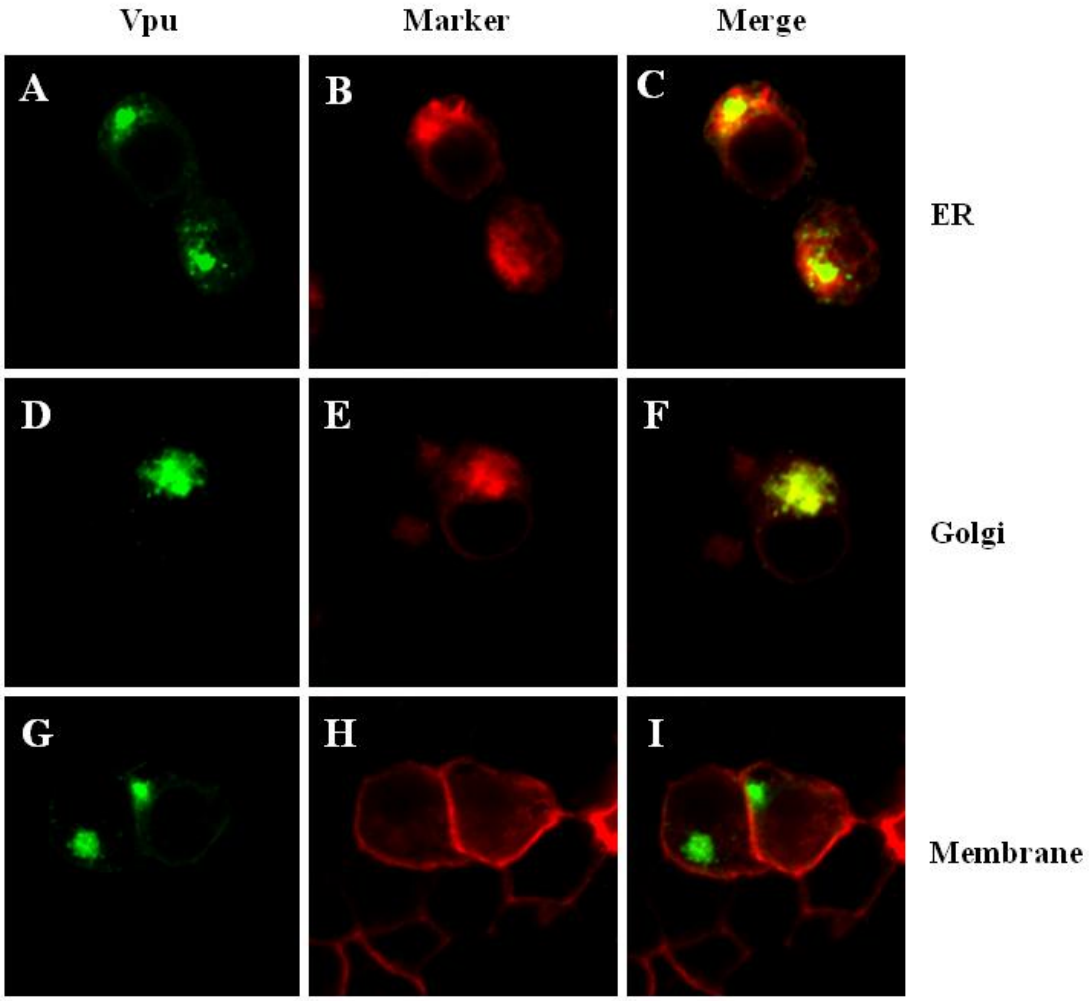
Vpu
Marker
Merge
A
B
C
ER
D
E
F
Golgi
G
H
I
Membrane

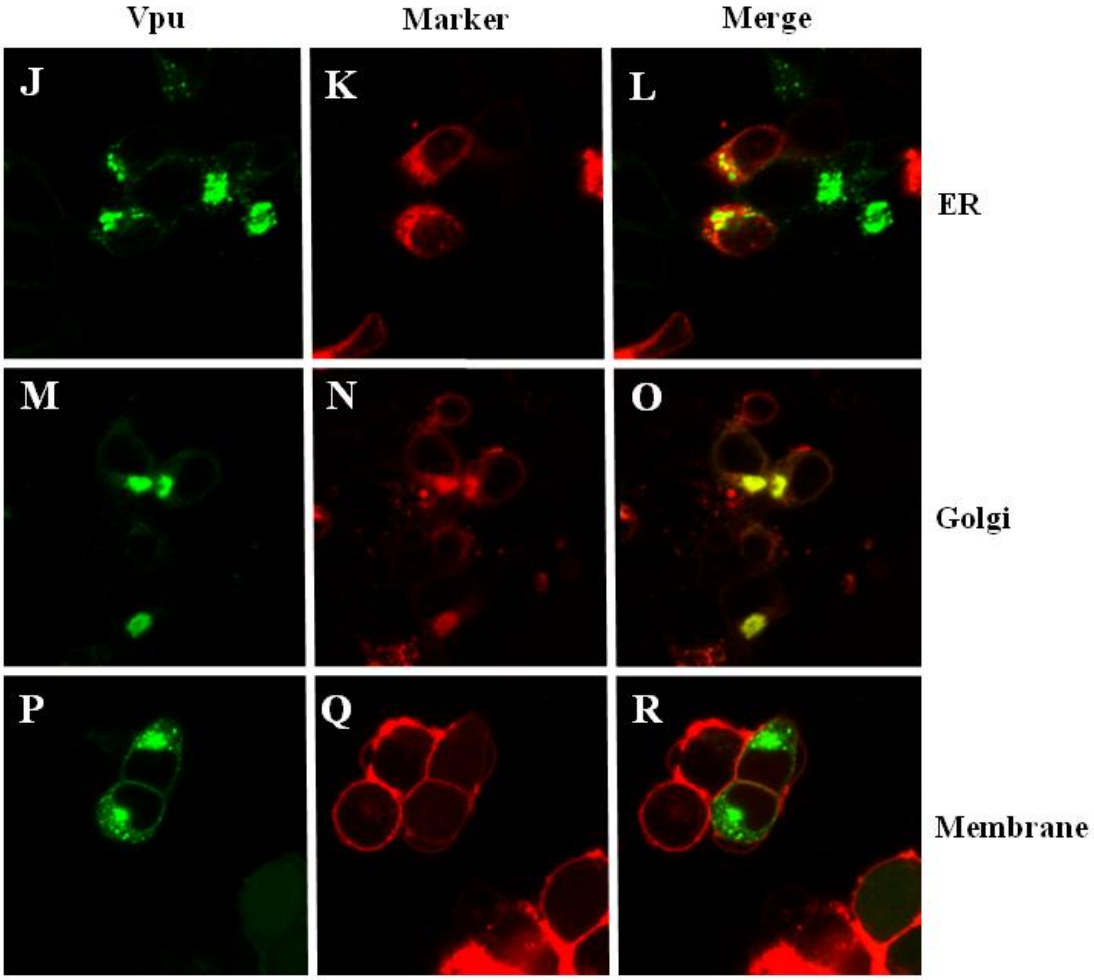
Vpu
Marker
Merge
J
K
L
ER
M
N
O
Golgi
P
Q
R
Membrane

Figure 40. Raft association correlates with enhanced virus release. The same mutants described in Figure 7A were used to determine the level of virus release in the presence of human BST-2. HeLa cells were co-transfected with $SHIV_{\Delta Vpu}$ and vectors expressing Vphu or the different transmembrane mutants. At 48 hours, the culture medium was collected and assayed for p27 and infectious virus released from cells. Panel A. The level of p27 released from transfected cells. Significance in the enhancement of p27 release was calculated with respect to the $SHIV_{KU\text{-}2MC4}$ using a Student's *t*-test with $p \leq 0.01$ considered significant (*). Panel B. The level of infectious virus released as determined by infection of TZM-bl cells and staining for the presence of β-galactosidase activity at 48 hours post-inoculation as described in the Materials and methods section. Significance in the enhancement of release of infectious units was determined with respect to the unmodified Vphu using a Student's *t*-test with $p \leq 0.01$ considered significant (*).

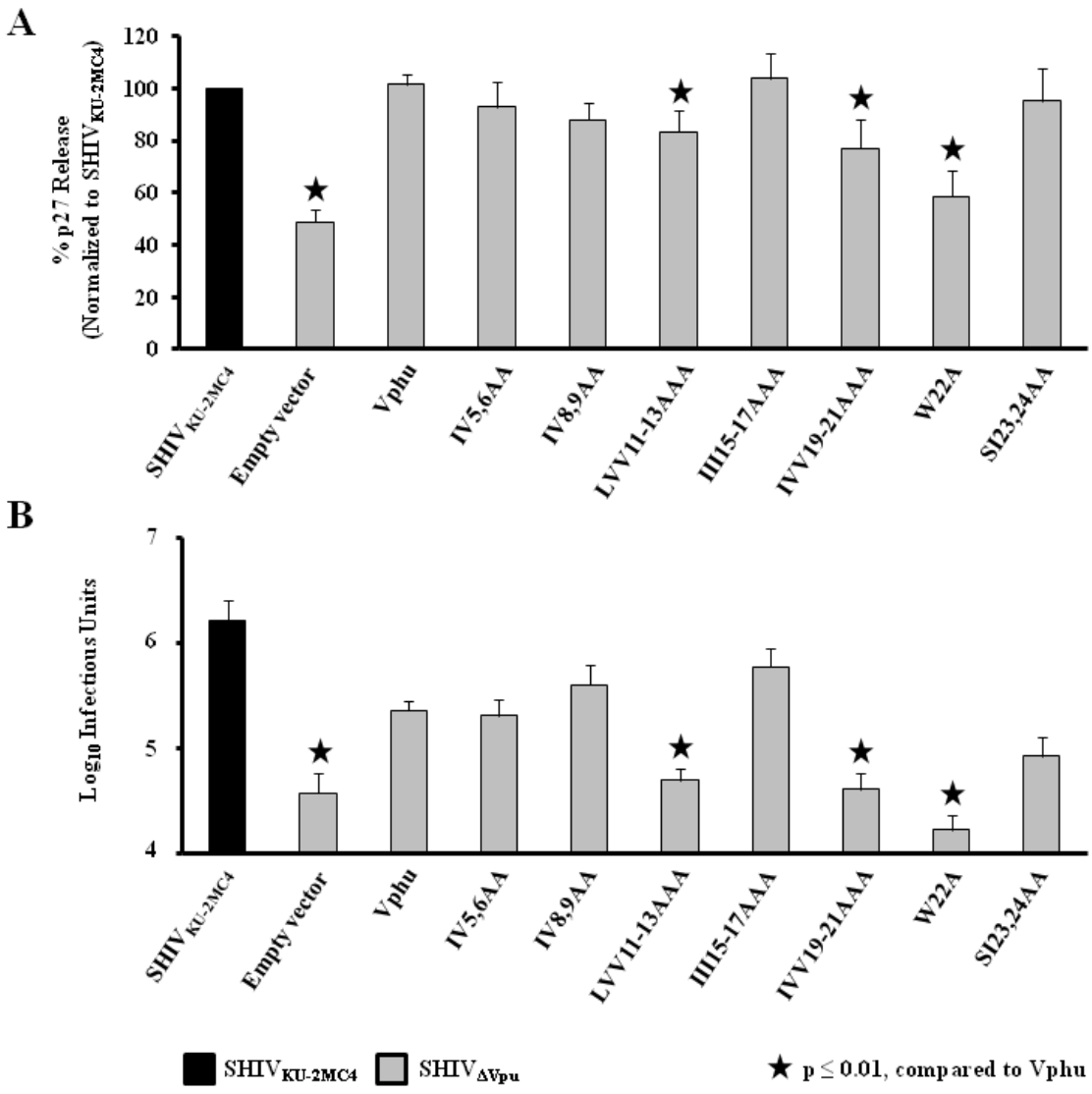
A
% p27 Release
(Normalized to SHIV KU-2MC4)
120
100
80
60
40
20
0
SHIV KU-2MC4
Empty vector
Vphu
IV5,6AA
IV8,9AA
LVV11-13AAA
IIII5-17AAA
IVV19-21AAA
W22A
SI23,24AA
B
Log10 Infectious Units
7
6
5
4
SHIV KU-2MC4
Empty vector
Vphu
IV5,6AA
IV8,9AA
LVV11-13AAA
IIII5-17AAA
IVV19-21AAA
W22A
SI23,24AA
SHIV KU-2MC4
SHIV ΔVpu
★ p ≤ 0.01, compared to Vphu

Membrane raft association is not required for CD4 down-regulation

As the other major function of Vpu is shunting of CD4 to the proteasome for degradation, we also examined surface expression of CD4 in the presence of these Vpu mutants. HeLa $CD4^+$ cells were transfected with vectors expressing Vphu or the mutants described above and EGFP. Cells were analyzed for CD4 surface expression by flow cytometry as previously described (Hill et al., 2008; Hill et al., 2010; Ruiz et al., 2008). All conditions were run three separate times and the average CD4 surface expression and standard error calculated. This Vpu function was not impaired with the majority of these mutants (Figure 41). The two Vphu mutants that were not detected in rafts, Vphu-IVV19-21AAA and W22A, had normal (VphuIVV19-21AAA) or slightly impaired (W22A) surface CD4 down-modulation compared to the unmodified Vphu protein. Taken together, these results indicate that raft association was not a requirement for Vpu-mediated down-modulation of CD4.

Figure 41. CD4 down-regulation by Vphu transmembrane mutants. HeLa $CD4^+$ cells were transfected with plasmids expressing the unmodified Vphu or each of the mutant Vphu proteins and one expressing EGFP. At 48 hours, live cells were immunostained for CD4. Cells were assessed for CD4 surface expression using flow cytometry. A mean fluorescent intensity (MFI) ratio of transfected (EGFP positive) to untransfected cells (EGFP negative) was calculated for each sample with the EGFP transfection control normalized to 1.0. Normalized ratios from three separate experiments were averaged and the standard error calculated.

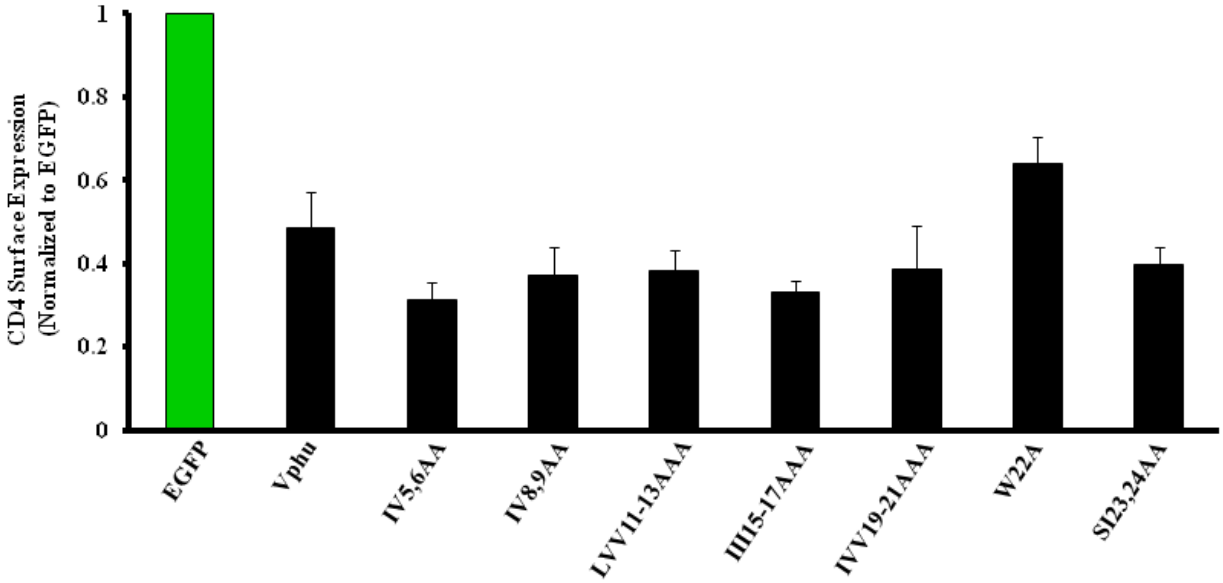
CD4 Surface Expression
(Normalized to EGFP)
1
0.8
0.6
0.4
0.2
0
EGFP
Vphu
IV5,6AA
IV8,9AA
LVV11-13AAA
IHI5-17AAA
IVV19-21AAA
W22A
SI23,24AA

Discussion

Many enveloped viruses such as vaccinia virus, the orthomyxoviruses (influenza), paramyxoviruses (measles, RSV), filoviruses (Ebola, Marburg) herpesviruses (EBV, HSV-1, pseudorabies), flaviviruses (West Nile virus), rhabdoviruses (VSV), and retroviruses (MLV) use membrane rafts as portals for entry and/or egress from cells (Barman and Nayak, 2000; Bavari et al., 2002; Bender et al., 2003; Brown and Lyles, 2003; Chung et al., 2005; Keller and Simons, 1998; Li et al., 2002; Manie et al., 2000; Marty et al., 2004; Medigeshi et al., 2008; Scheiffele et al., 1999). In addition to the viruses listed above, HIV-1 also exploits membrane rafts at several steps in its replication cycle. The HIV-1 envelope is known to be enriched in cholesterol and both Gag and Env have been found in detergent resistant membranes (Aloia et al., 1993; Brugger et al., 2006; Nguyen and Hildreth, 2000). These investigators found that GPI-anchored proteins such as Thy1 and CD59 as well as GM-1 ganglioside were present but that a non-raft protein, CD45, was largely absent from viral particles. It was subsequently shown that membrane rafts were critical for virus assembly and release (Ono and Freed, 2001). These investigators found that the myristylated N-terminal domain of Gag and the I domain of the nucleocapsid protein were critical for raft association and that the cholesterol depleting compound, M-β-CD, reduced the efficiency of virus release. The palmitoylation of Env gp41 was initially shown to be important for raft targeting and infectivity but later studies showed that substitution of the cysteines in the cytoplasmic domain of gp41 (thus resulting in no palmitoylation) only partially affected infectivity or had no effect (Bhattacharya et al., 2004; Chan et al., 2005; Rousso et al., 2000). It was later shown that mutations in the Gag p17 protein would prevent Env incorporation into rafts and virions, suggesting that Gag regulates Env incorporation into rafts (Bhattacharya et al., 2006; Patil et al., 2010). Other investigators have shown that the HIV-1

Env has a **c**holesterol **r**ecognition/interaction **a**mino acid **c**onsensus (CRAC) domain that is responsible for raft association (Epand et al., 2006; Vishwanathan et al., 2008).

In this study, we have determined that the Vpu protein partially associates with membrane rafts. We have shown this using biochemical fractionation, through the use of cholesterol reducing drugs and co-patching experiments. In the results presented here, Vpu expressed either exogenously in the absence of other viral proteins or in virus-infected T cells (C8166 cell line), partitions into DRMs. Our studies used Triton-X-100 as it is the most stringent with respect to extraction of DRMs (Schuck et al., 2003; Shogomori and Brown, 2003). We also showed that Vpu partially partitions into DRMs when extracted at physiological temperature as rafts isolated at 37C are thought to be more similar to rafts in live cells. In addition to showing that Vpu partitions into DRMs, it was necessary to show that disruption of membrane rafts by cholesterol depletion would prevent Vpu from partitioning into DRMs. Drugs that reduce cholesterol levels in cells, either by inhibiting an HMGCoA reductase in the cholesterol synthesis pathway (e.g. Lovastatin) or by extracting cholesterol from cell membranes (e.g. methyl-β-cyclodextrin; M-β-CD), are known to disrupt membrane rafts. We determined if a combination of Lovastatin and M-β-CD would eliminate Vpu from DRMs, which would indicate that Vpu resistance to Triton-X-100 is a specific property of raft inclusion. This treatment significantly reduced the level of Vpu in membrane rafts. Finally, Vpu association with lipid rafts was confirmed by co-localization of Vpu_{SC}EGFP1 with a raft marker in live cells. As the subtype B Vpu used in most of the experiments in this study is found predominantly in the Golgi, ER, and endosomes, and only small amounts are found at the surface, we used Vpu_{SC}, which is efficiently transported to the cell surface for this assay. While it seems likely that Vpu is associated with rafts internally, these rafts are, as yet, difficult to visualize. Most studies of rafts

in Golgi bodies or endosomes have been done using biochemical lipidomic techniques rather than live cell imaging. Taken together, these experiments provide strong evidence that Vpu is partially localized to membrane rafts and at least some rafts containing GPI-anchored proteins.

As the transmembrane (TM) or membrane proximal domains are most likely to be involved in membrane raft targeting, we examined the detergent resistance of a Vpu fusion protein with a scrambled TM domain (Vpu_{TM}EGFP). This protein was not associated with DRM fractions, indicating that the TM domain may be involved in membrane raft association. However, since this scrambled TM domain has a total of 15 amino acid changes, it is possible that these substitutions may have caused an alteration of the spatial orientation of the protein in the membrane, the flexible linker region following the TM domain or the first α-helical region proximal to the membrane. Also, previous modeling studies have indicated that changes in the Vpu TM domain have the ability to cause secondary structure changes downstream (Candler et al., 2005; Sramala et al., 2003). In order to address this concern, we used Vpu mutants with more targeted mutations. Our results indicate that Vpu mutants Vphu-IVV19-21AAA and Vphu-W22A were no longer associated with membrane raft fractions. While these results show that amino acid substitutions in the TM domain can affect incorporation into rafts, they do not necessarily rule out that other amino acids in the TM domain (i.e. the alanine residues) or residues in the cytoplasmic domain may also be involved. Recent computer modeling studies have suggested that the transmembrane domain of Vpu is flexible in adapting to different lipid environments (Kruger and Fischer, 2008). When Vpu was simulated moving through various lipid environments representative of the Golgi apparatus, Vpu exhibited no particular preference for lipid thickness or composition. Rather, the tilt angle and kink around the region I17 to S23 adjust to the membrane. This modeling data correlates well with the loss of DRM association of

IVV19-21AAA and W22A. If these residues are important to the structural flexibility of the Vpu transmembrane domain, substitution with alanines could reduce the ability of the protein to adapt to a changing lipid environment, thus excluding it from membrane rafts. Substitution of the W23 with a longer, more hydrophobic leucine resulted in a protein which was still found in the DRMs. As this protein was more similar to wild-type Vpu in efficiency of CD4 down-modulation than W23A (data not shown), this further suggests that structural changes are involved in raft inclusion and exclusion of Vpu.

To demonstrate that membrane raft association was relevant to Vpu functions and to virus replication, we assayed the various Vphu TM mutants for the ability to down-modulate CD4 surface expression and enhance virus release. Our results showed that all of the Vphu TM mutants down-modulated CD4 surface expression although Vphu-W22A was slightly impaired compared to the other mutants. We measured enhanced virus release by two methods, release of p27 antigen from cells and by quantifying levels of infectious virus released from cells. The two assays were in agreement and indicate that virus release was significantly reduced by the LVV11-13AAA, IVV19-21AAA and W22A mutants with the W22A consistently displaying the most reduction in particle release. Of these three mutants, both IVV19-21AAA and W22A were not incorporated into rafts, implying a correlation between membrane raft association and Vpu-mediated virus release. One question that arises is, "Why did LVV11-13AAA have impaired release since it was clearly observed in DRM fractions?" While the answer is presently unknown, it is possible that substitution of three hydrophobic residues with less hydrophobic alanines may have altered the structure/flexibility of the protein or protein-protein interactions (such as with BST-2) of the domain although it had no effect on CD4 down-modulation. As is a caveat of all mutagenesis based studies, it is unknown whether the results observed in this study

were based on structural alterations of the protein or roles for specific amino acids. Further studies will be needed to determine the affects the mutations introduced in this study have on the overall protein structure as well as any protein-protein interactions. However, regardless of the mechanisms by which the membrane raft association and enhanced virion release function of the Vpu proteins were altered these results demonstrate the ability of exogenous forces to disrupt function. This introduces the potential for therapeutic molecules designed to alter the spatial orientation of the TMD such that membrane raft association and/or protein-protein interactions (such as BST-2) would be disrupted.

Recently, Vpu was shown to antagonize the activity of a molecule known as bone marrow stromal cell antigen 2 (BST-2) or tetherin (Neil et al., 2008; Van Damme et al., 2008). BST-2 is thought to work by "tethering" particles at the cell surface, which may account for the observed maturation of HIV-1Δ*vpu* (adherence of particles to the cell plasma membrane with a common observation of several virus particles in the "string of pearls" arrangement and the observation of virus particles being taken or maturing into vesicles). BST-2 has been shown to associate with membrane rafts, including the sites of HIV-1 maturation and release (Kupzig et al., 2003; Perez-Caballero et al., 2009; Rollason et al., 2007). In the absence of Vpu, BST-2 may become associated with rafts that are ultimately involved in virus assembly and release from cells. This is supported by findings that HIV-1 Gag and BST-2 co-localize in intracellular compartments of the cell (Neil et al., 2008; Van Damme et al., 2008). Vpu is not incorporated into virions suggesting that Vpu may associate with membrane rafts that are not involved in virus assembly and release (Strebel et al., 1989). It is known that membrane rafts are diverse in both lipid and protein composition and it has been shown that distinct rafts can be isolated using immune selection procedures (Drevot et al., 2002; Knorr et al., 2009). One group of

investigators showed that wild type BST-2 was found in several different clusters on the plasma membrane and that removal of the GPI anchor resulted in a BST-2 exclusively associated with sites of budding (Perez-Caballero et al., 2009). This implies that wild type BST-2 is found in more than one type of membrane raft. Thus, it is conceivable that Vpu could possibly interact with BST-2 before or after transport to the Golgi complex and become associated with a subpopulation of membrane rafts not associated with virus assembly and release at the cell surface. Membrane rafts were originally shown to initially form in the Golgi complex (Simons and van Meer, 1988) and to be enriched in the *trans* Golgi network. However, more recent studies have shown that the ER and *cis* Golgi are also sites for sorting of proteins and lipids (Alfalah et al., 2005; Browman et al., 2006). BST-2 was found in membrane rafts only after its N-linked carbohydrate chains were fully processed, suggesting that raft association of this protein occurs in the Golgi complex (Kupzig et al., 2003). Recent data has been presented that suggests the presence of Vpu in the *trans* Golgi is important for Vpu antagonism of BST-2 (Dube et al., 2009). It will be of interest to determine if Vpu and BST-2 can be co-immunoprecipitated from similar rafts and if so, where does this association occur? Finally, identification of Vpu mutants that are functional for either CD4 down-modulation or enhanced virus release will be useful in determining if one function is more important for pathogenesis using the SHIV/macaque model.

Materials and Methods

Plasmids, Viruses and Cell Culture

The HeLa cell line was obtained through the AIDS Research and Reference Reagent Program, Division of AIDS, NIAID, NIH: (specify cell line) from Dr. Richard Axel. The 293

and HeLa cell lines were maintained in Dulbecco's minimal essential medium supplemented with 10% fetal bovine serum, gentamicin (5 μg per ml) and penicillin/streptomycin (100 U per ml and 100 μg per mL, respectively). The TZM-bl cell line was obtained through the NIH AIDS Research and Reference Reagent Program, Division of AIDS, NIAID, NIH: TZM-bl from Dr. John C. Kappes, Dr. Xiaoyun Wu and Tranzyme Inc. The HeLa $CD4^+$ cell line was obtained through the AIDS Research and Reference Reagent Program, Division of AIDS, NIAID, NIH: HeLa CD4 Clone 1022 from Dr. Bruce Chesebro. TZM-bl cells were maintained in DMEM containing 10% fetal bovine serum with antibiotics. HeLa CD4+ cells were maintained in DMEM containing 10% fetal bovine serum antibioics and 1 mg per mL of G-418. The derivation and pathogenicity of $SHIV_{KU\text{-}1bMC33}$ and no*vpu*$SHIV_{KU\text{-}1bMC33}$ have been described (McCormick-Davis et al., 2000a; Singh et al., 2003; Stephens et al., 2002). The derivation of the $SHIV_{KU\text{-}2MC4\Delta Vpu}$ plasmid has been described (Ruiz et al., 2010b). Vectors expressing the subtype B (pcv*puegfp*) and C Vpu (pcvpu_{SC}*egfp*) proteins fused to enhanced green fluorescent protein (eGFP) and the Vpu_{TM}EGFP (pcvpu_{TM}*egfp*) mutant have been previously described (Gomez et al., 2005; Pacyniak et al., 2005; Ruiz et al., 2008; Singh et al., 2003). The pcVphu construct was obtained through the NIH AIDS Research and Reference Reagent Program, Division of AIDS, NIAID, NIH: pcDNA-Vphu from Dr. Stephan Bour and Dr. Klaus Strebel (Nguyen et al., 2004). The YFP-GPI and NFP-GPI constructs were kindly provided by Dr. Akira Ono. The YFP-GPI construct has the ER translocation signal from rabbit phlorizin hydrolase fused to the N-terminus of Venus YFP and a GPI anchor sequence from CD59 fused to the C-terminus. The non-fluorescent version (NFP-YFP) contains the mutation Y67C that abolishes fluorophore formation. The vectors expressing ER-DsRed2, Golgi-DsRed2, and Mem-DsRed2 were obtained from Clontech. Mutations introduced into all plasmids used in this study were

accomplished using a QuikChange site-directed mutagenesis kit (Stratagene) according to the manufacturer's protocol. All plasmid inserts were sequenced to ensure the validity of the mutations and that no other mutations were introduced during the cloning process.

Isolation of Detergent Resistant Membranes (DRMs)

293 cells were cultured in 60 mm well dishes for 24 hours, then transfected using branched polyethylenimine (PEI; Sigma). At 48 hours post-transfection, cells were lysed in ice cold DRM buffer (25 mM Tris pH 7.5, 150 mM NaCl, 10 mM EDTA) containing 1% Triton-X-100. Cells remained on ice in lysis buffer for 20min before being pushed through a 22 gauge needle at least 7 times. The lysate was then mixed with an equal volume of 80% sucrose (w/v) in DRM buffer to a final concentration of 40% sucrose. The lysate was placed in the bottom of a SW41 ultracentrifuge tube and overlaid with 8 mL 30% sucrose and 2 mL 5% sucrose. Gradients were spun to equilibrium at 38,000 rpm (247,000x g) for 18 hours (SW41 rotor, Beckman Coulter). One mL fractions were taken from the top, concentrated, and analyzed by Western blot using a rabbit anti-EGFP antibody or a rabbit Vpu antiserum obtained through the AIDS Research and Reference Reagent Program, Division of AIDS, NIAID, NIH: HIV-1_{NL4-3} Vpu Antiserum from Dr Frank Maldarelli and Dr. Klaus Strebel. Controls include the raft protein flotillin-1 (mouse anti-flotillin-1, BD Biosciences) and the non-raft protein, transferrin receptor (mouse anti-transferrin receptor, BD Biosciences). For isolation of DRMs from virus infected cells, C8166 cells were inoculated with 10^4 $TCID_{50}$ of either $SHIV_{KU\text{-}1bMC33}$ or no*vpu*$SHIV_{KU\text{-}1bMC33}$ for 4 hours. At this time, cells were washed twice and incubated in fresh medium for 5 days at 37C. Cultures were starved and radiolabled with 1 mCi of ^{35}S-methionine/cysteine for 2

hours. The cells were centrifuged at low speed (800x g) to pellet the cells, washed three times in medium without serum and processed as above. One ml fractions were taken from the top and raft (fractions 1-3), middle (fractions 6-7), and non-raft (fractions 10-12) fractions were analyzed by immunoprecipitation using the rabbit Vpu antiserum antibody and by Western blot for raft and non-raft control proteins.

Isolation of Detergent Resistant Membranes (DRMs) at Physiological Temperature

For these experiments, we used the procedure of (Chen et al., 2009). 293 cells were cultured in 12 well dishes for 24 hours and then transfected using PEI. At 36-48 hours post-transfection, cells were lysed in DRM37 (10 mM HEPES pH 7.0, 50 mM KOAc, 1 mM $Mg(OAc)_2$, 1 mM EDTA, 200 mM sucrose). The lysates were pushed through a 22 gauge needle at least 7 times, then incubated at 37C for 5 minutes. Lysates were then mixed with an equal volume of 2% Triton X-100 in DRM37 and incubated at 37C for 5 minutes. The lysates were mixed with an equal volume of 80% sucrose in DRM37, layered at the bottom of an ultracentrifuge tube and overlaid with 7 ml 30% sucrose/DRM37 and 2 ml DRM37 (6.5% sucrose). Gradients were spun to equilibrium at 38,000 rpm overnight (SW41 rotor, Beckman Coulter) at 4C. One ml fractions were taken from the top and analyzed for various proteins by Western blot.

Cholesterol Depletion Experiments

293 cells were transfected with a plasmid expressing VpuEGFP or Vpu_{SC}EGFP and treated with 4μM Lovastatin for 48 hours. Thirty minutes prior to lysis of cells, the cultures were incubated with M-β-cyclodextrin (M-β-CD; 10 mg/ml). Lysates were prepared, and subjected to ultracentrifugation as described above. One mL fractions were collected from the top of the gradient. Fractions 1-3, 6-7, and 10-12 were each pooled, methanol precipitated and resuspended in 1X sample reducing buffer. The samples were then analyzed for the presence of VpuEGFP or Vpu_{SC}EGFP by Western blot using an antibody directed against EGFP.

Co-patching Experiments

293 cells cultured on cover slips were transfected with YFP-GPI or NFP-GPI and Vpu_{SC}EGFP using PEI. At 48 hours post-transfection, cover slips were washed three times in 1X PBS, then incubated in primary antibody (mouse anti-GFP, Clontech) for 30 minutes at 37C. Unbound antibody was removed by washing three times in 1X PBS followed by reaction with a secondary antibody (goat anti-mouse-Cy5, Molecular Probes) at 37C for 30 minutes. Unbound antibody was removed by washing three times in 1X PBS and cells fixed in 2% paraformaldehyde/PBS for 15 minutes. Cover slips were mounted in SlowFade Antifade solution A (Molecular Probes). A Nikon A1 confocal microscope was used to collect 100X images with a 2X digital zoom, using EZ-C1 software. The pinhole was set to large (100 nm) for all wavelengths. EGFP was excited using an argon 488 nm laser and viewed through the FITC filter (525/25 nm) and Cy5 was excited at 638 nm and viewed through a Cy5 filter (700/38 nm).

Pulse-Chase Analysis of Vphu TMD Mutant Proteins

293 cells were transfected with vectors expressing each mutant protein. At 48 hours post-transfection, the medium was removed and cells were incubated in methionine/cysteine-free medium for 2 hours. The cells were then radiolabeled with 200 µCi of ^{35}S-Translabel (methionine and cysteine, MP Biomedical) for 1 hour. The radiolabel was chased in DMEM containing 100X unlabeled methionine/cysteine medium for 0 and 6 hours. Vphu proteins were immunoprecipitated using a rabbit anti-Vpu serum and collected on Protein A-Sepharose beads overnight on a rotator for 18 hours. Non-transfected 293 cells, starved, radiolabeled and chased for 0 hours served as a negative control. Beads were washed three times with 1X radioimmunoprecipitation buffer (RIPA: (50 mM Tris-HCl, pH 7.5; 50 mM NaCl; 0.5% deoxycholate; 0.2% SDS; 10 mM EDTA), and the samples resuspended in sample reducing buffer. Samples were boiled and the Vphu proteins separated by SDS-PAGE (12% gel). Proteins were then visualized using standard autoradiographic techniques. All conditions were run in duplicate, the pixel densities of each band determined using ImageJ software, normalized to the hour 0 sample, and the average percent protein remaining calculated.

Confocal Microscopy Studies

293 cells were cultured on cover slips one day prior to being transiently transfected with plasmids expressing either VpuEGFP or VpuEGFPW23A and one of the intracellular marker proteins (ER-DsRed2, Golgi-DsRed2 or Membrane-DsRed2) using PEI (Sigma). Cultures were maintained for 36-48 hours before being washed three times in PBS, and fixed in 2% paraformaldehyde/PBS. Cover slips were mounted in glycerol containing mounting media

(Slowfade Antifade solution A). A Nikon A1 confocal microscope was used to collect 100X images with a 2X digital zoom, using EZ-C1 software. The pinhole was set to large (100 nm) for all wavelengths. EGFP was excited using an argon 488 nm laser and viewed through the FITC filter (525/25 nm). DsRed2 were excited using a 561 DPSS laser and viewed through the Texas Red filter (595/50 nm).

Virion Release Assays

Hela cells (10^5) were seeded into a 24-well tissue culture plate 24 hours prior to transfection. Cells were transfected as described above with 1 µg of plasmid expressing full length SHIV proviral DNA (either $SHIV_{KU\text{-}2MC4}$ or $SHIV_{\Delta Vpu}$) and 200 ng of plasmid expressing various mutant *vphu* genes. Cells were incubated at 37C in 5% CO_2 atmosphere for 48 hours. Supernatants were collected and cellular debris removed through low speed centrifugation. Cells were lysed in 250 µl of 1X RIPA buffer and the nuclei removed through high speed centrifugation. The amount of p27 present within the supernatant and the cell lysates was determined using a commercially available p27 ELISA kit (Zeptometrix Incorporated) and the percent of p27 release calculated. All conditions were run at least four separate times and the average percent p27 release and standard error calculated. Significance with respect to the unmodified Vphu was calculated using a Student's *t*-test with a $p<0.01$ considered significant.

Infectious Units Release Assays

TZM-bl cells (10^4) were seeded into a 96-well tissue culture plate 24 hours prior to infection. Supernatants collected from HeLa cells co-transfected with $SHIV_{\Delta Vpu}$ and Vphu expressing plasmids as described above were added to the TZM-bl cells and serially diluted. At 48 hours post-infection, cells were washed twice in 1X PBS and incubated in a fixative solution (0.25% glutaraldehyde, 0.8% formaldehyde in phosphate buffered saline) for 5 minutes at room temperature. The cells were washed three times in 1X PBS and covered in staining solution (400 µg/ml X-gal, 4 mM $MgCl_2$, 4 mM $K_3Fe(CN)_6$, 4 mM $K_4Fe(CN)_6$-$3H_2O$ in phosphate buffered saline) and incubated for 2 hours at 37C. Cells were washed once in 1X PBS and then immersed in 1X PBS during counting. The $TCID_{50}$ for each supernatant was calculated based on wells containing cells expressing β-galactosidase. All conditions were run at least four times and the $TCID_{50}$ calculated. The average $TCID_{50}$ and standard error were calculated. Significance in the restriction of infectivity was determined with respect to the unmodified Vphu using a Student's *t*-test with $p<0.01$ considered significant.

Assessment of CD4 cell surface expression

For analysis of cell surface CD4 expression in the presence of the various Vphu mutant proteins, HeLa $CD4^+$ cells were seeded into each well of a 6-well tissue culture plate 1 day prior to transfection. Cells were co-transfected with plasmids expressing one of the various Vphu mutant proteins and EGFP. Cells transfected with EGFP only were used as the control. At 48 hours post-transfection, cells were removed from the plate using Ca^{2+}/Mg^{2+}-free PBS containing 10mM EDTA and stained with PE-Cy5 conjugated anti-CD4 (BD Bioscience). Cells were

analyzed using an LSRII flow cytometer and the mean fluorescence intensity (MFI) of PE-Cy5 for transfected cells (EGFP positive) and untransfected cells (EGFP negative) was calculated. An MFI ratio was calculated for each sample with the EGFP control (no Vphu) normalized to 1.0 and untransfected cells (EGFP negative). Normalized ratios from three separate experiments were averaged and the standard error calculated. All groups were compared to the EGFP control as well as the Vphu only control using a Student's t-test (unpaired, $p<0.05$ significant).

XI. Chapter 6: Requirements of the Membrane Proximal Tyrosine and Dileucine Based Sorting Signals for Efficient Transport of the Subtype C Vpu Protein to the Plasma Membrane and in Virus Release

Abstract

Previously, we showed that the Vpu protein from HIV-1 subtype C is more efficiently transported to the cell surface than the well studied subtype B Vpu (Pacyniak et al., 2005) and that a SHIV expressing the subtype C Vpu exhibited a decreased rate of $CD4^+$ T cell loss following inoculation in macaques (Hill et al., 2008). In this study, we examined the role of overlapping tyrosine-based (YxxΦ) and dileucine-based ([D/E]xxxL[L/I]) motifs in the membrane proximal region of the subtype C Vpu (EYRKLL) in Vpu intracellular transport, CD4 surface expression and virus release from the cell surface. We constructed three site-directed mutants of the subtype C *vpu* and fused these genes to the gene for enhanced green fluorescent protein (EGFP). The first mutation altered the tyrosine (E**A**RKLL; Vpu_{SC}EGFPY35A) , the second altered the dileucine motif (EYRKL**G**; Vpu_{SC}EGFPL39G), and the third contained both amino acid substitutions (E**A**RKL**G**; Vpu_{SC}EGFPYL35,39AG) in this region of the Vpu protein. The Vpu_{SC}EGFPY35A protein was transported to the cell surface similar to the unmodified Vpu_{SC}EGFP1 while Vpu_{SC}EGFPL39G was expressed at the cell surface at significantly reduced levels. The Vpu_{SC}EGFPYL35,39AG was found to have an intermediate level of cell surface expression. All three mutant Vpu proteins were analyzed for the ability to prevent cell surface expression of CD4. We found that both single mutants did not significantly affect CD4 surface expression while the double mutant (Vpu_{SC}EGFPYL35,39AG) was significantly less efficient at preventing cell surface CD4 expression. Chimeric simian-human immunodeficiency viruses

were constructed with these mutations in *vpu* ($SHIV_{SCVpuY35A}$, $SHIV_{SCVpuL39G}$ and $SHIV_{SCVpuYL35,39AG}$). Our results indicate that $SHIV_{SCVpuL39G}$ replicated much more efficiently and was much more cytopathic than $SHIV_{SCVpu.}$ In contrast, $SHIV_{SCVpuY35A}$ and $SHIV_{SCVpuYL35,39AG}$ replicated less efficiently when compared to the parental $SHIV_{SCVpu}$. Taken together, these results show for the first time that the tyrosine-based sorting motif in the cytoplasmic domain of Vpu is essential for efficient virus release. These results also indicate that the dileucine-based sorting motif affects the intracellular trafficking of clade C Vpu proteins, virus replication, and release.

Introduction

Subtype C HIV-1 accounts for over 50% of the infections worldwide (Hemelaar et al., 2006; Takeb et al., 2004). While the reasons for the rapid spread of these viruses in the human population is currently unknown, several studies have suggested differences between the subtype C HIV-1 and viruses from the other subtypes of HIV-1 group M. In one study, both non-syncytia-inducing (NSI)/R5 and syncytia inducing (SI)/X4 subtype C HIV-1 isolates were found to be significantly less fit in peripheral blood mononuclear cells (PBMC) competition assays than all other group M isolates of the same phenotype (Ball et al., 2003). Another study evaluated the replicative fitness of representative strains from subtypes A, B, C, D and CRF01_AE. In this study, subtype C viruses were found to have less replicative fitness in PBMC compared to the other subtypes but were 100 fold more fit in these assays than HIV-2 or group O isolates (Arien et al., 2005). More recently, a study evaluating the fitness and transmission efficiency of 33 different isolates from various HIV-1 subtypes found that while the subtype C HIV-1 viruses were the least replicatively fit in PBMC, these viruses were able to

compete with other subtypes in primary human explants of penial, cervical and rectal tissues (Abraha et al., 2009). In addition to replication in *in vitro* assays, the Vpu proteins from subtype C HIV-1 isolates have biological properties and structural features that differ from the well studied subtype B Vpu protein. Previously, we showed that the subtype C Vpu protein was efficiently transported to the cell surface while the subtype B Vpu protein appears to be predominantly localized to intracellular compartments (Pacyniak et al., 2005). Recently, we also showed that the subtype C Vpu was less efficient at preventing surface expression of CD4 than the subtype B protein and that replacement of the subtype B *vpu* from a pathogenic molecular clone of SHIV ($SHIV_{KU\text{-}1bMC33}$) with the *vpu* gene from a subtype C clinical isolate resulted in a decreased rate of $CD4^+$ T cell loss following inoculation into macaques (Hill et al., 2008). Taken together, these studies suggest that specific molecular determinants within different Vpu subtypes mediate protein trafficking and function and in turn, affect the role of the Vpu in HIV-1 pathogenesis.

The distinct biological properties exhibited by different HIV-1 Vpu subtypes suggest that their function and effects on HIV-1 pathogenesis are mediated by different domains within each protein. Tyrosine and dileucine motifs have been implicated in the intracellular sorting of a multitude of viral and cellular proteins. For the human and simian immunodeficiency viruses, the intracellular trafficking function of the envelope (Env) protein as well as the negative factor (Nef) protein have been shown to be modulated by conserved GYxxΦ and ExxxLL motifs, respectively (Aiken et al., 1994; Day et al., 2006; Greenberg et al., 1998a). HIV-1 Vpu also contains several potential sorting signal sequences within the cytoplasmic domain. The subtype C Vpu contains overlapping conserved EYxxΦ and [D/E]xxxL[L/I] motifs at the membrane proximal region of the cytoplasmic domain. It also contains an ExxxLL motif at the carboxy

terminus region of the cytoplasmic domain. The membrane proximal YxxΦ motif is highly conserved among all Vpu subtypes while the two dileucine motifs are only highly conserved among subtype C Vpu. Finally, an invariant leucine residue is present within the predicted second α-helical domain of all Vpu. This leucine residue is part of a potential dileucine-based sorting signal (ExxxLV) within the subtype B Vpu protein. The presence or absence of these dileucine motifs may play a role in the differences in biological properties exhibited by subtype C Vpu as well as the reduced replicative fitness of this subset of viruses. In this study, we examined the role of the unique overlapping tyrosine (YxxΦ; with Φ being an amino acid with a large hydrophobic amino acid) and dileucine ([D/E]xxxL[L/I]) motifs on the intracellular trafficking of the subtype C Vpu, CD4 surface expression and viral release from infected cells. Our results show for the first time that a dileucine-based sorting signal can affect trafficking of the Vpu protein, the level of cytopathology, the enhanced release function of Vpu and the efficiency of cell surface CD4 surface expression .

Results

Substitution in the dileucine motif causes retention of subtype C Vpu in ER/Golgi compartments

The sequences of the Vpu mutants analyzed in this study are shown in Figure 42. We first analyzed the ability of the Vpu mutants to be transported to the cell surface using two different assays. 293 cells were transfected with vectors expressing either Vpu_{SC}EGFP1, Vpu_{SC}EGFPY35A, Vpu_{SC}EGFPL39G, or Vpu_{SC}EGFPYL35,39AG. At 36 hours post-transfection, cells were analyzed by laser scanning confocal microscopy. As shown in Figure 43A-D, the Vpu_{SC}EGFP1 and Vpu_{SC}EGFPY35A predominately localized at the cell plasma

Figure 42. Sequence alignment of the Vpu proteins analyzed in this study. The putative transmembrane domain (black), tyrosine motif (blue), and dileucine motifs (green) within each protein are identified by color and bottom-line. The parental proteins used in this study were used as references.

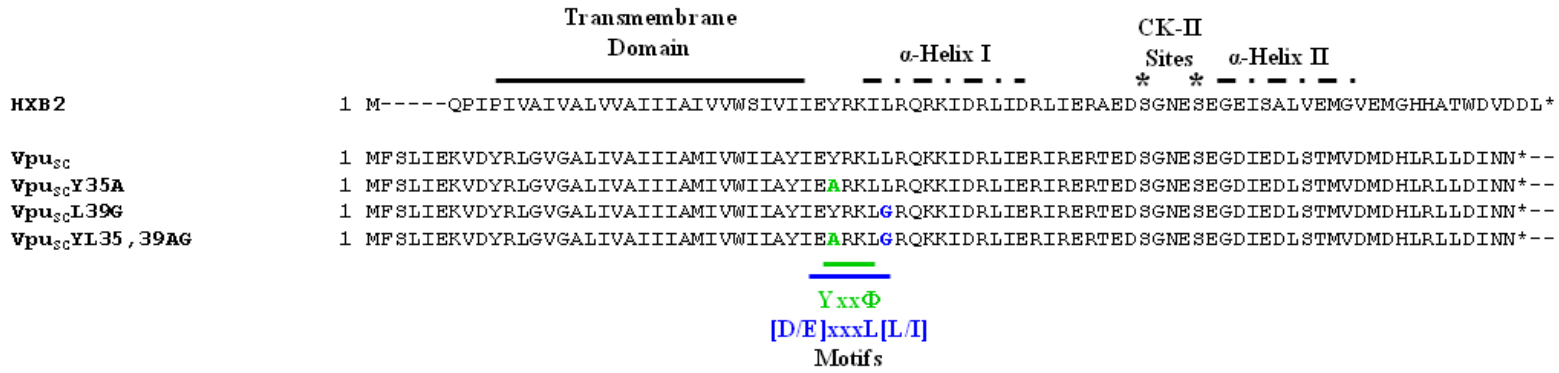
Transmembrane Domain
α-Helix I
CK-II Sites
α-Helix II
HXB2 1 M-----QPIPIVAIVALVVAIIIAIVVWSIVIIEYRKILRQRKIDRLIDRLIERAEDSGNESEGEISALVEMGVEMGHHATWDVDDL*
Vpu$_{SC}$ 1 MFSLIEKVDYRLGVGALIVAIIIAMIVWIIAYIEYRKLLRQKKIDRLIERIRERTEDSGNESEGDIEDLSTMVDMDHLRLLDINN*--
Vpu$_{SC}$Y35A 1 MFSLIEKVDYRLGVGALIVAIIIAMIVWIIAYIEARKLLRQKKIDRLIERIRERTEDSGNESEGDIEDLSTMVDMDHLRLLDINN*--
Vpu$_{SC}$L39G 1 MFSLIEKVDYRLGVGALIVAIIIAMIVWIIAYIEYRKLGRQKKIDRLIERIRERTEDSGNESEGDIEDLSTMVDMDHLRLLDINN*--
Vpu$_{SC}$YL35,39AG 1 MFSLIEKVDYRLGVGALIVAIIIAMIVWIIAYIEARKLGRQKKIDRLIERIRERTEDSGNESEGDIEDLSTMVDMDHLRLLDINN*--
YxxΦ
[D/E]xxxL[L/I]
Motifs

membrane. In contrast, the Vpu_{SC}EGFPL39G and Vpu_{SC}EGFPYL35,39AG clearly had reduced expression at the cell surface (Figure 43E-H). Of these two constructs, the Vpu_{SC}EGFPL39A consistently had the lowest surface expression. As the results in Figure 43 suggested that Vpu_{SC}EGFPL39G and Vpu_{SC}EGFPYL35,39AG were expressed at reduced levels, we analyzed which compartment these proteins were predominantly localized. 293 cells were transfected with vectors expressing Vpu_{SC}EGFP1, Vpu_{SC}EGFPY35A, Vpu_{SC}EGFPL39G, or Vpu_{SC}EGFPYL35,39AG and DsRed2-Golgi. As shown in Figure 44, Vpu_{SC}EGFPY35A (Figure 44E-H) was efficiently expressed at the cell surface while the majority of the Vpu_{SC}EGFPL39G (Figure 44I-L) and Vpu_{SC}EGFPYL35,39AG (Figure 44M-P) co-localized with the DsRed2-Golgi marker. To confirm the differences in surface expression of each mutant, transfected cells were surface biotinylated followed by immunoprecipitation with an anti-EGFP antibody. As shown in Figure 45, biotinylated Vpu_{SC}EGFP1 (100%) and Vpu_{SC}EGFPY35A (110-120%) were easily detected at the cell surface. In contrast, decreased levels of Vpu_{SC}EGFPL39G (30%) and Vpu_{SC}EGFPYL35,39AG (40%) were found at the cell surface. Together, these results indicate that Vpu_{SC}EGFPY35A had slightly higher (but not statistically significant) levels at the cell surface, Vpu_{SC}EGFPYL35,39AG had an intermediate level of expression and Vpu_{SC}EGFPL39G had the lowest level of surface expression.

The reduction in surface expression of Vpu_{SC}EGFPL39G and Vpu_{SC}EGFPYL39AG was not due to enhanced turnover of the protein

One possible explanation for the reduced expression of Vpu_{SC}EGFPL39G and Vpu_{SC}EGFPYL35,39AG at the cell surface could be due to the stability of the viral proteins. Pulse-chase experiments were performed to examine the rate of turnover of Vpu_{SC}EGFP1 and

Figure 43. Expression of EGFP, Vpu_{SC}EGFP1, Vpu_{SC}EGFPY35A, Vpu_{SC}EGFPL39G, or Vpu_{SC}EGFPYL35,39AG in 293 cells. 293 cells were co-transfected with vectors expressing Vpu_{SC}EGFP1, Vpu_{SC}EGFPY35A, Vpu_{SC}EGFPL39G, Vpu_{SC}EGFPYL35,39AG or EGFP. At 48 hours, cells expressing EGFP were identified and images collected using laser scanning confocal microscopy as described in the Materials and methods section. Panel A. Phase image merged with fluorescence micrograph of a cell expressing Vpu_{SC}EGFP1. Panel B. Fluorescence micrograph of a cell expressing Vpu_{SC}EGFP1. Panel C. Phase image merged with fluorescence micrograph of a cell expressing Vpu_{SC}EGFPY35A. Panel D. Fluorescence micrograph of a cell expressing Vpu_{SC}EGFPY35A. Panel E. Phase image merged with fluorescence micrograph of a cell expressing Vpu_{SC}EGFPL39G. Panel F. Fluorescence micrograph of a cell expressing Vpu_{SC}EGFPL39G. Panel G. Phase image merged with fluorescence micrograph of a cell expressing Vpu_{SC}EGFPYL35,39AG. Panel H. Fluorescence micrograph of a cell expressing Vpu_{SC}EGFPYL35,39AG.

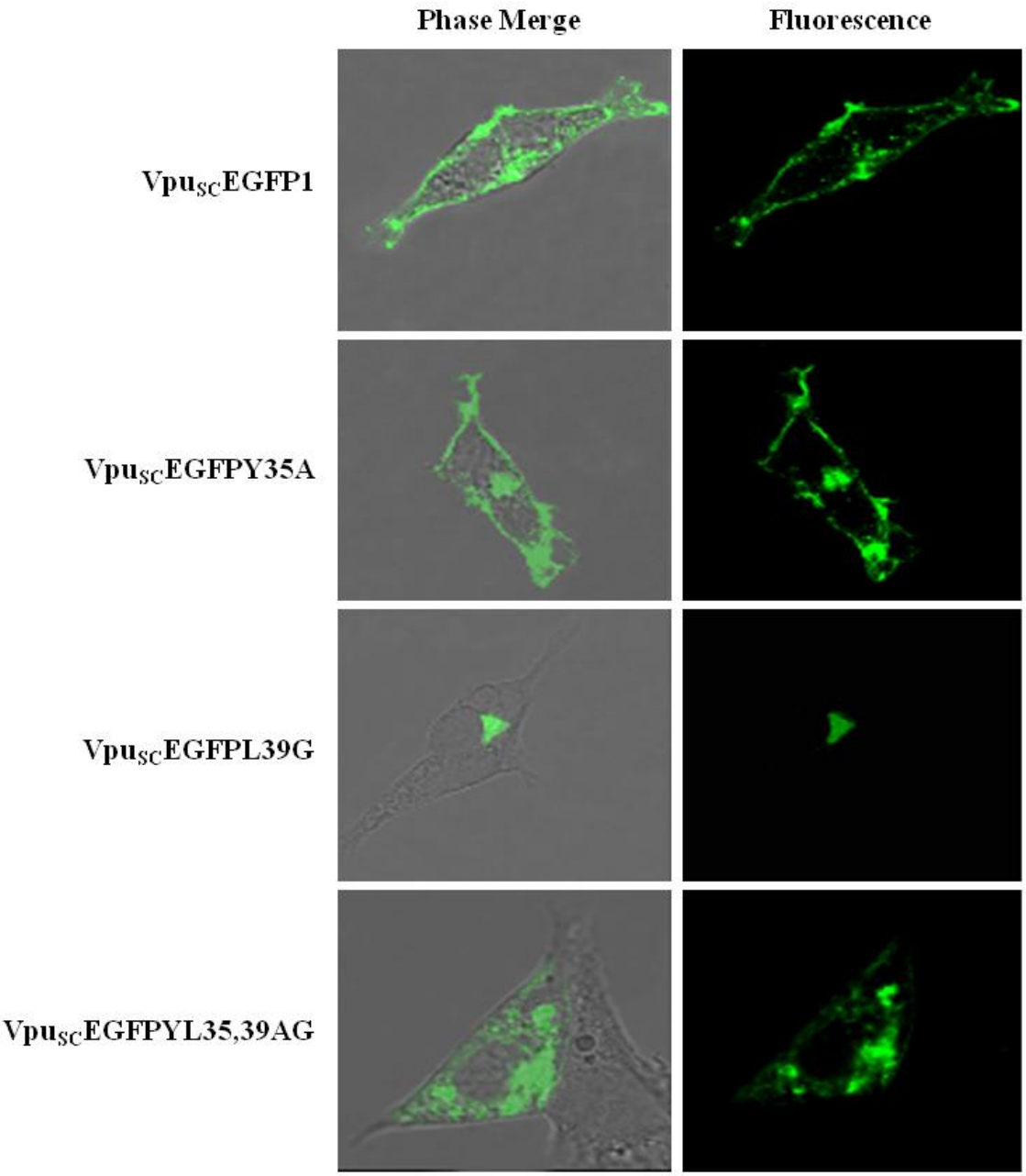
Phase Merge
Fluorescence
Vpu$_{SC}$EGFP1
Vpu$_{SC}$EGFPY35A
Vpu$_{SC}$EGFPL39G
Vpu$_{SC}$EGFPYL35,39AG

Figure 44. Expression of EGFP, Vpu_{SC}EGFP1, Vpu_{SC}EGFPY35A, Vpu_{SC}EGFPL39G or Vpu_{SC}EGFPYL35,39AG and DsRed2-Golgi in 293 cells. 293 cells were co-transfected with vectors expressing Vpu_{SC}EGFP1, Vpu_{SC}EGFPY35A, Vpu_{SC}EGFPL39G, Vpu_{SC}EGFPYL35,39AG or EGFP and DsRed2-Golgi. At 48 h, cells expressing EGFP were identified and images collected using laser scanning confocal microscopy as described in the Materials and methods section. Panels A-D. 293 cells co-transfected with Vpu_{SC}EGFP1 and DsRed2-Golgi. Panel A. Phase contrast image of a cell expressing Vpu_{SC}EGFP1 and DsRed2-Golgi. Panel B. Fluorescence micrograph of a cell expressing Vpu_{SC}EGFP1. Panel C. Fluorescence micrograph of a cell expressing DsRed2-Golgi. Panel D. Merge of panels B and C. Panels E-H. 293 cells co-transfected with Vpu_{SC}EGFPY35A and DsRed2-Golgi. Panel E. Phase contrast image of a cell expressing Vpu_{SC}EGFPY35A and DsRed2-Golgi. Panel F. Fluorescence micrograph of a cell expressing Vpu_{SC}EGFPY35A. Panel G. Fluorescence micrograph of a cell expressing DsRed2-Golgi. Panel H. Merge of panels F and G. Panels I-L. 293 cells co-transfected with Vpu_{SC}EGFPL39G and DsRed2-Golgi. Panel I. Phase contrast image of a cell expressing Vpu_{SC}EGFPL39G and DsRed2-Golgi. Panel J. Fluorescence micrograph of a cell expressing Vpu_{SC}EGFPL39G. Panel K. Fluorescence micrograph of a cell expressing DsRed2-Golgi. Panel L. Merge of panels J and K. Panels M-P. 293 cells co-transfected with Vpu_{SC}EGFPYL35,39AG and DsRed2-Golgi. Panel M. Phase contrast image of a cell expressing Vpu_{SC}EGFPYL35,39AG and DsRed2-Golgi. Panel N. Fluorescence micrograph of a cell expressing Vpu_{SC}EGFPYL35,39AG. Panel O. Fluorescence micrograph of a cell expressing DsRed2-Golgi. Panel P. Merge of panels N and O.

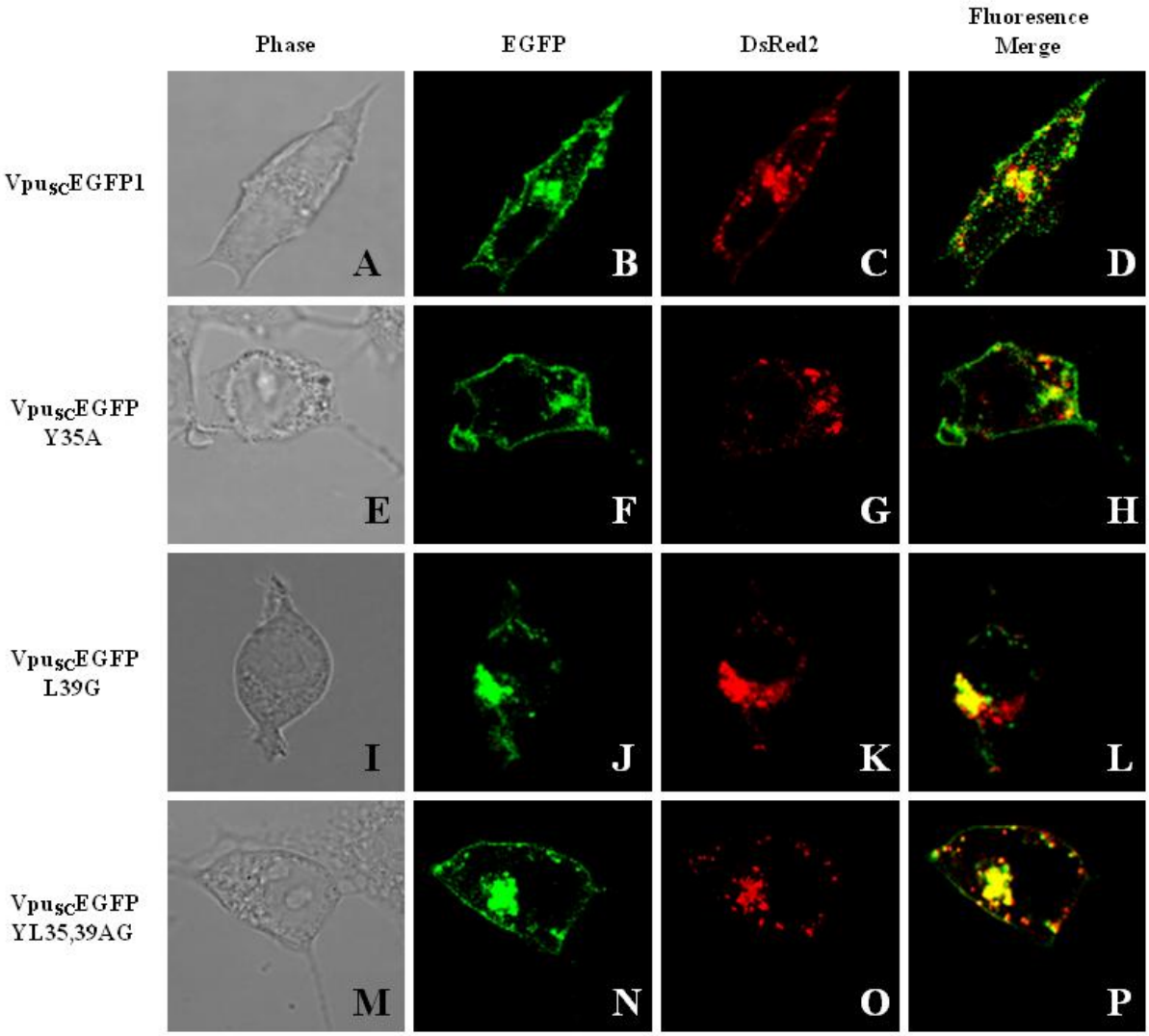
Phase
EGFP
DsRed2
Fluoresence Merge
VpusCEGFP1
VpusCEGFP Y35A
VpusCEGFP L39G
VpusCEGFP YL35,39AG
A
B
C
D
E
F
G
H
I
J
K
L
M
N
O
P

Figure 45. Detection of subtype C Vpu mutants by surface biotinylation. 293 cells were transfected with vectors expressing Vpu_{SC}EGFP1, Vpu_{SC}EGFPY35A, Vpu_{SC}EGFPL39G, Vpu_{SC}EGFPYL35,39AG, or EGFP. At 48 hours, cells were radiolabeled and surface biotinylated as described in the Materials and methods section. EGFP containing proteins were immunoprecipitated using an anti-EGFP serum and run on SDS-PAGE. The proteins were transferred to membranes and reacted with a substrate to visualize the biotinylated proteins. (Lane 1) Cells transfected with EGFP. (Lane 2) Cells transfected with Vpu_{SC}EGFP1. (Lane 3) Cells transfected with Vpu_{SC}EGFPY35A. (Lane 4) Cells transfected with Vpu_{SC}EGFPL39G. (Lane 5) Cells transfected with Vpu_{SC}EGFPYL35,39AG. (Lane 6) Untransfected cells, control.

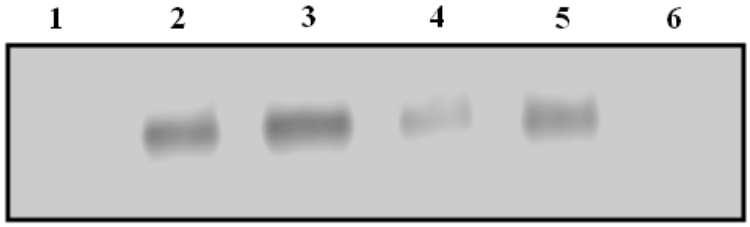
1
2
3
4
5
6

the three mutant Vpu proteins. As shown in Figure 46A-D, Vpu_{SC}EGFP1 and the three mutant Vpu proteins had 62-69% of the protein remaining at the 6 hour chase period. These results indicate that protein stability was not the reason for the observed results in Figures 43-45.

Cell surface expression of CD4 in the presence of tyrosine and dileucine mutants

We examined the ability of Vpu_{SC}EGFP1 and the three Vpu mutants to down-regulate cell surface CD4 expression. HeLa $CD4^+$ cells were transfected with vectors expressing Vpu_{SC}EGFP1 and the three Vpu mutants. At 48 hours, cells were removed from the plates, stained for surface CD4 and analyzed by flow cytometry. The results in Figure 47 show that CD4 surface expression levels in cells expressing either Vpu_{SC}EGFPL39G or Vpu_{SC}EGFPY35A were not statistically significant when compared to Vpu_{SC}EGFP1. However, cells transfected with Vpu_{SC}EGFPYL35,39AG had a statistically significant reduction in CD4 cell surface expression when compared to Vpu_{SC}EGFP1 ($p < 0.05$). These results indicate that removal of both the tyrosine and dileucine signals effected CD4 surface level down-modulation.

SHIVs expressing Vpu proteins with mutations in the dileucine motif replicate with increased kinetics compared to those with mutations in the tyrosine motif

We constructed simian human immunodeficiency viruses that expressed a Vpu protein with either the Y35A ($SHIV_{SCVpuY35A}$), the L39G ($SHIV_{SCVpuL39G}$) or the YL35,39AG ($SHIV_{SCVpuYL35,39AG}$) amino acid substitutions. The replication of these viruses and the unmodified $SHIV_{SCVpu}$ were compared using p27 growth curves. The results of these assays are shown in Figure 48 and indicate that $SHIV_{SCVpuL39G}$ released p27 into the culture medium at a faster rate and was 5.6-fold higher than parental $SHIV_{SCVpu}$ at day 7 post-inoculation.

Figure 46. Pulse-chase analyses of the Vpu fusion proteins. To determine if the amino acid substitutions resulted in altered turnover of the Vpu fusion proteins, 293 cells were transfected with vectors expressing Vpu_{SC}EGFP1, Vpu_{SC}EGFPY35A, Vpu_{SC}EGFPL39G, or Vpu_{SC}EGFPYL35,39AG. At 48 hours post-transfection, the medium was removed and cells were incubated in methionine/cysteine-free medium for 2 hours. The cells were then radiolabeled for 30 minutes with 1 mCi of ^{35}S-Translabel (methionine and cysteine, ICN Biomedical, Costa Mesa, CA) and the radiolabel chased for various periods of time (0-6 hours) in DMEM containing 100X unlabeled methionine/cysteine. Vpu fusion proteins were immunoprecipitated using an anti-EGFP serum as described in the Material and methods section. Non-transfected 293 cells, radiolabeled and chased for 0 hours served as a negative control (lane C). All immune precipitates were collected on protein A Sepharose, the beads washed three times with RIPA buffer, and the samples resuspended in sample reducing buffer. Samples were boiled and the SHIV specific proteins analyzed by SDS-PAGE (10% gel). Proteins were then visualized by standard autoradiographic techniques. Panel A. Results of pulse-chase analysis of viral proteins immunoprecipitated from Vpu_{SC}EGFP1 transfected cells. Panel B. Results of pulse-chase analysis of viral proteins immunoprecipitated from Vpu_{SC}EGFPY35A transfected cells. Panel C. Results of pulse-chase analysis of viral proteins immunoprecipitated from Vpu_{SC}EGFPL39G transfected cells. Panel D. Results of pulse-chase analysis of viral proteins immunoprecipitated from Vpu_{SC}EGFPYL35,39AG transfected cells.

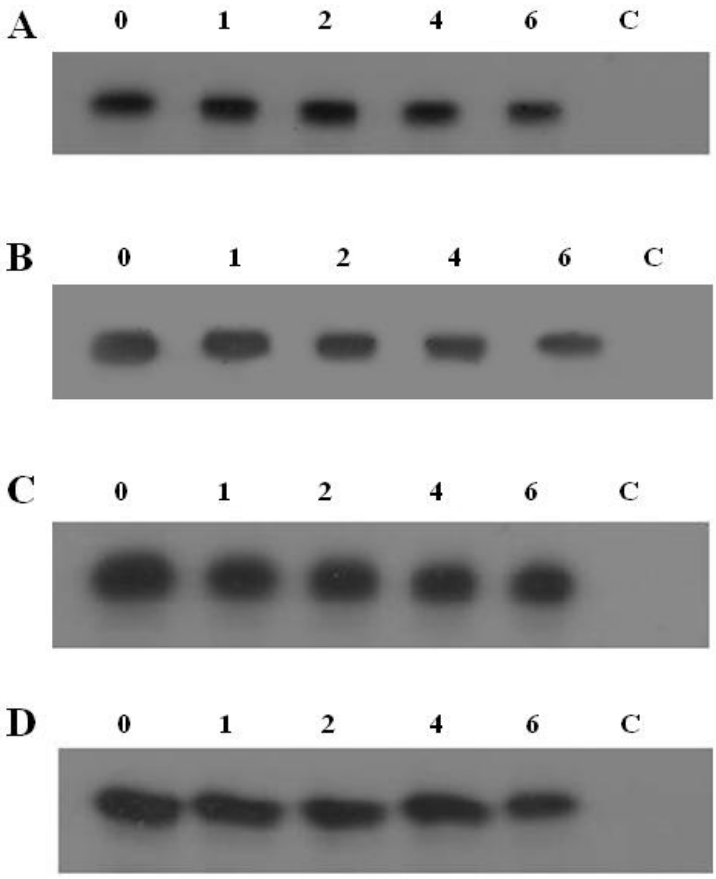
A
0 1 2 4 6 C
B
0 1 2 4 6 C
C
0 1 2 4 6 C
D
0 1 2 4 6 C

Figure 47. Substitution of tyrosine and leucine residues at positions 35 and 39 results in a protein that is less efficient at down-regulating cell surface CD4 expression. HeLa $CD4^+$ cells were transfected with plasmids expressing EGFP, $Vpu_{SC}EGFP1$, $Vpu_{SC}EGFPY35A$, $Vpu_{SC}EGFPL39G$, or $Vpu_{SC}EGFPYL35,39AG$. At 48 hours, live cells were immunostained for CD4. Cells expressing EGFP or EGFP fusion proteins were assessed for CD4 surface expression using flow cytometry. CD4 expression in cells expressing the various Vpu proteins was normalized to CD4 expression in EGFP expressing cells. (*) symbol above bar represents Vpu proteins that were less efficient at down-modulating CD4 from the cell surface compared to VpuEGFP, with a $p \leq 0.05$ considered significant.

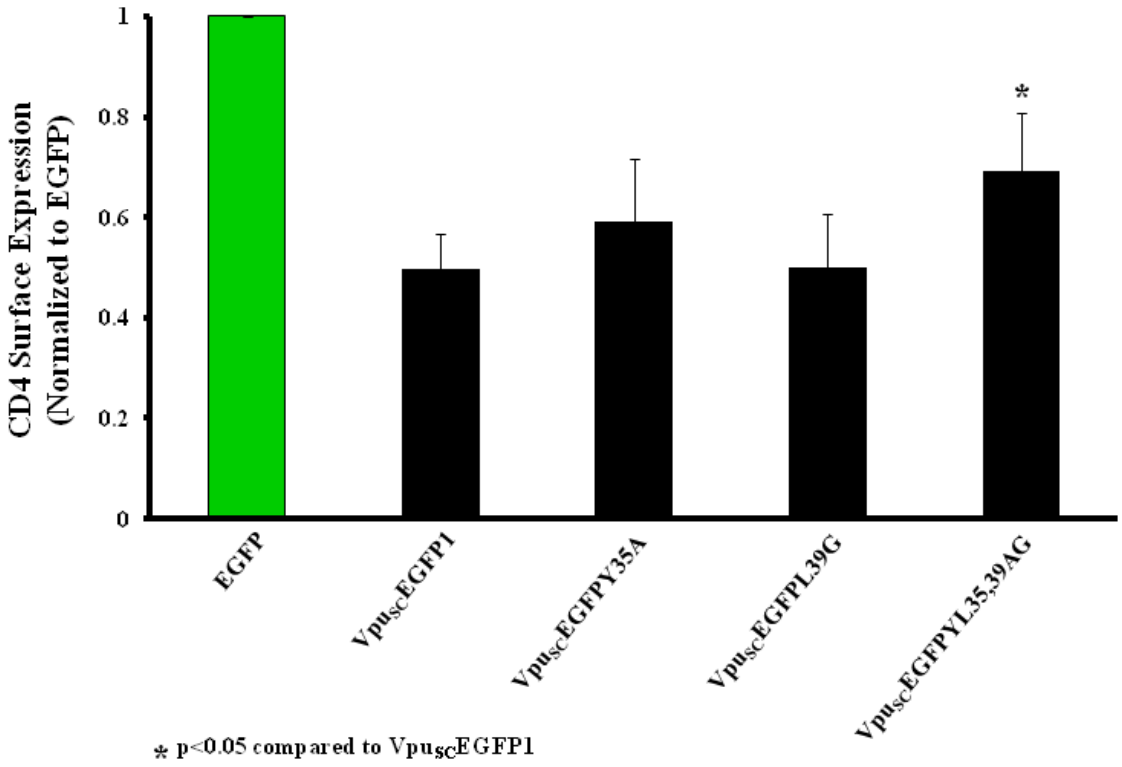
CD4 Surface Expression
(Normalized to EGFP)
1
0.8
0.6
0.4
0.2
0
*
EGFP
Vpu$_{SC}$EGFP1
Vpu$_{SC}$EGFPY35A
Vpu$_{SC}$EGFPL39G
Vpu$_{SC}$EGFPYL35,39AG
* p<0.05 compared to Vpu$_{SC}$EGFP1

Figure 48. Growth curves of $SHIV_{SCVpu}$, $SHIV_{SCVpuY35A}$, $SHIV_{SCVpuL39G}$ and $SHIV_{SCVpuYL35,39AG}$ in C8166 cells. Cultures of C8166 cells were inoculated with $SHIV_{SCVpu}$ (♦), $SHIV_{SCVpuY35A}$ (■), $SHIV_{SCVpuL39G}$ (▲), and $SHIV_{SCVpuYL35,39AG}$ (●) as described in the text. Aliquots of the culture medium were assayed for the presence of p27 antigen. The growth curves were performed in triplicate and the mean of the three experiments plotted.

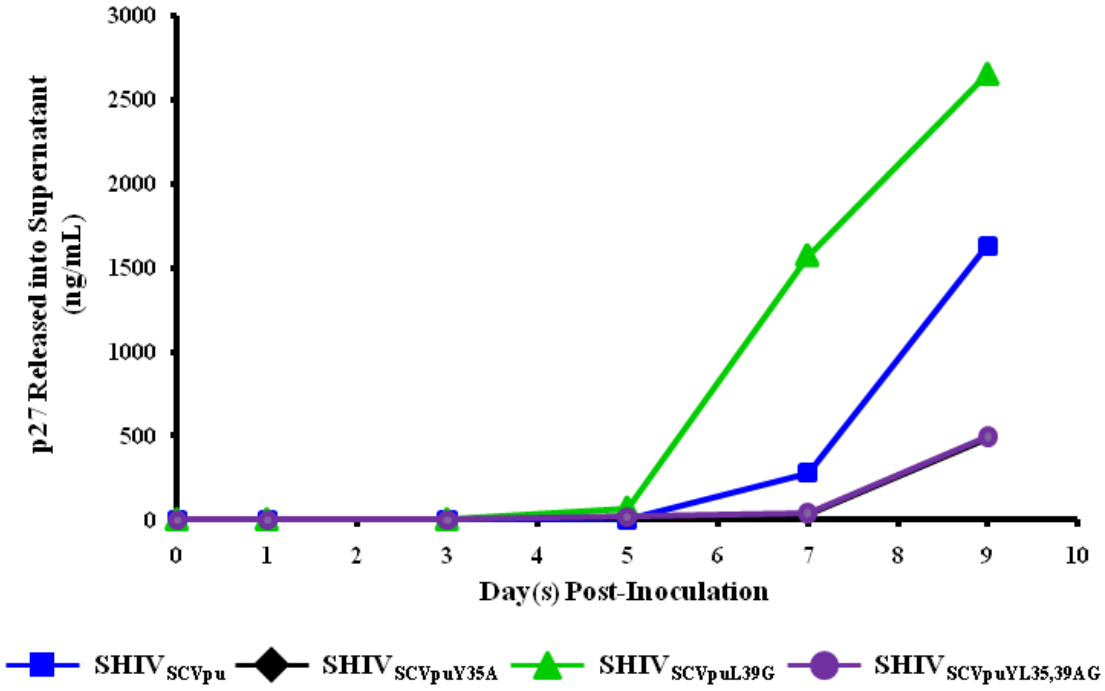
p27 Released into Supernatant (ng/mL)
3000
2500
2000
1500
1000
500
0
0
1
2
3
4
5
6
7
8
9
10
Day(s) Post-Inoculation
SHIV SCVpu
SHIV SCVpuY35A
SHIV SCVpuL39G
SHIV SCVpuYL35,39AG

Additionally, we observed that cultures inoculated with $SHIV_{SCVpuL39G}$ developed syncytial cytopathology at a faster rate (and larger) compared to the other three viruses (data not shown). In contrast, the $SHIV_{SCVpuY35A}$ and $SHIV_{SCVpuYL35,39AG}$ released p27 into the culture medium at a slower rate and at day 7 were 10.3 and 7.4-fold less, respectively, when compared to the parental $SHIV_{SCVpu}$. It should be noted that in four attempts to prepare stocks of $SHIV_{SCVpuY35A}$, three of the stocks selected for a highly cytopathic variant. Sequence analysis of the *vpu* gene amplified from cells isolated from infected cultures revealed a premature stop codon in *vpu* at amino acid position 28 (data not shown). Since we have never encountered this problem in construction of other SHIVs, it suggests that the lack of a tyrosine residue at this position is being compensated for by truncation of the protein. Taken together, these results indicate that the tyrosine residue appeared to be required for efficient virus particle release and that removal of the dileucine motif resulted in a virus that replicated much more efficiently.

$SHIV_{SCVpuL39G}$ processes Gag and Env precursors faster than $SHIV_{SCVpuY35A}$ and $SHIV_{SCVpuYL35,39AG}$

Pulse-chase experiments were used to analyze the processing of viral Gag and Env proteins. C8166 cells were inoculated with either $SHIV_{SCVpu}$, $SHIV_{SCVpuY35A}$ $SHIV_{SCVpuL39G}$, or $SHIV_{SCVpuYL35,39AG}$ for 5 days at which time pulse-chase analyses were performed. The results of the pulse-chase analysis for $SHIV_{SCVpu}$ are shown in Figure 49A and have been previously described (Hill et al., 2008). The results of the pulse-chase analyses for $SHIV_{SCVpuL39G}$ (Figure 49B) indicate that Env and Gag protein precursors were processed similar to $SHIV_{SCVpu}$ but faster than either $SHIV_{SCVpuY35A}$ (Figure 49C) but not $SHIV_{SCVpuYL35,39AG}$ (Figure 49D). This

Figure 49. Pulse-chase analyses revealed that $SHIV_{SCVpuY35A}$, $SHIV_{SCVpuL39G}$ and $SHIV_{SCVpuYL35,39AG}$ have altered processing of viral proteins. To determine if viral structural proteins were released with reduced efficiency in $SHIV_{SCVpu}$-inoculated cultures, C8166 cells were inoculated with 10^3 $TCID_{50}$ of $SHIV_{SCVpu}$, $SHIV_{SCVpuY35A}$, $SHIV_{SCVpuL39G}$ or $SHIV_{SCVpuYL35,39AG}$. At 7 days post-infection, the medium was removed and infected cells were incubated in methionine/cysteine-free medium for 2 hours. The cells were then radiolabeled for 30 minutes with 1 mCi of ^{35}S-Translabel (methionine and cysteine, ICN Biomedical, Costa Mesa, CA) and the radiolabel chased for various periods of time (0-6 hours) in DMEM containing 100X unlabeled methionine/cysteine. SHIV proteins were immunoprecipitated from cell lysates using plasma pooled from several pig-tailed monkeys infected previously with SHIV as described in the Material and methods section. Uninfected C8166 cells, radiolabeled and chased for 0 hours served as a negative control (lane C). All immune precipitates were collected on protein A-Sepharose, the beads washed three times with RIPA buffer, and the samples resuspended in sample reducing buffer. Samples were boiled and the SHIV specific proteins analyzed by SDS-PAGE (10% gel). Proteins were then visualized by standard autoradiographic techniques. Panel A. Results of pulse-chase analysis of viral proteins immunoprecipitated from $SHIV_{SCVpu}$ infected cell lysates. Panel B. Results of pulse-chase analysis of viral proteins immunoprecipitated from $SHIV_{SCVpuL39G}$ infected cell lysates. Panel C. Results of pulse-chase analysis of viral proteins immunoprecipitated from $SHIV_{SCVpuY35A}$ infected cell lysates. Panel D. Results of pulse-chase analysis of viral proteins immunoprecipitated from $SHIV_{SCVpuYL35,39AG}$ infected cell lysates.

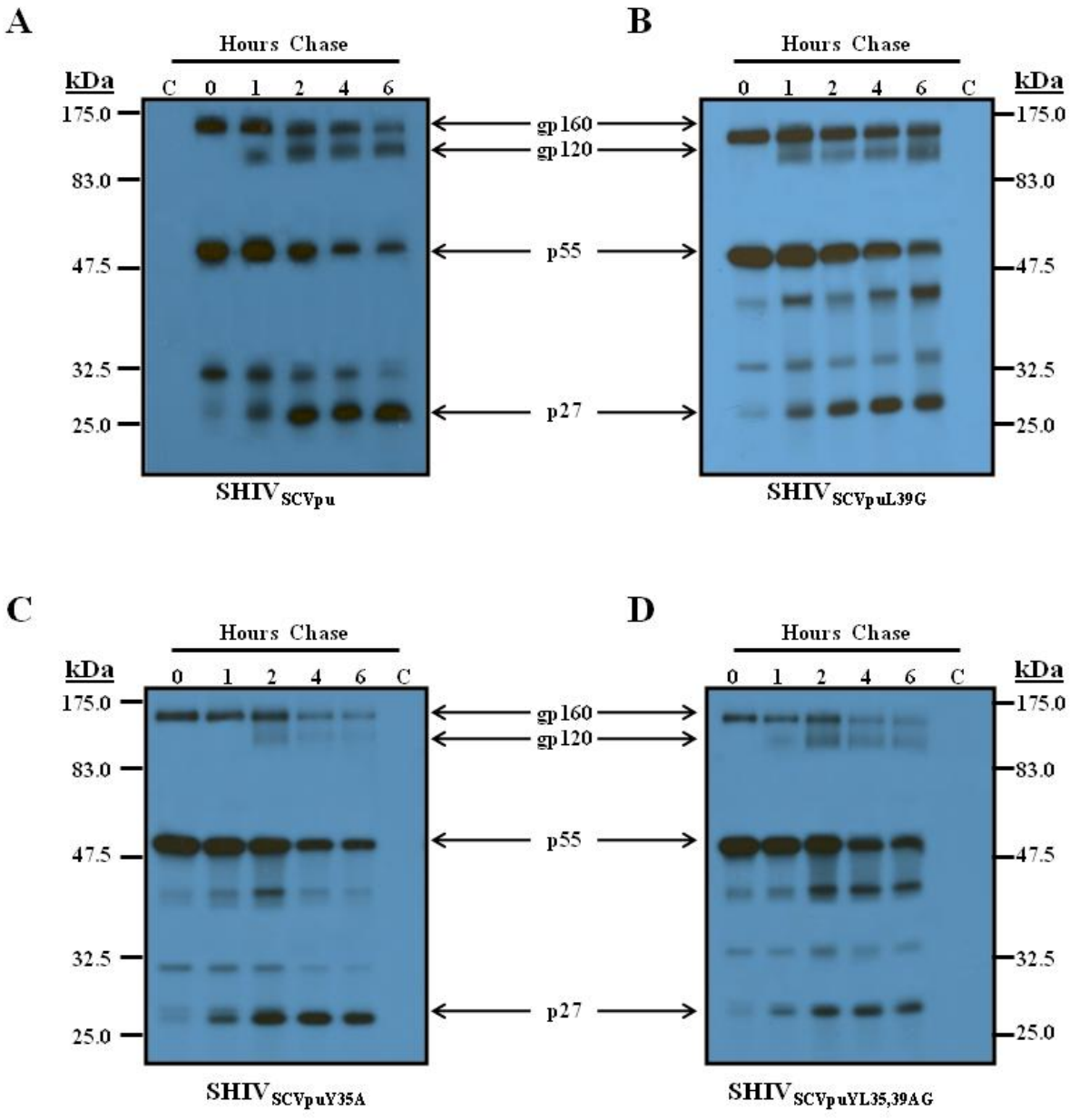
A
Hours Chase
kDa
C 0 1 2 4 6
175.0
83.0
47.5
32.5
25.0
gp160
gp120
p55
p27
SHIV SCVpu
B
Hours Chase
0 1 2 4 6 C
kDa
175.0
83.0
47.5
32.5
25.0
SHIV SCVpuL39G
C
Hours Chase
kDa
0 1 2 4 6 C
175.0
83.0
47.5
32.5
25.0
gp160
gp120
p55
p27
SHIV SCVpuY35A
D
Hours Chase
0 1 2 4 6 C
kDa
175.0
83.0
47.5
32.5
25.0
SHIV SCVpuYL35,39AG

was also reflected in the release of the viral proteins into the culture medium (data not shown). Together, these data correlated well with the p27 growth curves.

SHIVs with the L39G amino acid substitution exhibit more particles on the cell surface

We examined the maturation of $SHIV_{SCVpu}$, $SHIV_{SCVpuY35A}$, $SHIV_{SCVpuL39G}$ and $SHIV_{SCVpuYL35,39AG}$ by electron microscopy to determine if these amino acid substitutions altered the pattern of virus maturation. As shown in Figure 50A, the $SHIV_{SCVpu}$ was found to mature at the cell surface as we recently reported (Hill et al., 2008). $SHIV_{SCVpuY35A}$, $SHIV_{SCVpuL39G}$, and $SHIV_{SCVpuYL35,39AG}$ were also found to mature predominantly at the cell surface (Figure 50B-D) although viral particles were occasionally observed within vesicles of $SHIV_{SCVpuL39G}$-infected cells (Figure 50E). The salient feature of the electron microscopy studies was the number of viral particles associated per infected cell. We determined the mean number of particles per 50 cells at five days post-inoculation. As shown in Figure 51A, the mean number of virus particles from 50 $SHIV_{SCVpu}$-infected C8166 cells was approximately 16. The number of particles per cell for $SHIV_{SCVpuY35A}$ and $SHIV_{SCVpuYL35,39AG}$-infected cells was approximately 3 and 8, respectively (Figure 51B-C). Contrasting with these results, $SHIV_{SCVpuL39G}$ had a mean of approximately 75 particles per cell or approximately 5 times as many particles as parental $SHIV_{SCVpu}$ (Figure 51D). The difference in the mean number of particles per cell between $SHIV_{SCVpu}$ and $SHIV_{SCVpuL39G,}$ $SHIV_{SCVpu}$ and $SHIV_{SCVpuYL35,39AG}$, and $SHIV_{SCVpu}$ and $SHIV_{SCVpuY35A}$ were found to be very significant ($p < 0.001$). Analysis of the distribution of the number of particles per cell also showed a clear difference between $SHIV_{SCVpuL39G}$ and the other three viruses. For $SHIV_{SCVpu}$, the number of particles per cell was generally less than 30 (Figure 51A) while for $SHIV_{SCVpuYL35,39AG}$ and $SHIV_{SCVpuY35A}$ the number of particles per cell was less

Figure 50. Electron microscopic examination of C8166 cells inoculated with $SHIV_{SCVpu}$, $SHIV_{SCVpuY35A}$, $SHIV_{SCVpuL39G}$, or $SHIV_{SCVpuYL35,39AG}$. C8166 cells were inoculated with each virus for 7 days. Cells were washed three times with PBS and processed for electron microscopy as described in the Materials and methods section. Panel A. C8166 cells inoculated with parental $SHIV_{SCVpu}$. Panel B. C8166 cells inoculated with $SHIV_{SCVpuY35A}$. Panels C and D. C8166 cells inoculated with $SHIV_{SCVpuYL35,39AG}$. Panels E and F. C8166 cells inoculated with $SHIV_{SCVpuL39G}$.

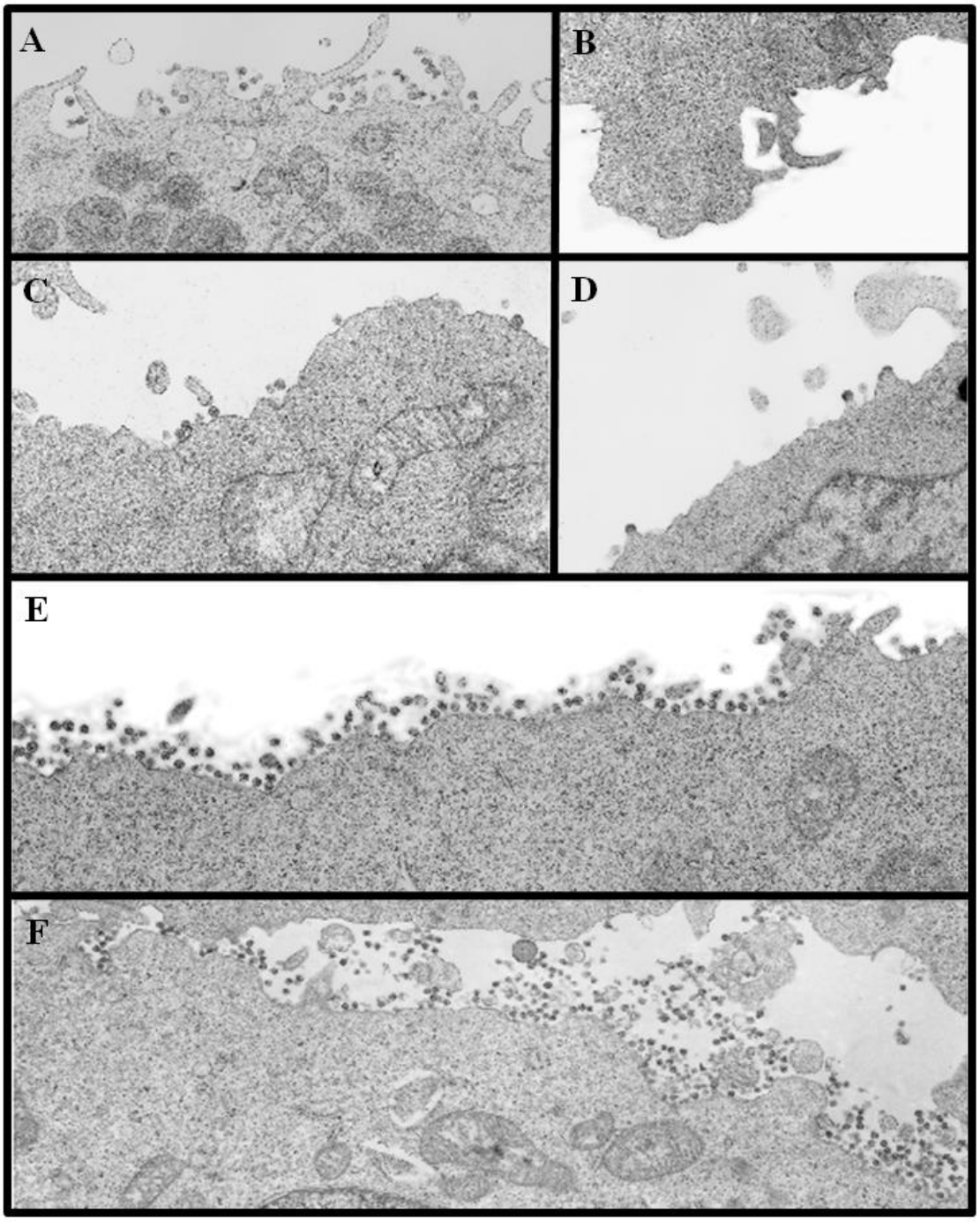
A
B
C
D
E
F

Figure 51. Enumeration of the number of viral particles associated with the infected C8166 cells following inoculation with $SHIV_{SCVpu}$, $SHIV_{SCVpuY35A}$, $SHIV_{SCVpuL39G,}$ or $SHIV_{SCVpuYL35,39AG}$. Cells were inoculated with equivalent doses of infectious virus and at 5 days processed for electron microscopy as described in the Material and methods section. The number of viral particles associated with 50 cells per virus and mean values calculated.

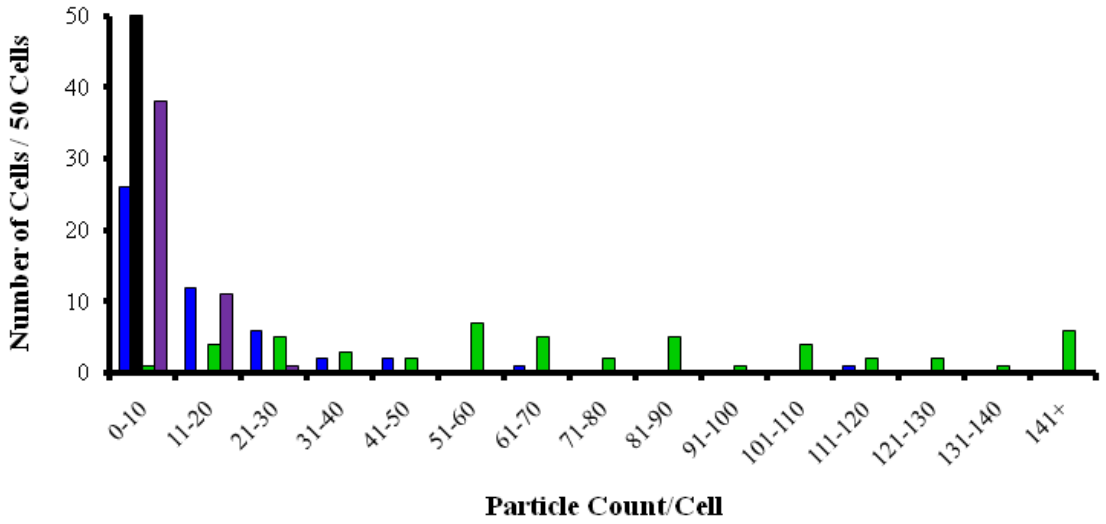

Mean Particle Counts:	15.7	2.8	75.0	8.3
	$SHIV_{SCVpu}$	$SHIV_{SCVpuY35A}$	$SHIV_{SCVpuL39G}$	$SHIV_{SCVpuYL35,39AG}$

than 20 and 10, respectively (Figure 51B-C). These results were in contrast with those for $SHIV_{SCVpuL39G}$, which showed a more even distribution in the number of particles per cell (Figure 51D). Combined with the p27 growth curves, while there were increased numbers of virus particles on the surface, the virus replicated with increased kinetics and released more p27 into the culture medium.

Discussion

The subtype C Vpu proteins have canonical tyrosine (YxxΦ) and dileucine ([D/ExxxL[L/I]) motifs that could be involved in the targeting of this protein to different intracellular compartments. The targeting of proteins containing these motifs is generally mediated through interactions with various adaptor protein complexes (AP-1, AP-2, AP-3, AP-4). The YxxΦ signals have been shown to be involved in endocytosis of membrane proteins from the cell plasma membrane as well as targeting of membrane proteins to lysosomes and lysosome-related vesicles. The YxxΦ motifs that are involved in endocytic functions generally have a glycine residue at the Y+1 position and are located 10-40 amino acids from the transmembrane of the protein. Those YxxΦ motifs that are involved in lysosomal targeting generally have an acidic residue at the Y+1 position and are generally located 6-9 residues from the transmembrane domain (Bonifacino and Traub, 2003). Tyrosine signals generally interact with the μ subunit of adaptor protein complexes. The best-studied interactions with the AP complexes have been predominantly with μ2, although the μ1, μ3, and μ4 subunits can interact with these motifs. The μ3A and μ3B subunits have a preference for binding to tyrosine signals with an acidic amino acid before and/or after the tyrosine residue. The most characteristic feature of the μ4 subunit binding is the presence of aromatic amino acids near the tyrosine

residue. With dileucine motifs, the first leucine is generally invariant and replacement of the first leucine with an isoleucine reduces the potency of the signal. However, the second leucine can be replaced with an isoleucine and in some cases a methionine residue with an acidic amino acid at the +4 and/or +5 position and retain signal function. Dileucine motifs also interact with adaptor protein complexes AP-1, AP-2, and AP-3 (Bonifacino and Traub, 2003), but they appear to interact with a hemi-complex formed by the small subunit and the large specific subunit (Janvier et al., 2003). Similar to the tyrosine motifs, the proximity to the transmembrane domain appears to affect whether it is involved in endocytosis or lysosomal targeting. As the overlapping tyrosine and dileucine motifs of Vpu are membrane proximal, it suggests that they may be involved in lysosomal targeting.

In this study we analyzed the role of overlapping tyrosine and dileucine signals within the cytoplasmic domain of the subtype C Vpu in intracellular targeting. The two other membrane proteins of HIV-1, Env and Nef, use tyrosine and dileucine motifs for either trafficking within the cell and/or removal of cellular proteins from the cell surface (Boge et al., 1998; Bresnahan et al., 1998; Byland et al., 2007; Chaudhuri et al., 2007; Coleman et al., 2005; Craig et al., 1998; Day et al., 2006; Greenberg et al., 1998a; Lodge et al., 1997; Noviello et al., 2008; Roeth et al., 2004; Schwartz et al., 1996). Our findings indicate that the tyrosine motif within Vpu may have a role in enhanced virus release. The finding that the tyrosine based motif was important to virus release is not entirely surprising as this motif is conserved in virtually all of the Vpu sequences from the different HIV-1 subtypes in the Los Alamos National Laboratory (LANL)-HIV-1 group M database. Bone marrow stromal antigen 2 (BST-2) was recently identified as a target for Vpu identifying a mechanism by which Vpu enhances virion release in certain cell types (Neil et al., 2008; Van Damme et al., 2008). However, the physiological relevance of BST-2 antagonism as

a mechanism for Vpu mediated enhancement of pathogenesis has been brought under question based on several observations: 1) human PBMC do not express high levels of BST-2 even following treatment with interferon-α; 2) HIV-1 Vpu has been shown to enhance pathogenesis in a macaque model even though the BST-2 protein expressed by these species is not antagonized by HIV-1 Vpu and 3) subtype B and subtype C Vpu exhibit distinct replication kinetics in C8166 cells and pig-tailed PBMC even though they display equal antagonistic properties against human BST-2 (Hill et al., 2008; Joag et al., 1996; Liu et al., 1999; McCormick-Davis et al., 2000a; Miyagi et al., 2009; Singh et al., 2001; Stephens et al., 2002). Also, no studies have been conducted to determine whether endogenous expression of BST-2 in C8166 cells significantly affects virion release and determines the Vpu phenotype of this cell line. Therefore, as changing the tyrosine residue at position 35 to an alanine in the subtype C Vpu protein resulted in a virus, $SHIV_{SCVpuY35A,}$ that replicated very poorly in C8166 cells, it raises several questions. First, is the membrane proximal tyrosine motif important in the Vpu interactions with BST-2? Secondly, if it is important, does it affect binding (perhaps through structural alterations of the transmembrane domain) or does it affect the mechanism by which Vpu antagonizes BST-2? Finally, is the tyrosine motif involved in alternate mechanisms of Vpu mediated enhancement of virion release that are not associated with BST-2? Additional studies are needed to determine the affects these amino acid substitutions have on the interaction of Vpu with BST-2 and whether these results correlate with what remains to be seen in cells that express high levels of BST-2 (i.e. HeLa cells). This would provide additional insight into the physiological relevance of Vpu mediated antagonism of BST-2 for enhancement of pathogenesis.

Dileucine motifs are found in a high percentage of subtype C Vpu sequences in the LANL-HIV-1 database, with approximately 80% of the sequences having a dileucine, leucine-

isoleucine or leucine-valine motif at the membrane proximal location. In contrast, of 271 subtype B Vpu sequences in the LANL-HIV database, the majority (~95%) of the sequences have an isoleucine in place of the primary leucine (EYRK**I**L) with only 5.2% of the sequences having dileucine, leucine-isoleucine or leucine-valine motif. Similar to YxxΦ signals, [D/E]xxxL[L/I] signals in mammalian membrane proteins can mediate both rapid internalization as well as targeting to endosomal and lysosomal compartments. This indicates that they can be recognized at the plasma membrane and the intracellular compartments. In addition, [D/E]xxxL[L/I] signals have been implicated in trafficking of membrane proteins to basolateral membranes in polarized epithelial cells (Hunziker and Fumey, 1994; Matter et al., 1994; Miranda et al., 2001). Our results indicate that the dileucine sorting signal within the subtype C Vpu protein was important for efficient transport and expression at the cell surface. Substitution of the second leucine with a glycine resulted in a protein (Vpu_{SC}EGFPL39G) that was transported to the cell surface less efficiently with the majority being retained within the Golgi complex. The virus constructed with this mutation, $SHIV_{SCVpuL39G}$, was found to replicate much better than the SHIV with the unmodified subtype C Vpu protein ($SHIV_{SCVpu}$). We also find that $SHIV_{SCVpuL39G}$ replicates as well as the SHIV expressing the subtype B Vpu protein ($SHIV_{KU\text{-}1bMC33}$). While speculative at this juncture, one possible explanation for these observations is that the presence of the [D/E]xxxL[L/I] motif may interfere with the function of the tyrosine-based signal. Possibly, the subtype C Vpu protein does not interact with AP complexes for sorting of the protein to intracellular compartments resulting in the transport of the protein to the cell surface. By removing the dileucine sequence, the protein may be allowed to interact with cellular components that target the protein to an intracellular compartment.

Our results raise the important question, "Why would the subtype C viruses select for a dileucine signal that would hinder virus replication?" It has been hypothesized that subtype C HIV-1 may be evolving to a less virulent form (Arien et al., 2007). Data to support this hypothesis include that the subtype C viruses were found to be less fit in PBMC competition assays (Arien et al., 2005; Ball et al., 2003). Additional support comes from our recent study using $SHIV_{SCVpu}$ where we exchanged the subtype B *vpu* with one from a clinical subtype C isolate (Hill et al., 2008). In this study, we showed that inoculation of pig-tailed macaques with this virus resulted in a slower rate of $CD4^+$ T cell loss compared to our highly pathogenic subtype B $SHIV_{KU\text{-}1bMC33}$. It will be of interest to determine if inoculation of macaques with the $SHIV_{SCVpuL39G}$ causes a more rapid loss of $CD4^+$ T cells.

Materials and Methods

Plasmids and Cell Culture

The derivation and pathogenicity of $SHIV_{KU\text{-}1bMC33}$ has been described (McCormick-Davis et al., 2000a; Singh et al., 2003; Stephens et al., 2002). A derivative of this virus, known as $SHIV_{SCVpu}$, is identical to $SHIV_{KU\text{-}1bMC33}$ except that this virus expresses the subtype C Vpu protein (Hill et al., 2008). Vectors expressing the subtype B (pcv*puegfp*) and C Vpu (pcvpu_{sc}*egfp*) proteins fused to enhanced green fluorescent protein (EGFP) have been previously described (Gomez et al., 2005; Pacyniak et al., 2005; Singh et al., 2003). The vector expressing the DsRed2-Golgi was obtained from Clontech. For the construction of the subtype C Vpu mutants, site-directed mutagenesis was performed on the parental plasmid, pcvpu_{SC}*egfp*. Site directed mutagenesis was performed using this plasmid in the Quik Change Mutagenesis kit (Stratagene) according to the manufacturer's instructions. With all mutants, the entire insert was

sequenced (both *vpu* and *egfp* genes) to ensure the validity of the mutations introduced and that no additional changes were introduced during the mutagenesis process.

The 293 cell line was maintained in DMEM supplemented with 10% fetal bovine serum, gentamicin (5 ug per mL) and penicillin/streptomycin (100 U per mL and 100 µg per mL, respectively). A C8166 cell line was used as the indicator cells to measure infectivity and cytopathicity of the viruses used in this study. C8166 cells were maintained in RPMI-1640, supplemented with 10 mM Hepes buffer pH 7.3, 2 mM glutamine, gentamicin (5 µg per mL) and 10% fetal bovine serum (R10FBS). HeLa $CD4^+$ cells were obtained through the AIDS Research and Reference Reagent Program, Division of AIDS, NIAID, NIH: HeLa CD4 Clone 1022 from Dr. Bruce Chesebro and were maintained in DMEM supplemented with 10% fetal bovine serum, gentamicin (5 µg per mL), and G-418 (1 mg per mL).

Laser Scanning Confocal Fluorescence Microscopy Analysis

VpuEGFP and other plasmids were transfected into human 293 cells to assess their subcellular localization using ExGen^{TM} 500 (MBI Fermentas) using the manufacturer's protocol. Briefly, 10^5 cells were seeded onto cover slips in each well of a 6-well tissue culture plate 24 hours prior to transfection. Plasmid DNA (4.75 µg) was diluted in 300 µl of 150 mM sodium chloride solution and vortexed gently. Polyethylenimine was then added to the solution, vortexed and allowed to stand at room temperature for 10 minutes. The 293 cells were washed and 3.0 mL of media was added. The polyethylenimine/DNA mixture was added to the cells dropwise and the cultures were incubated at 37C in 5% CO_2 atmosphere. At 48 hours post-transfection, cells were washed in phosphate buffered saline (PBS, pH 7.2) and fixed in ice cold 2% paraformaldehyde for 5 minutes. The cells were washed again in PBS and the cover slips

mounted onto microscope slides using mounting media (Slowfade Antifade, Molecular Probes). The cells were imaged with a Zeiss LSM 510 confocal microscope in the upright configuration. The objective used was a 63X 1.4n.a. Plan Apochromat. Images were captured at 12 bit resolution with a pixel array of 2048 x 2048 and a zoom of 2.0X. The EGFP was excited with light at 488 nm with a constant laser intensity, and the emitted light was collected after passing through a 505 nm long pass filter. The amplifier offset and gain were identical for all images. The pinhole was set to 96 µm which at this wavelength represents one airey unit. The optical section had a width of 0.7 µm.

To confirm the presence of the Vpu fusion protein at different subcellular compartments, a series of co-transfection studies were performed using vectors expressing a Golgi marker fused to the fluorescent protein DsRed2 (DsRed2-Golgi). 293 cells were co-transfected with vectors expressing the various Vpu fusion proteins and a vector expressing one of the subcellular markers. At 48 hours post-transfection, cells were processed for confocal microscopy as described above, and cells identified expressing both proteins. Fluorescent digital images were obtained using a Zeiss LSM510 confocal microscope equipped with Argon and HeNe2 lasers (25 mW) for the excitation (488 nm, 50% laser power) and detection (band pass 505-530 nm filter; BP505-530) of EGFP and for excitation (558 nm, 100% laser power) and detection (band pass 583 nm filter; LP560) of DsRed2. Images were acquired in Multitrack channel mode (sequential excitation/emission) with LSM510 (v 3.2) software and a Plan-Apochromat 63/1.4 Oil DIC objective with frame size of 2048 x 2048 pixels. Detector gain was set initially to cover the full range of all the samples and background corrected by setting the amplifier gain, and all images were then collected under the same photomultiplier detector conditions and pinhole diameter.

Construction of Viruses with the Tyrosine and Dileucine Mutations

For the construction of a subtype C SHIV containing tyrosine and dileucine mutations, we used plasmid pUCvpu$_{SC}$, which contains the *tat* and *rev* of HIV-1 (HXB2), the subtype C *vpu* and 5' end of the *env* gene. To introduce the tyrosine and dileucine mutations, we used this plasmid and procedures used for site-directed mutagenesis as described above for the construction of the Vpu/EGFP fusion proteins. Simian-human immunodeficiency viruses expressing subtype C Vpu proteins with the Y35A (SHIV$_{SCVpuY35A}$), the L39G (SHIV$_{SCVpuL39G}$), and YL35,39AG (SHIV$_{SCVpuYL35,39AG}$) amino acid substitutions were constructed as previously described (Hill et al., 2008; Hout et al., 2006b; Hout et al., 2005; McCormick-Davis et al., 2000a; Singh et al., 2003; Stephens et al., 2002). Stocks were prepared, titrated in C8166 cells and frozen at -86C until used.

Pulse-Chase Analysis of Viral Proteins

To analyze the viral proteins synthesized and released from cells, C8166 cells were inoculated with 10 ng of p27 of either SHIV$_{SCVpuY35A}$, SHIV$_{SCVpuL39G,}$ SHIV$_{SCVpuYL35,39AG}$ or SHIV$_{SCVpu}$. At 7 days post-inoculation, the medium was removed and infected cells were incubated in methionine/cysteine-free Dulbecco's modified Eagle's medium (DMEM) for 2 hours. The cells were then radiolabeled for 30 minutes with 1 mCi per ml of ^{35}S-Translabel (methionine and cysteine, ICN Biomedical, Costa Mesa, CA) and the radiolabel chased for various periods of time in DMEM containing 100X unlabeled methionine/cysteine. SHIV proteins were immunoprecipitated from the cell culture medium and infected cell lysates using plasma pooled from several rhesus monkeys infected previously with non-pathogenic SHIV-4. Briefly, the cell culture medium was clarified (16,000x g) for 2 minutes. The supernatant was

transferred and made 1X with respect to cell lysis buffer (50 mM Tris-HCl, pH 7.5; 50 mM NaCl; 0.5% deoxycholate; 0.2% SDS; 10 mM EDTA) and SHIV proteins were immunoprecipitated with 10 μl of a pooled serum. For immunoprecipitation of cell associated SHIV proteins, cell lysates were prepared as previously described (Hout et al., 2005; McCormick-Davis et al., 2000a; Stephens et al., 1995) prior to incubation with antiserum. Lysates were centrifuged in a microfuge to remove nuclei prior to the addition of antibody. Cell lysates and culture medium were then incubated with antibody for 16 hours at 4C. All immunoprecipitates were collected on protein A-Sepharose beads, the beads washed three times with RIPA buffer, and the samples resuspended in sample reducing buffer. Samples were boiled and the SHIV specific proteins analyzed by SDS-PAGE. Proteins were then visualized by standard autoradiographic techniques.

Assays for Examining Cell Surface Vpu Expression

To determine if Vpu proteins were expressed on the plasma membrane, 293 cells were transfected with 4.75μg of plasmid DNA expressing EGFP, Vpu_{SC}EGFP, Vpu_{SC}EGFPY35A, Vpu_{SC}EGFPL39G, or Vpu_{SC}EGFPYL35,39AG. At 48 hours post-transfection, cells were incubated in methionine/cysteine-free media for 2 hours and then labeled with 200 μCi of ^{35}S-Translabel for 1 hour. Cells were washed three times in ice-cold 1X PBS and the surface of cells labeled with EZ-Link Sulfo-NHS-LC-Biotin (Pierce) at a concentration of 10 mg/ml for 1 hour on ice. Cells were then washed three times in 1X PBS containing 100 mM glycine. The cells were lysed in 1 ml of 1X RIPA buffer and nuclei were removed by centrifugation at 14,000 rpm for 15 minutes. Cell lysates were incubated overnight at 4C with a rabbit polyclonal anti-EGFP antibody and protein A-Sepharose beads. Lysate immunoprecipitates were washed three times in

1X RIPA, resuspended in sample reducing buffer, and boiled for 5 minutes. Proteins were separated on a 10% SDS-PAGE gel and densitometry was used to quantify the total amount of VpuEGFP fusion expressed in each sample. Equal amounts of fusion proteins were then separated on a 10% SDS-PAGE gel, the proteins were transferred to nitrocellulose and a Western blot was used to detect biotin-labeled proteins. Biotin-labeled proteins were detected using a Vectastain-ABC-AmP chemiluminescent detection kit (Vector Laboratories). A BioRad chemiluminescent imager was used to quantify the total amount of biotin-labeled VpuEGFP in each sample. The experiments were conducted in triplicate and a Student's t-test was used to determine statistical significance with $p<0.05$ considered significant.

CD4 Surface Expression Analysis

For analysis of cell surface CD4 expression in the presence of various VpuEGFP proteins, HeLa $CD4^+$ cells were seeded into each well of six well plates 24 hours prior to transfection. Cells were transfected with plasmids expressing EGFP or various Vpu proteins fused to EGFP. Cultures were monitored for 48 hours, cells removed from the six well plates using Ca^{2+} /Mg^{2+}-free PBS containing 1 mM EDTA and stained with PE-Cy5 conjugated anti-CD4 (BD Bioscience). Cells were analyzed using an LSR II flow cytometer, determining mean fluorescence intensity (MFI) of PE-Cy5 for transfected (EGFP positive) and untransfected (EGFP negative) cells within the same well. An MFI ratio was calculated for each sample with the EGFP control normalized to 1.0. Normalized ratios from at least five separate experiments were averaged and the standard deviation calculated. Statisitcal significance for all groups were compared using a Student's *t*-test, with $p<0.05$ considered significant.

Viral Replication Kinetics Analysis

Standard p27 assays (Zeotometrix Incorporated, SIV core antigen kit) were used to assess release of viral particles from cells infected with $SHIV_{SCVpu,}$ $SHIV_{SCVpuY35A}$, $SHIV_{SCVpuL39G}$ or $SHIV_{SCVpuYL35,39AG}$. Cultures of 10^6 C8166 cells were inoculated with 10 ng of p27 (determined by commercial p27 antigen kits) for 4 hours. At the end of 4 hours, the cells were centrifuged at 400x g for 10 minutes and the pellet washed with 10 mL of medium. This was repeated two additional times. The cells were resuspended in RPMI-1640 supplemented with 10% FBS and antibiotics and this was considered the 0 time point of the assay. Cultures were incubated at 37C and aliquots of the culture were removed at 0, 1, 3, 5, 7, and 9 days with fresh media added to cultures at days 3 and 6. The culture medium was separated from the cells by centrifugation and assayed for p27 according to the manufacturer's instructions.

Electron Microscopy

To determine the site(s) of intracellular maturation, infected cells were examined by transmission electron microscopy. Cultures of 10^6 C8166 cells were inoculated with 10 ng of $SHIV_{SCVpu,}$ $SHIV_{SCVpuY35A}$, $SHIV_{SCVpuL39G}$ or $SHIV_{SCVpuYL35,39AG}$. Cells were incubated for 5 days at which time cells were pelleted at 400x g for 10 minutes. Cells were washed three times with 10 mL of PBS (pH 7.4) and fixed in 2% glutaraldehyde overnight at 4C. Cells were post-fixed in 2% osmium tetroxide (OsO_4) for 1 hour. The cells were washed twice with water and dehydrated through a series of alcohols (30-100%) followed by embedding in Embed 812 resin. Thin sections were cut at 80Å, stained with uranyl acetate and lead citrate and examined under a JEOL 100CXII transmission electron microscope. The number of virus particles associated with

50 infected cells (either at the surface or within the cell) were enumerated and data analyzed by planned comparisons using unpaired *t*-test.

XII. Chapter 7: The Transmembrane Domain of Human Immunodeficiency Virus Type 1 Vpu is the Major Influence of the Protein on the Rate of $CD4^+$ T Cell Loss in Pig-tailed Macaques Inoculated with SHIV

Abstract

Previously, we showed that a subtype C Vpu protein from a clinical isolate of HIV-1 displayed biological properties distinct from those exhibited by a laboratory-adapted subtype B Vpu (HXB2). Inoculation of pig-tailed macaques with a simian-human immunodeficiency virus (SHIV) expressing a subtype C Vpu protein ($SHIV_{SCVpu}$) resulted in a more gradual loss of $CD4^+$ T-cells compared to those inoculated with a SHIV expressing a subtype B Vpu ($SHIV_{KU\text{-}1bMC33}$) (Hill et al., 2008). In this study, we sought to determine the contributions of the N-terminus/transmembrane domain and the cytoplasmic domain of each of these subtypes to the differences observed. We constructed chimeric Vpu expressing either the subtype B or subtype C N-terminal region/transmembrane domain and the opposing cytoplasmic domain. Both chimeric *vpu* genes were fused in frame with the gene for enhanced green fluorescence protein (EGFP). Our results indicate that the cytoplasmic domain is responsible for localization of the protein and the difference in molecular weight of the fusion proteins. Both proteins down-modulated CD4 from the surface similar to the subtype C Vpu. We constructed SHIV expressing either of the chimeric Vpu ($SHIV_{VpuBC}$ and $SHIV_{VpuCB}$). Both SHIV expressing the chimeric Vpu proteins replicated at intermediate rates compared to the two parental viruses, however $SHIV_{VpuBC}$ replicated with increased kinetics compared to $SHIV_{VpuCB}$. Inoculation of three pig-tailed macaques with $SHIV_{VpuBC}$ resulted in a rapid loss of circulating $CD4^+$ T cells and high viral loads similar to results in macaques inoculated with $SHIV_{KU\text{-}1bMC33}$. Inoculation of

three pig-tailed macaques with $SHIV_{VpuCB}$ resulted in a more gradual loss of circulating $CD4^+$ T cells than observed in $SHIV_{VpuBC}$ inoculated macaques, however, more rapid than resulted in macaques inoculated with $SHIV_{SCVpu}$. These results demonstrate the potential impact of the individual domains of the Vpu protein on biological properties, protein function and pathogenesis.

Introduction

Two major functions of Vpu in HIV-1 pathogenesis have been identified. These are the down-modulation of CD4 from the surface of infected cells by shunting CD4 molecules to the proteasome and facilitating virion release from the surface of cells. Both the transmembrane domain and the cytoplasmic domain have been implicated to play a role in both of these functions. However, whether these implications are due to alterations in protein interactions or modifications of protein structure remains in question. The extent to which each of these functions and the contributions that each of the domains that mediated them contribute to disease progression *in vivo* also remains unknown.

During the last several years, our laboratory has generated a series of pathogenic chimeric simian-human immunodeficiency virus molecular clones that have greatly facilitated the study of the role of HIV-1 Vpu in pathogenesis. Using $SHIV_{KU\text{-}1bMC33}$, our laboratory showed that the Vpu protein can play a role in disease progression and that the Vpu from another subtype of HIV-1 affected SHIV pathogenesis differentially (Hill et al., 2008; Stephens et al., 2002). Additional studies from our laboratory have shown that subtype B Vpu and subtype C Vpu exhibit distinct structural and biological properties that could potentially affect overall HIV-1 pathogenesis (Hill et al., 2008; Pacyniak et al., 2005; Singh et al., 2003). Using a VpuEGFP

fusion system we determined that subtype B Vpu predominately localizes to the Golgi complex, while subtype C Vpu is efficiently transported to the plasma membrane. The subtype B Vpu is more efficient at down-modulating CD4 surface expression than subtype C Vpu. Both proteins associate with detergent resistant membranes, which appears to correlate with the BST-2 associated enhancement of virion release function. However, membrane raft association does not appear to impact the CD4 down-modulation function of Vpu. Finally, a SHIV expressing a subtype C Vpu ($SHIV_{SCVpu}$) has reduced replication kinetics and results in a decreased rate of $CD4^+$ T cell loss and lower viral loads in infected pig-tailed macaques when compared to a SHIV expressing a subtype B Vpu ($SHIV_{KU\text{-}1bMC33}$) (Hill et al., 2008; Pacyniak et al., 2005; Singh et al., 2003). In this study, we sought to determine the contributions of the N-terminus/transmembrane domain and the cytoplasmic domain of the subtype B and subtype C Vpu proteins to the structural and functional properties of each of these isolates and their impact on disease pathogenesis. Our results indicate that while both domains impact both functions of the Vpu protein, the transmembrane domain appears to have a major influence on the rate of $CD4^+$ T cell loss in infected pig-tailed macaques. As the transmembrane domain is critical to the enhanced virion release function of Vpu, these results again question, "To what extent is the antagonism of BST-2 relevant in Vpu mediated enhancement of disease progression?" as pig-tailed macaques do not express a BST-2 protein that is susceptible to HIV-1 Vpu.

Results

The cytoplasmic domain of the Vpu protein dictates intracellular localization and molecular weight

The sequences of the chimeric Vpu proteins analyzed in this study are shown in Figure 52. 293 cells were transfected with vectors expressing VpuEGFP, Vpu_{SC}EGFP1, Vpu_{BC}EGFP or Vpu_{CB}EGFP. At 48 hours post-transfection, cells were analyzed by laser scanning confocal microscopy. As shown in Figure 53A-D, Vpu_{BC}EGFP was predominately localized within intracellular compartments, similar to VpuEGFP, while the Vpu_{CB}EGFP was efficiently transported to the plasma membrane parallel to results observed in cells transfected with Vpu_{SC}EGFP1.

We next examined the stability of these chimeric proteins using pulse-chase analysis. The results shown in Figure 54, indicate that exchanging the domains of the subtypes B and C Vpu proteins does not modify the rate of protein turnover. These results identify the cytoplasmic domain as a determinant of the differential molecular weights (M_r) of VpuEGFP and Vpu_{SC}EGFP1.

Both domains impact the ability of Vpu to down-modulate CD4 surface expression

In order to examine the influence of each of the domains to the CD4 surface down-modulation function, HeLa $CD4^+$ cells were transfected with plasmids expressing VpuEGFP, Vpu_{SC}EGFP1, Vpu_{BC}EGFP, or Vpu_{CB}EGFP and CD4 surface expression was analyzed by flow cytometry. Expression of either Vpu_{BC}EGFP or Vpu_{CB}EGFP results in CD4 surface expression levels similar to cells expressing Vpu_{SC}EGFP1 (Figure 55). Statistical analysis using a Student's *t*-test indicated that both chimeric Vpu fusion proteins were significantly less efficient at down-

Figure 52. Sequence alignments of parental and chimeric Vpu proteins used in this study. Base pairs similar to subtype B Vpu (B.US.HXB2) are highlighted in blue. Base pairs similar to subtype C Vpu (C.BW16B01) are highlighted in yellow.

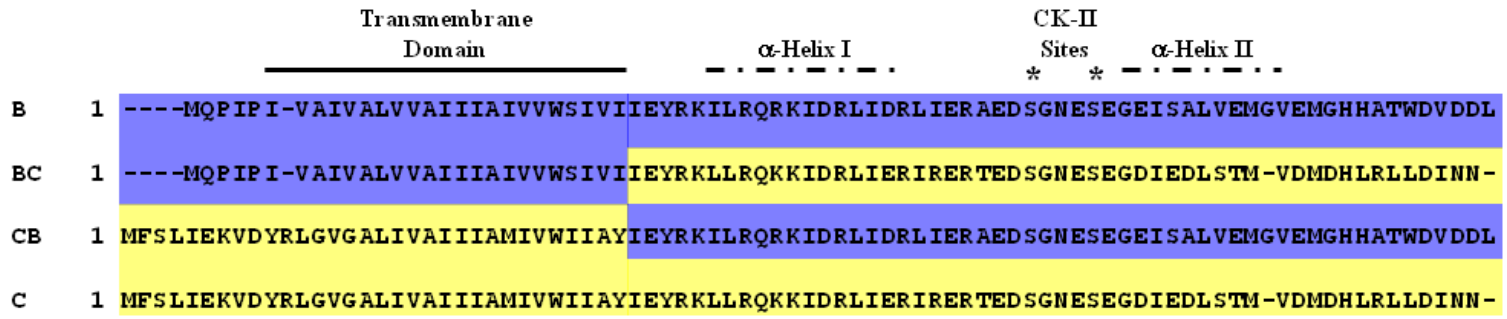
Transmembrane Domain
α-Helix I
CK-II Sites
α-Helix II
B 1 ----MQPIPI-VAIVALVVAIIIAIVVWSIVIIEYRKILRQRKIDRLIDRLIERAEDSGNESEGEISALVEMGVEMGHHATWDVDDL
BC 1 ----MQPIPI-VAIVALVVAIIIAIVVWSIVIIEYRKLLRQKKIDRLIERIRERTEDSGNESEGDIEDLSTM-VDMDHLRLLDINN-
CB 1 MFSLIEKVDYRLGVGALIVAIIIAMIVWIIAYIEYRKILRQRKIDRLIDRLIERAEDSGNESEGEISALVEMGVEMGHHATWDVDDL
C 1 MFSLIEKVDYRLGVGALIVAIIIAMIVWIIAYIEYRKLLRQKKIDRLIERIRERTEDSGNESEGDIEDLSTM-VDMDHLRLLDINN-

Figure 53. Cellular localization of chimeric Vpu fusion proteins. 293 cells plated on glass coverslips were transfected with vectors expressing VpuEGFP, Vpu_{SC}EGFP1, Vpu_{BC}EGFP or Vpu_{CB}EGFP. At 48 hours post transfection, cells expressing EGFP were identified and images collected using laser scanning confocal microscopy as described in the Materials and methods section.

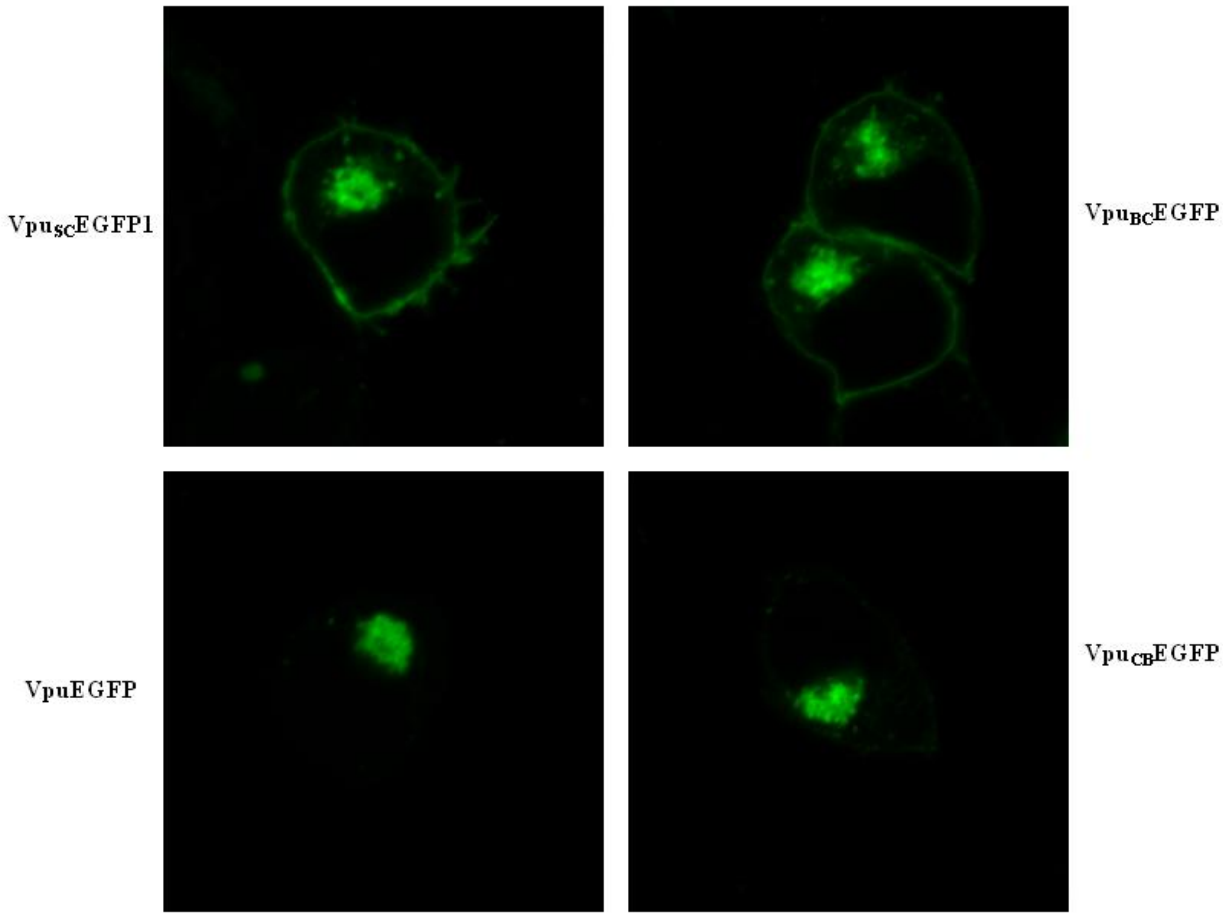
Vpu$_{SC}$EGFP1
Vpu$_{BC}$EGFP
VpuEGFP
Vpu$_{CB}$EGFP

Figure 54. Protein stability of parental and chimeric Vpu fusion proteins. 293 cells were transfected with vectors expressing VpuEGFP, Vpu_{SC}EGFP1, Vpu_{BC}EGFP or Vpu_{CB}EGFP. At 48 hours post-transfection, the cells were washed and starved in DMEM lacking methionine and cysteine. Cells were radiolabeled with ^{35}S-Translabel (MP Biomedical) for 1 hour and chased in DMEM containing 100X unlabeled methionine/cysteine for 6 hours. Samples were collected at hours 0, 3, and 6 post-label. Cells were lysed in 1X RIPA and immunoprecipitated using a rabbit anti-EGFP serum and protein A-Sepharose beads. All immune precipitates were washed, resuspended in reducing buffer and boiled. Proteins were separated on a 10% SDS-PAGE gel and visualized by standard autoradiography techniques. Pixel density was determined using ImageJ software and the percent protein remaining determined. Panel A. Representative autoradiographs. Numbers above lanes represent hours post-chase. Panel B. Graphical representation of the percent protein remaining at the 6-hour post-chase period.

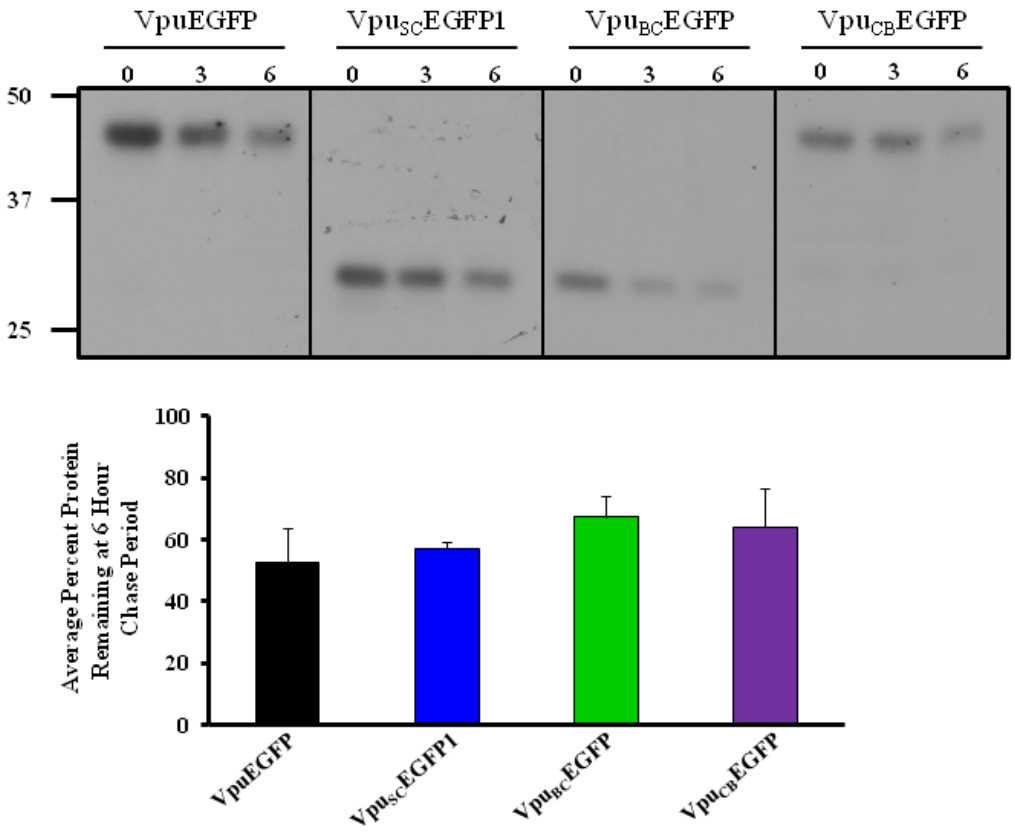
VpuEGFP
Vpu$_{SC}$EGFP1
Vpu$_{BC}$EGFP
Vpu$_{CB}$EGFP
0 3 6 0 3 6 0 3 6 0 3 6
50
37
25
Average Percent Protein Remaining at 6 Hour Chase Period
100
80
60
40
20
0
VpuEGFP
Vpu$_{SC}$EGFP1
Vpu$_{BC}$EGFP
Vpu$_{CB}$EGFP

Figure 55. CD4 surface expression in the presence of chimeric Vpu fusion proteins. HeLa $CD4^+$ cells were transfected with plasmids expressing VpuEGFP, Vpu_{SC}EGFP1, Vpu_{BC}EGFP or Vpu_{CB}EGFP. At 48 hours post-transfection the cells were removed from the plate and stained with PE-Cy5 conjugated to anti-CD4. Cells were analyzed using a LSR II flow cytometer, determining mean fluorescence intensity (MFI) of PE-Cy5 for transfected (EGFP positive) and untransfected (EGFP negative) cells within the same well. An MFI ratio was calculated for each; EGFP was normalized to 1. At least five separate experiments were performed, the normalized ratios averaged and the standard deviation calculated. Groups were compared using the unpaired Student's *t*-test, with $p \leq 0.05$ considered significant (*).

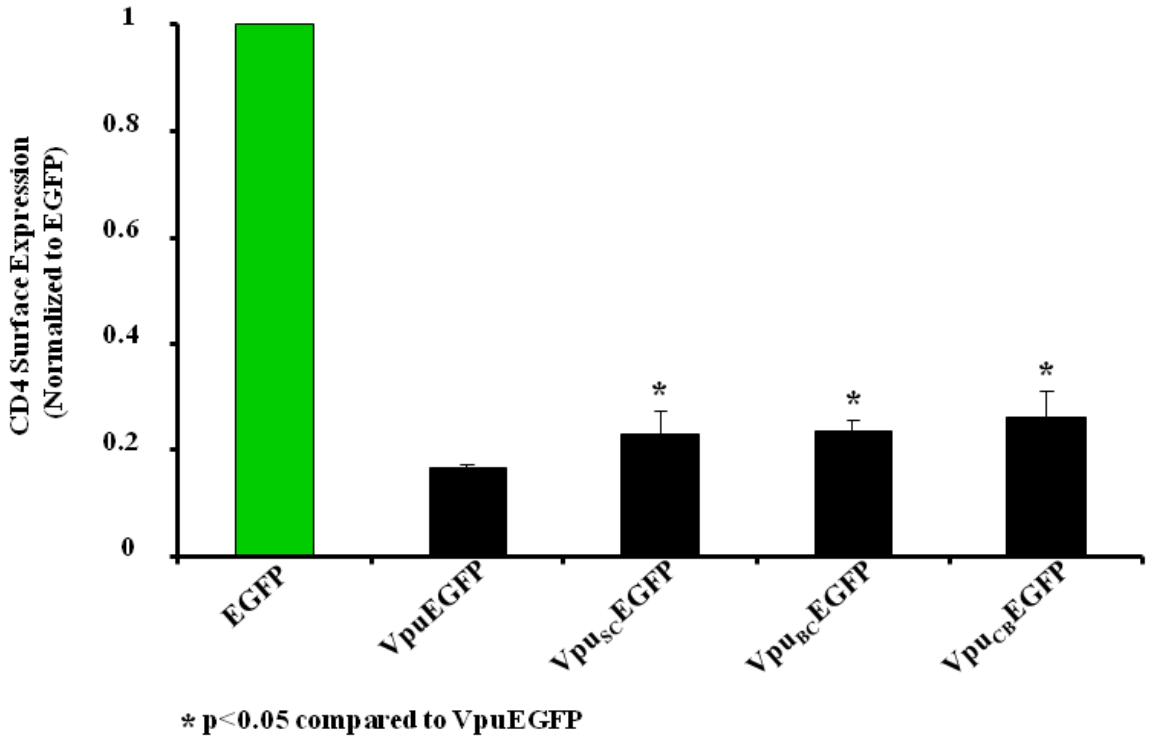
CD4 Surface Expression
(Normalized to EGFP)
1
0.8
0.6
0.4
0.2
0
*
*
*
EGFP
VpuEGFP
Vpu$_{SC}$EGFP
Vpu$_{BC}$EGFP
Vpu$_{CB}$EGFP
* p<0.05 compared to VpuEGFP

modulating CD4 surface expression compared to VpuEGFP and were similar to Vpu_{SC}EGFP1. These results suggest that both the N-terminal transmembrane domain and the cytoplasmic domain have the ability to influence Vpu mediated CD4 surface down-modulation.

Exchange of subtype B and subtype C Vpu domains does not alter biosynthesis or rate of turnover of other SHIV proteins

In order to examine the processing of other viral proteins, including the Gag and Env proteins. C8166 cells were inoculated with $SHIV_{VpuBC}$ or $SHIV_{VpuCB}$ and 5 days post-inoculation viral proteins were immunoprecipitated as described in the Materials and methods section. The results in Figure 56 show that the Gag and Env proteins expressed in the chimeric Vpu SHIV viruses are synthesized and processed similar to the parental viruses.

SHIV expressing chimeric Vpu replicate with intermediate kinetics compared to the parental SHIVs

We constructed SHIV expressing either the VpuBC ($SHIV_{VpuBC}$) or the VpuCB ($SHIV_{VpuCB}$) protein and examined the replication kinetics of these viruses in C8166 cells. Cells were inoculated with 10^3 $TCID_{50}$ of $SHIV_{KU\text{-}1bMC33}$, $SHIV_{SCVpu}$, $SHIV_{VpuBC}$, or $SHIV_{VpuCB}$ and the cultures analyzed using p27 growth curves as described in the Materials and methods section. Growth curve analysis was repeated in triplicate and the average p27 concentrations for each time point determined. The average results of these assays are shown in Figure 57 and indicate that the two chimeric Vpu expressing SHIVs replicated with intermediate kinetics compared to $SHIV_{KU\text{-}1bMC33}$ and $SHIV_{VpuSC}$. Of the two chimeric Vpu SHIVs, $SHIV_{VpuBC}$ replicated more

Figure 56. C8166 cells were infected with 10^4 $TCID_{50}$ of $SHIV_{VpuBC}$ or $SHIV_{VpuCB}$ stock cultures and incubated at 37C. After 4 hours cells were washed and resuspended in fresh culture media. 5 days post-infection cells were incubated in DMEM lacking methionine and cysteine for 2 hours. Cells were radiolabeled with 500 µCi of ^{35}S Translabel (MP Biomedical) for an hour. Cells were lysed in 1X RIPA buffer and the nuclei removed through centrifugation. SHIV proteins were immunoprecipitated from both the cell lysates using pooled serum from macaques inoculated with a non-pathogenic SHIV and protein A-Sepharose beads. Immune precipitates were washed and separated on a 10% SDS-PAGE gel and visualized using standard autoradiography techniques.

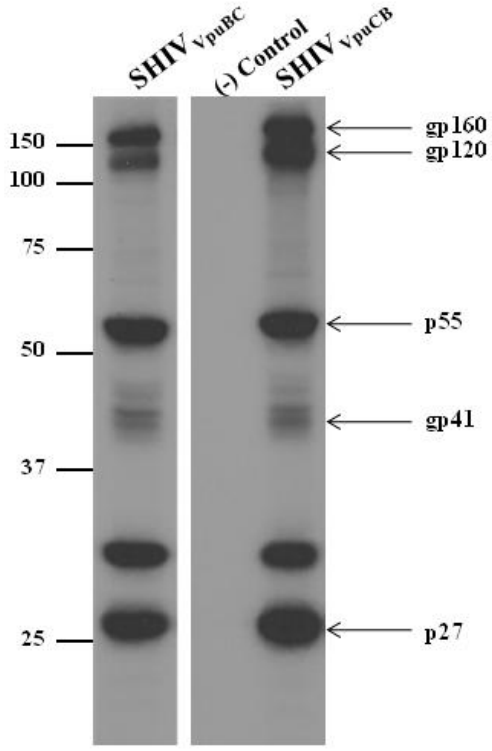
SHIV VpuBC
(-) Control
SHIV VpuCB
150
100
75
50
37
25
gp160
gp120
p55
gp41
p27

Figure 57. C8166 cells were infected with 10^3 $TCID_{50}$ of SHIV expressing the parental (B or C) or chimeric (BC or CB) Vpu proteins. 4 hours post-infection the cells were washed, resuspended in fresh culture media and incubated at 37C. Samples were collected at days 0, 1, 3, 5, 7 and 9 post-inoculation. The amount of p27 protein present within the supernatant samples was quantified using a commercially available p27 antigen capture ELISA (Zeptometrix).

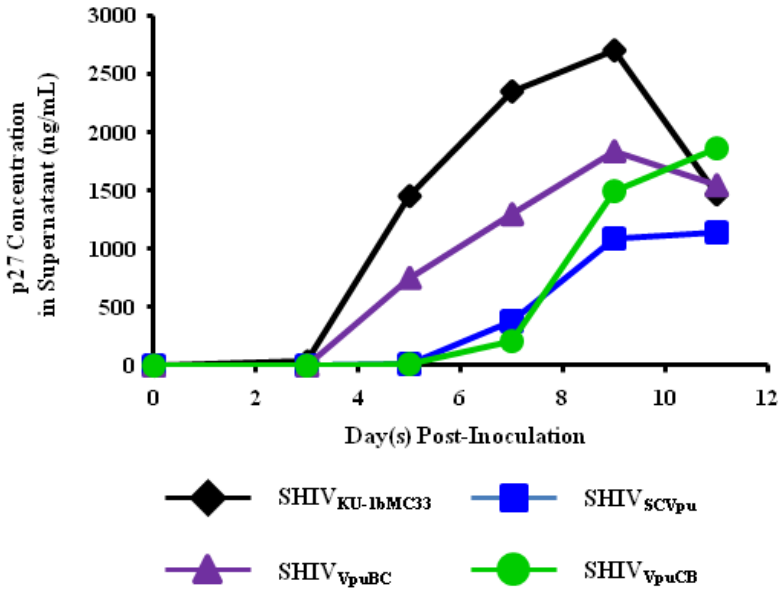
3000
2500
2000
1500
1000
500
0
p27 Concentration
in Supernatant (ng/mL)
0
2
4
6
8
10
12
Day(s) Post-Inoculation
SHIV KU-1bMC33
SHIV SCVpu
SHIV VpuBC
SHIV VpuCB

efficiently than $SHIV_{VpuCB}$, which replicated similar to $SHIV_{SCVpu}$ until around day 7 at which time the accumulation of p27 in the culture media increased through day 11.

$SHIV_{VpuCB}$ inoculated cells exhibited an increased number of particles on the cell surface

We also compared the pattern of virus maturation in C8166 cells inoculated with $SHIV_{KU\text{-}1bMC33}$, $SHIV_{VpuSC}$, $SHIV_{VpuBC}$ or $SHIV_{VpuCB}$ using electron microscopy. The results shown in Figure 58A-B indicate that both parental viruses ($SHIV_{KU\text{-}1bMC33}$ (Panel A); $SHIV_{SCVpu}$ (Panel B)) mature at the plasma membrane as we have previously reported (Hill et al., 2008). SHIVs expressing either VpuBC (Panel C) or VpuCB (Panels D and E) were also found to mature at the plasma membrane (Figure 58C-E), however, $SHIV_{VpuCB}$ exhibited an increased number of particles associated per infected cell compared to the other three. We determined the mean number of particles per cell of 50 cells at five days post-inoculation. As shown in Figure 59, the mean number of particles per cell for $SHIV_{KU\text{-}1bMC33}$, $SHIV_{SCVpu}$, and $SHIV_{VpuBC}$ were 35, 21, and 34, respectively. In contrast, $SHIV_{VpuCB}$ had a mean of approximately 84 particles per cell. There was a clear difference in the distribution of the number of particles per cell between $SHIV_{VpuCB}$ and the other three viruses. For the two parental viruses and $SHIV_{VpuBC}$, the number of particles per cell was generally less than 60, while $SHIV_{VpuCB}$ showed a more even distribution. The results for $SHIV_{VpuCB}$ were similar to results we reported previously for a SHIV expressing a Vpu with a glycine substitution at position 39 ($SHIV_{SCVpuL39G}$). However, $SHIV_{SCVpuL39G}$ was found to replicate better than $SHIV_{VpuCB}$.

Figure 58. Electron microscopic examination of C8166 cells inoculated with $SHIV_{KU-1bMC33}$, $SHIV_{SCVpu}$, $SHIV_{VpuBC}$, or $SHIV_{VpuCB}$. C8166 cells were inoculated with each virus for 5 days. Cells were washed three times with PBS and processed for electron microscopy as described in the Materials and methods section. Panel A. C8166 cells inoculated with parental $SHIV_{KU-1bMC33}$. Panel B. C8166 cells inoculated with parental $SHIV_{SCVpu}$. Panel C. C8166 cells inoculated with $SHIV_{VpuBC}$. Panels D and E. C8166 cells inoculated with $SHIV_{VpuCB}$.

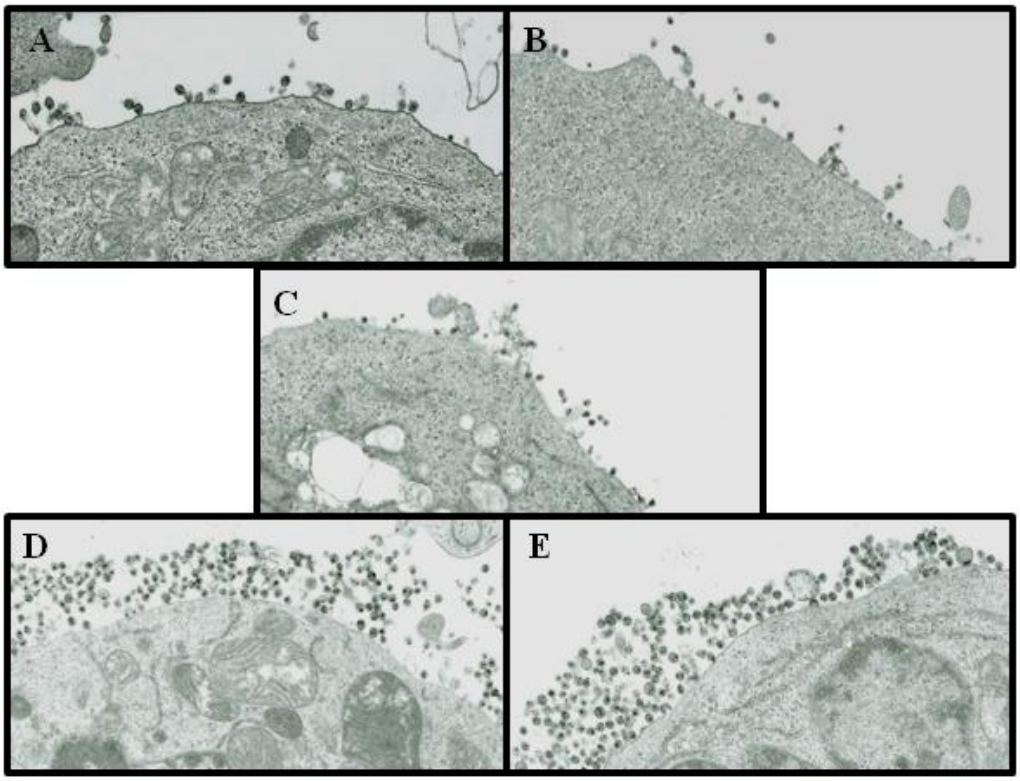
A
B
C
D
E

Figure 59. Enumeration of the number of viral particles associated with the infected C8166 cells following inoculation with $SHIV_{KU\text{-}1bMC33}$ (Black), $SHIV_{SCVpu}$ (Blue), $SHIV_{VpuBC}$ (Green), or $SHIV_{VpuCB}$ (Purple). Cells were inoculated with equivalent doses of infectious virus and at 5 days processed for electron microscopy as described in the Materials and methods section. The number of viral particles associated with 50 cells per virus and mean values was calculated.

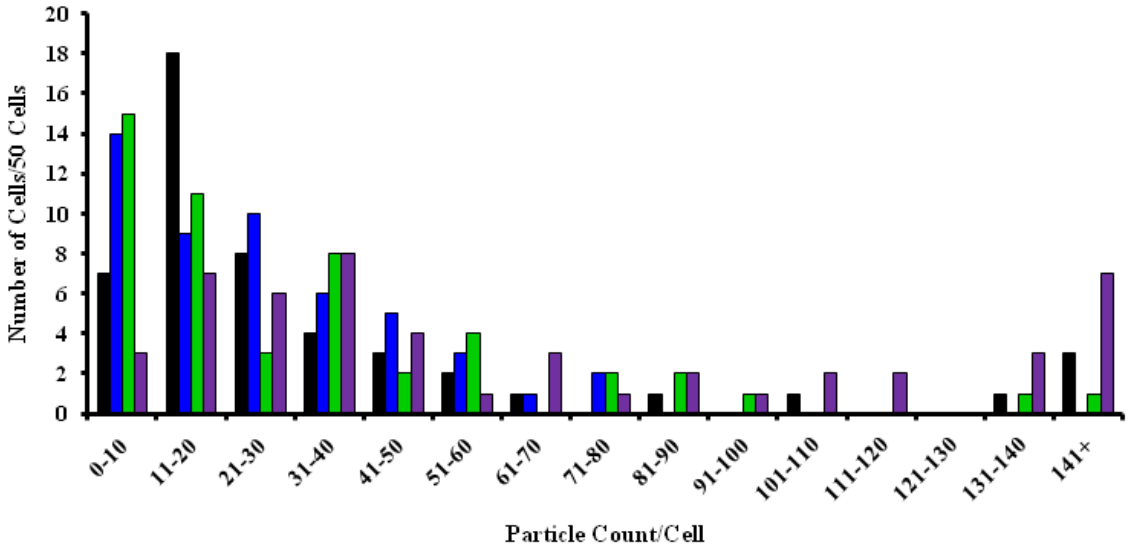

Mean Particle Count:	35	21	34	84
	$SHIV_{KU-1bMC33}$	$SHIV_{SCVpu}$	$SHIV_{VpuBC}$	$SHIV_{VpuCB}$

The rate of $CD4^+$ T cell loss was decreased and plasma viral loads lower in macaques inoculated with $SHIV_{VpuCB}$

In order to determine the contributions of the different domains to pathogenesis, two sets of three pig-tailed macaques (Set 1: W005, W018, W030 and Set 2: W004, W007, W013) were inoculated with 10^4 $TCID_{50}$ of either $SHIV_{VpuBC}$ or $SHIV_{VpuCB}$, respectively, and their circulating $CD4^+$ T cell levels and plasma viral loads monitored. Macaques W030, W005, and W018 were euthanized in a moribund condition at weeks 10, 24 and 24 post-inoculation, respectively. Macaques W004, W007 and W013 are still being monitored and the results presented from this study are presented through week 24 post-inoculation. The circulating $CD4^+$ T cell levels are shown in Figure 60 in conjunction with results published previously for macaques inoculated with either $SHIV_{KU\text{-}1bMC33}$ or $SHIV_{SCVpu}$. These results demonstrate a rapid and severe loss of $CD4^+$ T cells in all three macaques inoculated with $SHIV_{VpuBC}$, similar to results observed in $SHIV_{KU\text{-}1bMC33}$ inoculated macaques. Macaques inoculated with $SHIV_{VpuCB}$ exhibited a more gradual loss of $CD4^+$ T cells, however, not to the extent observed in macaques inoculated with $SHIV_{SCVpu}$. We also found that early peak viral loads (weeks 1-3) in macaques inoculated with $SHIV_{VpuCB}$ were approximately 10-fold less than in macaques W018 and W030 (inoculated with $SHIV_{VpuBC}$) (Figure 61).

Figure 60. Circulating $CD4^+$ T cell levels in infected macaques. Alterations in the levels of $CD4^+$ T cells after experimental inoculations were monitored sequentially by FACS analysis (Becton Dickinson). T cell subsets were labeled with OKT4 (CD4; Ortho Diagnostics Systems, Inc.), SP34 (CD3; Pharmingen) or FN18 (CD3; Biosource International) monoclonal antibodies. Panel A. The levels of circulating $CD4^+$ T cells in three macaques (2000, CM4G and CM4K) inoculated with $SHIV_{KU\text{-}1bMC33}$. Panel B. The levels of circulating $CD4^+$ T cells in three macaques (CX56, CX57 and PLg2) inoculated with $SHIV_{SCVpu}$. Panel C. The levels of circulating $CD4^+$ T cells in three macaques (W005, W018 and W030) inoculated with $SHIV_{VpuBC}$. Macaque W030 was euthanized at 10 weeks post-inoculation in a moribund condition with severe anemia (†). Macaques W005 and W018 were euthanized at 24 weeks post-inoculation (†). Macaque W018 was diagnosed with a Candadiasis infection. Macaque W005 did not exhibit an AIDS-defining illnesses aside from $CD4^+$ T cell levels below 200 per µl. Panel D. The levels of circulating $CD4^+$ T cells in three macaques (W004, W007 and W013) inoculated with $SHIV_{VpuCB}$. All three macaques inoculated with $SHIV_{VpuCB}$ are still being monitored.

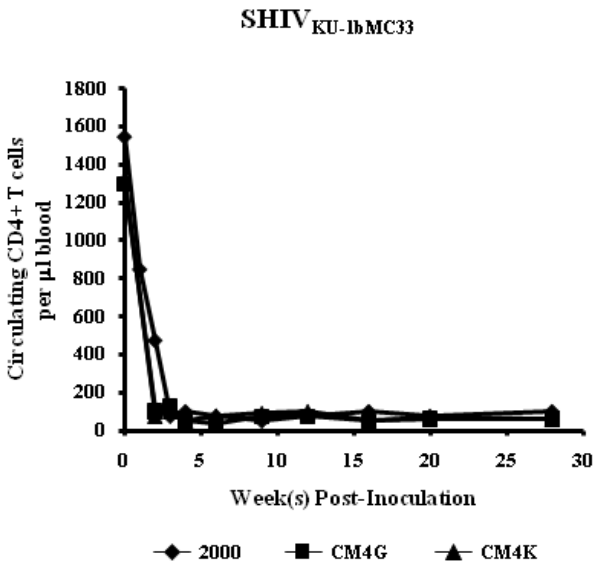
SHIV KU-1bMC33
Circulating CD4+ T cells per µl blood
1800
1600
1400
1200
1000
800
600
400
200
0
0
5
10
15
20
25
30
Week(s) Post-Inoculation
2000
CM4G
CM4K

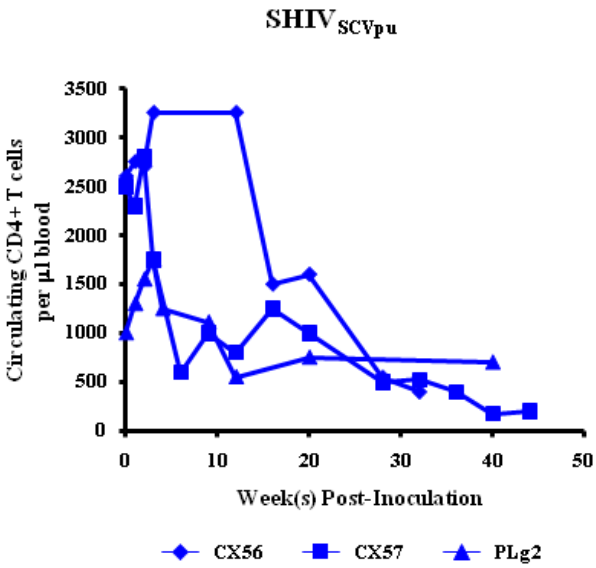
SHIV SCVpu
Circulating CD4+ T cells per µl blood
3500
3000
2500
2000
1500
1000
500
0
0
10
20
30
40
50
Week(s) Post-Inoculation
CX56
CX57
PLg2

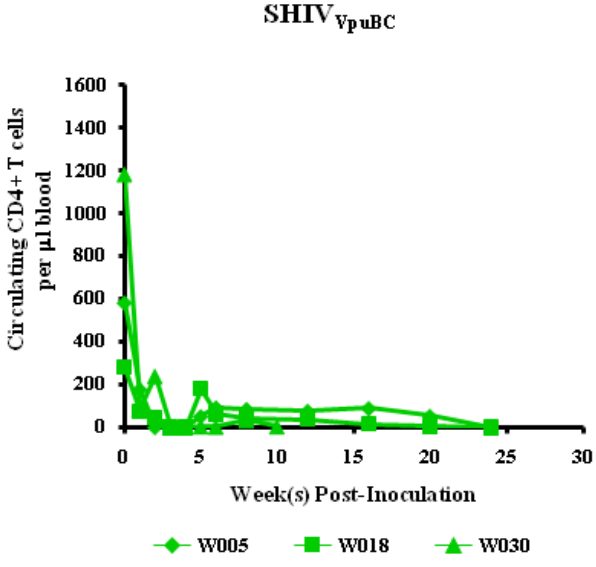
SHIV VpuBC
Circulating CD4+ T cells per µl blood
1600
1400
1200
1000
800
600
400
200
0
0
5
10
15
20
25
30
Week(s) Post-Inoculation
W005
W018
W030

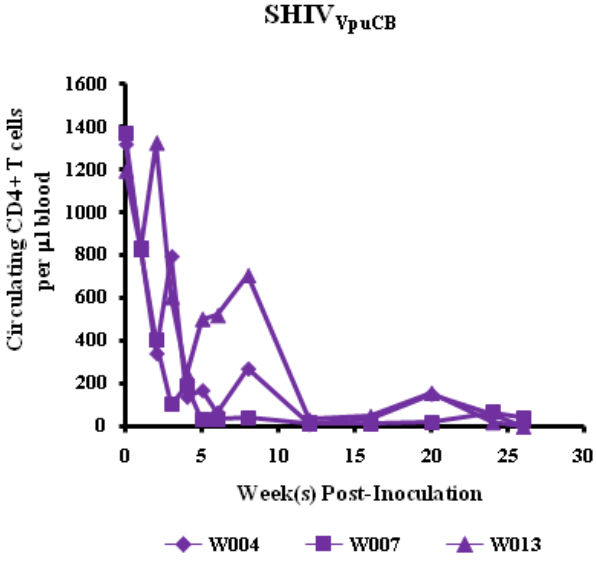
SHIV VpuCB
Circulating CD4+ T cells per µl blood
1600
1400
1200
1000
800
600
400
200
0
0
5
10
15
20
25
30
Week(s) Post-Inoculation
W004
W007
W013

Figure 61. Plasma viral loads in infected macaques. Virus was pelleted from 1 mL of EDTA-treated plasma through ultracentrifugation (Beckman SW55Ti, 38,000rpm, 1 hour) and viral RNA extracted using a QIAamp viral RNA kit (Qiagen). RNA samples were analyzed by real-time RT-PCR using *gag* primers and a 5'FAM/3'TAMRA labeled Sigma probe that was homologous to the SIV *gag* gene. Standard curves were prepared using a series of twelve ten-fold dilutions of T7 transcribed SIV *gag* mRNA of known concentration. The sensitivity of this assay was 100 RNA equivalents per mL. Samples were analyzed in duplicate and the number of RNA equivalents were calculated per mL of plasma. Panel A. Viral loads in three macaques (2000, CM4G and CM4K) inoculated with $SHIV_{KU\text{-}1bMC33}$. Panel B. Viral loads in three macaques (CX56, CX57 and PLg2) inoculated with $SHIV_{SCVpu}$. Panel C. Viral loads in three macaques (W005, W018 and W030) inoculated with $SHIV_{VpuBC}$. Macaque W030 was euthanized at 10 weeks post-inoculation in a moribund condition with severe anemia (†). Macaques W005 and W018 were euthanized at 24 weeks post-inoculation (†). Macaque W018 was diagnosed with a Candadiasis infection. Macaque W005 did not exhibit an AIDS-defining illness aside from $CD4^+$ T cell levels below 200 per µl. Panel D. Viral loads in three macaques (W004, W007 and W013) inoculated with $SHIV_{VpuCB}$. All three macaques inoculated with $SHIV_{VpuCB}$ are still being monitored.

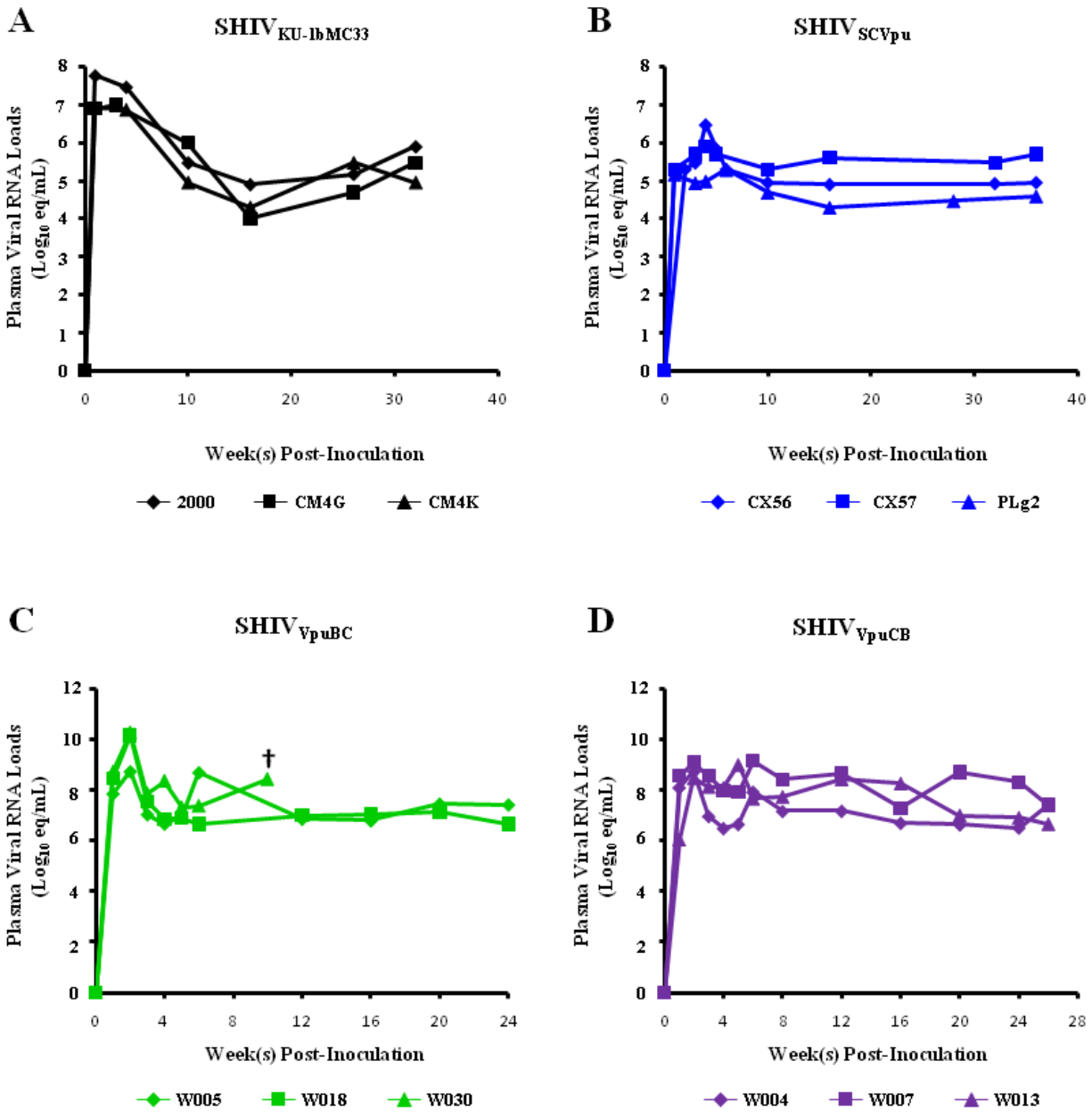
A
SHIV KU-1bMC33
Plasma Viral RNA Loads (Log10 eq/mL)
Week(s) Post-Inoculation
2000
CM4G
CM4K
B
SHIV SCVpu
Plasma Viral RNA Loads (Log10 eq/mL)
Week(s) Post-Inoculation
CX56
CX57
PLg2
C
SHIV VpuBC
†
Plasma Viral RNA Loads (Log10 eq/mL)
Week(s) Post-Inoculation
W005
W018
W030
D
SHIV VpuCB
Plasma Viral RNA Loads (Log10 eq/mL)
Week(s) Post-Inoculation
W004
W007
W013

Discussion

The biological relevance of the two separate functions of Vpu has been difficult to assess since alterations within either the transmembrane or cytoplasmic domain have the ability to modify the other region and in turn both functions. Previously, we and other investigators showed that while the two domains of Vpu can influence the other, the two functions of Vpu are dictated by the two separable structural domains (Hout et al., 2005; Schubert et al., 1996a). We have also shown that subtype B and subtype C Vpu proteins exhibit distinct biological properties and contain differential sorting signals that could potentially contribute to the differences in pathogenesis observed in macaques inoculated with SHIV expressing either of these proteins (Hill et al., 2008; Pacyniak et al., 2005; Ruiz et al., 2008; Singh et al., 2003). Therefore, in this study we determined the impact each domain had on pathogenesis. These studies increase our understanding of the role of both structural domains of Vpu and the biological significance of each of its functions.

In order to examine the role of each domain in Vpu-mediated modification of pathogenesis, we constructed two chimeric Vpu proteins in which we exchanged the N-terminal/transmembrane domain regions of a subtype B and a subtype C Vpu protein (VpuBC and VpuCB). Using flow cytometric analysis to determine the efficiency of each of these proteins to down-modulate CD4 surface expression, we found that both chimeric Vpu proteins were statistically less efficient at preventing cell surface expression of CD4, which is similar to results we previously reported for the parental subtype C Vpu protein (Hill et al., 2008). Previous studies examining the contributions of each domain to the ability of Vpu to degrade CD4 have involved mutational analysis (Hout et al., 2005; Schubert et al., 1996a). In this study, we used proteins that contained unmodified transmembrane (TM) domains, and therefore these

results suggest that the two domains either directly influence the ability of Vpu to down-modulate CD4 surface expression or that each subtype has evolved intricate structural features that allow for differential modification of this function.

We constructed SHIVs expressing each of these chimeric Vpu proteins and examining the replication kinetics. In support of the hypothesis that both domains contribute to each function of Vpu, SHIV expressing either of the proteins replicated at rates intermediate of those observed with either the $SHIV_{KU\text{-}1bMC33}$ or $SHIV_{SCVpu}$ parental viruses. However, the $SHIV_{VpuBC}$ replicated more rapidly than the $SHIV_{VpuCB}$, suggesting that the transmembrane domain is the major influence on viral propagation as was previously hypothesized. Inoculation of pig-tailed macaques yielded results parallel to those observed with growth curve analysis. Macaques inoculated with $SHIV_{VpuBC}$ displayed rapid $CD4^+$ T cell loss, while macaques inoculated with $SHIV_{VpuCB}$ showed a more gradual rate of loss. The rate of $CD4^+$ T cell loss in the macaques inoculated with $SHIV_{VpuCB}$ was not as decreased as that observed in macaques inoculated with $SHIV_{SCVpu}$. These results provide additional support for the contribution of each domain to both functions of Vpu, however, the transmembrane domain appears to have a major influence on the rate of $CD4^+$ T cell loss in infected macaques.

Another possible factor in the rate of $CD4^+$ T cell loss is the differential efficiencies of subtype B and subtype C Vpu proteins to down-modulate CD4 surface expression. Even though both chimeric Vpu proteins were significantly less efficient at down-regulating CD4 surface expression, macaques inoculated with SHIV expressing either of these proteins, displayed differential rates of $CD4^+$ T cell loss. These results suggest that the statistical significance observed *in vitro* for these two proteins and for all four of the subtype C Vpu/EGFP fusion proteins analyzed previously, may not be physiologically relevant. This also suggests that the

ability of the subtype B and subtype C Vpu proteins to down-modulate CD4 from the surface is not a major contributing factor in the differences in pathogenesis caused by these two viruses. These results insinuate that the major influence in the differences in pathogenesis caused by these two viruses is the enhanced virion release function. Previously, we demonstrated that subtype B and subtype C displayed a similar ability to overcome BST-2 mediated restriction of virion release in HeLa cells (See Chapter 3). Taken together, these results suggest that the enhanced virion release function of Vpu *in vivo* and the differential rates of $CD4^+$ T cell loss in macaques inoculated with SHIV expressing different Vpu subtypes is not associated with overcoming BST-2 restriction or CD4 down-modulation. This suggests that Vpu enhances virion release and in turn modifies disease pathogenesis *in vivo*, via an unknown mechanism, potentially associated with the ion channel function of Vpu, intra- or interprotein oligomerization of Vpu, or the antagonism of another yet unknown viral restriction factor. As these results are based on an intravenous route of inoculation, it is possible different affects would be observed with mucosal transmission and additional studies are needed to fully understand the impact of this variable.

Materials and Methods

Plasmids, Viruses and Cell Culture

In order to construct plasmids expressing subtype B and subtype C chimeric *vpuegfp* fusion genes an EcoRV site was inserted into each parental *vpu* gene expressed in a pcDNA(+) expression vector at the interface between the putative transmembrane domain and the cytoplasmic domain using site-directed mutagenesis. The N-terminal regions were excised from the parental plasmids using KpnI and EcoRV restriction enzymes. The N-terminal region

fragments were ligated into the opposing digested vector. The EcoRV sites were then removed using site-directed mutagenesis and the resulting plasmids (pc*vpu*$_{BC}$*egfp* and pc*vpu*$_{CB}$*egfp*) sequenced to ensure validity of the genes and that no other mutations were introduced during the cloning process.

For the construction of SHIVs expressing chimeric subtype B and subtype C Vpu, site-directed mutagenesis was performed on the pGEM3zf(+) vector containing the *tat, rev, vpu* and *env* from either SHIV$_{KU\text{-}1bMC33}$ or SHIV$_{SCVpu}$, respectively to introduce an EcoRV site at the interface between the putative transmembrane domain and the cytoplasmic domain. The DNA fragment containing the *vpu* cytoplasmic and *env* regions was isolated by digesting each resulting plasmid with EcoRV and KpnI restriction enzymes. Each fragment was gel purified and ligated into the opposing digested vector. The EcoRV sites were then removed using site-directed mutagenesis and the resulting plasmids were sequenced to ensure validity of the genes and that no other mutations were introduced during the cloning process. Each plasmid was then digested with KpnI and SphI restriction enzymes and the resulting fragments were purified and directly cloned into p3'SHIV$_{KU\text{-}1bMC33}$ to yield p3'SHIV$_{VpuBC}$ and p3'SHIV$_{VpuCB}$. The resulting plasmids were sequenced to ensure that the *tat, rev, vpu* and *env* genes were intact. For the production of p3'SHIV$_{VpuBC}$ and p3'SHIV$_{VpuCB}$ each 3'SHIV plasmid was digested in conjunction with p5'SHIV-4 with SphI overnight, purified, ligated and used to transfect C8166 cells as previously described (Hout et al., 2006b; Hout et al., 2005; McCormick-Davis et al., 2000a; McCormick-Davis et al., 2000b; Singh et al., 2003; Stephens et al., 2002). Stocks were prepared, titrated in C8166 and TZM-bl cells and stored at -80C until used. The 293 cell line was maintained DMEM supplemented with 10% fetal bovine serum, gentamicin (5 ug per mL) and penicillin/streptomycin (100 U per mL and 100 μg per mL, respectively). The TZM-bl cell line

was obtained through the NIH AIDS Research and Reference Reagent Program, Division of AIDS, NIAID, NIH: TZM-bl from Dr. John C. Kappes, Dr. Xiaoyun Wu and Tranzyme Inc. The HeLa $CD4^+$ cell line was obtained through the AIDS Research and Reference Reagent Program, Division of AIDS, NIAID, NIH: HeLa CD4 Clone 1022 from Dr. Bruce Chesebro. TZM-bl cells were maintained in Dulbecco's minimal essential medium supplemented with 10% fetal bovine serum, gentamicin (5 µg per mL), and penicillin/streptomycin (100 U per mL and 100 µg per mL, respectively). HeLa $CD4^+$ cells were maintained in Dulbecco's minimal essential medium supplemented with 10% fetal bovine serum, gentamicin (5 µg per mL), penicillin/streptomycin (100 U per mL and 100 µg per mL, respectively) and G-418 (1 mg per mL). C8166 cells were maintained in RPMI-1640, supplemented with 10mM Hepes buffer pH 7.3, 2mM glutamine, gentamicin (5 µg per mL) and 10% fetal bovine serum (R10FBS). Uninfected pig-tailed PBMC were isolated as described above and activated in RPMI-1640 supplemented with 10% FBS, penicillin/streptomycin (100 U per mL and 100 µg per mL, respectively), gentamicin (5 µg per mL), Concavalin A (1 mg per mL), and human recombinant IL-2 (100 U per mL). Activated PBMC cultures were maintained in RPMI-1640 supplemented with 10% FBS, penicillin/streptomycin (100 U per mL and 100 µg per mL, respectively), gentamicin (5 µg per mL), and human recombinant IL-2 (100 U per mL).

Laser Scanning Confocal Microscopy Analysis

293 cells were cultured on cover slips one day prior to being transiently transfected with plasmids expressing either Vpu_{BC}EGFP or Vpu_{CB}EGFP using PEI (Sigma). Following transfection, cultures were maintained for 36-48 hours before being washed three times in PBS, and fixed in 2% paraformaldehyde/PBS. Cover slips were mounted in glycerol containing

mounting media (Slowfade Antifade solution A). A Nikon A1 confocal microscope was used to collect 100X images with a 2X digital zoom, using EZ-C1 software. The pinhole was set to large (100 nm) for all wavelengths. EGFP was excited using an argon 488 nm laser and viewed through the FITC filter (525/25 nm).

Pulse-Chase Analysis of Chimeric Vpu Proteins

293 cells were transfected with vectors expressing either the Vpu_{BC}EGFP or Vpu_{CB}EGFP protein. At 48 hours post-transfection, the medium was removed and cells were incubated in methionine/cysteine-free medium for 2 hours. The cells were then radiolabeled with 200 µCi of ^{35}S-Translabel (methionine and cysteine, MP Biomedical) for 1 hour. The radiolabel was chased in DMEM containing 100X unlabeled methionine/cysteine medium for 0 and 6 hours. Vpu proteins were immunoprecipitated using a rabbit anti-EGFP serum and collected on protein A-Sepharose beads on a rotator for 18 hours. Non-transfected 293 cells, starved, radiolabeled and chased for 0 hours served as a negative control. Beads were washed three times with 1X radioimmunoprecipitation buffer (RIPA: (50mM TrisHCl, pH 7.5; 50mM NaCl; 0.5% deoxycholate; 0.2% SDS; 10mM EDTA), and the samples resuspended in sample reducing buffer. Samples were boiled and the VpuEGFP fusion proteins separated by SDS-PAGE (12% gel). Proteins were then visualized using standard autoradiographic techniques. All conditions were run in duplicate, the pixel densities of each band determined using ImageJ software, normalized to the hour 0 sample, and the average percent protein remaining calculated.

CD4 Surface Expression Analysis

For analysis of cell surface CD4 expression in the presence of each chimeric VpuEGFP protein, HeLa $CD4^+$ cells (2.5×10^5) were seeded into each well of a six well plate 24 hours prior to transfection. Cells were transfected with plasmids expressing EGFP, VpuEGFP, Vpu_{SC}EGFP, Vpu_{BC}EGFP, or Vpu_{CB}EGFP. Cultures were monitored for 48 hours, cells removed from the six well plate using Ca^{2+}/Mg^{2+}-free PBS containing 1mM EDTA and stained with PE-Cy5 conjugated anti-CD4 (BD Bioscience). Cells were analyzed using an LSR II flow cytometer, determining mean fluorescence intensity (MFI) of PE-Cy5 for transfected (EGFP positive) and untransfected (EGFP negative) cells within the same well. An MFI ratio was calculated for each sample with the EGFP control normalized to 1.0. Normalized ratios from three separate experiments were averaged and the standard deviation calculated. Significance of CD4 surface down-regulation by each chimeric Vpu/EGFP was determined by comparing each sample to the EGFP only control as well as to the subtype B VpuEGFP sample, using a Student's *t*-test, with $p<0.05$ considered significant.

Pulse-Chase Analysis of Viral Proteins

To analyze the viral proteins synthesized and released from cells, C8166 cells were inoculated with 10^4 $TCID_{50}$ of either $SHIV_{VpuBC}$ or $SHIV_{VpuCB}$. At 5 days post-inoculation, the medium was removed and infected cells were incubated in methionine/cysteine-free Dulbecco's modified Eagle's medium (DMEM) for 2 hours. The cells were then radiolabeled for 1 hour with 500 µCi of ^{35}S-Translabel (MP Biomedicals). Cells were lysed in 1X RIPA buffer and the nuclei removed through centrifugation. SHIV proteins were immunoprecipitated from the cell lysates

using plasma pooled from several pig-tailed macaques infected previously with a non-pathogenic SHIV and protein A-Sepharose beads on a rotator for 18 hours. Immunoprecipitates were washed three times in 1X RIPA buffer and the samples resuspended in sample reducing buffer. Samples were boiled and the SHIV specific proteins analyzed by SDS-PAGE. Proteins were then visualized by standard autoradiographic techniques.

Viral Replication Kinetics Analysis

Standard p27 assays (Zeotometrix Incorporated, SIV core antigen kit) were used to assess release of viral particles from cells infected with $SHIV_{KU\text{-}1bMC33}$, $SHIV_{SCVpu}$, $SHIV_{VpuBC}$ or $SHIV_{VpuCB}$. Cultures of 10^6 C8166 cells or pig-tailed PBMC were inoculated with 10^4 $TCID_{50}$ of each virus stock for 4 hours. At the end of 4 hours, the cells were centrifuged at 400x g for 10 minutes and the pellet washed with 10 ml of medium. This was repeated two additional times. The cells were resuspended in propagation medium as described above and this was considered the 0 time point of the assay. Cultures were incubated at 37C and aliquots of the culture were removed at 0, 1, 3, 5, 7, 9, 11 and 13 days with fresh media added to cultures at days 3, 6, 9, and 12. The culture medium was separated from the cells by centrifugation and assayed for p27 according to the manufacturer's instructions.

Macaques and Virus Inoculation

Pig-tailed macaques were obtained from the Caribbean Primate Center in Puerto Rico. All macaques were housed in the AAALAC-approved animal facility at the University of Kansas Medical Center. Six pig-tailed macaques (Set 1: W005, W018 and W030) (Set 2: W004, W007

and W013) were inoculated intravenously with 10^4 $TCID_{50}$ of either $SHIV_{VpuBC}$ or $SHIV_{VpuCB}$, respectively. EDTA-treated blood was collected weekly for 6 weeks, then at 3-week intervals for the next 6 weeks, and thereafter at monthly intervals.

Processing of Blood Samples

PBMC were prepared by centrifugation on Ficoll-Hypaque gradients as described previously (Joag et al., 1996; Joag et al., 1994). Ten-fold dilutions of PBMC (10^6 cells per ml) were inoculated into replicate cultures and were examined for development of cytopathic effects as previously described (McCormick-Davis et al., 2000a; Stephens et al., 2002). Alterations in circulating levels of $CD4^+$ T-lymphocytes after experimental inoculations were monitored sequentially by flow cytometric analysis. T-lymphocyte subsets were labeled with OKT4 (CD4; Ortho Diagnostics Systems, Inc), SP34 (CD3; Pharmingen) or FN18 (CD3; Biosource International) monoclonal antibodies.

Plasma Virus Loads

Plasma viral RNA loads were determined on RNA extracted from EDTA-treated plasma. Virus was pelleted and RNA extracted using the Qiagen viral RNA kit (Qiagen). RNA samples were analyzed by real-time RT-PCR using *gag* specific primers and a 5'FAM and 3'TAMRA labeled probe (Sigma) that was homologous to the SIV *gag* gene. Standard curves were prepared using a series of six 10-fold dilutions of viral RNA of known concentration. The sensitivity of the assay was 100 RNA equivalents per milliliter. Samples were analyzed in triplicate and the number of RNA equivalents was calculated per ml of plasma.

XIII. Conclusions

Human immunodeficiency virus type 1 (HIV-1) is one of the most devastating public health concerns facing the world today. While the development of highly active anti-retroviral therapies (HAART) has led to a global stabilization of the HIV/AIDS epidemic, the continued emergence of mutated strains and recombinant viruses emphasizes the need for new anti-viral therapeutics and vaccine development. In addition, the responsiveness of HIV-1 to current anti-retroviral drugs and the selection of drug resistant mutant strains has been shown to vary among subtypes (Champenois et al., 2008; Desai et al., 2007; Palmer et al., 1998; Poonpiriya et al., 2008; Snoeck et al., 2006). The first round of anti-retroviral therapy is the most important and therefore the predication of the potential for drug resistance as well as the general virological and immunological responses of patients with similar strains is essential for administering the optimum treatment (Martinez-Cajas et al., 2008). Epidemiological and genotypic studies are necessary for detecting/identifying mutations and trends involved in drug resistance/responsiveness of particular HIV-1 subtypes/strains found within different populations (Martinez-Cajas et al., 2008; Martinez-Cajas and Wainberg, 2008). Furthermore, characterization of different HIV-1 strains and their respective viral proteins is necessary in order to understand and develop the most favorable therapeutic regimens. Therefore, the main objective of this dissertation was to identify unique and conserved domains/motifs, crucial for structural and/or functional characteristics of different Vpu proteins that could potentially serve as novel targets for anti-retroviral therapy.

The main function of Vpu is to augment viral replication by down-modulating CD4 surface expression and enhancing virion release (Bour and Strebel, 2003; Fujita et al., 1997; Hout et al., 2004; Klimkait et al., 1990; Ruiz et al., 2010a; Schubert et al., 1998; Strebel et al.,

1989; Terwilliger et al., 1989; Willey et al., 1992a, b). The preservation of both functions was not found in Vpu proteins from any group O or group N isolates examined (Sauter et al., 2009). Therefore, the maintenance of both functions in group M Vpu proteins contributes to the ability of these viruses to establish and sustain the current global pandemic. While the mechanism by which HIV-1 Vpu down-modulates CD4 surface expression has been studied extensively, the mechanism(s) that the Vpu uses to enhance virion release is still ill-defined. Studies examining the mechanism(s) by which HIV-1 Vpu enhances virion release have identified three potential modes of action: 1) antagonism of BST-2; 2) modification of membrane permeability with ion-channel-like properties; or 3) inhibition of the cellular K^+ channel, TASK-1, resulting in depolarization of the plasma membrane (Bour and Strebel, 2003; Coady et al., 1998; Ewart et al., 1996; Hsu et al., 2010; Hsu et al., 2004; Neil et al., 2008; Schubert et al., 1996b; Strebel, 2004; Van Damme et al., 2008). While all three mechanisms have been demonstrated *in vitro*, the physiological relevance of each remains controversial. The majority of the studies analyzing these potential mechanisms have been conducted in cell lines not normally targeted by HIV-1 Vpu. While TASK-1 has been shown to be constitutively expressed in $CD3^+$ T lymphocytes, the levels of expression in $CD4^+$ T cells as well as macrophages remains unknown (Meuth et al., 2008). Additionally, BST-2 has only been shown to have high expression levels in macrophages (Miyagi et al., 2009; Schindler et al., 2010). Taken together, these results suggest that HIV-1 Vpu may use different mechanisms to enhance virion release in different cell types. The results presented herein, address the physiological relevance of HIV-1 Vpu-mediated BST-2 antagonism using both *in vitro* and *in vivo* models.

Our laboratory has used the SHIV/macaque model of disease extensively in order to provide insight into the physiological relevance of *in vitro* analyses of the HIV-1 Vpu protein. In

light of the discovery of BST-2 as a restriction factor targeted by the HIV-1 Vpu and SIV Nef proteins, we sought to determine the potential of SHIV viruses as a model for studying these interactions and identify domains/amino acids essential to hBST-2 susceptibility to HIV-1 Vpu. Our results demonstrate similar susceptibilities of the hBST-2 and the ptBST-2 proteins to SHIV Vpu and Nef, respectively, similar to what has been reported for HIV-1 and SIV. This emphasizes the suitability and value of SHIV viruses as models for studying the effects of HIV-1 Vpu in pathogenesis. These results also allow us to broaden our interpretation of previous *in vivo* analyses since rhesus and pig-tailed macaques do not express a BST-2 that is susceptible to HIV-1 Vpu. Instead, macaque BST-2 antagonism is likely overcome by Nef. These results do not, however, rule out a role for this interaction in a human HIV-1 infection and the analysis of the interaction between HIV-1 Vpu and hBST-2 is still warranted and provides a useful tool for identifying regions of the Vpu protein that represent potential targets for anti-retroviral therapy.

Mutagenesis-based analysis of the human and ptBST-2 proteins identified the transmembrane domain (TMD) and a small motif (^{13}DDIWK^{17}) in the N'terminal region as determinants of HIV-1 Vpu and SIV Nef susceptibility, respectively. Results of this study also suggested that the length and/or topology of the BST-2 TMD are more important than the amino acid identity in determining sensitivity and anti-viral activity similar to results observed by other investigators (Perez-Caballero et al., 2009). Together, these results provide a basis for the development of new Vpu targeted small molecule inhibitors designed to mimic the structural elements of the BST-2 protein.

To date, only a few studies have been conducted on the genomic contributions of different Vpu proteins on structure and function and even fewer have examined the impact different Vpu subtypes have on pathogenesis (Abraha et al., 2009; Arien et al., 2005; Ball et al.,

2003; Hill et al., 2008; Joag et al., 1996; McCormick-Davis et al., 1998; Sauter et al., 2009). We initiated our analyses by examining several biological properties associated with seven different HIV-1 Group M Vpu proteins. Using an EGFP fusion reporter system we determined that subtypes A, A2 and C Vpu proteins were more efficiently transported to the cell surface than other Vpu proteins. We did not establish a correlation of this transport with either the ability of each protein to down-modulate CD4 from the surface or their ability to overcome hBST-2-mediated restriction of particle release in HeLa cells. However, it remains to be determined whether the distinct localization of these proteins is physiologically relevant. It is possible that the sorting signals within these proteins are distinct from those of the other Vpu proteins. If these proteins lack a specific signal that retains the other Vpu proteins in the ER/Golgi compartments, the presence at the plasma membrane may be a default mechanism. It is also possible that these proteins contain localization signals or interact with distinct cellular proteins that target them to the cell surface as a decoy or default mechanism.

Based on our identification of distinct biological properties among different Vpu proteins that may impact viral pathogenesis and in turn contribute to the disproportionate global distribution of HIV-1 subtypes, we continued our analysis by focusing on our subtype B and subtype C Vpu proteins. These isolates displayed distinct localization patterns, slight variations in CD4 down-modulation efficiencies, which was maintained among four separate subtype C Vpu proteins examined, and similar abilities to overcome BST-2 restriction in HeLa cells. The drawback to the majority of studies conducted to date on the role of different subtypes in HIV pathogenesis and their abilities to overcome cell-type specific restriction factors, is that these studies are generally conducted in cell lines that are not normally infected by HIV-1 and therefore may yield cell-type specific results. Therefore, it is extremely important to verify these

results using either physiologically relevant cell types, *ex vivo* tissues, and/or appropriate animal models. Hence, we continued our analyses of the subtype B and subtype C Vpu proteins by observing the affects of these proteins on SHIV replication and pathogenesis in a macaque model. A SHIV expressing the subtype C Vpu protein ($SHIV_{SCVpu}$) replicated with delayed kinetics compared to a SHIV expressing the subtype B Vpu ($SHIV_{KU\text{-}1bMC33}$) and was not due to differential viral protein turnover or packaging within virions. Similar results have been reported for studies analyzing the replication fitness of subtype B and subtype C HIV-1 isolates in human PBMC. Subtype C HIV-1 isolates were found to be less replicatively fit than all other subtypes in PBMC, but equally efficient in Langerhans cells and *ex vivo* tissues (Abraha et al., 2009; Arien et al., 2005; Ball et al., 2003). Inoculation of $SHIV_{SCVpu}$ into pig-tailed macaques resulted in a more gradual rate of $CD4^+$ T cell lymphocytes and lower peak viral loads than observed in macaques inoculated with $SHIV_{KU\text{-}1bMC33}$. These results validate our hypothesis that the biological differences observed and/or specific differences yet undetermined between these Vpu proteins contribute to the modification of pathogenesis. As these studies utilized an intravenous route of inoculation, it remains unknown whether similar results would be observed with alternate inoculation routes where transmission is more dependent on the infection and replication of the virus within macrophages. Additional studies are needed to determine whether or not different subtypes have evolved distinct mechanisms designed to promote infection via specific transmission routes and whether Vpu is a determinant of this. Several epidemiological studies have provided evidence in favor of this phenomenon, however, similar to other epidemiological studies, the minimal number of subjects analyzed invokes uncertainty in the validity of the trends observed (Avila et al., 2002; Buonaguro et al., 2007a; Buonaguro et al.,

2007b; Buonaguro et al., 2004; Buonaguro et al., 2007c; Gao et al., 1996; van Harmelen et al., 1997).

The spread of progeny virions is clearly augmented by the HIV-1 Vpu protein and therefore this protein is undoubtedly a candidate for anti-retroviral therapy. Optimum design of anti-retroviral drugs requires a comprehensive understanding of the structural and functional features of the target protein and the specific elements that govern them. Consequently, we focused our studies on identifying specific genomic constituents of the subtype B and subtype C Vpu proteins that influence their structural and functional properties. Our initial examination concentrated on the transmembrane domain and the impact of combinatorial substitutions on membrane association and Vpu function. Since the Vpu protein is membrane bound and interacts with known lipid raft proteins (i.e. CD4 and BST-2), we hypothesized that Vpu also associated with lipid rafts. Using detergent resistant membrane (DRM) fractionation techniques, we determined that Vpu partially partitions into membrane rafts in a cholesterol dependent manner. We also observed co-localization of Vpu_{SC}EGFP1 with a known GPI-anchor protein in membrane rafts using co-patched live cell imaging, thus providing additional visual confirmation of Vpu association with lipid rafts. However, as these assays do not discriminate among different lipid compositions or distinct organelle membranes, the location where Vpu interacts with these membrane microdomains and the type of raft(s) Vpu favors remains unknown. Recent computer modeling studies suggest that Vpu does not exhibit a preference for lipid thickness or composition implying that Vpu may be able to adapt to different lipid environments and therefore may reside within multiple types of rafts (Kruger and Fischer, 2008).

The association of Vpu with lipid rafts has potential involvement in almost every aspect of Vpu function as the majority of proteins Vpu has been shown to associate with lipid rafts. In

order to establish a basis for this association, we examined the role of the transmembrane domain and the affects of combinatorial substitutions within this region on Vpu partitioning into DRM fractions. The Vpu/EGFP fusion protein with a scrambled TMD (Vpu_{TM}EGFP) did not partition into the DRM fractions, suggesting a role for the transmembrane domain or perhaps the membrane proximal region of the protein (as the potential for structural alterations is greatest within this region) in lipid raft association. Alanine scanning mutagenesis of the transmembrane domain revealed two mutants, IVV19-21AAA and W22A (or W23A), capable of abolishing Vpu association with lipid rafts. Based on recent findings that the region between I17 and S23 in the Vpu proteins encompasses the kink region of the TMD that adjusts to the membrane composition, these mutants most likely alter the ability of the protein to adapt to the changing lipid environment and thus exclude it from these microdomains (Kruger and Fischer, 2008). This hypothesis was supported by the finding that the Vpu fusion mutant, W23L, retained the ability to partition into DRM fractions and exhibited intracellular localization and CD4 down-modulation similar to the unmodified Vpu.

Our analysis of the TMD alanine substitution Vpu mutants also allowed us to show a correlation between membrane raft association and Vpu function. Flow cytometric analysis of CD4 surface expression in the presence and absence of each of these mutants revealed no direct correlation with the ability of Vpu to partition into lipid rafts and the ability to down-modulate CD4 from the cell surface. Both mutants deficient in lipid raft association retained the ability to down-modulate CD4 from the cell surface, even though W22A was slightly less efficient than the unmodified Vpu protein (similar to VphuC). Results from p27 and infectious unit release assays did suggest a direct correlation between the ability of Vpu to partition to DRM fractions and the enhancement of SHIV virion release. Both the IVV19-21AAA and W22A mutants were

significantly reduced in the ability to enhance virion release compared to both the $SHIV_{KU-2MC4}$ empty vector control and the cells co-transfected with $SHIV_{\Delta Vpu}$ and the unmodified Vphu protein. The Vpu TMD mutant, LVV11-13AAA, was also reduced in its capacity to enhance virion release. As this mutant retained the ability to partition into DRM fractions as well as down-modulate CD4 from the cell surface, it may represent a region of the TMD that has the ability to alter the orientation/flexibility of the membrane such that it is reduced in its ability to interact with proteins necessary for the enhancement of virion release (such as BST-2 or perhaps oligomerization with other Vpu proteins).

While these studies have identified the transmembrane domain and several specific areas within this domain as possible targets for anti-retroviral therapy, they do not address the specific mechanisms involved in Vpu-mediated enhanced virion release. In order to fully understand the significance of these results, additional studies are needed to determine: 1) the cellular location in which Vpu associates with lipid rafts; 2) whether the correlation of lipid raft association and enhanced virion release function remains valid in physiologically relevant cells (i.e. macrophages and $CD4^+$ T cells; and 3) what protein-protein interactions, if any, are involved. Even though the association of Vpu with lipid rafts in the ER is possible, incorporation is more likely in the Golgi complex and/or the plasma membrane. It has been reported previously that artificial retention of the Vpu protein in the ER completely eliminates its function in the enhancement of virion release and that this function is only partially dependent on phosphorylation of the two CK-II sites in the cytoplasmic domain (Schubert and Strebel, 1994). Also, previous studies have provided evidence in favor of BST-2 lipid raft association occurring in the Golgi complex (Kupzig et al., 2003). More recently, data has been presented that suggests the presence of Vpu in the *trans* Golgi is important for Vpu antagonism of BST-2 (Dube et al.,

2009). In conjunction with our results indicating that CD4 down-modulation is not dependent on lipid raft association, the most likely intracellular compartment for Vpu association with lipid rafts would be the Golgi complex. However, as previously mentioned, Vpu has also been shown to interact with a background K^+ channel, TASK-1. TASK-1 has been shown to localize to the plasma membrane and this is where its interaction with Vpu is thought to occur, although the relevance of this interaction in macrophages and/or $CD4^+$ T cells remains to be determined (Hsu et al., 2010; Hsu et al., 2004; Strebel, 2004). In addition, if this is the major mechanism by which HIV-1 Vpu enhances virion release, Vpu subtypes that predominately localize to the plasma membrane would be expected to have increased enhanced virion release, which our results indicate is not the case. Since HIV-1 Vpu function requires a certain level of promiscuity, the interactions with BST-2 and TASK-1 may represent unintentional, cell-type specific interactions that may or may not be physiologically relevant. However, our identification of Vpu as a lipid raft associated protein, distinguishes the transmembrane domain as a target for anti-retroviral therapy that could be utilized against all subtypes, as well as provides an additional means to uncovering the exact mechanisms by which Vpu promotes the spread of HIV-1 progeny virions. Based on the data available several potential mechanisms and sites for interaction of Vpu with cellular restriction factors are illustrated in Figure 62.

The majority of HIV-1 studies have focused on the subtype B HIV-1 because it is the most prevalent genotype in the United States and Western Europe (Hemelaar et al., 2006; Oliveira et al., 2000). However, the subtype C HIV-1 genotype currently accounts for approximately 50% of infections worldwide (Bjorndal et al., 1999; Essex, 1999). It is unclear why this particular subtype of viruses has spread so rapidly among the human population. It has been hypothesized that subtype C HIV-1 may be evolving to a less pathogenic form based on

Figure 62. Possible mechanisms by which Vpu enhances virion release from cells. (1) Vpu allows efficient transport of Env proteins to the site of virion assembly. Vpu is synthesized on the rough endoplasmic reticulum and binds CD4 releasing gp160 for processing and cleavage into gp120/gp41 which may be transported to the site of assembly. Vpu may function as a viroporin. (2) Vpu resides within the rough endoplasmic reticulum, *trans*-Golgi network and at the cell surface. It is unknown whether the ability of Vpu to serve as an ion channel functions to enhance virion release at any of these intracellular locations. Vpu may oligomerize with TASK-1 at the cell surface forming non-functional ion channels which could result in the depolarization of the membrane and enhanced membrane scission and separation of budding virions from the plasma membrane. (3) Vpu removes BST-2 from the site of virion assembly. In the absence of Vpu, BST-2 is expressed at the cell surface. Both proteins are known to associate with lipid rafts. It is possible that Vpu is targeted to lipid rafts that BST-2 normally resides within and causes an alteration in its targeting, potentially via an endo-lysosomal, lysosomal or proteasomal degradation pathway. Vpu may also interact with BST-2 and target it to different lipid rafts in order to alter the intracellular localization and/or turnover of BST-2 such that it cannot restrict virion release at the cell surface.

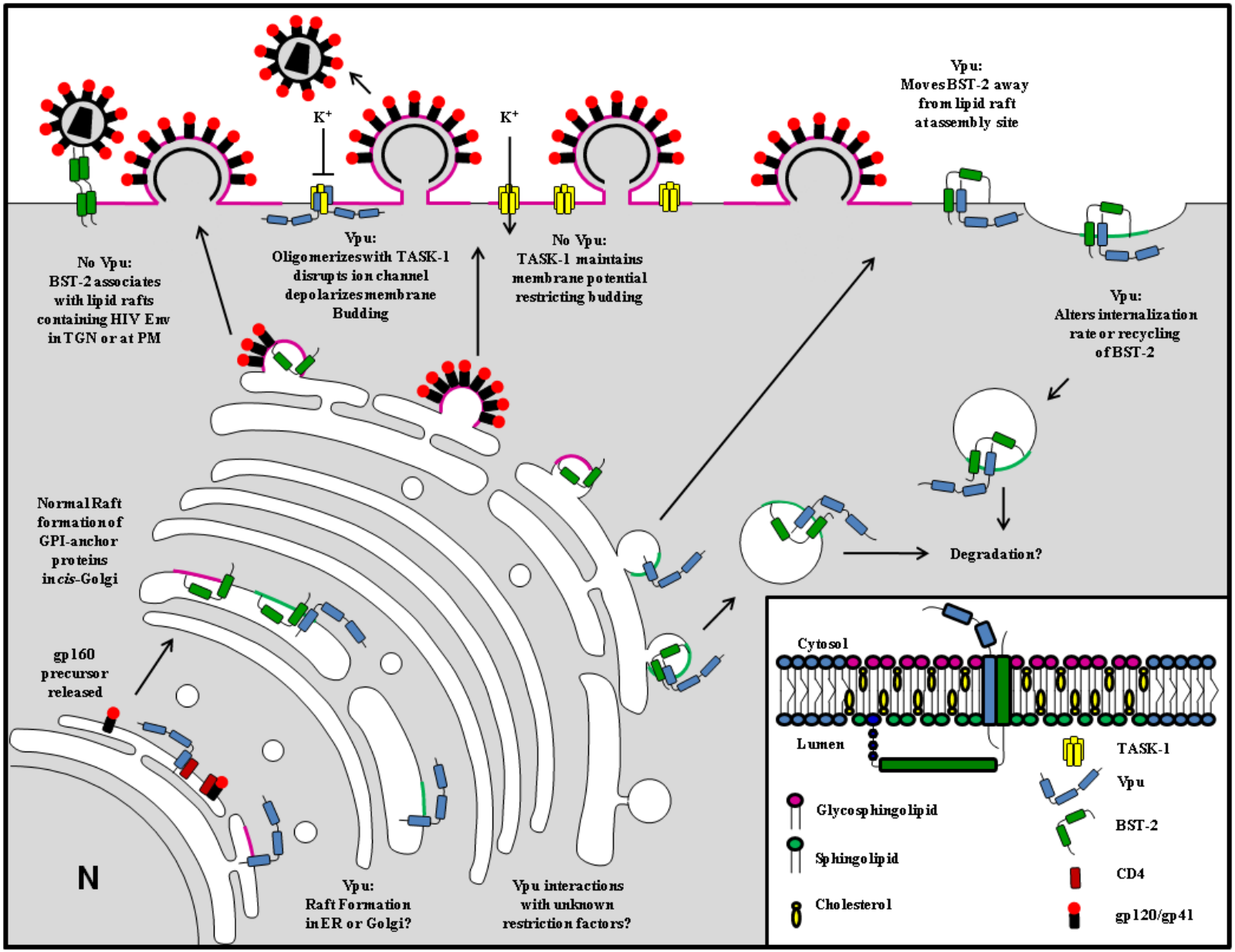
K+
K+
Vpu:
Moves BST-2 away
from lipid raft
at assembly site
No Vpu:
BST-2 associates
with lipid rafts
containing HIV Env
in TGN or at PM
Vpu:
Oligomerizes with TASK-1
disrupts ion channel
depolarizes membrane
Budding
No Vpu:
TASK-1 maintains
membrane potential
restricting budding
Vpu:
Alters internalization
rate or recycling
of BST-2
Degradation?
Normal Raft
formation of
GPI-anchor
proteins
in cis-Golgi
gp160
precursor
released
N
Vpu:
Raft Formation
in ER or Golgi?
Vpu interactions
with unknown
restriction factors?
Cytosol
Lumen
TASK-1
Vpu
BST-2
CD4
gp120/gp41
Glycosphingolipid
Sphingolipid
Cholesterol

data indicating that subtype C viruses are less fit in PBMC competition assays than all other group M isolates (Abraha et al., 2009; Arien et al., 2005; Ball et al., 2003). Analysis of 338 HIV-1 Vpu sequences from different subtypes revealed several unique as well as conserved features within the cytoplasmic domain that may contribute to the effects these Vpu have on viral pathogenesis. The first feature we observed was a YxxΦ sequence proximal to the membrane present in 98% of the sequences we analyzed. Among the subtype C Vpu proteins we analyzed, more than 80% contained a membrane proximal dileucine motif ([D/E]xxxL[L/I]) overlapping the tyrosine motif (EYRKLL). While the dileucine motif was present in several other isolates, it was not as highly conserved in the other subtypes of HIV-1. Both of these motifs include an upstream acidic residue, a property implicated in internalization and endosomal/lysosomal targeting (Bonifacino and Traub, 2003). Based on our analysis we hypothesized that the tyrosine motif and/or dileucine motif within subtype C Vpu dictated the differential trafficking of the protein and in turn resulted in a reduction in the proteins ability to enhance virion release in $CD4^+$ T cells. Mutational analysis of the tyrosine residue at position 35 and the leucine residue at 39 demonstrated that neither residue/motif affected CD4 surface down-regulation. A significant reduction in the efficiency of Vpu_{SC} to down-regulate CD4 was only observed with mutation of both the tyrosine and leucine residues. This reduction was most likely due to slight structural alterations to either the TMD or the first cytoplasmic α-helix. Substitution of the tyrosine residue at position 35 with an alanine increased the expression of the Vpu_{SC} at the cellular surface, while substitution of the leucine residue at position 39 with a glycine significantly reduced the trafficking of the Vpu_{SC} to the plasma membrane. In contrast, substitution of the tyrosine residue at position 30 in the subtype B Vpu protein did not alter protein localization (data not shown). Previously our laboratory reported that the signal for

retention of the subtype B Vpu protein in the ER/Golgi complex compartments was localized to the C-terminal region of the protein as deletion of the last 23 residues within a subtype B Vpu protein (VpuΔ23EGFP) resulted in a protein that was efficiently transported to the surface (Pacyniak et al., 2005). Originally, we hypothesized that the signal for this retention was a dileucine motif that contained the invariant leucine residue at position 63. However, laser scanning confocal microscopic analysis of a Vpu protein that contained an alanine at position 63 displayed similar intracellular localization as an unmodified VpuEGFP fusion protein (Hill et al., 2010). While the specific signals within each of these proteins and the mechanisms by which they dictate intracellular localization remains unknown, these results suggest that both proteins evolved to display specific localization patterns. The potential importance of this observation is supported by the idea that subtype A HIV-1 represents the second major group of HIV-1 infections worldwide and the subtype A Vpu protein we analyzed was also efficiently trafficked to the plasma membrane. Additionally, a SHIV expressing a mutant Vpu_{SC} protein that was retained within intracellular compartments (Vpu_{SCL39G}) replicated with increased kinetics compared to the parental $SHIV_{SCVpu}$. While the evidence for this hypothesis is speculative at this point, the necessity for further analysis of other Vpu isolates that are efficiently trafficked to the cellular plasma membrane and the trends observed with viruses that express them is evident.

We continued our analysis of the role of the overlapping tyrosine and dileucine motifs present within the Vpu_{SC} cytoplasmic domain by constructing SHIV that expressed each of the mutant Vpu proteins. Our findings demonstrated a clear role for the tyrosine residue in the enhanced virion release function of Vpu_{SC}, while the leucine residue appeared to have an inhibitory role in this function. We also analyzed the replication kinetics of a SHIV expressing the Vpu_{Y30A} protein and found that this virus also replicated with greatly reduced kinetics

compared to the $SHIV_{KU\text{-}1bMC33}$ parental virus (data not shown). Based on the proximity of the tyrosine motif to the membrane and the existence of the acidic residue at the Y+1 position, we hypothesize that this motif is involved in lysosomal targeting. Since the tyrosine motif is highly conserved among all HIV-1 Vpu subtypes and because the substitution of this residue did not alter the rate of Vpu protein turnover, it is possible this motif is involved in the targeting of cellular restriction factors for degradation via the lysosome. While it is possible this targeted destruction applies to the BST-2 protein, the observation that in HeLa cells the subtype B and subtype C Vpu were equally efficient at rescuing virion release, suggests that this is not the mechanism utilized by these two proteins in $CD4^+$ T cells (C8166 cells) or that it is not the sole means by which Vpu can enhance virion release. The mechanisms by which Vpu antagonizes BST-2 is still controversial and differential results among separate studies suggests that the mechanism may be cell-type specific (Douglas et al., 2009; Goffinet et al., 2009; Gupta et al., 2009b; Iwabu et al., 2009; Mitchell et al., 2009). If the tyrosine motif is involved in this interaction, analysis of the ability of the tyrosine mutants to bind and inhibit BST-2 mediated virion restriction may aid in the elucidation of the mechanism(s) used in cells normally targeted by HIV-1.

In contrast to SHIV expressing Vpu with disrupted tyrosine motifs, p27 growth curve analysis demonstrated a significant increase in the replication kinetics of $SHIV_{SCVpuL39G}$ as well as the number of particles associated with the cell surface compared to the parental $SHIV_{SCVpu}$ virus. At this juncture, our hypothesis is that the dileucine motif may interfere with other signals present within the cytoplasmic domain such as the tyrosine motif. It is possible that the tyrosine motif is involved in the inhibition of a cellular restriction factor, be it BST-2 or a yet unknown protein, and the dileucine motif may interfere with the necessary protein-protein interactions. By

removing the dileucine motif and possibly the competing interactions, the tyrosine motif is able to function similar to that of the subtype B Vpu protein. The explication of any protein-protein interactions mediated by these motifs is necessary to fully understand their role in dictating Vpu function and providing the necessary information for developing optimal therapeutics.

While the results are not presented within this thesis, three pig-tailed macaques were inoculated with $SHIV_{SCVpuL39G}$ and all three selected for a Vpu protein truncated at position 28 less than 2 weeks post-inoculation. The virus replicated within these macaques however, the viral loads were relatively low and they did not exhibit a loss in circulating $CD4^+$ T cell levels. These macaques were euthanized in a healthy condition approximately 28 weeks post-inoculation. While we were unable to determine the specific role of the dileucine motif in SHIV pathogenesis, the immediate and perpetual selection of a Vpu protein truncated prior to the cytoplasmic domain suggests that the dileucine motif may play a significant role in Vpu_{SC} function *in vivo* and the removal of this motif is pessimal, if not detrimental to the function of the protein and replication of the virus. It is possible that all functional Vpu proteins utilize a dileucine motif-based trafficking signal within the cytoplasmic domain to counteract BST-2 and/or other unknown cellular restriction factors. Recent data has suggested a role for the ExxxLV-based motif in the second α-helix of the subtype B Vpu in antagonizing BST-2 providing support for the forementioned hypothesis (Kueck et al., 2010). The positioning of this dileucine motif within the cytoplasmic domain and its proximity to the transmembrane domain may be an evolutionary adaptation of different subtypes to either promote or subdue Vpu function in specific cell types.

Although our studies have identified specific regions within the transmembrane and cytoplasmic domains of the subtype B and subtype C Vpu proteins, the level of impact that these

regions would have on Vpu enhancement of disease progression remained unknown. Therefore, we analyzed the specific contributions of the transmembrane domain versus the cytoplasmic domain of both the subtype B and subtype C Vpu proteins by creating chimeric Vpu proteins. These chimeric proteins verified the role of the cytoplasmic domain in determining protein localization and molecular weight. Both proteins down-modulated CD4 surface expression similar to the Vpu_{SC}EGFP1 fusion protein suggesting that both domains either directly influence the ability of Vpu to down-modulate CD4 or the membrane interface region of each protein is designed to allow for differential modification of this function. However, while the ability of HIV-1 Vpu to down-modulate CD4 from the cell surface appears to be crucial to enhanced pathogenesis, the slight variability in efficiencies among the Vpu proteins analyzed in this study and thus different Group M proteins, does not appear to be a major determinant of the rate of $CD4^+$ T cell loss in infected macaques. Instead, the transmembrane domain was identified as the major influence on differential modification of $CD4^+$ T cell loss in macaques inoculated with SHIV expressing either a subtype B or subtype C Vpu protein. Macaques inoculated with either the $SHIV_{SCVpu}$ parental virus or the $SHIV_{VpuCB}$ virus containing the subtype C Vpu TMD displayed a more gradual loss in circulating $CD4^+$ T cells than macaques inoculated with either the $SHIV_{KU\text{-}1bMC33}$ parental virus or $SHIV_{VpuBC}$. Considering the impact individual mutations can have on the structural and functional properties of any given Vpu protein, it is tempting to suggest that different subtypes have evolved an intricate balance between the signals contained within their transmembrane and cytoplasmic domains such that Vpu function in viral pathogenesis is optimized for the intended targets.

Even though these studies focused on the subtype B and subtype C Vpu proteins, our analyses demonstrate a clear potential for differential signaling and functional efficiency among

all HIV-1 Vpu subtypes with the ability to modify pathogenesis. Additionally, our analyses provided evidence for Vpu association with lipid rafts and its correlation with enhancement of virion release, identifying a potentially significant biological property associated with Vpu augmentation of HIV-1 pathogenesis. We have also provided evidence suggesting a minimal role for BST-2 antagonism in Vpu enhancement of pathogenesis associated via the intravenous route of inoculation, suggesting that additional undefined mechanisms may be involved in Vpu mediated enhanced virion release. Finally, we have identified the transmembrane domain and membrane proximal regions as crucial components to Vpu-mediated modification of pathogenesis and establish these areas as focal points for anti-retroviral therapeutic development. Further analysis of individual Vpu proteins is necessary to identify other signaling motifs and/or areas critical in governing the structural and functional properties of different Vpu subtypes and distinct isolates. Identification of these targeted domains and the mechanisms associated with their regulation of Vpu function will provide the information necessary for the development of novel effective anti-virals against the Vpu protein essential for combating the current HIV/AIDS pandemic.

XIV. References

Abraha, A., Nankya, I.L., Gibson, R., Demers, K., Tebit, D.M., Johnston, E., Katzenstein, D., Siddiqui, A., Herrera, C., Fischetti, L., *et al.* (2009). CCR5- and CXCR4-tropic subtype C human immunodeficiency virus type 1 isolates have a lower level of pathogenic fitness than other dominant group M subtypes: implications for the epidemic. J Virol *83*, 5592-5605.

Accola, M.A., Bukovsky, A.A., Jones, M.S., and Gottlinger, H.G. (1999). A conserved dileucine-containing motif in p6(gag) governs the particle association of Vpx and Vpr of simian immunodeficiency viruses SIV(mac) and SIV(agm). J Virol *73*, 9992-9999.

Aiken, C. (1997). Pseudotyping human immunodeficiency virus type 1 (HIV-1) by the glycoprotein of vesicular stomatitis virus targets HIV-1 entry to an endocytic pathway and suppresses both the requirement for Nef and the sensitivity to cyclosporin A. J Virol *71*, 5871-5877.

Aiken, C., Konner, J., Landau, N.R., Lenburg, M.E., and Trono, D. (1994). Nef induces CD4 endocytosis: requirement for a critical dileucine motif in the membrane-proximal CD4 cytoplasmic domain. Cell *76*, 853-864.

Aiken, C., Krause, L., Chen, Y.L., and Trono, D. (1996). Mutational analysis of HIV-1 Nef: identification of two mutants that are temperature-sensitive for CD4 downregulation. Virology *217*, 293-300.

Aiken, C., and Trono, D. (1995). Nef stimulates human immunodeficiency virus type 1 proviral DNA synthesis. J Virol *69*, 5048-5056.

Alexander, M., Bor, Y.C., Ravichandran, K.S., Hammarskjold, M.L., and Rekosh, D. (2004). Human immunodeficiency virus type 1 Nef associates with lipid rafts to downmodulate cell surface CD4 and class I major histocompatibility complex expression and to increase viral infectivity. J Virol *78*, 1685-1696.

Alfalah, M., Wetzel, G., Fischer, I., Busche, R., Sterchi, E.E., Zimmer, K.P., Sallmann, H.P., and Naim, H.Y. (2005). A novel type of detergent-resistant membranes may contribute to an early protein sorting event in epithelial cells. J Biol Chem *280*, 42636-42643.

Ali, M.S., Hammonds, J., Ding, L., and Spearman, P. (2010). CAML does not modulate tetherin-mediated restriction of HIV-1 particle release. PLoS One *5*, e9005.

Aloia, R.C., Tian, H., and Jensen, F.C. (1993). Lipid composition and fluidity of the human immunodeficiency virus envelope and host cell plasma membranes. Proc Natl Acad Sci U S A *90*, 5181-5185.

Anderson, S.J., Lenburg, M., Landau, N.R., and Garcia, J.V. (1994). The cytoplasmic domain of CD4 is sufficient for its down-regulation from the cell surface by human immunodeficiency virus type 1 Nef. J Virol *68*, 3092-3101.

Andrew, A.J., Miyagi, E., Kao, S., and Strebel, K. (2009). The formation of cysteine-linked dimers of BST-2/tetherin is important for inhibition of HIV-1 virus release but not for sensitivity to Vpu. Retrovirology *6*, 80.

Arens, M., Joseph, T., Nag, S., Miller, J.P., Powderly, W.G., and Ratner, L. (1993). Alterations in spliced and unspliced HIV-1-specific RNA detection in peripheral blood mononuclear cells of individuals with varying CD4-positive lymphocyte counts. AIDS Res Hum Retroviruses *9*, 1257-1263.

Arien, K.K., Abraha, A., Quinones-Mateu, M.E., Kestens, L., Vanham, G., and Arts, E.J. (2005). The replicative fitness of primary human immunodeficiency virus type 1 (HIV-1) group M, HIV-1 group O, and HIV-2 isolates. J Virol *79*, 8979-8990.

Arien, K.K., Vanham, G., and Arts, E.J. (2007). Is HIV-1 evolving to a less virulent form in humans? Nat Rev Microbiol *5*, 141-151.

Arora, V.K., Molina, R.P., Foster, J.L., Blakemore, J.L., Chernoff, J., Fredericksen, B.L., and Garcia, J.V. (2000). Lentivirus Nef specifically activates Pak2. J Virol *74*, 11081-11087.

Atkins, K.M., Thomas, L., Youker, R.T., Harriff, M.J., Pissani, F., You, H., and Thomas, G. (2008). HIV-1 Nef binds PACS-2 to assemble a multikinase cascade that triggers major histocompatibility complex class I (MHC-I) down-regulation: analysis using short interfering RNA and knock-out mice. J Biol Chem *283*, 11772-11784.

Avila, M.M., Pando, M.A., Carrion, G., Peralta, L.M., Salomon, H., Carrillo, M.G., Sanchez, J., Maulen, S., Hierholzer, J., Marinello, M., *et al.* (2002). Two HIV-1 epidemics in Argentina: different genetic subtypes associated with different risk groups. J Acquir Immune Defic Syndr *29*, 422-426.

Ayinde, D., Maudet, C., Transy, C., and Margottin-Goguet, F. (2010). Limelight on two HIV/SIV accessory proteins in macrophage infection: is Vpx overshadowing Vpr? Retrovirology *7*, 35.

Bachand, F., Yao, X.J., Hrimech, M., Rougeau, N., and Cohen, E.A. (1999). Incorporation of Vpr into human immunodeficiency virus type 1 requires a direct interaction with the p6 domain of the p55 gag precursor. J Biol Chem *274*, 9083-9091.

Ball, S.C., Abraha, A., Collins, K.R., Marozsan, A.J., Baird, H., Quinones-Mateu, M.E., Penn-Nicholson, A., Murray, M., Richard, N., Lobritz, M., *et al.* (2003). Comparing the ex vivo fitness of CCR5-tropic human immunodeficiency virus type 1 isolates of subtypes B and C. J Virol *77*, 1021-1038.

Barlow, K.L., Ajao, A.O., and Clewley, J.P. (2003). Characterization of a novel simian immunodeficiency virus (SIVmonNG1) genome sequence from a mona monkey (Cercopithecus mona). J Virol *77*, 6879-6888.

Barman, S., and Nayak, D.P. (2000). Analysis of the transmembrane domain of influenza virus neuraminidase, a type II transmembrane glycoprotein, for apical sorting and raft association. J Virol *74*, 6538-6545.

Barre-Sinoussi, F., Chermann, J.C., Rey, F., Nugeyre, M.T., Chamaret, S., Gruest, J., Dauguet, C., Axler-Blin, C., Vezinet-Brun, F., Rouzioux, C., *et al.* (1983). Isolation of a T-lymphotropic retrovirus from a patient at risk for acquired immune deficiency syndrome (AIDS). Science *220*, 868-871.

Bartee, E., McCormack, A., and Fruh, K. (2006). Quantitative membrane proteomics reveals new cellular targets of viral immune modulators. PLoS Pathog *2*, e107.

Bavari, S., Bosio, C.M., Wiegand, E., Ruthel, G., Will, A.B., Geisbert, T.W., Hevey, M., Schmaljohn, C., Schmaljohn, A., and Aman, M.J. (2002). Lipid raft microdomains: a gateway for compartmentalized trafficking of Ebola and Marburg viruses. J Exp Med *195*, 593-602.

Belzile, J.P., Duisit, G., Rougeau, N., Mercier, J., Finzi, A., and Cohen, E.A. (2007). HIV-1 Vpr-mediated G2 arrest involves the DDB1-CUL4AVPRBP E3 ubiquitin ligase. PLoS Pathog *3*, e85.

Bender, F.C., Whitbeck, J.C., Ponce de Leon, M., Lou, H., Eisenberg, R.J., and Cohen, G.H. (2003). Specific association of glycoprotein B with lipid rafts during herpes simplex virus entry. J Virol *77*, 9542-9552.

Bergamaschi, A., Ayinde, D., David, A., Le Rouzic, E., Morel, M., Collin, G., Descamps, D., Damond, F., Brun-Vezinet, F., Nisole, S., *et al.* (2009). The human immunodeficiency virus type 2 Vpx protein usurps the CUL4A-DDB1 DCAF1 ubiquitin ligase to overcome a postentry block in macrophage infection. J Virol *83*, 4854-4860.

Berger, E.A., Murphy, P.M., and Farber, J.M. (1999). Chemokine receptors as HIV-1 coreceptors: roles in viral entry, tropism, and disease. Annu Rev Immunol *17*, 657-700.

Besnard-Guerin, C., Belaidouni, N., Lassot, I., Segeral, E., Jobart, A., Marchal, C., and Benarous, R. (2004). HIV-1 Vpu sequesters beta-transducin repeat-containing protein (betaTrCP) in the cytoplasm and provokes the accumulation of beta-catenin and other SCFbetaTrCP substrates. J Biol Chem *279*, 788-795.

Bhattacharya, J., Peters, P.J., and Clapham, P.R. (2004). Human immunodeficiency virus type 1 envelope glycoproteins that lack cytoplasmic domain cysteines: impact on association with membrane lipid rafts and incorporation onto budding virus particles. J Virol *78*, 5500-5506.

Bhattacharya, J., Repik, A., and Clapham, P.R. (2006). Gag regulates association of human immunodeficiency virus type 1 envelope with detergent-resistant membranes. J Virol *80*, 5292-5300.

Bieniasz, P.D. (2006). Late budding domains and host proteins in enveloped virus release. Virology *344*, 55-63.

Binette, J., Dube, M., Mercier, J., Halawani, D., Latterich, M., and Cohen, E.A. (2007). Requirements for the selective degradation of CD4 receptor molecules by the human immunodeficiency virus type 1 Vpu protein in the endoplasmic reticulum. Retrovirology *4*, 75.

Bishop, K.N., Holmes, R.K., Sheehy, A.M., Davidson, N.O., Cho, S.J., and Malim, M.H. (2004). Cytidine deamination of retroviral DNA by diverse APOBEC proteins. Curr Biol *14*, 1392-1396.

Bjorndal, A., Sonnerborg, A., Tscherning, C., Albert, J., and Fenyo, E.M. (1999). Phenotypic characteristics of human immunodeficiency virus type 1 subtype C isolates of Ethiopian AIDS patients. AIDS Res Hum Retroviruses *15*, 647-653.

Blagoveshchenskaya, A.D., Thomas, L., Feliciangeli, S.F., Hung, C.H., and Thomas, G. (2002). HIV-1 Nef downregulates MHC-I by a PACS-1- and PI3K-regulated ARF6 endocytic pathway. Cell *111*, 853-866.

Boge, M., Wyss, S., Bonifacino, J.S., and Thali, M. (1998). A membrane-proximal tyrosine-based signal mediates internalization of the HIV-1 envelope glycoprotein via interaction with the AP-2 clathrin adaptor. J Biol Chem *273*, 15773-15778.

Bogerd, H.P., and Cullen, B.R. (2008). Single-stranded RNA facilitates nucleocapsid: APOBEC3G complex formation. RNA *14*, 1228-1236.

Bollinger, R.C., Egan, M.A., Chun, T.W., Mathieson, B., and Siliciano, R.F. (1996). Cellular immune responses to HIV-1 in progressive and non-progressive infections. AIDS *10 Suppl A*, S85-96.

Bonifacino, J.S., and Traub, L.M. (2003). Signals for sorting of transmembrane proteins to endosomes and lysosomes. Annu Rev Biochem *72*, 395-447.

Bour, S., Schubert, U., and Strebel, K. (1995). The human immunodeficiency virus type 1 Vpu protein specifically binds to the cytoplasmic domain of CD4: implications for the mechanism of degradation. J Virol *69*, 1510-1520.

Bour, S., and Strebel, K. (2003). The HIV-1 Vpu protein: a multifunctional enhancer of viral particle release. Microbes Infect *5*, 1029-1039.

Bouyac-Bertoia, M., Dvorin, J.D., Fouchier, R.A., Jenkins, Y., Meyer, B.E., Wu, L.I., Emerman, M., and Malim, M.H. (2001). HIV-1 infection requires a functional integrase NLS. Mol Cell *7*, 1025-1035.

Braaten, D., Franke, E.K., and Luban, J. (1996). Cyclophilin A is required for an early step in the life cycle of human immunodeficiency virus type 1 before the initiation of reverse transcription. J Virol *70*, 3551-3560.

Bresnahan, P.A., Yonemoto, W., Ferrell, S., Williams-Herman, D., Geleziunas, R., and Greene, W.C. (1998). A dileucine motif in HIV-1 Nef acts as an internalization signal for CD4 downregulation and binds the AP-1 clathrin adaptor. Curr Biol *8*, 1235-1238.

Briggs, J.A., Wilk, T., Welker, R., Krausslich, H.G., and Fuller, S.D. (2003). Structural organization of authentic, mature HIV-1 virions and cores. EMBO J *22*, 1707-1715.

Browman, D.T., Resek, M.E., Zajchowski, L.D., and Robbins, S.M. (2006). Erlin-1 and erlin-2 are novel members of the prohibitin family of proteins that define lipid-raft-like domains of the ER. J Cell Sci *119*, 3149-3160.

Brown, E.L., and Lyles, D.S. (2003). Organization of the vesicular stomatitis virus glycoprotein into membrane microdomains occurs independently of intracellular viral components. J Virol *77*, 3985-3992.

Brugger, B., Glass, B., Haberkant, P., Leibrecht, I., Wieland, F.T., and Krausslich, H.G. (2006). The HIV lipidome: a raft with an unusual composition. Proc Natl Acad Sci U S A *103*, 2641-2646.

Bukrinsky, M.I., Haggerty, S., Dempsey, M.P., Sharova, N., Adzhubel, A., Spitz, L., Lewis, P., Goldfarb, D., Emerman, M., and Stevenson, M. (1993). A nuclear localization signal within HIV-1 matrix protein that governs infection of non-dividing cells. Nature *365*, 666-669.

Buonaguro, L., Tagliamonte, M., Tornesello, M., and Buonaguro, F.M. (2007a). Evolution of the HIV-1 V3 region in the Italian epidemic. New Microbiol *30*, 1-11.

Buonaguro, L., Tagliamonte, M., Tornesello, M.L., and Buonaguro, F.M. (2007b). Genetic and phylogenetic evolution of HIV-1 in a low subtype heterogeneity epidemic: the Italian example. Retrovirology *4*, 34.

Buonaguro, L., Tagliamonte, M., Tornesello, M.L., Pilotti, E., Casoli, C., Lazzarin, A., Tambussi, G., Ciccozzi, M., Rezza, G., and Buonaguro, F.M. (2004). Screening of HIV-1 isolates by reverse heteroduplex mobility assay and identification of non-B subtypes in Italy. J Acquir Immune Defic Syndr *37*, 1295-1306.

Buonaguro, L., Tornesello, M.L., and Buonaguro, F.M. (2007c). Human immunodeficiency virus type 1 subtype distribution in the worldwide epidemic: pathogenetic and therapeutic implications. J Virol *81*, 10209-10219.

Buonocore, L., Turi, T.G., Crise, B., and Rose, J.K. (1994). Stimulation of heterologous protein degradation by the Vpu protein of HIV-1 requires the transmembrane and cytoplasmic domains of CD4. Virology *204*, 482-486.

Burnett, A., and Spearman, P. (2007). APOBEC3G multimers are recruited to the plasma membrane for packaging into human immunodeficiency virus type 1 virus-like particles in an RNA-dependent process requiring the NC basic linker. J Virol *81*, 5000-5013.

Butticaz, C., Michielin, O., Wyniger, J., Telenti, A., and Rothenberger, S. (2007). Silencing of both beta-TrCP1 and HOS (beta-TrCP2) is required to suppress human immunodeficiency virus type 1 Vpu-mediated CD4 down-modulation. J Virol *81*, 1502-1505.

Byland, R., Vance, P.J., Hoxie, J.A., and Marsh, M. (2007). A conserved dileucine motif mediates clathrin and AP-2-dependent endocytosis of the HIV-1 envelope protein. Mol Biol Cell *18*, 414-425.

Campbell, E.M., Nunez, R., and Hope, T.J. (2004a). Disruption of the actin cytoskeleton can complement the ability of Nef to enhance human immunodeficiency virus type 1 infectivity. J Virol *78*, 5745-5755.

Campbell, G.R., Pasquier, E., Watkins, J., Bourgarel-Rey, V., Peyrot, V., Esquieu, D., Barbier, P., de Mareuil, J., Braguer, D., Kaleebu, P., *et al.* (2004b). The glutamine-rich region of the HIV-1 Tat protein is involved in T-cell apoptosis. J Biol Chem *279*, 48197-48204.

Candler, A., Featherstone, M., Ali, R., Maloney, L., Watts, A., and Fischer, W.B. (2005). Computational analysis of mutations in the transmembrane region of Vpu from HIV-1. Biochim Biophys Acta *1716*, 1-10.

Cao, W., Bover, L., Cho, M., Wen, X., Hanabuchi, S., Bao, M., Rosen, D.B., Wang, Y.H., Shaw, J.L., Du, Q., *et al.* (2009). Regulation of TLR7/9 responses in plasmacytoid dendritic cells by BST2 and ILT7 receptor interaction. J Exp Med *206*, 1603-1614.

Casado, G., Thomson, M.M., Sierra, M., and Najera, R. (2005). Identification of a novel HIV-1 circulating ADG intersubtype recombinant form (CRF19_cpx) in Cuba. J Acquir Immune Defic Syndr *40*, 532-537.

Champenois, K., Bocket, L., Deuffic-Burban, S., Cotte, L., Andre, P., Choisy, P., and Yazdanpanah, Y. (2008). Expected response to protease inhibitors of HIV-1 non-B subtype viruses according to resistance algorithms. AIDS *22*, 1087-1089.

Chan, W.E., Lin, H.H., and Chen, S.S. (2005). Wild-type-like viral replication potential of human immunodeficiency virus type 1 envelope mutants lacking palmitoylation signals. J Virol *79*, 8374-8387.

Chang, F., Re, F., Sebastian, S., Sazer, S., and Luban, J. (2004). HIV-1 Vpr induces defects in mitosis, cytokinesis, nuclear structure, and centrosomes. Mol Biol Cell *15*, 1793-1801.

Chaudhuri, R., Lindwasser, O.W., Smith, W.J., Hurley, J.H., and Bonifacino, J.S. (2007). Downregulation of CD4 by human immunodeficiency virus type 1 Nef is dependent on clathrin and involves direct interaction of Nef with the AP2 clathrin adaptor. J Virol *81*, 3877-3890.

Chen, C.H., Matthews, T.J., McDanal, C.B., Bolognesi, D.P., and Greenberg, M.L. (1995). A molecular clasp in the human immunodeficiency virus (HIV) type 1 TM protein determines the anti-HIV activity of gp41 derivatives: implication for viral fusion. J Virol *69*, 3771-3777.

Chen, M.Y., Maldarelli, F., Karczewski, M.K., Willey, R.L., and Strebel, K. (1993). Human immunodeficiency virus type 1 Vpu protein induces degradation of CD4 in vitro: the cytoplasmic domain of CD4 contributes to Vpu sensitivity. J Virol *67*, 3877-3884.

Chen, X., Jen, A., Warley, A., Lawrence, M.J., Quinn, P.J., and Morris, R.J. (2009). Isolation at physiological temperature of detergent-resistant membranes with properties expected of lipid rafts: the influence of buffer composition. Biochem J *417*, 525-533.

Chen, Z., Huang, Y., Zhao, X., Skulsky, E., Lin, D., Ip, J., Gettie, A., and Ho, D.D. (2000). Enhanced infectivity of an R5-tropic simian/human immunodeficiency virus carrying human immunodeficiency virus type 1 subtype C envelope after serial passages in pig-tailed macaques (Macaca nemestrina). J Virol *74*, 6501-6510.

Chen, Z., Zhou, P., Ho, D.D., Landau, N.R., and Marx, P.A. (1997). Genetically divergent strains of simian immunodeficiency virus use CCR5 as a coreceptor for entry. J Virol *71*, 2705-2714.

Cheng, J., Nath, A., Knudsen, B., Hochman, S., Geiger, J.D., Ma, M., and Magnuson, D.S. (1998). Neuronal excitatory properties of human immunodeficiency virus type 1 Tat protein. Neuroscience *82*, 97-106.

Chiu, Y.L., and Greene, W.C. (2008). The APOBEC3 cytidine deaminases: an innate defensive network opposing exogenous retroviruses and endogenous retroelements. Annu Rev Immunol *26*, 317-353.

Choe, H. (1998). Chemokine receptors in HIV-1 and SIV infection. Arch Pharm Res *21*, 634-639.

Chowers, M.Y., Spina, C.A., Kwoh, T.J., Fitch, N.J., Richman, D.D., and Guatelli, J.C. (1994). Optimal infectivity in vitro of human immunodeficiency virus type 1 requires an intact nef gene. J Virol *68*, 2906-2914.

Chukkapalli, V., Hogue, I.B., Boyko, V., Hu, W.S., and Ono, A. (2008). Interaction between the human immunodeficiency virus type 1 Gag matrix domain and phosphatidylinositol-(4,5)-bisphosphate is essential for efficient gag membrane binding. J Virol *82*, 2405-2417.

Chung, C.S., Huang, C.Y., and Chang, W. (2005). Vaccinia virus penetration requires cholesterol and results in specific viral envelope proteins associated with lipid rafts. J Virol *79*, 1623-1634.

Clavel, F., Guyader, M., Guetard, D., Salle, M., Montagnier, L., and Alizon, M. (1986). Molecular cloning and polymorphism of the human immune deficiency virus type 2. Nature *324*, 691-695.

Coadou, G., Gharbi-Benarous, J., Megy, S., Bertho, G., Evrard-Todeschi, N., Segeral, E., Benarous, R., and Girault, J.P. (2003). NMR studies of the phosphorylation motif of the HIV-1 protein Vpu bound to the F-box protein beta-TrCP. Biochemistry *42*, 14741-14751.

Coady, M.J., Daniel, N.G., Tiganos, E., Allain, B., Friborg, J., Lapointe, J.Y., and Cohen, E.A. (1998). Effects of Vpu expression on Xenopus oocyte membrane conductance. Virology *244*, 39-49.

Coffin, J.M. (1996). HIV viral dynamics. AIDS *10 Suppl 3*, S75-84.

Cohen, E.A., Dehni, G., Sodroski, J.G., and Haseltine, W.A. (1990). Human immunodeficiency virus vpr product is a virion-associated regulatory protein. J Virol *64*, 3097-3099.

Cohen, E.A., Terwilliger, E.F., Sodroski, J.G., and Haseltine, W.A. (1988). Identification of a protein encoded by the vpu gene of HIV-1. Nature *334*, 532-534.

Coleman, S.H., Van Damme, N., Day, J.R., Noviello, C.M., Hitchin, D., Madrid, R., Benichou, S., and Guatelli, J.C. (2005). Leucine-specific, functional interactions between human immunodeficiency virus type 1 Nef and adaptor protein complexes. J Virol *79*, 2066-2078.

Conticello, S.G., Thomas, C.J., Petersen-Mahrt, S.K., and Neuberger, M.S. (2005). Evolution of the AID/APOBEC family of polynucleotide (deoxy)cytidine deaminases. Mol Biol Evol *22*, 367-377.

Cordes, F.S., Kukol, A., Forrest, L.R., Arkin, I.T., Sansom, M.S., and Fischer, W.B. (2001). The structure of the HIV-1 Vpu ion channel: modelling and simulation studies. Biochim Biophys Acta *1512*, 291-298.

Cortes, M.J., Wong-Staal, F., and Lama, J. (2002). Cell surface CD4 interferes with the infectivity of HIV-1 particles released from T cells. J Biol Chem *277*, 1770-1779.

Courcoul, M., Patience, C., Rey, F., Blanc, D., Harmache, A., Sire, J., Vigne, R., and Spire, B. (1995). Peripheral blood mononuclear cells produce normal amounts of defective Vif- human immunodeficiency virus type 1 particles which are restricted for the preretrotranscription steps. J Virol *69*, 2068-2074.

Courgnaud, V., Salemi, M., Pourrut, X., Mpoudi-Ngole, E., Abela, B., Auzel, P., Bibollet-Ruche, F., Hahn, B., Vandamme, A.M., Delaporte, E., *et al.* (2002). Characterization of a novel simian immunodeficiency virus with a vpu gene from greater spot-nosed monkeys (Cercopithecus nictitans) provides new insights into simian/human immunodeficiency virus phylogeny. J Virol *76*, 8298-8309.

Craig, H.M., Pandori, M.W., and Guatelli, J.C. (1998). Interaction of HIV-1 Nef with the cellular dileucine-based sorting pathway is required for CD4 down-regulation and optimal viral infectivity. Proc Natl Acad Sci U S A *95*, 11229-11234.

Crise, B., Buonocore, L., and Rose, J.K. (1990). CD4 is retained in the endoplasmic reticulum by the human immunodeficiency virus type 1 glycoprotein precursor. J Virol *64*, 5585-5593.

Cullen, B.R. (1998). HIV-1 auxiliary proteins: making connections in a dying cell. Cell *93*, 685-692.

Cunningham, A.L., Naif, H., Saksena, N., Lynch, G., Chang, J., Li, S., Jozwiak, R., Alali, M., Wang, B., Fear, W., *et al.* (1997). HIV infection of macrophages and pathogenesis of AIDS dementia complex: interaction of the host cell and viral genotype. J Leukoc Biol *62*, 117-125.

Dang, Y., Siew, L.M., Wang, X., Han, Y., Lampen, R., and Zheng, Y.H. (2008). Human cytidine deaminase APOBEC3H restricts HIV-1 replication. J Biol Chem *283*, 11606-11614.

Dang, Y., Wang, X., Esselman, W.J., and Zheng, Y.H. (2006). Identification of APOBEC3DE as another antiretroviral factor from the human APOBEC family. J Virol *80*, 10522-10533.

Day, J.R., Van Damme, N., and Guatelli, J.C. (2006). The effect of the membrane-proximal tyrosine-based sorting signal of HIV-1 gp41 on viral infectivity depends on sequences within gp120. Virology *354*, 316-327.

Dayton, A.I., Sodroski, J.G., Rosen, C.A., Goh, W.C., and Haseltine, W.A. (1986). The trans-activator gene of the human T cell lymphotropic virus type III is required for replication. Cell *44*, 941-947.

Dazza, M.C., Ekwalanga, M., Nende, M., Shamamba, K.B., Bitshi, P., Paraskevis, D., and Saragosti, S. (2005). Characterization of a novel vpu-harboring simian immunodeficiency virus from a Dent's Mona monkey (Cercopithecus mona denti). J Virol *79*, 8560-8571.

De Clercq, E. (2009). The history of antiretrovirals: key discoveries over the past 25 years. Rev Med Virol *19*, 287-299.

de Mareuil, J., Carre, M., Barbier, P., Campbell, G.R., Lancelot, S., Opi, S., Esquieu, D., Watkins, J.D., Prevot, C., Braguer, D., *et al.* (2005). HIV-1 Tat protein enhances microtubule polymerization. Retrovirology *2*, 5.

de Noronha, C.M., Sherman, M.P., Lin, H.W., Cavrois, M.V., Moir, R.D., Goldman, R.D., and Greene, W.C. (2001). Dynamic disruptions in nuclear envelope architecture and integrity induced by HIV-1 Vpr. Science *294*, 1105-1108.

Deacon, N.J., Tsykin, A., Solomon, A., Smith, K., Ludford-Menting, M., Hooker, D.J., McPhee, D.A., Greenway, A.L., Ellett, A., Chatfield, C., *et al.* (1995). Genomic structure of an attenuated quasi species of HIV-1 from a blood transfusion donor and recipients. Science *270*, 988-991.

DeHart, J.L., Zimmerman, E.S., Ardon, O., Monteiro-Filho, C.M., Arganaraz, E.R., and Planelles, V. (2007). HIV-1 Vpr activates the G2 checkpoint through manipulation of the ubiquitin proteasome system. Virol J *4*, 57.

Demarchi, F., Gutierrez, M.I., and Giacca, M. (1999). Human immunodeficiency virus type 1 tat protein activates transcription factor NF-kappaB through the cellular interferon-inducible, double-stranded RNA-dependent protein kinase, PKR. J Virol *73*, 7080-7086.

Demarest, J.F., Jack, N., Cleghorn, F.R., Greenberg, M.L., Hoffman, T.L., Ottinger, J.S., Fantry, L., Edwards, J., O'Brien, T.R., Cao, K., *et al.* (2001). Immunologic and virologic analyses of an acutely HIV type 1-infected patient with extremely rapid disease progression. AIDS Res Hum Retroviruses *17*, 1333-1344.

Deng, H., Liu, R., Ellmeier, W., Choe, S., Unutmaz, D., Burkhart, M., Di Marzio, P., Marmon, S., Sutton, R.E., Hill, C.M., *et al.* (1996). Identification of a major co-receptor for primary isolates of HIV-1. Nature *381*, 661-666.

Deng, H.K., Unutmaz, D., KewalRamani, V.N., and Littman, D.R. (1997). Expression cloning of new receptors used by simian and human immunodeficiency viruses. Nature *388*, 296-300.

Desai, S., Kyriakides, T., Holodniy, M., Al-Salman, J., Griffith, B., and Kozal, M. (2007). Evolution of genotypic resistance algorithms and their impact on the interpretation of clinical trials: an OPTIMA trial substudy. HIV Clin Trials *8*, 293-302.

Doehle, B.P., Schafer, A., and Cullen, B.R. (2005). Human APOBEC3B is a potent inhibitor of HIV-1 infectivity and is resistant to HIV-1 Vif. Virology *339*, 281-288.

Doms, R.W. (2004). Unwelcome guests with master keys: how HIV enters cells and how it can be stopped. Top HIV Med *12*, 100-103.

Doms, R.W., and Peiper, S.C. (1997). Unwelcomed guests with master keys: how HIV uses chemokine receptors for cellular entry. Virology *235*, 179-190.

Doranz, B.J., Rucker, J., Yi, Y., Smyth, R.J., Samson, M., Peiper, S.C., Parmentier, M., Collman, R.G., and Doms, R.W. (1996). A dual-tropic primary HIV-1 isolate that uses fusin and the beta-chemokine receptors CKR-5, CKR-3, and CKR-2b as fusion cofactors. Cell *85*, 1149-1158.

Douglas, J.L., Viswanathan, K., McCarroll, M.N., Gustin, J.K., Fruh, K., and Moses, A.V. (2009). Vpu directs the degradation of the human immunodeficiency virus restriction factor BST-2/Tetherin via a {beta}TrCP-dependent mechanism. J Virol *83*, 7931-7947.

Dragic, T., Trkola, A., Lin, S.W., Nagashima, K.A., Kajumo, F., Zhao, L., Olson, W.C., Wu, L., Mackay, C.R., Allaway, G.P., *et al.* (1998). Amino-terminal substitutions in the CCR5 coreceptor impair gp120 binding and human immunodeficiency virus type 1 entry. J Virol *72*, 279-285.

Drevot, P., Langlet, C., Guo, X.J., Bernard, A.M., Colard, O., Chauvin, J.P., Lasserre, R., and He, H.T. (2002). TCR signal initiation machinery is pre-assembled and activated in a subset of membrane rafts. EMBO J *21*, 1899-1908.

Dube, M., Roy, B.B., Guiot-Guillain, P., Mercier, J., Binette, J., Leung, G., and Cohen, E.A. (2009). Suppression of Tetherin-restricting activity upon human immunodeficiency virus type 1 particle release correlates with localization of Vpu in the trans-Golgi network. J Virol *83*, 4574-4590.

Edinger, A.L., Amedee, A., Miller, K., Doranz, B.J., Endres, M., Sharron, M., Samson, M., Lu, Z.H., Clements, J.E., Murphey-Corb, M., *et al.* (1997). Differential utilization of CCR5 by macrophage and T cell tropic simian immunodeficiency virus strains. Proc Natl Acad Sci U S A *94*, 4005-4010.

Epand, R.F., Thomas, A., Brasseur, R., Vishwanathan, S.A., Hunter, E., and Epand, R.M. (2006). Juxtamembrane protein segments that contribute to recruitment of cholesterol into domains. Biochemistry *45*, 6105-6114.

Essex, M. (1999). Human immunodeficiency viruses in the developing world. Adv Virus Res *53*, 71-88.

Estrabaud, E., Le Rouzic, E., Lopez-Verges, S., Morel, M., Belaidouni, N., Benarous, R., Transy, C., Berlioz-Torrent, C., and Margottin-Goguet, F. (2007). Regulated degradation of the HIV-1 Vpu protein through a betaTrCP-independent pathway limits the release of viral particles. PLoS Pathog *3*, e104.

Evrard-Todeschi, N., Gharbi-Benarous, J., Bertho, G., Coadou, G., Megy, S., Benarous, R., and Girault, J.P. (2006). NMR studies for identifying phosphopeptide ligands of the HIV-1 protein Vpu binding to the F-box protein beta-TrCP. Peptides *27*, 194-210.

Ewart, G.D., Mills, K., Cox, G.B., and Gage, P.W. (2002). Amiloride derivatives block ion channel activity and enhancement of virus-like particle budding caused by HIV-1 protein Vpu. Eur Biophys J *31*, 26-35.

Ewart, G.D., Nasr, N., Naif, H., Cox, G.B., Cunningham, A.L., and Gage, P.W. (2004). Potential new anti-human immunodeficiency virus type 1 compounds depress virus replication in cultured human macrophages. Antimicrob Agents Chemother *48*, 2325-2330.

Ewart, G.D., Sutherland, T., Gage, P.W., and Cox, G.B. (1996). The Vpu protein of human immunodeficiency virus type 1 forms cation-selective ion channels. J Virol *70*, 7108-7115.

Feng, Y., Broder, C.C., Kennedy, P.E., and Berger, E.A. (1996). HIV-1 entry cofactor: functional cDNA cloning of a seven-transmembrane, G protein-coupled receptor. Science *272*, 872-877.

Fisher, A.G., Ensoli, B., Ivanoff, L., Chamberlain, M., Petteway, S., Ratner, L., Gallo, R.C., and Wong-Staal, F. (1987). The sor gene of HIV-1 is required for efficient virus transmission in vitro. Science *237*, 888-893.

Fisher, A.G., Feinberg, M.B., Josephs, S.F., Harper, M.E., Marselle, L.M., Reyes, G., Gonda, M.A., Aldovini, A., Debouk, C., Gallo, R.C., *et al.* (1986). The trans-activator gene of HTLV-III is essential for virus replication. Nature *320*, 367-371.

Fitzpatrick, K., Skasko, M., Deerinck, T.J., Crum, J., Ellisman, M.H., and Guatelli, J. (2010). Direct restriction of virus release and incorporation of the interferon-induced protein BST-2 into HIV-1 particles. PLoS Pathog *6*, e1000701.

Foster, J.L., and Garcia, J.V. (2008). HIV-1 Nef: at the crossroads. Retrovirology *5*, 84.

Fouchier, R.A., and Malim, M.H. (1999). Nuclear import of human immunodeficiency virus type-1 preintegration complexes. Adv Virus Res *52*, 275-299.

Franke, E.K., Yuan, H.E., and Luban, J. (1994). Specific incorporation of cyclophilin A into HIV-1 virions. Nature *372*, 359-362.

Frankel, A.D., and Young, J.A. (1998). HIV-1: fifteen proteins and an RNA. Annu Rev Biochem *67*, 1-25.

Freed, E.O. (2001). HIV-1 replication. Somat Cell Mol Genet *26*, 13-33.

Freed, E.O. (2002). Viral late domains. J Virol *76*, 4679-4687.

Fujita, K., Omura, S., and Silver, J. (1997). Rapid degradation of CD4 in cells expressing human immunodeficiency virus type 1 Env and Vpu is blocked by proteasome inhibitors. J Gen Virol *78 (Pt 3)*, 619-625.

Gabuzda, D.H., Lawrence, K., Langhoff, E., Terwilliger, E., Dorfman, T., Haseltine, W.A., and Sodroski, J. (1992). Role of vif in replication of human immunodeficiency virus type 1 in CD4+ T lymphocytes. J Virol *66*, 6489-6495.

Gallo, R., Wong-Staal, F., Montagnier, L., Haseltine, W.A., and Yoshida, M. (1988). HIV/HTLV gene nomenclature. Nature *333*, 504.

Gallo, R.C., Salahuddin, S.Z., Popovic, M., Shearer, G.M., Kaplan, M., Haynes, B.F., Palker, T.J., Redfield, R., Oleske, J., Safai, B., *et al.* (1984). Frequent detection and isolation of cytopathic retroviruses (HTLV-III) from patients with AIDS and at risk for AIDS. Science *224*, 500-503.

Ganser, B.K., Li, S., Klishko, V.Y., Finch, J.T., and Sundquist, W.I. (1999). Assembly and analysis of conical models for the HIV-1 core. Science *283*, 80-83.

Gao, F., Bailes, E., Robertson, D.L., Chen, Y., Rodenburg, C.M., Michael, S.F., Cummins, L.B., Arthur, L.O., Peeters, M., Shaw, G.M., *et al.* (1999). Origin of HIV-1 in the chimpanzee Pan troglodytes troglodytes. Nature *397*, 436-441.

Gao, F., Robertson, D.L., Morrison, S.G., Hui, H., Craig, S., Decker, J., Fultz, P.N., Girard, M., Shaw, G.M., Hahn, B.H., *et al.* (1996). The heterosexual human immunodeficiency virus type 1 epidemic in Thailand is caused by an intersubtype (A/E) recombinant of African origin. J Virol *70*, 7013-7029.

Garber, M.E., Wei, P., and Jones, K.A. (1998). HIV-1 Tat interacts with cyclin T1 to direct the P-TEFb CTD kinase complex to TAR RNA. Cold Spring Harb Symp Quant Biol *63*, 371-380.

Garcia, J.V., and Miller, A.D. (1991). Serine phosphorylation-independent downregulation of cell-surface CD4 by nef. Nature *350*, 508-511.

Gartner, S. (2000). HIV infection and dementia. Science *287*, 602-604.

Gelderblom, H.R. (1991). Assembly and morphology of HIV: potential effect of structure on viral function. AIDS *5*, 617-637.

Geyer, M., Yu, H., Mandic, R., Linnemann, T., Zheng, Y.H., Fackler, O.T., and Peterlin, B.M. (2002). Subunit H of the V-ATPase binds to the medium chain of adaptor protein complex 2 and connects Nef to the endocytic machinery. J Biol Chem *277*, 28521-28529.

Giacca, M. (2005). HIV-1 Tat, apoptosis and the mitochondria: a tubulin link? Retrovirology *2*, 7.

Gibbs, J.S., Lackner, A.A., Lang, S.M., Simon, M.A., Sehgal, P.K., Daniel, M.D., and Desrosiers, R.C. (1995). Progression to AIDS in the absence of a gene for vpr or vpx. J Virol *69*, 2378-2383.

Gibbs, J.S., Regier, D.A., and Desrosiers, R.C. (1994). Construction and in vitro properties of SIVmac mutants with deletions in "nonessential" genes. AIDS Res Hum Retroviruses *10*, 607-616.

Giunta, B., Hou, H., Zhu, Y., Rrapo, E., Tian, J., Takashi, M., Commins, D., Singer, E., He, J., Fernandez, F., *et al.* (2009). HIV-1 Tat contributes to Alzheimer's disease-like pathology in PSAPP mice. Int J Clin Exp Pathol *2*, 433-443.

Gkantiragas, I., Brugger, B., Stuven, E., Kaloyanova, D., Li, X.Y., Lohr, K., Lottspeich, F., Wieland, F.T., and Helms, J.B. (2001). Sphingomyelin-enriched microdomains at the Golgi complex. Mol Biol Cell *12*, 1819-1833.

Goffinet, C., Allespach, I., Homann, S., Tervo, H.M., Habermann, A., Rupp, D., Oberbremer, L., Kern, C., Tibroni, N., Welsch, S., *et al.* (2009). HIV-1 antagonism of CD317 is species specific and involves Vpu-mediated proteasomal degradation of the restriction factor. Cell Host Microbe *5*, 285-297.

Goldsmith, M.A., Warmerdam, M.T., Atchison, R.E., Miller, M.D., and Greene, W.C. (1995). Dissociation of the CD4 downregulation and viral infectivity enhancement functions of human immunodeficiency virus type 1 Nef. J Virol *69*, 4112-4121.

Gomez, L.M., Pacyniak, E., Flick, M., Hout, D.R., Gomez, M.L., Nerrienet, E., Ayouba, A., Santiago, M.L., Hahn, B.H., and Stephens, E.B. (2005). Vpu-mediated CD4 down-regulation and degradation is conserved among highly divergent SIV(cpz) strains. Virology *335*, 46-60.

Gonzalez, M.E., and Carrasco, L. (2003). Viroporins. FEBS Lett *552*, 28-34.

Gottlinger, H.G., Dorfman, T., Sodroski, J.G., and Haseltine, W.A. (1991). Effect of mutations affecting the p6 gag protein on human immunodeficiency virus particle release. Proc Natl Acad Sci U S A *88*, 3195-3199.

Goujon, C., Arfi, V., Pertel, T., Luban, J., Lienard, J., Rigal, D., Darlix, J.L., and Cimarelli, A. (2008). Characterization of simian immunodeficiency virus SIVSM/human immunodeficiency virus type 2 Vpx function in human myeloid cells. J Virol *82*, 12335-12345.

Goujon, C., Riviere, L., Jarrosson-Wuilleme, L., Bernaud, J., Rigal, D., Darlix, J.L., and Cimarelli, A. (2007). SIVSM/HIV-2 Vpx proteins promote retroviral escape from a proteasome-dependent restriction pathway present in human dendritic cells. Retrovirology *4*, 2.

Grandgenett, D.P. (2005). Symmetrical recognition of cellular DNA target sequences during retroviral integration. Proc Natl Acad Sci U S A *102*, 5903-5904.

Greenberg, M., DeTulleo, L., Rapoport, I., Skowronski, J., and Kirchhausen, T. (1998a). A dileucine motif in HIV-1 Nef is essential for sorting into clathrin-coated pits and for downregulation of CD4. Curr Biol *8*, 1239-1242.

Greenberg, M.E., Iafrate, A.J., and Skowronski, J. (1998b). The SH3 domain-binding surface and an acidic motif in HIV-1 Nef regulate trafficking of class I MHC complexes. EMBO J *17*, 2777-2789.

Grice, A.L., Kerr, I.D., and Sansom, M.S. (1997). Ion channels formed by HIV-1 Vpu: a modelling and simulation study. FEBS Lett *405*, 299-304.

Grzesiek, S., Stahl, S.J., Wingfield, P.T., and Bax, A. (1996). The CD4 determinant for downregulation by HIV-1 Nef directly binds to Nef. Mapping of the Nef binding surface by NMR. Biochemistry *35*, 10256-10261.

Gummuluru, S., Kinsey, C.M., and Emerman, M. (2000). An in vitro rapid-turnover assay for human immunodeficiency virus type 1 replication selects for cell-to-cell spread of virus. J Virol *74*, 10882-10891.

Gupta, R.K., Hue, S., Schaller, T., Verschoor, E., Pillay, D., and Towers, G.J. (2009a). Mutation of a single residue renders human tetherin resistant to HIV-1 Vpu-mediated depletion. PLoS Pathog *5*, e1000443.

Gupta, R.K., Mlcochova, P., Pelchen-Matthews, A., Petit, S.J., Mattiuzzo, G., Pillay, D., Takeuchi, Y., Marsh, M., and Towers, G.J. (2009b). Simian immunodeficiency virus envelope glycoprotein counteracts tetherin/BST-2/CD317 by intracellular sequestration. Proc Natl Acad Sci U S A *106*, 20889-20894.

Habermann, A., Krijnse-Locker, J., Oberwinkler, H., Eckhardt, M., Homann, S., Andrew, A., Strebel, K., and Krausslich, H.G. (2010). CD317/tetherin is enriched in the HIV-1 envelope and downregulated from the plasma membrane upon virus infection. J Virol *84*, 4646-4658.

Hammes, S.R., Dixon, E.P., Malim, M.H., Cullen, B.R., and Greene, W.C. (1989). Nef protein of human immunodeficiency virus type 1: evidence against its role as a transcriptional inhibitor. Proc Natl Acad Sci U S A *86*, 9549-9553.

Harris, R.S., Bishop, K.N., Sheehy, A.M., Craig, H.M., Petersen-Mahrt, S.K., Watt, I.N., Neuberger, M.S., and Malim, M.H. (2003). DNA deamination mediates innate immunity to retroviral infection. Cell *113*, 803-809.

Haughey, N.J., and Mattson, M.P. (2002). Calcium dysregulation and neuronal apoptosis by the HIV-1 proteins Tat and gp120. J Acquir Immune Defic Syndr *31 Suppl 2*, S55-61.

He, J., Choe, S., Walker, R., Di Marzio, P., Morgan, D.O., and Landau, N.R. (1995). Human immunodeficiency virus type 1 viral protein R (Vpr) arrests cells in the G2 phase of the cell cycle by inhibiting p34cdc2 activity. J Virol *69*, 6705-6711.

Heinzinger, N.K., Bukinsky, M.I., Haggerty, S.A., Ragland, A.M., Kewalramani, V., Lee, M.A., Gendelman, H.E., Ratner, L., Stevenson, M., and Emerman, M. (1994). The Vpr protein of human immunodeficiency virus type 1 influences nuclear localization of viral nucleic acids in nondividing host cells. Proc Natl Acad Sci U S A *91*, 7311-7315.

Hemelaar, J., Gouws, E., Ghys, P.D., and Osmanov, S. (2006). Global and regional distribution of HIV-1 genetic subtypes and recombinants in 2004. AIDS *20*, W13-23.

Hill, M.S., Ruiz, A., Pacyniak, E., Pinson, D.M., Culley, N., Yen, B., Wong, S.W., and Stephens, E.B. (2008). Modulation of the severe CD4+ T-cell loss caused by a pathogenic simian-human immunodeficiency virus by replacement of the subtype B vpu with the vpu from a subtype C HIV-1 clinical isolate. Virology *371*, 86-97.

Hill, M.S., Ruiz, A., Schmitt, K., and Stephens, E.B. (2010). Identification of amino acids within the second alpha helical domain of the human immunodeficiency virus type 1 Vpu that are critical for preventing CD4 cell surface expression. Virology *397*, 104-112.

Hirsch, M.S., and Curran, J. (1996). Human Immunodeficiency Viruses.

Hirsch, V.M., Sharkey, M.E., Brown, C.R., Brichacek, B., Goldstein, S., Wakefield, J., Byrum, R., Elkins, W.R., Hahn, B.H., Lifson, J.D., *et al.* (1998). Vpx is required for dissemination and pathogenesis of SIV(SM) PBj: evidence of macrophage-dependent viral amplification. Nat Med *4*, 1401-1408.

Hoch, J., Lang, S.M., Weeger, M., Stahl-Hennig, C., Coulibaly, C., Dittmer, U., Hunsmann, G., Fuchs, D., Muller, J., Sopper, S., *et al.* (1995). vpr deletion mutant of simian immunodeficiency virus induces AIDS in rhesus monkeys. J Virol *69*, 4807-4813.

Holman, A.G., and Coffin, J.M. (2005). Symmetrical base preferences surrounding HIV-1, avian sarcoma/leukosis virus, and murine leukemia virus integration sites. Proc Natl Acad Sci U S A *102*, 6103-6107.

Holsinger, L.J., and Lamb, R.A. (1991). Influenza virus M2 integral membrane protein is a homotetramer stabilized by formation of disulfide bonds. Virology *183*, 32-43.

Holsinger, L.J., Nichani, D., Pinto, L.H., and Lamb, R.A. (1994). Influenza A virus M2 ion channel protein: a structure-function analysis. J Virol *68*, 1551-1563.

Hope, T.J. (1999). The ins and outs of HIV Rev. Arch Biochem Biophys *365*, 186-191.

Hout, D.R., Gomez, L.M., Pacyniak, E., Miller, J.M., Hill, M.S., and Stephens, E.B. (2006a). A single amino acid substitution within the transmembrane domain of the human immunodeficiency virus type 1 Vpu protein renders simian-human immunodeficiency virus (SHIV(KU-1bMC33)) susceptible to rimantadine. Virology *348*, 449-461.

Hout, D.R., Gomez, M.L., Pacyniak, E., Gomez, L.M., Fegley, B., Mulcahy, E.R., Hill, M.S., Culley, N., Pinson, D.M., Nothnick, W., *et al.* (2006b). Substitution of the transmembrane domain of Vpu in simian-human immunodeficiency virus (SHIVKU1bMC33) with that of M2 of influenza A results in a virus that is sensitive to inhibitors of the M2 ion channel and is pathogenic for pig-tailed macaques. Virology *344*, 541-559.

Hout, D.R., Gomez, M.L., Pacyniak, E., Gomez, L.M., Inbody, S.H., Mulcahy, E.R., Culley, N., Pinson, D.M., Powers, M.F., Wong, S.W., *et al.* (2005). Scrambling of the amino acids within the transmembrane domain of Vpu results in a simian-human immunodeficiency virus (SHIVTM) that is less pathogenic for pig-tailed macaques. Virology *339*, 56-69.

Hout, D.R., Mulcahy, E.R., Pacyniak, E., Gomez, L.M., Gomez, M.L., and Stephens, E.B. (2004). Vpu: a multifunctional protein that enhances the pathogenesis of human immunodeficiency virus type 1. Curr HIV Res *2*, 255-270.

Hrecka, K., Gierszewska, M., Srivastava, S., Kozaczkiewicz, L., Swanson, S.K., Florens, L., Washburn, M.P., and Skowronski, J. (2007). Lentiviral Vpr usurps Cul4-DDB1[VprBP] E3 ubiquitin ligase to modulate cell cycle. Proc Natl Acad Sci U S A *104*, 11778-11783.

Hsu, K., Han, J., Shinlapawittayatorn, K., Deschenes, I., and Marban, E. (2010). Membrane Potential Depolarization as a Triggering Mechanism for Vpu-Mediated HIV-1 Release. Biophys J *99*, 1718-1725.

Hsu, K., Seharaseyon, J., Dong, P., Bour, S., and Marban, E. (2004). Mutual functional destruction of HIV-1 Vpu and host TASK-1 channel. Mol Cell *14*, 259-267.

Hu, D.J., Buve, A., Baggs, J., van der Groen, G., and Dondero, T.J. (1999). What role does HIV-1 subtype play in transmission and pathogenesis? An epidemiological perspective. AIDS *13*, 873-881.

Hua, J., and Cullen, B.R. (1997). Human immunodeficiency virus types 1 and 2 and simian immunodeficiency virus Nef use distinct but overlapping target sites for downregulation of cell surface CD4. J Virol *71*, 6742-6748.

Huang, M., Orenstein, J.M., Martin, M.A., and Freed, E.O. (1995). p6Gag is required for particle production from full-length human immunodeficiency virus type 1 molecular clones expressing protease. J Virol *69*, 6810-6818.

Huet, T., Cheynier, R., Meyerhans, A., Roelants, G., and Wain-Hobson, S. (1990). Genetic organization of a chimpanzee lentivirus related to HIV-1. Nature *345*, 356-359.

Hunziker, W., and Fumey, C. (1994). A di-leucine motif mediates endocytosis and basolateral sorting of macrophage IgG Fc receptors in MDCK cells. EMBO J *13*, 2963-2969.

Hwang, S., Tamilarasu, N., Kibler, K., Cao, H., Ali, A., Ping, Y.H., Jeang, K.T., and Rana, T.M. (2003). Discovery of a small molecule Tat-trans-activation-responsive RNA antagonist that potently inhibits human immunodeficiency virus-1 replication. J Biol Chem *278*, 39092-39103.

Ishikawa, J., Kaisho, T., Tomizawa, H., Lee, B.O., Kobune, Y., Inazawa, J., Oritani, K., Itoh, M., Ochi, T., Ishihara, K., *et al.* (1995). Molecular cloning and chromosomal mapping of a bone marrow stromal cell surface gene, BST2, that may be involved in pre-B-cell growth. Genomics *26*, 527-534.

Iwabu, Y., Fujita, H., Kinomoto, M., Kaneko, K., Ishizaka, Y., Tanaka, Y., Sata, T., and Tokunaga, K. (2009). HIV-1 accessory protein Vpu internalizes cell-surface BST-2/tetherin through transmembrane interactions leading to lysosomes. J Biol Chem *284*, 35060-35072.

Jabbar, M.A., and Nayak, D.P. (1990). Intracellular interaction of human immunodeficiency virus type 1 (ARV-2) envelope glycoprotein gp160 with CD4 blocks the movement and maturation of CD4 to the plasma membrane. J Virol *64*, 6297-6304.

Jacotot, E., Ferri, K.F., El Hamel, C., Brenner, C., Druillennec, S., Hoebeke, J., Rustin, P., Metivier, D., Lenoir, C., Geuskens, M., *et al.* (2001). Control of mitochondrial membrane permeabilization by adenine nucleotide translocator interacting with HIV-1 viral protein rR and Bcl-2. J Exp Med *193*, 509-519.

Jaffe, H.W., and Schochetman, G. (1998). Group O human immunodeficiency virus-1 infections. Infect Dis Clin North Am *12*, 39-46.

Janvier, K., Kato, Y., Boehm, M., Rose, J.R., Martina, J.A., Kim, B.Y., Venkatesan, S., and Bonifacino, J.S. (2003). Recognition of dileucine-based sorting signals from HIV-1 Nef and LIMP-II by the AP-1 gamma-sigma1 and AP-3 delta-sigma3 hemicomplexes. J Cell Biol *163*, 1281-1290.

Jarmuz, A., Chester, A., Bayliss, J., Gisbourne, J., Dunham, I., Scott, J., and Navaratnam, N. (2002). An anthropoid-specific locus of orphan C to U RNA-editing enzymes on chromosome 22. Genomics *79*, 285-296.

Jenkins, Y., McEntee, M., Weis, K., and Greene, W.C. (1998). Characterization of HIV-1 vpr nuclear import: analysis of signals and pathways. J Cell Biol *143*, 875-885.

Jia, B., Serra-Moreno, R., Neidermyer, W., Rahmberg, A., Mackey, J., Fofana, I.B., Johnson, W.E., Westmoreland, S., and Evans, D.T. (2009). Species-specific activity of SIV Nef and HIV-1 Vpu in overcoming restriction by tetherin/BST2. PLoS Pathog *5*, e1000429.

Joag, S.V., Li, Z., Foresman, L., Pinson, D.M., Raghavan, R., Zhuge, W., Adany, I., Wang, C., Jia, F., Sheffer, D., *et al.* (1997). Characterization of the pathogenic KU-SHIV model of acquired immunodeficiency syndrome in macaques. AIDS Res Hum Retroviruses *13*, 635-645.

Joag, S.V., Li, Z., Foresman, L., Stephens, E.B., Zhao, L.J., Adany, I., Pinson, D.M., McClure, H.M., and Narayan, O. (1996). Chimeric simian/human immunodeficiency virus that causes progressive loss of CD4+ T cells and AIDS in pig-tailed macaques. J Virol *70*, 3189-3197.

Joag, S.V., Li, Z., Wang, C., Jia, F., Foresman, L., Adany, I., Pinson, D.M., Stephens, E.B., and Narayan, O. (1998a). Chimeric SHIV that causes CD4+ T cell loss and AIDS in rhesus macaques. J Med Primatol *27*, 59-64.

Joag, S.V., Liu, Z.Q., Stephens, E.B., Smith, M.S., Kumar, A., Li, Z., Wang, C., Sheffer, D., Jia, F., Foresman, L., *et al.* (1998b). Oral immunization of macaques with attenuated vaccine virus induces protection against vaginally transmitted AIDS. J Virol *72*, 9069-9078.

Joag, S.V., Stephens, E.B., Adams, R.J., Foresman, L., and Narayan, O. (1994). Pathogenesis of SIVmac infection in Chinese and Indian rhesus macaques: effects of splenectomy on virus burden. Virology *200*, 436-446.

John-Stewart, G.C., Nduati, R.W., Rousseau, C.M., Mbori-Ngacha, D.A., Richardson, B.A., Rainwater, S., Panteleeff, D.D., and Overbaugh, J. (2005). Subtype C Is associated with increased vaginal shedding of HIV-1. J Infect Dis *192*, 492-496.

Jouvenet, N., Neil, S.J., Zhadina, M., Zang, T., Kratovac, Z., Lee, Y., McNatt, M., Hatziioannou, T., and Bieniasz, P.D. (2009). Broad-spectrum inhibition of retroviral and filoviral particle release by tetherin. J Virol *83*, 1837-1844.

Jowett, J.B., Xie, Y.M., and Chen, I.S. (1999). The presence of human immunodeficiency virus type 1 Vpr correlates with a decrease in the frequency of mutations in a plasmid shuttle vector. J Virol *73*, 7132-7137.

Ju, S.M., Song, H.Y., Lee, J.A., Lee, S.J., Choi, S.Y., and Park, J. (2009). Extracellular HIV-1 Tat up-regulates expression of matrix metalloproteinase-9 via a MAPK-NF-kappaB dependent pathway in human astrocytes. Exp Mol Med *41*, 86-93.

Kaletsky, R.L., Francica, J.R., Agrawal-Gamse, C., and Bates, P. (2009). Tetherin-mediated restriction of filovirus budding is antagonized by the Ebola glycoprotein. Proc Natl Acad Sci U S A *106*, 2886-2891.

Kandathil, A.J., Ramalingam, S., Kannangai, R., David, S., and Sridharan, G. (2005). Molecular epidemiology of HIV. Indian J Med Res *121*, 333-344.

Karlsson, G.B., Halloran, M., Li, J., Park, I.W., Gomila, R., Reimann, K.A., Axthelm, M.K., Iliff, S.A., Letvin, N.L., and Sodroski, J. (1997). Characterization of molecularly cloned simian-human immunodeficiency viruses causing rapid CD4+ lymphocyte depletion in rhesus monkeys. J Virol *71*, 4218-4225.

Kasper, M.R., Roeth, J.F., Williams, M., Filzen, T.M., Fleis, R.I., and Collins, K.L. (2005). HIV-1 Nef disrupts antigen presentation early in the secretory pathway. J Biol Chem *280*, 12840-12848.

Kaul, M., Garden, G.A., and Lipton, S.A. (2001). Pathways to neuronal injury and apoptosis in HIV-associated dementia. Nature *410*, 988-994.

Kawamura, M., Sakai, H., and Adachi, A. (1994). Human immunodeficiency virus Vpx is required for the early phase of replication in peripheral blood mononuclear cells. Microbiol Immunol *38*, 871-878.

Keller, P., and Simons, K. (1998). Cholesterol is required for surface transport of influenza virus hemagglutinin. J Cell Biol *140*, 1357-1367.

Kestler, H.W., 3rd, Ringler, D.J., Mori, K., Panicali, D.L., Sehgal, P.K., Daniel, M.D., and Desrosiers, R.C. (1991). Importance of the nef gene for maintenance of high virus loads and for development of AIDS. Cell *65*, 651-662.

Kewalramani, V.N., and Emerman, M. (1996). Vpx association with mature core structures of HIV-2. Virology *218*, 159-168.

Khan, M.A., Kao, S., Miyagi, E., Takeuchi, H., Goila-Gaur, R., Opi, S., Gipson, C.L., Parslow, T.G., Ly, H., and Strebel, K. (2005). Viral RNA is required for the association of APOBEC3G with human immunodeficiency virus type 1 nucleoprotein complexes. J Virol *79*, 5870-5874.

Kim, E.Y., Busch, M., Abel, K., Fritts, L., Bustamante, P., Stanton, J., Lu, D., Wu, S., Glowczwskie, J., Rourke, T., *et al.* (2005). Retroviral recombination in vivo: viral replication patterns and genetic structure of simian immunodeficiency virus (SIV) populations in rhesus macaques after simultaneous or sequential intravaginal inoculation with SIVmac239Deltavpx/Deltavpr and SIVmac239Deltanef. J Virol *79*, 4886-4895.

Kim, Y.K., Bourgeois, C.F., Isel, C., Churcher, M.J., and Karn, J. (2002). Phosphorylation of the RNA polymerase II carboxyl-terminal domain by CDK9 is directly responsible for human immunodeficiency virus type 1 Tat-activated transcriptional elongation. Mol Cell Biol *22*, 4622-4637.

Kimata, J.T., Gosink, J.J., KewalRamani, V.N., Rudensey, L.M., Littman, D.R., and Overbaugh, J. (1999). Coreceptor specificity of temporal variants of simian immunodeficiency virus Mne. J Virol *73*, 1655-1660.

Kirchhoff, F., Greenough, T.C., Brettler, D.B., Sullivan, J.L., and Desrosiers, R.C. (1995). Brief report: absence of intact nef sequences in a long-term survivor with nonprogressive HIV-1 infection. N Engl J Med *332*, 228-232.

Klimkait, T., Strebel, K., Hoggan, M.D., Martin, M.A., and Orenstein, J.M. (1990). The human immunodeficiency virus type 1-specific protein vpu is required for efficient virus maturation and release. J Virol *64*, 621-629.

Knorr, R., Karacsonyi, C., and Lindner, R. (2009). Endocytosis of MHC molecules by distinct membrane rafts. J Cell Sci *122*, 1584-1594.

Kobayashi, M., Takaori-Kondo, A., Miyauchi, Y., Iwai, K., and Uchiyama, T. (2005). Ubiquitination of APOBEC3G by an HIV-1 Vif-Cullin5-Elongin B-Elongin C complex is essential for Vif function. J Biol Chem *280*, 18573-18578.

Kondo, E., and Gottlinger, H.G. (1996). A conserved LXXLF sequence is the major determinant in p6gag required for the incorporation of human immunodeficiency virus type 1 Vpr. J Virol *70*, 159-164.

Kondo, M., Shima, T., Nishizawa, M., Sudo, K., Iwamuro, S., Okabe, T., Takebe, Y., and Imai, M. (2005). Identification of attenuated variants of HIV-1 circulating recombinant form 01_AE that are associated with slow disease progression due to gross genetic alterations in the nef/long terminal repeat sequences. J Infect Dis *192*, 56-61.

Krambovitis, E., and Spandidos, D.A. (2006). HIV-1 infection: is it time to reconsider our concepts? Int J Mol Med *18*, 3-8.

Kruger, J., and Fischer, W.B. (2008). Exploring the conformational space of Vpu from HIV-1: a versatile adaptable protein. J Comput Chem *29*, 2416-2424.

Kueck, T., Vigan, R., and Neil, S.J. (2010). A conserved ExxxLV-based sorting signal in the Vpu cytoplasmic tail is required for tetherin antagonism and cell-surface downregulation (London, King's College London, Department of Infectious Disease).

Kupzig, S., Korolchuk, V., Rollason, R., Sugden, A., Wilde, A., and Banting, G. (2003). Bst-2/HM1.24 is a raft-associated apical membrane protein with an unusual topology. Traffic *4*, 694-709.

Kusumi, A., and Suzuki, K. (2005). Toward understanding the dynamics of membrane-raft-based molecular interactions. Biochim Biophys Acta *1746*, 234-251.

Kwong, P.D., Wyatt, R., Sattentau, Q.J., Sodroski, J., and Hendrickson, W.A. (2000). Oligomeric modeling and electrostatic analysis of the gp120 envelope glycoprotein of human immunodeficiency virus. J Virol *74*, 1961-1972.

Lang, S.M., Weeger, M., Stahl-Hennig, C., Coulibaly, C., Hunsmann, G., Muller, J., Muller-Hermelink, H., Fuchs, D., Wachter, H., Daniel, M.M., *et al.* (1993). Importance of vpr for infection of rhesus monkeys with simian immunodeficiency virus. J Virol *67*, 902-912.

Le Rouzic, E., Belaidouni, N., Estrabaud, E., Morel, M., Rain, J.C., Transy, C., and Margottin-Goguet, F. (2007). HIV1 Vpr arrests the cell cycle by recruiting DCAF1/VprBP, a receptor of the Cul4-DDB1 ubiquitin ligase. Cell Cycle *6*, 182-188.

Le Rouzic, E., and Benichou, S. (2005). The Vpr protein from HIV-1: distinct roles along the viral life cycle. Retrovirology *2*, 11.

Le Rouzic, E., Mousnier, A., Rustum, C., Stutz, F., Hallberg, E., Dargemont, C., and Benichou, S. (2002). Docking of HIV-1 Vpr to the nuclear envelope is mediated by the interaction with the nucleoporin hCG1. J Biol Chem *277*, 45091-45098.

Lenburg, M.E., and Landau, N.R. (1993). Vpu-induced degradation of CD4: requirement for specific amino acid residues in the cytoplasmic domain of CD4. J Virol *67*, 7238-7245.

Levesque, K., Zhao, Y.S., and Cohen, E.A. (2003). Vpu exerts a positive effect on HIV-1 infectivity by down-modulating CD4 receptor molecules at the surface of HIV-1-producing cells. J Biol Chem *278*, 28346-28353.

Li, J., Lord, C.I., Haseltine, W., Letvin, N.L., and Sodroski, J. (1992). Infection of cynomolgus monkeys with a chimeric HIV-1/SIVmac virus that expresses the HIV-1 envelope glycoproteins. J Acquir Immune Defic Syndr *5*, 639-646.

Li, J.C., Lee, D.C., Cheung, B.K., and Lau, A.S. (2005a). Mechanisms for HIV Tat upregulation of IL-10 and other cytokine expression: kinase signaling and PKR-mediated immune response. FEBS Lett *579*, 3055-3062.

Li, L., Li, H.S., Pauza, C.D., Bukrinsky, M., and Zhao, R.Y. (2005b). Roles of HIV-1 auxiliary proteins in viral pathogenesis and host-pathogen interactions. Cell Res *15*, 923-934.

Li, M., Yang, C., Tong, S., Weidmann, A., and Compans, R.W. (2002). Palmitoylation of the murine leukemia virus envelope protein is critical for lipid raft association and surface expression. J Virol *76*, 11845-11852.

Liao, F., Alkhatib, G., Peden, K.W., Sharma, G., Berger, E.A., and Farber, J.M. (1997). STRL33, A novel chemokine receptor-like protein, functions as a fusion cofactor for both macrophage-tropic and T cell line-tropic HIV-1. J Exp Med *185*, 2015-2023.

Liddament, M.T., Brown, W.L., Schumacher, A.J., and Harris, R.S. (2004). APOBEC3F properties and hypermutation preferences indicate activity against HIV-1 in vivo. Curr Biol *14*, 1385-1391.

Lindwasser, O.W., Smith, W.J., Chaudhuri, R., Yang, P., Hurley, J.H., and Bonifacino, J.S. (2008). A diacidic motif in human immunodeficiency virus type 1 Nef is a novel determinant of binding to AP-2. J Virol *82*, 1166-1174.

Liner, K.J., 2nd, Hall, C.D., and Robertson, K.R. (2007). Impact of human immunodeficiency virus (HIV) subtypes on HIV-associated neurological disease. J Neurovirol *13*, 291-304.

Liu, Z.Q., Muhkerjee, S., Sahni, M., McCormick-Davis, C., Leung, K., Li, Z., Gattone, V.H., 2nd, Tian, C., Doms, R.W., Hoffman, T.L., *et al.* (1999). Derivation and biological characterization of a molecular clone of SHIV(KU-2) that causes AIDS, neurological disease, and renal disease in rhesus macaques. Virology *260*, 295-307.

Lodge, R., Lalonde, J.P., Lemay, G., and Cohen, E.A. (1997). The membrane-proximal intracytoplasmic tyrosine residue of HIV-1 envelope glycoprotein is critical for basolateral targeting of viral budding in MDCK cells. EMBO J *16*, 695-705.

Lopez, C.F., Montal, M., Blasie, J.K., Klein, M.L., and Moore, P.B. (2002). Molecular dynamics investigation of membrane-bound bundles of the channel-forming transmembrane domain of viral protein U from the human immunodeficiency virus HIV-1. Biophys J *83*, 1259-1267.

Lu, M., Blacklow, S.C., and Kim, P.S. (1995). A trimeric structural domain of the HIV-1 transmembrane glycoprotein. Nat Struct Biol *2*, 1075-1082.

Luban, J., Bossolt, K.L., Franke, E.K., Kalpana, G.V., and Goff, S.P. (1993). Human immunodeficiency virus type 1 Gag protein binds to cyclophilins A and B. Cell *73*, 1067-1078.

Lundquist, C.A., Tobiume, M., Zhou, J., Unutmaz, D., and Aiken, C. (2002). Nef-mediated downregulation of CD4 enhances human immunodeficiency virus type 1 replication in primary T lymphocytes. J Virol *76*, 4625-4633.

Luo, K., Liu, B., Xiao, Z., Yu, Y., Yu, X., Gorelick, R., and Yu, X.F. (2004). Amino-terminal region of the human immunodeficiency virus type 1 nucleocapsid is required for human APOBEC3G packaging. J Virol *78*, 11841-11852.

Luo, K., Wang, T., Liu, B., Tian, C., Xiao, Z., Kappes, J., and Yu, X.F. (2007). Cytidine deaminases APOBEC3G and APOBEC3F interact with human immunodeficiency virus type 1 integrase and inhibit proviral DNA formation. J Virol *81*, 7238-7248.

Luo, T., Livingston, R.A., and Garcia, J.V. (1997). Infectivity enhancement by human immunodeficiency virus type 1 Nef is independent of its association with a cellular serine/threonine kinase. J Virol *71*, 9524-9530.

Madani, N., and Kabat, D. (1998). An endogenous inhibitor of human immunodeficiency virus in human lymphocytes is overcome by the viral Vif protein. J Virol *72*, 10251-10255.

Mahalingam, S., Van Tine, B., Santiago, M.L., Gao, F., Shaw, G.M., and Hahn, B.H. (2001). Functional analysis of the simian immunodeficiency virus Vpx protein: identification of packaging determinants and a novel nuclear targeting domain. J Virol *75*, 362-374.

Maldarelli, F., Chen, M.Y., Willey, R.L., and Strebel, K. (1993). Human immunodeficiency virus type 1 Vpu protein is an oligomeric type I integral membrane protein. J Virol *67*, 5056-5061.

Malim, M.H. (2009). APOBEC proteins and intrinsic resistance to HIV-1 infection. Philos Trans R Soc Lond B Biol Sci *364*, 675-687.

Mangasarian, A., Foti, M., Aiken, C., Chin, D., Carpentier, J.L., and Trono, D. (1997). The HIV-1 Nef protein acts as a connector with sorting pathways in the Golgi and at the plasma membrane. Immunity *6*, 67-77.

Mangeat, B., Gers-Huber, G., Lehmann, M., Zufferey, M., Luban, J., and Piguet, V. (2009). HIV-1 Vpu neutralizes the antiviral factor Tetherin/BST-2 by binding it and directing its beta-TrCP2-dependent degradation. PLoS Pathog *5*, e1000574.

Mangeat, B., Turelli, P., Caron, G., Friedli, M., Perrin, L., and Trono, D. (2003). Broad antiretroviral defence by human APOBEC3G through lethal editing of nascent reverse transcripts. Nature *424*, 99-103.

Manie, S.N., de Breyne, S., Vincent, S., and Gerlier, D. (2000). Measles virus structural components are enriched into lipid raft microdomains: a potential cellular location for virus assembly. J Virol *74*, 305-311.

Mansouri, M., Viswanathan, K., Douglas, J.L., Hines, J., Gustin, J., Moses, A.V., and Fruh, K. (2009). Molecular mechanism of BST2/tetherin downregulation by K5/MIR2 of Kaposi's sarcoma-associated herpesvirus. J Virol *83*, 9672-9681.

Margottin, F., Bour, S.P., Durand, H., Selig, L., Benichou, S., Richard, V., Thomas, D., Strebel, K., and Benarous, R. (1998). A novel human WD protein, h-beta TrCp, that interacts with HIV-1 Vpu connects CD4 to the ER degradation pathway through an F-box motif. Mol Cell *1*, 565-574.

Mariani, R., Chen, D., Schrofelbauer, B., Navarro, F., Konig, R., Bollman, B., Munk, C., Nymark-McMahon, H., and Landau, N.R. (2003). Species-specific exclusion of APOBEC3G from HIV-1 virions by Vif. Cell *114*, 21-31.

Marin, M., Rose, K.M., Kozak, S.L., and Kabat, D. (2003). HIV-1 Vif protein binds the editing enzyme APOBEC3G and induces its degradation. Nat Med *9*, 1398-1403.

Marshall, H.M., Ronen, K., Berry, C., Llano, M., Sutherland, H., Saenz, D., Bickmore, W., Poeschla, E., and Bushman, F.D. (2007). Role of PSIP1/LEDGF/p75 in lentiviral infectivity and integration targeting. PLoS One *2*, e1340.

Martin-Serrano, J., Zang, T., and Bieniasz, P.D. (2003). Role of ESCRT-I in retroviral budding. J Virol *77*, 4794-4804.

Martinez-Cajas, J.L., Pant-Pai, N., Klein, M.B., and Wainberg, M.A. (2008). Role of genetic diversity amongst HIV-1 non-B subtypes in drug resistance: a systematic review of virologic and biochemical evidence. AIDS Rev *10*, 212-223.

Martinez-Cajas, J.L., and Wainberg, M.A. (2008). Antiretroviral therapy : optimal sequencing of therapy to avoid resistance. Drugs *68*, 43-72.

Marty, A., Meanger, J., Mills, J., Shields, B., and Ghildyal, R. (2004). Association of matrix protein of respiratory syncytial virus with the host cell membrane of infected cells. Arch Virol *149*, 199-210.

Masuyama, N., Kuronita, T., Tanaka, R., Muto, T., Hirota, Y., Takigawa, A., Fujita, H., Aso, Y., Amano, J., and Tanaka, Y. (2009). HM1.24 is internalized from lipid rafts by clathrin-mediated endocytosis through interaction with alpha-adaptin. J Biol Chem *284*, 15927-15941.

Matter, K., Yamamoto, E.M., and Mellman, I. (1994). Structural requirements and sequence motifs for polarized sorting and endocytosis of LDL and Fc receptors in MDCK cells. J Cell Biol *126*, 991-1004.

McCormick-Davis, C., Dalton, S.B., Hout, D.R., Singh, D.K., Berman, N.E., Yong, C., Pinson, D.M., Foresman, L., and Stephens, E.B. (2000a). A molecular clone of simian-human immunodeficiency virus (DeltavpuSHIV(KU-1bMC33)) with a truncated, non-membrane-bound vpu results in rapid CD4(+) T cell loss and neuro-AIDS in pig-tailed macaques. Virology *272*, 112-126.

McCormick-Davis, C., Dalton, S.B., Singh, D.K., and Stephens, E.B. (2000b). Comparison of Vpu sequences from diverse geographical isolates of HIV type 1 identifies the presence of highly

variable domains, additional invariant amino acids, and a signature sequence motif common to subtype C isolates. AIDS Res Hum Retroviruses *16*, 1089-1095.

McCormick-Davis, C., Zhao, L.J., Mukherjee, S., Leung, K., Sheffer, D., Joag, S.V., Narayan, O., and Stephens, E.B. (1998). Chronology of genetic changes in the vpu, env, and Nef genes of chimeric simian-human immunodeficiency virus (strain HXB2) during acquisition of virulence for pig-tailed macaques. Virology *248*, 275-283.

McCullough, J., Fisher, R.D., Whitby, F.G., Sundquist, W.I., and Hill, C.P. (2008). ALIX-CHMP4 interactions in the human ESCRT pathway. Proc Natl Acad Sci U S A *105*, 7687-7691.
McCutchan, F.E. (2006). Global epidemiology of HIV. J Med Virol *78 Suppl 1*, S7-S12.

McDonald, B., and Martin-Serrano, J. (2009). No strings attached: the ESCRT machinery in viral budding and cytokinesis. J Cell Sci *122*, 2167-2177.

McNatt, M.W., Zang, T., Hatziioannou, T., Bartlett, M., Fofana, I.B., Johnson, W.E., Neil, S.J., and Bieniasz, P.D. (2009). Species-specific activity of HIV-1 Vpu and positive selection of tetherin transmembrane domain variants. PLoS Pathog *5*, e1000300.

Medigeshi, G.R., Hirsch, A.J., Streblow, D.N., Nikolich-Zugich, J., and Nelson, J.A. (2008). West Nile virus entry requires cholesterol-rich membrane microdomains and is independent of alphavbeta3 integrin. J Virol *82*, 5212-5219.

Megy, S., Bertho, G., Gharbi-Benarous, J., Evrard-Todeschi, N., Coadou, G., Segeral, E., Iehle, C., Quemeneur, E., Benarous, R., and Girault, J.P. (2005). STD and TRNOESY NMR studies on the conformation of the oncogenic protein beta-catenin containing the phosphorylated motif DpSGXXpS bound to the beta-TrCP protein. J Biol Chem *280*, 29107-29116.

Mehle, A., Goncalves, J., Santa-Marta, M., McPike, M., and Gabuzda, D. (2004a). Phosphorylation of a novel SOCS-box regulates assembly of the HIV-1 Vif-Cul5 complex that promotes APOBEC3G degradation. Genes Dev *18*, 2861-2866.

Mehle, A., Strack, B., Ancuta, P., Zhang, C., McPike, M., and Gabuzda, D. (2004b). Vif overcomes the innate antiviral activity of APOBEC3G by promoting its degradation in the ubiquitin-proteasome pathway. J Biol Chem *279*, 7792-7798.

Melikyan, G.B., Markosyan, R.M., Hemmati, H., Delmedico, M.K., Lambert, D.M., and Cohen, F.S. (2000). Evidence that the transition of HIV-1 gp41 into a six-helix bundle, not the bundle configuration, induces membrane fusion. J Cell Biol *151*, 413-423.

Meusser, B., and Sommer, T. (2004). Vpu-mediated degradation of CD4 reconstituted in yeast reveals mechanistic differences to cellular ER-associated protein degradation. Mol Cell *14*, 247-258.

Meuth, S.G., Bittner, S., Meuth, P., Simon, O.J., Budde, T., and Wiendl, H. (2008). TWIK-related acid-sensitive K+ channel 1 (TASK1) and TASK3 critically influence T lymphocyte effector functions. J Biol Chem *283*, 14559-14570.

Miller, M.D., Warmerdam, M.T., Gaston, I., Greene, W.C., and Feinberg, M.B. (1994). The human immunodeficiency virus-1 nef gene product: a positive factor for viral infection and replication in primary lymphocytes and macrophages. J Exp Med *179*, 101-113.

Miranda, K.C., Khromykh, T., Christy, P., Le, T.L., Gottardi, C.J., Yap, A.S., Stow, J.L., and Teasdale, R.D. (2001). A dileucine motif targets E-cadherin to the basolateral cell surface in Madin-Darby canine kidney and LLC-PK1 epithelial cells. J Biol Chem *276*, 22565-22572.

Mitchell, R.S., Katsura, C., Skasko, M.A., Fitzpatrick, K., Lau, D., Ruiz, A., Stephens, E.B., Margottin-Goguet, F., Benarous, R., and Guatelli, J.C. (2009). Vpu antagonizes BST-2-mediated restriction of HIV-1 release via beta-TrCP and endo-lysosomal trafficking. PLoS Pathog *5*, e1000450.

Miyagi, E., Andrew, A.J., Kao, S., and Strebel, K. (2009). Vpu enhances HIV-1 virus release in the absence of Bst-2 cell surface down-modulation and intracellular depletion. Proc Natl Acad Sci U S A *106*, 2868-2873.

Morita, E., and Sundquist, W.I. (2004). Retrovirus budding. Annu Rev Cell Dev Biol *20*, 395-425.

Moulard, M., Lortat-Jacob, H., Mondor, I., Roca, G., Wyatt, R., Sodroski, J., Zhao, L., Olson, W., Kwong, P.D., and Sattentau, Q.J. (2000). Selective interactions of polyanions with basic surfaces on human immunodeficiency virus type 1 gp120. J Virol *74*, 1948-1960.

Narayan, O., Zink, M.C., Huso, D., Sheffer, D., Crane, S., Kennedy-Stoskopf, S., Jolly, P.E., and Clements, J.E. (1988). Lentiviruses of animals are biological models of the human immunodeficiency viruses. Microb Pathog *5*, 149-157.

Narayan, S.V., Mukherjee, S., Jia, F., Li, Z., Wang, C., Foresman, L., McCormick-Davis, C., Stephens, E.B., Joag, S.V., and Narayan, O. (1999). Characterization of a neutralization-escape variant of SHIVKU-1, a virus that causes acquired immune deficiency syndrome in pig-tailed macaques. Virology *256*, 54-63.

Navarro, F., Bollman, B., Chen, H., Konig, R., Yu, Q., Chiles, K., and Landau, N.R. (2005). Complementary function of the two catalytic domains of APOBEC3G. Virology *333*, 374-386.

Ndung'u, T., Lu, Y., Renjifo, B., Touzjian, N., Kushner, N., Pena-Cruz, V., Novitsky, V.A., Lee, T.H., and Essex, M. (2001). Infectious simian/human immunodeficiency virus with human immunodeficiency virus type 1 subtype C from an African isolate: rhesus macaque model. J Virol *75*, 11417-11425.

Neil, S.J., Zang, T., and Bieniasz, P.D. (2008). Tetherin inhibits retrovirus release and is antagonized by HIV-1 Vpu. Nature *451*, 425-430.

Neilson, J.R., John, G.C., Carr, J.K., Lewis, P., Kreiss, J.K., Jackson, S., Nduati, R.W., Mbori-Ngacha, D., Panteleeff, D.D., Bodrug, S., *et al.* (1999). Subtypes of human immunodeficiency virus type 1 and disease stage among women in Nairobi, Kenya. J Virol *73*, 4393-4403.

Newman, E.N., Holmes, R.K., Craig, H.M., Klein, K.C., Lingappa, J.R., Malim, M.H., and Sheehy, A.M. (2005). Antiviral function of APOBEC3G can be dissociated from cytidine deaminase activity. Curr Biol *15*, 166-170.

Nguyen, D.H., and Hildreth, J.E. (2000). Evidence for budding of human immunodeficiency virus type 1 selectively from glycolipid-enriched membrane lipid rafts. J Virol *74*, 3264-3272.

Nguyen, K.L., llano, M., Akari, H., Miyagi, E., Poeschla, E.M., Strebel, K., and Bour, S. (2004). Codon optimization of the HIV-1 vpu and vif genes stabilizes their mRNA and allows for highly efficient Rev-independent expression. Virology *319*, 163-175.

Nisole, S., Stoye, J.P., and Saib, A. (2005). TRIM family proteins: retroviral restriction and antiviral defence. Nat Rev Microbiol *3*, 799-808.

Noviello, C.M., Benichou, S., and Guatelli, J.C. (2008). Cooperative binding of the class I major histocompatibility complex cytoplasmic domain and human immunodeficiency virus type 1 Nef to the endosomal AP-1 complex via its mu subunit. J Virol *82*, 1249-1258.

OhAinle, M., Kerns, J.A., Malik, H.S., and Emerman, M. (2006). Adaptive evolution and antiviral activity of the conserved mammalian cytidine deaminase APOBEC3H. J Virol *80*, 3853-3862.

Okada, A., Miura, T., and Takeuchi, H. (2001). Protonation of histidine and histidine-tryptophan interaction in the activation of the M2 ion channel from influenza a virus. Biochemistry *40*, 6053-6060.

Oliveira, D.C., Wu, S.W., and de Lencastre, H. (2000). Genetic organization of the downstream region of the mecA element in methicillin-resistant Staphylococcus aureus isolates carrying different polymorphisms of this region. Antimicrob Agents Chemother *44*, 1906-1910.

Ono, A. (2009). HIV-1 Assembly at the Plasma Membrane: Gag Trafficking and Localization. Future Virol *4*, 241-257.

Ono, A., Ablan, S.D., Lockett, S.J., Nagashima, K., and Freed, E.O. (2004). Phosphatidylinositol (4,5) bisphosphate regulates HIV-1 Gag targeting to the plasma membrane. Proc Natl Acad Sci U S A *101*, 14889-14894.

Ono, A., and Freed, E.O. (2001). Plasma membrane rafts play a critical role in HIV-1 assembly and release. Proc Natl Acad Sci U S A *98*, 13925-13930.

Ono, A., and Freed, E.O. (2004). Cell-type-dependent targeting of human immunodeficiency virus type 1 assembly to the plasma membrane and the multivesicular body. J Virol *78*, 1552-1563.

Orenstein, J.M., Meltzer, M.S., Phipps, T., and Gendelman, H.E. (1988). Cytoplasmic assembly and accumulation of human immunodeficiency virus types 1 and 2 in recombinant human colony-stimulating factor-1-treated human monocytes: an ultrastructural study. J Virol *62*, 2578-2586.

Pacyniak, E., Gomez, M.L., Gomez, L.M., Mulcahy, E.R., Jackson, M., Hout, D.R., Wisdom, B.J., and Stephens, E.B. (2005). Identification of a region within the cytoplasmic domain of the subtype B Vpu protein of human immunodeficiency virus type 1 (HIV-1) that is responsible for retention in the golgi complex and its absence in the Vpu protein from a subtype C HIV-1. AIDS Res Hum Retroviruses *21*, 379-394.

Pagans, S., Pedal, A., North, B.J., Kaehlcke, K., Marshall, B.L., Dorr, A., Hetzer-Egger, C., Henklein, P., Frye, R., McBurney, M.W., *et al.* (2005). SIRT1 regulates HIV transcription via Tat deacetylation. PLoS Biol *3*, e41.

Palmer, S., Alaeus, A., Albert, J., and Cox, S. (1998). Drug susceptibility of subtypes A,B,C,D, and E human immunodeficiency virus type 1 primary isolates. AIDS Res Hum Retroviruses *14*, 157-162.

Pantophlet, R., and Burton, D.R. (2006). GP120: target for neutralizing HIV-1 antibodies. Annu Rev Immunol *24*, 739-769.

Park, S.H., Mrse, A.A., Nevzorov, A.A., Mesleh, M.F., Oblatt-Montal, M., Montal, M., and Opella, S.J. (2003). Three-dimensional structure of the channel-forming trans-membrane domain of virus protein "u" (Vpu) from HIV-1. J Mol Biol *333*, 409-424.

Park, S.H., and Opella, S.J. (2005). Tilt angle of a trans-membrane helix is determined by hydrophobic mismatch. J Mol Biol *350*, 310-318.

Patil, A., Gautam, A., and Bhattacharya, J. (2010). Evidence that Gag facilitates HIV-1 envelope association both in GPI-enriched plasma membrane and detergent resistant membranes and facilitates envelope incorporation onto virions in primary CD4+ T cells. Virol J *7*, 3.

Paul, M., and Jabbar, M.A. (1997). Phosphorylation of both phosphoacceptor sites in the HIV-1 Vpu cytoplasmic domain is essential for Vpu-mediated ER degradation of CD4. Virology *232*, 207-216.

Paxton, W., Connor, R.I., and Landau, N.R. (1993). Incorporation of Vpr into human immunodeficiency virus type 1 virions: requirement for the p6 region of gag and mutational analysis. J Virol *67*, 7229-7237.

Perez-Caballero, D., Zang, T., Ebrahimi, A., McNatt, M.W., Gregory, D.A., Johnson, M.C., and Bieniasz, P.D. (2009). Tetherin inhibits HIV-1 release by directly tethering virions to cells. Cell *139*, 499-511.

Piguet, V., Chen, Y.L., Mangasarian, A., Foti, M., Carpentier, J.L., and Trono, D. (1998). Mechanism of Nef-induced CD4 endocytosis: Nef connects CD4 with the mu chain of adaptor complexes. EMBO J *17*, 2472-2481.

Piguet, V., Gu, F., Foti, M., Demaurex, N., Gruenberg, J., Carpentier, J.L., and Trono, D. (1999a). Nef-induced CD4 degradation: a diacidic-based motif in Nef functions as a lysosomal targeting signal through the binding of beta-COP in endosomes. Cell *97*, 63-73.

Piguet, V., Schwartz, O., Le Gall, S., and Trono, D. (1999b). The downregulation of CD4 and MHC-I by primate lentiviruses: a paradigm for the modulation of cell surface receptors. Immunol Rev *168*, 51-63.

Pinto, L.H., Holsinger, L.J., and Lamb, R.A. (1992). Influenza virus M2 protein has ion channel activity. Cell *69*, 517-528.

Pizzato, M., Helander, A., Popova, E., Calistri, A., Zamborlini, A., Palu, G., and Gottlinger, H.G. (2007). Dynamin 2 is required for the enhancement of HIV-1 infectivity by Nef. Proc Natl Acad Sci U S A *104*, 6812-6817.

Poignard, P., Saphire, E.O., Parren, P.W., and Burton, D.R. (2001). gp120: Biologic aspects of structural features. Annu Rev Immunol *19*, 253-274.

Poonpiriya, V., Sungkanuparph, S., Leechanachai, P., Pasomsub, E., Watitpun, C., Chunhakan, S., and Chantratita, W. (2008). A study of seven rule-based algorithms for the interpretation of HIV-1 genotypic resistance data in Thailand. J Virol Methods *151*, 79-86.

Pralle, A., Keller, P., Florin, E.L., Simons, K., and Horber, J.K. (2000). Sphingolipid-cholesterol rafts diffuse as small entities in the plasma membrane of mammalian cells. J Cell Biol *148*, 997-1008.

Prior, I.A., Muncke, C., Parton, R.G., and Hancock, J.F. (2003). Direct visualization of Ras proteins in spatially distinct cell surface microdomains. J Cell Biol *160*, 165-170.

Qi, M., and Aiken, C. (2007). Selective restriction of Nef-defective human immunodeficiency virus type 1 by a proteasome-dependent mechanism. J Virol *81*, 1534-1536.

Qi, M., and Aiken, C. (2008). Nef enhances HIV-1 infectivity via association with the virus assembly complex. Virology *373*, 287-297.

Quinones-Mateu, M.E., Ball, S.C., Marozsan, A.J., Torre, V.S., Albright, J.L., Vanham, G., van Der Groen, G., Colebunders, R.L., and Arts, E.J. (2000). A dual infection/competition assay

shows a correlation between ex vivo human immunodeficiency virus type 1 fitness and disease progression. J Virol *74*, 9222-9233.

Raghavan, R., Stephens, E.B., Joag, S.V., Adany, I., Pinson, D.M., Li, Z., Jia, F., Sahni, M., Wang, C., Leung, K., *et al.* (1997). Neuropathogenesis of chimeric simian/human immunodeficiency virus infection in pig-tailed and rhesus macaques. Brain Pathol *7*, 851-861.

Ramanathan, M.P., Curley, E., 3rd, Su, M., Chambers, J.A., and Weiner, D.B. (2002). Carboxyl terminus of hVIP/mov34 is critical for HIV-1-Vpr interaction and glucocorticoid-mediated signaling. J Biol Chem *277*, 47854-47860.

Rao, T.K. (1991). Human immunodeficiency virus (HIV) associated nephropathy. Annu Rev Med *42*, 391-401.

Reeves, J.D., and Doms, R.W. (2002). Human immunodeficiency virus type 2. J Gen Virol *83*, 1253-1265.

Reeves, J.D., Hibbitts, S., Simmons, G., McKnight, A., Azevedo-Pereira, J.M., Moniz-Pereira, J., and Clapham, P.R. (1999). Primary human immunodeficiency virus type 2 (HIV-2) isolates infect CD4-negative cells via CCR5 and CXCR4: comparison with HIV-1 and simian immunodeficiency virus and relevance to cell tropism in vivo. J Virol *73*, 7795-7804.

Renjifo, B., Chaplin, B., Mwakagile, D., Shah, P., Vannberg, F., Msamanga, G., Hunter, D., Fawzi, W., and Essex, M. (1998). Epidemic expansion of HIV type 1 subtype C and recombinant genotypes in Tanzania. AIDS Res Hum Retroviruses *14*, 635-638.

Renkema, G.H., Manninen, A., Mann, D.A., Harris, M., and Saksela, K. (1999). Identification of the Nef-associated kinase as p21-activated kinase 2. Curr Biol *9*, 1407-1410.

Rinaldo, C., Huang, X.L., Fan, Z.F., Ding, M., Beltz, L., Logar, A., Panicali, D., Mazzara, G., Liebmann, J., Cottrill, M., *et al.* (1995). High levels of anti-human immunodeficiency virus type 1 (HIV-1) memory cytotoxic T-lymphocyte activity and low viral load are associated with lack of disease in HIV-1-infected long-term nonprogressors. J Virol *69*, 5838-5842.

Robertson, D.L., Anderson, J.P., Bradac, J.A., Carr, J.K., Foley, B., Funkhouser, R.K., Gao, F., Hahn, B.H., Kalish, M.L., Kuiken, C., *et al.* (2000). HIV-1 nomenclature proposal. Science *288*, 55-56.

Robinson, M.S., and Bonifacino, J.S. (2001). Adaptor-related proteins. Curr Opin Cell Biol *13*, 444-453.

Roeth, J.F., Williams, M., Kasper, M.R., Filzen, T.M., and Collins, K.L. (2004). HIV-1 Nef disrupts MHC-I trafficking by recruiting AP-1 to the MHC-I cytoplasmic tail. J Cell Biol *167*, 903-913.

Rogel, M.E., Wu, L.I., and Emerman, M. (1995). The human immunodeficiency virus type 1 vpr gene prevents cell proliferation during chronic infection. J Virol *69*, 882-888.

Rollason, R., Korolchuk, V., Hamilton, C., Jepson, M., and Banting, G. (2009). A CD317/tetherin-RICH2 complex plays a critical role in the organization of the subapical actin cytoskeleton in polarized epithelial cells. J Cell Biol *184*, 721-736.

Rollason, R., Korolchuk, V., Hamilton, C., Schu, P., and Banting, G. (2007). Clathrin-mediated endocytosis of a lipid-raft-associated protein is mediated through a dual tyrosine motif. J Cell Sci *120*, 3850-3858.

Romani, B., Engelbrecht, S., and Glashoff, R.H. (2010). Functions of Tat: the versatile protein of human immunodeficiency virus type 1. J Gen Virol *91*, 1-12.

Rong, L., Zhang, J., Lu, J., Pan, Q., Lorgeoux, R.P., Aloysius, C., Guo, F., Liu, S.L., Wainberg, M.A., and Liang, C. (2009). The transmembrane domain of BST-2 determines its sensitivity to down-modulation by human immunodeficiency virus type 1 Vpu. J Virol *83*, 7536-7546.

Ross, E.K., Buckler-White, A.J., Rabson, A.B., Englund, G., and Martin, M.A. (1991). Contribution of NF-kappa B and Sp1 binding motifs to the replicative capacity of human immunodeficiency virus type 1: distinct patterns of viral growth are determined by T-cell types. J Virol *65*, 4350-4358.

Rossi, A., Mukerjee, R., Ferrante, P., Khalili, K., Amini, S., and Sawaya, B.E. (2006). Human immunodeficiency virus type 1 Tat prevents dephosphorylation of Sp1 by TCF-4 in astrocytes. J Gen Virol *87*, 1613-1623.

Rousso, I., Mixon, M.B., Chen, B.K., and Kim, P.S. (2000). Palmitoylation of the HIV-1 envelope glycoprotein is critical for viral infectivity. Proc Natl Acad Sci U S A *97*, 13523-13525.

Rudner, L., Nydegger, S., Coren, L.V., Nagashima, K., Thali, M., and Ott, D.E. (2005). Dynamic fluorescent imaging of human immunodeficiency virus type 1 gag in live cells by biarsenical labeling. J Virol *79*, 4055-4065.

Ruiz, A., Guatelli, J.C., and Stephens, E.B. (2010a). The Vpu protein: new concepts in virus release and CD4 down-modulation. Curr HIV Res *8*, 240-252.

Ruiz, A., Hill, M.S., Schmitt, K., Guatelli, J., and Stephens, E.B. (2008). Requirements of the membrane proximal tyrosine and dileucine-based sorting signals for efficient transport of the subtype C Vpu protein to the plasma membrane and in virus release. Virology *378*, 58-68.

Ruiz, A., Lau, D., Mitchell, R.S., Hill, M.S., Schmitt, K., Guatelli, J.C., and Stephens, E.B. (2010b). BST-2 mediated restriction of simian-human immunodeficiency virus. Virology *406*, 312-321.

Ryser, H.J., and Fluckiger, R. (2005). Progress in targeting HIV-1 entry. Drug Discov Today *10*, 1085-1094.

Saad, J.S., Miller, J., Tai, J., Kim, A., Ghanam, R.H., and Summers, M.F. (2006). Structural basis for targeting HIV-1 Gag proteins to the plasma membrane for virus assembly. Proc Natl Acad Sci U S A *103*, 11364-11369.

Salvi, R., Garbuglia, A.R., Di Caro, A., Pulciani, S., Montella, F., and Benedetto, A. (1998). Grossly defective nef gene sequences in a human immunodeficiency virus type 1-seropositive long-term nonprogressor. J Virol *72*, 3646-3657.

Sansom, M.S., Forrest, L.R., and Bull, R. (1998). Viral ion channels: molecular modeling and simulation. Bioessays *20*, 992-1000.

Sauter, D., Schindler, M., Specht, A., Landford, W.N., Munch, J., Kim, K.A., Votteler, J., Schubert, U., Bibollet-Ruche, F., Keele, B.F., *et al.* (2009). Tetherin-driven adaptation of Vpu and Nef function and the evolution of pandemic and nonpandemic HIV-1 strains. Cell Host Microbe *6*, 409-421.

Sawaya, B.E., Khalili, K., Gordon, J., Taube, R., and Amini, S. (2000). Cooperative interaction between HIV-1 regulatory proteins Tat and Vpr modulates transcription of the viral genome. J Biol Chem *275*, 35209-35214.

Sayah, D.M., and Luban, J. (2004). Selection for loss of Ref1 activity in human cells releases human immunodeficiency virus type 1 from cyclophilin A dependence during infection. J Virol *78*, 12066-12070.

Schafer, A., Bogerd, H.P., and Cullen, B.R. (2004). Specific packaging of APOBEC3G into HIV-1 virions is mediated by the nucleocapsid domain of the gag polyprotein precursor. Virology *328*, 163-168.

Scheiffele, P., Rietveld, A., Wilk, T., and Simons, K. (1999). Influenza viruses select ordered lipid domains during budding from the plasma membrane. J Biol Chem *274*, 2038-2044.

Schindler, M., Munch, J., Kutsch, O., Li, H., Santiago, M.L., Bibollet-Ruche, F., Muller-Trutwin, M.C., Novembre, F.J., Peeters, M., Courgnaud, V., *et al.* (2006). Nef-mediated suppression of T cell activation was lost in a lentiviral lineage that gave rise to HIV-1. Cell *125*, 1055-1067.

Schindler, M., Rajan, D., Banning, C., Wimmer, P., Koppensteiner, H., Iwanski, A., Specht, A., Sauter, D., Dobner, T., and Kirchhoff, F. (2010). Vpu serine 52 dependent counteraction of tetherin is required for HIV-1 replication in macrophages, but not in ex vivo human lymphoid tissue. Retrovirology *7*, 1.

Schrofelbauer, B., Hakata, Y., and Landau, N.R. (2007). HIV-1 Vpr function is mediated by interaction with the damage-specific DNA-binding protein DDB1. Proc Natl Acad Sci U S A *104*, 4130-4135.

Schrofelbauer, B., Yu, Q., Zeitlin, S.G., and Landau, N.R. (2005). Human immunodeficiency virus type 1 Vpr induces the degradation of the UNG and SMUG uracil-DNA glycosylases. J Virol *79*, 10978-10987.

Schubert, U., Anton, L.C., Bacik, I., Cox, J.H., Bour, S., Bennink, J.R., Orlowski, M., Strebel, K., and Yewdell, J.W. (1998). CD4 glycoprotein degradation induced by human immunodeficiency virus type 1 Vpu protein requires the function of proteasomes and the ubiquitin-conjugating pathway. J Virol *72*, 2280-2288.

Schubert, U., Bour, S., Ferrer-Montiel, A.V., Montal, M., Maldarell, F., and Strebel, K. (1996a). The two biological activities of human immunodeficiency virus type 1 Vpu protein involve two separable structural domains. J Virol *70*, 809-819.

Schubert, U., Ferrer-Montiel, A.V., Oblatt-Montal, M., Henklein, P., Strebel, K., and Montal, M. (1996b). Identification of an ion channel activity of the Vpu transmembrane domain and its involvement in the regulation of virus release from HIV-1-infected cells. FEBS Lett *398*, 12-18.

Schubert, U., Henklein, P., Boldyreff, B., Wingender, E., Strebel, K., and Porstmann, T. (1994). The human immunodeficiency virus type 1 encoded Vpu protein is phosphorylated by casein kinase-2 (CK-2) at positions Ser52 and Ser56 within a predicted alpha-helix-turn-alpha-helix-motif. J Mol Biol *236*, 16-25.

Schubert, U., Schneider, T., Henklein, P., Hoffmann, K., Berthold, E., Hauser, H., Pauli, G., and Porstmann, T. (1992). Human-immunodeficiency-virus-type-1-encoded Vpu protein is phosphorylated by casein kinase II. Eur J Biochem *204*, 875-883.

Schubert, U., and Strebel, K. (1994). Differential activities of the human immunodeficiency virus type 1-encoded Vpu protein are regulated by phosphorylation and occur in different cellular compartments. J Virol *68*, 2260-2271.

Schuck, S., Honsho, M., Ekroos, K., Shevchenko, A., and Simons, K. (2003). Resistance of cell membranes to different detergents. Proc Natl Acad Sci U S A *100*, 5795-5800.

Schwartz, O., Marechal, V., Le Gall, S., Lemonnier, F., and Heard, J.M. (1996). Endocytosis of major histocompatibility complex class I molecules is induced by the HIV-1 Nef protein. Nat Med *2*, 338-342.

Seelamgari, A., Maddukuri, A., Berro, R., de la Fuente, C., Kehn, K., Deng, L., Dadgar, S., Bottazzi, M.E., Ghedin, E., Pumfery, A., *et al.* (2004). Role of viral regulatory and accessory proteins in HIV-1 replication. Front Biosci *9*, 2388-2413.

Sharma, P., Varma, R., Sarasij, R.C., Ira, Gousset, K., Krishnamoorthy, G., Rao, M., and Mayor, S. (2004). Nanoscale organization of multiple GPI-anchored proteins in living cell membranes. Cell *116*, 577-589.

Sharova, N., Wu, Y., Zhu, X., Stranska, R., Kaushik, R., Sharkey, M., and Stevenson, M. (2008). Primate lentiviral Vpx commandeers DDB1 to counteract a macrophage restriction. PLoS Pathog *4*, e1000057.

Sharp, P.M., Robertson, D.L., and Hahn, B.H. (1995). Cross-species transmission and recombination of 'AIDS' viruses. Philos Trans R Soc Lond B Biol Sci *349*, 41-47.

Sheehy, A.M., Gaddis, N.C., Choi, J.D., and Malim, M.H. (2002). Isolation of a human gene that inhibits HIV-1 infection and is suppressed by the viral Vif protein. Nature *418*, 646-650.

Sheehy, A.M., Gaddis, N.C., and Malim, M.H. (2003). The antiretroviral enzyme APOBEC3G is degraded by the proteasome in response to HIV-1 Vif. Nat Med *9*, 1404-1407.

Sherman, M.P., De Noronha, C.M., Williams, S.A., and Greene, W.C. (2002). Insights into the biology of HIV-1 viral protein R. DNA Cell Biol *21*, 679-688.

Sherman, M.P., and Greene, W.C. (2002). Slipping through the door: HIV entry into the nucleus. Microbes Infect *4*, 67-73.

Shibata, R., Maldarelli, F., Siemon, C., Matano, T., Parta, M., Miller, G., Fredrickson, T., and Martin, M.A. (1997). Infection and pathogenicity of chimeric simian-human immunodeficiency viruses in macaques: determinants of high virus loads and CD4 cell killing. J Infect Dis *176*, 362-373.

Shogomori, H., and Brown, D.A. (2003). Use of detergents to study membrane rafts: the good, the bad, and the ugly. Biol Chem *384*, 1259-1263.

Simmons, A., Aluvihare, V., and McMichael, A. (2001). Nef triggers a transcriptional program in T cells imitating single-signal T cell activation and inducing HIV virulence mediators. Immunity *14*, 763-777.

Simon, F., Mauclere, P., Roques, P., Loussert-Ajaka, I., Muller-Trutwin, M.C., Saragosti, S., Georges-Courbot, M.C., Barre-Sinoussi, F., and Brun-Vezinet, F. (1998a). Identification of a new human immunodeficiency virus type 1 distinct from group M and group O. Nat Med *4*, 1032-1037.

Simon, J.H., Gaddis, N.C., Fouchier, R.A., and Malim, M.H. (1998b). Evidence for a newly discovered cellular anti-HIV-1 phenotype. Nat Med *4*, 1397-1400.

Simon, J.H., and Malim, M.H. (1996). The human immunodeficiency virus type 1 Vif protein modulates the postpenetration stability of viral nucleoprotein complexes. J Virol *70*, 5297-5305.

Simon, J.H., Miller, D.L., Fouchier, R.A., Soares, M.A., Peden, K.W., and Malim, M.H. (1998c). The regulation of primate immunodeficiency virus infectivity by Vif is cell species restricted: a role for Vif in determining virus host range and cross-species transmission. EMBO J *17*, 1259-1267.

Simons, K., and van Meer, G. (1988). Lipid sorting in epithelial cells. Biochemistry *27*, 6197-6202.

Singh, D.K., Griffin, D.M., Pacyniak, E., Jackson, M., Werle, M.J., Wisdom, B., Sun, F., Hout, D.R., Pinson, D.M., Gunderson, R.S., *et al.* (2003). The presence of the casein kinase II phosphorylation sites of Vpu enhances the CD4(+) T cell loss caused by the simian-human immunodeficiency virus SHIV(KU-lbMC33) in pig-tailed macaques. Virology *313*, 435-451.

Singh, D.K., McCormick, C., Pacyniak, E., Lawrence, K., Dalton, S.B., Pinson, D.M., Sun, F., Berman, N.E., Calvert, M., Gunderson, R.S., *et al.* (2001). A simian human immunodeficiency virus with a nonfunctional Vpu (deltavpuSHIV(KU-1bMC33)) isolated from a macaque with neuroAIDS has selected for mutations in env and nef that contributed to its pathogenic phenotype. Virology *282*, 123-140.

Smit, T.K., Wang, B., Ng, T., Osborne, R., Brew, B., and Saksena, N.K. (2001). Varied tropism of HIV-1 isolates derived from different regions of adult brain cortex discriminate between patients with and without AIDS dementia complex (ADC): evidence for neurotropic HIV variants. Virology *279*, 509-526.

Snoeck, J., Kantor, R., Shafer, R.W., Van Laethem, K., Deforche, K., Carvalho, A.P., Wynhoven, B., Soares, M.A., Cane, P., Clarke, J., *et al.* (2006). Discordances between interpretation algorithms for genotypic resistance to protease and reverse transcriptase inhibitors of human immunodeficiency virus are subtype dependent. Antimicrob Agents Chemother *50*, 694-701.

Sova, P., and Volsky, D.J. (1993). Efficiency of viral DNA synthesis during infection of permissive and nonpermissive cells with vif-negative human immunodeficiency virus type 1. J Virol *67*, 6322-6326.

Sramala, I., Lemaitre, V., Faraldo-Gomez, J.D., Vincent, S., Watts, A., and Fischer, W.B. (2003). Molecular dynamics simulations on the first two helices of Vpu from HIV-1. Biophys J *84*, 3276-3284.

Srivastava, S., Swanson, S.K., Manel, N., Florens, L., Washburn, M.P., and Skowronski, J. (2008). Lentiviral Vpx accessory factor targets VprBP/DCAF1 substrate adaptor for cullin 4 E3 ubiquitin ligase to enable macrophage infection. PLoS Pathog *4*, e1000059.

Stephens, E.B., McClure, H.M., and Narayan, O. (1995). The proteins of lymphocyte- and macrophage-tropic strains of simian immunodeficiency virus are processed differently in macrophages. Virology *206*, 535-544.

Stephens, E.B., McCormick, C., Pacyniak, E., Griffin, D., Pinson, D.M., Sun, F., Nothnick, W., Wong, S.W., Gunderson, R., Berman, N.E., *et al.* (2002). Deletion of the vpu sequences prior to the env in a simian-human immunodeficiency virus results in enhanced Env precursor synthesis but is less pathogenic for pig-tailed macaques. Virology *293*, 252-261.

Stephens, E.B., Mukherjee, S., Sahni, M., Zhuge, W., Raghavan, R., Singh, D.K., Leung, K., Atkinson, B., Li, Z., Joag, S.V., *et al.* (1997). A cell-free stock of simian-human immunodeficiency virus that causes AIDS in pig-tailed macaques has a limited number of amino acid substitutions in both SIVmac and HIV-1 regions of the genome and has offered cytotropism. Virology *231*, 313-321.

Stephens, E.B., Sahni, M., Leung, K., Raghavan, R., Joag, S.V., and Narayan, O. (1998). Nucleotide substitutions in the long terminal repeat are not required for development of neurovirulence by simian immunodeficiency virus strain mac. J Gen Virol *79 (Pt 5)*, 1089-1100.

Stephens, E.B., Tian, C., Dalton, S.B., and Gattone, V.H., 2nd (2000). Simian-human immunodeficiency virus-associated nephropathy in macaques. AIDS Res Hum Retroviruses *16*, 1295-1306.

Stettner, M.R., Nance, J.A., Wright, C.A., Kinoshita, Y., Kim, W.K., Morgello, S., Rappaport, J., Khalili, K., Gordon, J., and Johnson, E.M. (2009). SMAD proteins of oligodendroglial cells regulate transcription of JC virus early and late genes coordinately with the Tat protein of human immunodeficiency virus type 1. J Gen Virol *90*, 2005-2014.

Stevenson, M., Meier, C., Mann, A.M., Chapman, N., and Wasiak, A. (1988). Envelope glycoprotein of HIV induces interference and cytolysis resistance in CD4+ cells: mechanism for persistence in AIDS. Cell *53*, 483-496.

Strebel, K. (2004). HIV-1 Vpu: putting a channel to the TASK. Mol Cell *14*, 150-152.

Strebel, K., Daugherty, D., Clouse, K., Cohen, D., Folks, T., and Martin, M.A. (1987). The HIV 'A' (sor) gene product is essential for virus infectivity. Nature *328*, 728-730.

Strebel, K., Klimkait, T., Maldarelli, F., and Martin, M.A. (1989). Molecular and biochemical analyses of human immunodeficiency virus type 1 vpu protein. J Virol *63*, 3784-3791.

Strebel, K., Klimkait, T., and Martin, M.A. (1988). A novel gene of HIV-1, vpu, and its 16-kilodalton product. Science *241*, 1221-1223.

Stuchell, M.D., Garrus, J.E., Muller, B., Stray, K.M., Ghaffarian, S., McKinnon, R., Krausslich, H.G., Morham, S.G., and Sundquist, W.I. (2004). The human endosomal sorting complex required for transport (ESCRT-I) and its role in HIV-1 budding. J Biol Chem *279*, 36059-36071.

Sullivan, N., Sun, Y., Binley, J., Lee, J., Barbas, C.F., 3rd, Parren, P.W., Burton, D.R., and Sodroski, J. (1998). Determinants of human immunodeficiency virus type 1 envelope glycoprotein activation by soluble CD4 and monoclonal antibodies. J Virol *72*, 6332-6338.

Svarovskaia, E.S., Xu, H., Mbisa, J.L., Barr, R., Gorelick, R.J., Ono, A., Freed, E.O., Hu, W.S., and Pathak, V.K. (2004). Human apolipoprotein B mRNA-editing enzyme-catalytic polypeptide-like 3G (APOBEC3G) is incorporated into HIV-1 virions through interactions with viral and nonviral RNAs. J Biol Chem *279*, 35822-35828.

Swann, S.A., Williams, M., Story, C.M., Bobbitt, K.R., Fleis, R., and Collins, K.L. (2001). HIV-1 Nef blocks transport of MHC class I molecules to the cell surface via a PI 3-kinase-dependent pathway. Virology *282*, 267-277.

Szczech, L.A. (2001). Renal diseases associated with human immunodeficiency virus infection: epidemiology, clinical course, and management. Clin Infect Dis *33*, 115-119.

Takeb, E.Y., Kusagawa, S., and Motomura, K. (2004). Molecular epidemiology of HIV: tracking AIDS pandemic. Pediatr Int *46*, 236-244.

Takeuchi, H., Okada, A., and Miura, T. (2003). Roles of the histidine and tryptophan side chains in the M2 proton channel from influenza A virus. FEBS Lett *552*, 35-38.

Tan, L., Ehrlich, E., and Yu, X.F. (2007). DDB1 and Cul4A are required for human immunodeficiency virus type 1 Vpr-induced G2 arrest. J Virol *81*, 10822-10830.

Tanaka, M., Ueno, T., Nakahara, T., Sasaki, K., Ishimoto, A., and Sakai, H. (2003). Downregulation of CD4 is required for maintenance of viral infectivity of HIV-1. Virology *311*, 316-325.

Tang, Y., Zaitseva, F., Lamb, R.A., and Pinto, L.H. (2002). The gate of the influenza virus M2 proton channel is formed by a single tryptophan residue. J Biol Chem *277*, 39880-39886.

Terwilliger, E.F., Cohen, E.A., Lu, Y.C., Sodroski, J.G., and Haseltine, W.A. (1989). Functional role of human immunodeficiency virus type 1 vpu. Proc Natl Acad Sci U S A *86*, 5163-5167.

Thali, M., Bukovsky, A., Kondo, E., Rosenwirth, B., Walsh, C.T., Sodroski, J., and Gottlinger, H.G. (1994). Functional association of cyclophilin A with HIV-1 virions. Nature *372*, 363-365.

Tiganos, E., Friborg, J., Allain, B., Daniel, N.G., Yao, X.J., and Cohen, E.A. (1998). Structural and functional analysis of the membrane-spanning domain of the human immunodeficiency virus type 1 Vpu protein. Virology *251*, 96-107.

Tiganos, E., Yao, X.J., Friborg, J., Daniel, N., and Cohen, E.A. (1997). Putative alpha-helical structures in the human immunodeficiency virus type 1 Vpu protein and CD4 are involved in binding and degradation of the CD4 molecule. J Virol *71*, 4452-4460.

Towers, G.J. (2007). The control of viral infection by tripartite motif proteins and cyclophilin A. Retrovirology *4*, 40.

Towers, G.J., Hatziioannou, T., Cowan, S., Goff, S.P., Luban, J., and Bieniasz, P.D. (2003). Cyclophilin A modulates the sensitivity of HIV-1 to host restriction factors. Nat Med *9*, 1138-1143.

Tristem, M., Marshall, C., Karpas, A., and Hill, F. (1992). Evolution of the primate lentiviruses: evidence from vpx and vpr. EMBO J *11*, 3405-3412.

Tristem, M., Marshall, C., Karpas, A., Petrik, J., and Hill, F. (1990). Origin of vpx in lentiviruses. Nature *347*, 341-342.

Tristem, M., Purvis, A., and Quicke, D.L. (1998). Complex evolutionary history of primate lentiviral vpr genes. Virology *240*, 232-237.

Ueno, F., Shiota, H., Miyaura, M., Yoshida, A., Sakurai, A., Tatsuki, J., Koyama, A.H., Akari, H., Adachi, A., and Fujita, M. (2003). Vpx and Vpr proteins of HIV-2 up-regulate the viral infectivity by a distinct mechanism in lymphocytic cells. Microbes Infect *5*, 387-395.

UNAIDS (2008). 2008 Report on the Global AIDS Epidemic.

Van Damme, N., Goff, D., Katsura, C., Jorgenson, R.L., Mitchell, R., Johnson, M.C., Stephens, E.B., and Guatelli, J. (2008). The interferon-induced protein BST-2 restricts HIV-1 release and is downregulated from the cell surface by the viral Vpu protein. Cell Host Microbe *3*, 245-252.

van Harmelen, J., Wood, R., Lambrick, M., Rybicki, E.P., Williamson, A.L., and Williamson, C. (1997). An association between HIV-1 subtypes and mode of transmission in Cape Town, South Africa. AIDS *11*, 81-87.

Van Heuverswyn, F., Li, Y., Neel, C., Bailes, E., Keele, B.F., Liu, W., Loul, S., Butel, C., Liegeois, F., Bienvenue, Y., *et al.* (2006). Human immunodeficiency viruses: SIV infection in wild gorillas. Nature *444*, 164.

Van Maele, B., and Debyser, Z. (2005). HIV-1 integration: an interplay between HIV-1 integrase, cellular and viral proteins. AIDS Rev *7*, 26-43.

Varin, A., Decrion, A.Z., Sabbah, E., Quivy, V., Sire, J., Van Lint, C., Roques, B.P., Aggarwal, B.B., and Herbein, G. (2005). Synthetic Vpr protein activates activator protein-1, c-Jun N-terminal kinase, and NF-kappaB and stimulates HIV-1 transcription in promonocytic cells and primary macrophages. J Biol Chem *280*, 42557-42567.

Vendeville, A., Rayne, F., Bonhoure, A., Bettache, N., Montcourrier, P., and Beaumelle, B. (2004). HIV-1 Tat enters T cells using coated pits before translocating from acidified endosomes and eliciting biological responses. Mol Biol Cell *15*, 2347-2360.

Vincent, M.J., Raja, N.U., and Jabbar, M.A. (1993). Human immunodeficiency virus type 1 Vpu protein induces degradation of chimeric envelope glycoproteins bearing the cytoplasmic and

anchor domains of CD4: role of the cytoplasmic domain in Vpu-induced degradation in the endoplasmic reticulum. J Virol *67*, 5538-5549.

Vishwanathan, S.A., Thomas, A., Brasseur, R., Epand, R.F., Hunter, E., and Epand, R.M. (2008). Hydrophobic substitutions in the first residue of the CRAC segment of the gp41 protein of HIV. Biochemistry *47*, 124-130.

Vodicka, M.A., Koepp, D.M., Silver, P.A., and Emerman, M. (1998). HIV-1 Vpr interacts with the nuclear transport pathway to promote macrophage infection. Genes Dev *12*, 175-185.

von Schwedler, U., Song, J., Aiken, C., and Trono, D. (1993). Vif is crucial for human immunodeficiency virus type 1 proviral DNA synthesis in infected cells. J Virol *67*, 4945-4955.

von Schwedler, U.K., Stuchell, M., Muller, B., Ward, D.M., Chung, H.Y., Morita, E., Wang, H.E., Davis, T., He, G.P., Cimbora, D.M., *et al.* (2003). The protein network of HIV budding. Cell *114*, 701-713.

Wallace, D.R., Dodson, S.L., Nath, A., and Booze, R.M. (2006). Delta opioid agonists attenuate TAT(1-72)-induced oxidative stress in SK-N-SH cells. Neurotoxicology *27*, 101-107.

Wei, B.L., Arora, V.K., Raney, A., Kuo, L.S., Xiao, G.H., O'Neill, E., Testa, J.R., Foster, J.L., and Garcia, J.V. (2005). Activation of p21-activated kinase 2 by human immunodeficiency virus type 1 Nef induces merlin phosphorylation. J Virol *79*, 14976-14980.

Weissenhorn, W., Dessen, A., Harrison, S.C., Skehel, J.J., and Wiley, D.C. (1997). Atomic structure of the ectodomain from HIV-1 gp41. Nature *387*, 426-430.

Wen, X., Duus, K.M., Friedrich, T.D., and de Noronha, C.M. (2007). The HIV1 protein Vpr acts to promote G2 cell cycle arrest by engaging a DDB1 and Cullin4A-containing ubiquitin ligase complex using VprBP/DCAF1 as an adaptor. J Biol Chem *282*, 27046-27057.

Wiegand, H.L., Doehle, B.P., Bogerd, H.P., and Cullen, B.R. (2004). A second human antiretroviral factor, APOBEC3F, is suppressed by the HIV-1 and HIV-2 Vif proteins. EMBO J *23*, 2451-2458.

Wildum, S., Schindler, M., Munch, J., and Kirchhoff, F. (2006). Contribution of Vpu, Env, and Nef to CD4 down-modulation and resistance of human immunodeficiency virus type 1-infected T cells to superinfection. J Virol *80*, 8047-8059.

Willey, R.L., Maldarelli, F., Martin, M.A., and Strebel, K. (1992a). Human immunodeficiency virus type 1 Vpu protein induces rapid degradation of CD4. J Virol *66*, 7193-7200.

Willey, R.L., Maldarelli, F., Martin, M.A., and Strebel, K. (1992b). Human immunodeficiency virus type 1 Vpu protein regulates the formation of intracellular gp160-CD4 complexes. J Virol *66*, 226-234.

Williams, K.C., Corey, S., Westmoreland, S.V., Pauley, D., Knight, H., deBakker, C., Alvarez, X., and Lackner, A.A. (2001). Perivascular macrophages are the primary cell type productively infected by simian immunodeficiency virus in the brains of macaques: implications for the neuropathogenesis of AIDS. J Exp Med *193*, 905-915.

Williams, S.A., Chen, L.F., Kwon, H., Ruiz-Jarabo, C.M., Verdin, E., and Greene, W.C. (2006). NF-kappaB p50 promotes HIV latency through HDAC recruitment and repression of transcriptional initiation. EMBO J *25*, 139-149.

Winston, J.A., and Klotman, P.E. (1996). Are we missing an epidemic of HIV-associated nephropathy? J Am Soc Nephrol *7*, 1-7.

Wolfrum, N., Muhlebach, M.D., Schule, S., Kaiser, J.K., Kloke, B.P., Cichutek, K., and Schweizer, M. (2007). Impact of viral accessory proteins of SIVsmmPBj on early steps of infection of quiescent cells. Virology *364*, 330-341.

Wonderlich, E.R., Williams, M., and Collins, K.L. (2008). The tyrosine binding pocket in the adaptor protein 1 (AP-1) mu1 subunit is necessary for Nef to recruit AP-1 to the major histocompatibility complex class I cytoplasmic tail. J Biol Chem *283*, 3011-3022.

Wray, V., Kinder, R., Federau, T., Henklein, P., Bechinger, B., and Schubert, U. (1999). Solution structure and orientation of the transmembrane anchor domain of the HIV-1-encoded virus protein U by high-resolution and solid-state NMR spectroscopy. Biochemistry *38*, 5272-5282.

Wu, G., Xu, G., Schulman, B.A., Jeffrey, P.D., Harper, J.W., and Pavletich, N.P. (2003). Structure of a beta-TrCP1-Skp1-beta-catenin complex: destruction motif binding and lysine specificity of the SCF(beta-TrCP1) ubiquitin ligase. Mol Cell *11*, 1445-1456.

Wu, X., Conway, J.A., Kim, J., and Kappes, J.C. (1994). Localization of the Vpx packaging signal within the C terminus of the human immunodeficiency virus type 2 Gag precursor protein. J Virol *68*, 6161-6169.

Wu, X., Li, Y., Crise, B., Burgess, S.M., and Munroe, D.J. (2005). Weak palindromic consensus sequences are a common feature found at the integration target sites of many retroviruses. J Virol *79*, 5211-5214.

Wyatt, R., Kwong, P.D., Desjardins, E., Sweet, R.W., Robinson, J., Hendrickson, W.A., and Sodroski, J.G. (1998). The antigenic structure of the HIV gp120 envelope glycoprotein. Nature *393*, 705-711.

Wyatt, R., and Sodroski, J. (1998). The HIV-1 envelope glycoproteins: fusogens, antigens, and immunogens. Science *280*, 1884-1888.

Yamada, T., and Iwamoto, A. (2000). Comparison of proviral accessory genes between long-term nonprogressors and progressors of human immunodeficiency virus type 1 infection. Arch Virol *145*, 1021-1027.

Yang, Y., Guo, F., Cen, S., and Kleiman, L. (2007). Inhibition of initiation of reverse transcription in HIV-1 by human APOBEC3F. Virology *365*, 92-100.

Yao, X.J., Garzon, S., Boisvert, F., Haseltine, W.A., and Cohen, E.A. (1993). The effect of vpu on HIV-1-induced syncytia formation. J Acquir Immune Defic Syndr *6*, 135-141.

Yap, M.W., Nisole, S., and Stoye, J.P. (2005). A single amino acid change in the SPRY domain of human Trim5alpha leads to HIV-1 restriction. Curr Biol *15*, 73-78.

Yeager, M., Wilson-Kubalek, E.M., Weiner, S.G., Brown, P.O., and Rein, A. (1998). Supramolecular organization of immature and mature murine leukemia virus revealed by electron cryo-microscopy: implications for retroviral assembly mechanisms. Proc Natl Acad Sci U S A *95*, 7299-7304.

Yedavalli, V.S., Shih, H.M., Chiang, Y.P., Lu, C.Y., Chang, L.Y., Chen, M.Y., Chuang, C.Y., Dayton, A.I., Jeang, K.T., and Huang, L.M. (2005). Human immunodeficiency virus type 1 Vpr interacts with antiapoptotic mitochondrial protein HAX-1. J Virol *79*, 13735-13746.

Yoon, K., Kestler, H.W., and Kim, S. (1998). Growth properties of HSIVnef: HIV-1 containing the nef gene from pathogenic molecular clone SIVmac239. Virus Res *57*, 27-34.

Yu, Q., Konig, R., Pillai, S., Chiles, K., Kearney, M., Palmer, S., Richman, D., Coffin, J.M., and Landau, N.R. (2004). Single-strand specificity of APOBEC3G accounts for minus-strand deamination of the HIV genome. Nat Struct Mol Biol *11*, 435-442.

Yu, X., Yu, Y., Liu, B., Luo, K., Kong, W., Mao, P., and Yu, X.F. (2003). Induction of APOBEC3G ubiquitination and degradation by an HIV-1 Vif-Cul5-SCF complex. Science *302*, 1056-1060.

Yu, X.F., Yu, Q.C., Essex, M., and Lee, T.H. (1991). The vpx gene of simian immunodeficiency virus facilitates efficient viral replication in fresh lymphocytes and macrophage. J Virol *65*, 5088-5091.

Zauli, G., Milani, D., Mirandola, P., Mazzoni, M., Secchiero, P., Miscia, S., and Capitani, S. (2001). HIV-1 Tat protein down-regulates CREB transcription factor expression in PC12 neuronal cells through a phosphatidylinositol 3-kinase/AKT/cyclic nucleoside phosphodiesterase pathway. FASEB J *15*, 483-491.

Zeitler, B., and Weis, K. (2004). The FG-repeat asymmetry of the nuclear pore complex is dispensable for bulk nucleocytoplasmic transport in vivo. J Cell Biol *167*, 583-590.

Zekeng, L., Gurtler, L., Afane Ze, E., Sam-Abbenyi, A., Mbouni-Essomba, G., Mpoudi-Ngolle, E., Monny-Lobe, M., Tapka, J.B., and Kaptue, L. (1994). Prevalence of HIV-1 subtype O infection in Cameroon: preliminary results. AIDS *8*, 1626-1628.

Zennou, V., and Bieniasz, P.D. (2006). Comparative analysis of the antiretroviral activity of APOBEC3G and APOBEC3F from primates. Virology *349*, 31-40.

Zennou, V., Perez-Caballero, D., Gottlinger, H., and Bieniasz, P.D. (2004). APOBEC3G incorporation into human immunodeficiency virus type 1 particles. J Virol *78*, 12058-12061.

Zhang, F., Wilson, S.J., Landford, W.C., Virgen, B., Gregory, D., Johnson, M.C., Munch, J., Kirchhoff, F., Bieniasz, P.D., and Hatziioannou, T. (2009). Nef proteins from simian immunodeficiency viruses are tetherin antagonists. Cell Host Microbe *6*, 54-67.

Zheng, Y.H., Irwin, D., Kurosu, T., Tokunaga, K., Sata, T., and Peterlin, B.M. (2004). Human APOBEC3F is another host factor that blocks human immunodeficiency virus type 1 replication. J Virol *78*, 6073-6076.

Zimmerman, C., Klein, K.C., Kiser, P.K., Singh, A.R., Firestein, B.L., Riba, S.C., and Lingappa, J.R. (2002). Identification of a host protein essential for assembly of immature HIV-1 capsids. Nature *415*, 88-92.

XV. Appendix

List of Publications

Hill MS, **Ruiz A**, Gomez LM, Miller JM, Berman NE, Stephens EB. APOBEC3G Expression is Restricted to Epithelial Cells of the Proximal Convoluted Tubules and is not Expressed in the Glomeruli of Macaques. J Histochem Cytochem. 2007 Jan;55(1):63-70.

Hill MS, **Ruiz A**, Pacyniak E, Pinson DM, Culley N, Yen B, Wong SW, Stephens EB. Modulation of the Severe CD4+ T-Cell Loss Caused by a Pathogenic Simian-Human Immunodeficiency Virus by Replacement of the Subtype B Vpu with the Vpu from a Subtype C HIV-1 Clinical Isolate. Virology. 2008 Feb 5;371(1):86-97.

Ruiz A, Hill MS, Schmitt K, Guatelli J, Stephens EB. Requirements of the Membrane Proximal Tyrosine and Dileucine-Based Sorting Signals for Efficient Transport of the Subtype C Vpu Protein to the Plasma Membrane and in Virus Release. Virology. 2008 Aug 15;378(1):58-68.

Schmitt K, Hill MS, **Ruiz A**, Culley N, Pinson DM, Wong SW, Stephens EB. Mutations in the Highly Conserved SLQYLA Motif of Vif in a Simian-Human Immunodeficiency Virus Result in a Less Pathogenic Virus and are Associated with G-to-A Mutations in the Viral Genome. Virology. 2009 Jan 20;383(2):362-72.

Mitchell RS, Katsura C, Skasko MA, Fitzpatrick K, Lau D, **Ruiz A**, Stephens EB, Margottin-Goguet F, Benarous R, Guatelli JC. Vpu Antagonizes BST-2-Mediated Restriction of HIV-1

Release via Beta-TrCP and Endo-Lysosomal Trafficking. PLoS Pathog. 2009 May;5(5):e1000450.

Hill MS, **Ruiz A**, Schmitt K, Stephens EB. Identification of Amino Acids within the Second Alpha Helical Domain of the Human Immunodeficiency Virus Type 1 Vpu that are Critical for Preventing CD4 Cell Surface Expression. Virology. 2010 Feb 5;397(1):104-12.

Ruiz A, Guatelli JC, Stephens EB. The Vpu Protein: New Concepts in Virus Release and CD4 Down-Modulation. Curr HIV Res. 2010 Apr 1;8(3):240-52. Review.

Schmitt K, Hill MS, Liu Z, **Ruiz A**, Culley N, Pinson DM, Stephens EB. Comparison of the Replication and Persistence of Simian-Human Immunodeficiency Viruses Expressing Vif Proteins with Mutation of the SLQYLA or HCCH Domains in Macaques. Virology. 2010 Sep 1;404(2):187-203.

Ruiz A, Lau D, Mitchell RS, Hill MS, Schmitt K, Guatelli JC, Stephens EB. BST-2 Mediated Restriction of Simian-Human Immunodeficiency Virus. Virology 2010 Oct 25;406(2):312-21.

Ruiz A, Hill MS, Schmitt K, Stephens EB. Membrane Raft Association of the Vpu Protein of Human Immunodeficiency Virus Type I Correlates with Enhanced Virus Release. Virology. 2010. [Epub Ahead of Print].